APPLICATION OF BRIDGE SPECIFIC FRAGILITY ANALYSIS IN THE SEISMIC DESIGN PROCESS OF BRIDGES IN CALIFORNIA

A Thesis
Presented to
The Academic Faculty

by

Jazalyn Denise Dukes

In Partial Fulfillment
of the Requirements for the Degree
Doctor of Philosophy in the
School of Civil and Environmental Engineering

Georgia Institute of Technology
May, 2013

APPLICATION OF BRIDGE SPECIFIC FRAGILITY ANALYSIS IN THE SEISMIC DESIGN PROCESS OF BRIDGES IN CALIFORNIA

Approved by:

Dr. Reginald Desroches, Advisor
School of Civil and Environmental
Engineering
Georgia Institute of Technology

Dr. Glenn Rix
School of Civil and Environmental
Engineering
Georgia Institute of Technology

Dr. Roberto Leon
Department of Civil and Environmental
Engineering
Virginia Tech

Dr. Jamie E. Padgett, Co-advisor
Department of Civil and Environmental
Engineering
Rice University

Dr. Barry Goodno
School of Civil and Environmental
Engineering
Georgia Institute of Technology

Dr. Steven French
College of Architecture, School of City
and Regional Planning
Georgia Institute of Technology

Date Approved: March 6, 2013

To the memory of James M. Walton, Sr.

ACKNOWLEDGEMENTS

My journey towards the PhD has been a great one, and I have so many people to thank for making it so. First, many thanks go to my academic advisor and mentor, Dr. Reginald Desroches, who saw the potential in me to complete this journey. He has been supportive, patient, and encouraging from the very beginning, and I couldn't have asked for a better advisor.

I extend my gratitude to the faculty members that served on my thesis committee: Drs. Jamie Padgett, Glenn Rix, Barry Goodno, Roberto Leon, and Steven French. Special thanks to Dr. Jamie Padgett, for also serving as my co-advisor, and providing great technical guidance throughout my research project. I extend my gratitude to Dr. Roberto Leon, who afforded me a great opportunity to get involved in an earthquake reconnaissance research experience in New Zealand, which greatly enhanced my experience during my PhD program. Many thanks to the numerous faculty members at Georgia Tech, past and present, for the willingness to impart their academic expertise to students both in and outside the classroom.

Many people outside of Tech have made the completion of this journey possible. I'd like to thank Caltrans for sponsoring this research project, and the team at Caltrans, in particular Cliff Roblee and Loren Turner, for their guidance throughout the project and support of the final results. Thanks to Jayadipta Ghosh, for his help with my research, as well as his friendship. I appreciate the National Science Foundation and the National Defense Education Program for funding my tenure here at Tech. Other entities enhanced my program while at Tech, including FACES, the Mundy Fund, and others.

The people I have met while at Georgia Tech have made this journey better than I could have imagined. Special thanks to Karthik, who worked on the same research project, for providing invaluable support throughout the process. Thanks to my former and current officemates and research fellows: Masahiro, Ben, Lynne, Niki, Tim, Matthew, Abdollah, Jieun, Stephanie, Jong-Su, Laura J., Laura R., Passarin, Dapeng, and Xiaohua. Thanks to the many friends I've made in the department, including Chris, Amal, Falak, Boyeon, and many, many others. Special thanks to the students in the Fellowship of Christian Graduate Students for their prayers and support. Many thanks to Zakiya and Denise for their friendship and support, and to the many other students I have met throughout my time in Tech that have made this experience unforgettable.

The immense amount of love and support that came from my family was truly a blessing during this time. My mom, Janet Dukes, encourages me at all times to achieve my goals; this work is dedicated to her, in addition to my late grandfather. My grandmother, brothers, aunts, uncles, and cousins continue to express their pride in my achievements and celebrate with me at every milestone. Much love and appreciation is extended to them all. Finally, I end this by saying that without God, none of this would have been possible.

TABLE OF CONTENTS

LIST OF TABLES

LIST OF FIGURES

xvii

SUMMARY

The California Department of Transportation (Caltrans) seismic bridge design process for an Ordinary Bridge described in the Seismic Design Criteria (SDC) directs the design engineer to meet minimum requirements resulting in the design of a bridge that should remain standing in the event of a Design Seismic Hazard. A bridge can be designed to sustain significant damage; however it should avoid the collapse limit state, where the bridge is unable to resist loads due to self-weight. Seismic hazards, in the form of a design spectrum or ground motion time histories, are used to determine the demands of the bridge components and bridge system. These demands are compared to the capacity of the components to ensure that the bridge meets key performance criteria. The SDC also specifies design detailing of various components, including abutments, foundations, hinge seats and bent caps. The expectation of following the guidelines set forth by the SDC during the design process is that the resulting bridge design will avoid collapse under anticipated seismic loads. While the code provisions provide different analyses to follow and component detailing to adhere to in order to ensure a proper bridge design, the SDC does not provide a way to quantitatively determine whether the bridge design has met the requirement of no-collapse.

The objectives of this research are to introduce probabilistic fragility analysis into the Caltrans design process and address the gap of information in the current design process, namely the determination of whether the bridge design meets the performance criteria of no-collapse at the design hazard level. The motivation for this project is to improve the designer's understanding of the probabilistic performance of their bridge

design as a function of important design details. To accomplish these goals, a new bridge fragility method is presented as well as a design support tool that provides design engineers with instant access to fragility information during the design process. These products were developed for one specific bridge type that is common in California, the two-span concrete box girder bridge. The end product, the design support tool, is a bridge-specific fragility generator that provides probabilistic performance information on the bridge design. With this tool, a designer can check the bridge design, after going through the SDC design process, to determine the performance of the bridge and its components at any hazard level. The design support tool can provide the user with the probability of failure or collapse for the specific bridge design, which will give insight to the user about whether the bridge design has achieved the performance objective set out in the SDC. The designer would also be able to determine the effect of a change in various design details on the performance and therefore make more informed design decisions.

CHAPTER 1

INTRODUCTION

1.1 Background and Motivation of Project

Through a study of the history of seismic design, one can see that the seismic design of bridges has gone through many iterations of progress over the past century. The first seismic design code provisions in the US appeared after the 1906 San Francisco earthquake (FEMA, 2006). In 1940, the first seismic design provisions for bridges were developed in California. Early provisions were based on limited knowledge of seismic loadings and only included provisions against lateral loads proportional to the weight (AASHO, 1961). Over time, seismically damaged bridges revealed design shortcomings, and analytical and experimental research revealed new information about the design and behavior of bridge structures under seismic loads. Thus, design provisions continually evolved to be much more comprehensive, ultimately leading to provisions requiring special detailing and additional dynamic analyses of the structure, among other things. The bridges of today, as a result, are designed based on much more knowledge from the failures of the past and about the characteristics of design that lead to preferable behavior during an earthquake.

The California Department of Transportation (Caltrans) seismic bridge design process for an Ordinary Bridge described in the Seismic Design Criteria (SDC) directs the design engineer to meet minimum requirements resulting in a bridge that should remain standing in the event of a Design Seismic Hazard (Caltrans, 2010). A bridge can be designed to sustain significant damage; however it should avoid the collapse limit state, where the bridge is unable to resist loads due to self-weight (Caltrans, 2010). Seismic hazards, in the form of a design spectrum or ground motion time histories, are used to determine the demands of the bridge components and bridge system. These

demands are compared to the capacity of the components to ensure that the bridge meets key performance criteria. The SDC also specifies design detailing of various components, including columns, abutments, foundations, hinge seats and bent caps. The expectation of following the guidelines set forth by the SDC during the design process is that the resulting bridge design will avoid collapse under anticipated seismic loads.

The procedure set forth in the SDC is a prescriptive approach which does not provide quantitative information on the bridge performance during a Design Seismic Hazard (DSH). Although the SDC is designed to produce bridge designs that will not collapse during a DSH, the collapse capacity of the structure is uncertain in itself (Luco, et al., 2007) and is not addressed by the SDC. Moreover, the current approach does not account for the performance of the bridge at hazard levels other than the Design Seismic Hazard. The current design process also does not directly provide information on the expected performance as a function of different design details. Therefore, there is a need for a supplement to this design process that will provide statistical information on the performance of a bridge at a Design Seismic Hazard, as well as for other hazard levels. Quantification of the uncertainty of the collapse capacity of the bridge and the sources of uncertainty would also be beneficial to append to the design process. There is also a need for designers to have an understanding of the effects of certain design decisions on the probabilistic performance of a bridge, and the performance of the bridge at different limit state levels.

Fragility analysis of bridges has been an important used in seismic risk assessment of bridges. Fragility analysis has had applications in lifeline network assessment of interdependent network systems, post-event planning, and retrofit planning (Duenas-Osorio, et al., 2007) (Mackie, et al., 2005)(Basoz, et al., 1999) (Padgett, et al., 2008). The knowledge of the performance of bridge and transportation networks during an earthquake event is very important to ensure the safety of the public and protection against damages and loss. Fragility curves in the past have been created using different

methods and for different purposes. The research presented in this dissertation was developed as part of a project that looks to improve the fragility relationships Caltrans uses for risk assessment and to incorporate fragility analysis in different ways. The following describes the applications Caltrans intends for fragility analysis in their engineering applications.

- Emergency Response:
  - Optimize initial bridge inspection priorities (through ShakeCast near-real-time alerting system);
  - Rapid initial estimate of loss (for support of emergency declarations).
- Design Support - Performance-Based Earthquake Engineering:
  - Bridge-Specific: Develop bridge-specific fragility curves to serve as a design check and support design strategy decisions.
  - Bridge Classes: Evaluate classes of bridge systems to optimize design guidelines for safety, cost, and functionality.
- Planning Support:
  - Traffic impacts from scenario earthquakes (e.g. Golden Guardian);
  - Performance of specific transportation corridors (e.g. Lifeline routes);
  - Cost-effectiveness of alternate bridge hardening strategies;
  - Screening for additional seismic retrofit needs.
- Policy Support - Risk Nomenclature
  - Capacity for issuing scientifically-defensible (internal, interagency, or public) statements regarding anticipated transportation system performance that accounts for unavoidable uncertainties in earthquake shaking and variable bridge design/construction/age.

Within the context of the one of the applications in which Caltrans intends to use fragility relationships, the present research is presented. That application is the

performance based earthquake engineering and design support, specifically, bridge-specific fragility relationships. Overall, the goal of this project is to introduce probabilistic fragility analysis into the Caltrans design process and address the lack of specific performance information provided to the engineer during the current design process. The motivation for this project is to improve the design engineer's understanding of the probabilistic performance of their bridge design as a function of several design details. To accomplish these goals, a bridge-specific fragility method is presented as well as a design support tool that provides design engineers with instant access to fragility information during the design process. These products are presented for one specific bridge type that is common in California, the two-span concrete box girder bridge. The end product, the design support tool, is a bridge-specific fragility generator that provides probabilistic performance information for specific bridge designs. With this tool, a designer can check the bridge design after going through the SDC procedure in order to determine the performance of the bridge and its components at any hazard level. The designer would then be able to determine the effect of a change in the design on the performance and therefore make more informed design decisions.

1.2 Research Objectives

The main objective of this research is to incorporate fragility analysis into the Caltrans seismic design process as a design check and a method to support design decisions made by design engineers. In order to complete the objectives of this research, the following tasks were performed:

1. Review the seismic design provisions made for bridge design in California in order to determine how the process can be improved with the use of fragility analysis.

2. Develop a fragility methodology that would create fragility curves specific to the details of a new bridge design.

3. Determine the design properties most significant to the response of the bridge for use in the method.

4. Perform the bridge specific fragility method for one class of bridge in California that is commonly built in the modern era.

5. Compare the BSFM against other fragility analysis methods and results to determine the similarities and differences in results and advantages over other methods.

6. Create the DST that encompasses the BSFM in an accessible format for Caltrans engineers to obtain fragility information specific to their bridge design.

7. Present the results of this research to Caltrans engineers for comments and feedback in order to improve the method for it to be used in practice.

1.3 Outline of Dissertation

This dissertation is divided into nine chapters as follows:

Chapter 2 details the history of seismic bridge design around the world, with a special focus on seismic bridge design in California. A detailed summary of the Caltrans seismic design provisions is given, and a motivation for incorporating fragility in the design process is presented.

Chapter 3 gives an overview of the analytical fragility analysis. Past research on the topic is given. The history of key components of the present research is also given in this chapter.

Chapter 4 describes the ground motion suite and the capacity model used in this research.

Chapter 5 includes details on the analytical bridge modeling used in this research. Details on the source of information on California bridges and inventory are given. The

material and structural models developed in OpenSees are detailed. The method of using these models in the fragility framework is described.

Chapter 6 contains the sensitivity studies of the design parameters, which are a major component of the bridge-specific fragility method presented in this research. The sensitivity studies were designed to show the significance of the design parameters on the response of the bridge components in order to determine which parameters should be used in the bridge-specific fragility framework.

Chapter 7 outlines the bridge-specific fragility method and framework, which is the focus of this research. This chapter contains details on the multi-parameter probabilistic seismic demand model (PSDM) created using the concepts of metamodels. It also includes information on how the multi-parameter PSDM and capacity models are convolved to determine bridge-specific fragility estimation using Monte Carlo simulation and logistic regression. Examples of the fragility curves developed with the BSFM and a validation of the method is included which compares the BSFM to other methods of bridge fragility analysis established in past research.

Chapter 8 describes the design support tool (DST) developed to house the BSFM. The DST presents this method for practical use by Caltrans engineers as a tool to check the new bridge designs for compliance with seismic design criteria for their specific projects.

Chapter 9 presents a summary of this thesis, along with conclusions, research impact, and future work related to this research.

CHAPTER 2

SEISMIC BRIDGE DESIGN PROVISIONS

Bridges are an important component of the transportation network and are vulnerable to damage from natural disasters such as earthquakes (Elnashai, et al., 2008). Because of this, the proper design of bridges to withstand the effects of seismic loads has been a major focus of designers and researchers for many years. Major earthquake events and the aftermath have provided guidance for needed improvements and advancement in design, as has research findings from labs and universities (Duan, et al., 2003). Today, design codes are in place in many earthquake prone areas to provide guidance for the bridge to perform in a manner acceptable by the designers and governing officials of that region. This chapter provides the history of seismic design from different locations around the world. It further details the current state of seismic design of bridges in California, which is considered a leader in the area of seismic design of bridges. Finally this chapter concludes with a summary of the design philosophies and an introduction to the focus of this thesis, which is to further improve the design process with the use of fragility analysis.

2.1 History of Bridge Seismic Design Provisions around the world

2.1.1 United States

2.1.1.1 AASHTO

In the AASHTO Standard Specifications for Highway Bridges, consideration for earthquake loads on bridges did not appear in the specifications until the 1961 edition (AASHO 1961). In the design division, a short provision for considering lateral earthquake loads is given in the following formula. According to the specifications, it is

applicable in regions where earthquakes may be anticipated. In Eq. (2.1), EQ is the lateral force applied horizontally in any directions at the center of gravity of the structure. D is the dead load of the bridge. C is a factor specified for different foundation types, ranging from 0.02 to 0.06. In other words, the maximum lateral force considered on the structure due to earthquakes would be 2-6% of the dead load (AASHO 1961). These specifications were based partly on the lateral force requirements in place for buildings set forth by the Structural Engineers Association of California (Rojahn 1997).

$$EQ = C * D$$

(2.1)

After the 1971 San Fernando earthquake, the extensive damage to bridges led to a push for better seismic design of bridges (Rojahn 1997). In the 12th edition of the AASHTO Standard Specifications for Highway Bridges (AASHTO 1977), the procedure to determine the load on a structure was updated. Three methods of seismic analysis were given for simple bridges, complex bridges and special cases. For bridges that have supporting members with similar stiffness, one can use the equivalent static force method to find an equivalent static force to apply to the structure. Eqn. (2.2) shows this method. The F is a framing factor based on the column structure and W is the total dead weight of the bridge. The C in the equation is the combined response coefficient. C can also be found with given charts based on the period of the structure and the maximum expected acceleration (A) at bedrock. The minimum value of C is 0.06 for sites with A less than 0.3 g, and 0.10 for A greater than 0.3 g.

$$EQ = C * F * W$$
$$C = A * R * S / Z$$

(2.2)

For more complex structures, a response spectrum method should be used for seismic analysis. The design response spectrum can be the combined response curves given in the code. For special cases, for bridges that are adjacent to active faults, unusual geologic conditions, unusual structures, and structures with periods greater than 3 seconds, these structures will have to be designed with current seismicity, soil response,

and dynamic analysis techniques. This edition also specifies the design force of retraining components such as hinge ties and shear blocks, to be 25% of the contributing dead load minus column shears (AASHTO 1977).

Changes to the seismic design of bridges continued to occur over several years. In 1981, the Applied Technology Council created guidelines for the design of bridges to be used nationally, Seismic Design Guidelines for Highway Bridges, known as ATC-6. AASHTO eventually integrated those guidelines into the Specifications in 1991(Rojahn 1997). In the most recent AASHTO LRFD Bridge Design Specifications, Customary U.S. Units, 5th Edition (AASHTO 2010), it specifies that bridges should be designed with a low probability of collapse during earthquake loads that have a 7% probability of exceedance in 75 years. The bridge may, however, suffer significant damage during said earthquake. The seismic hazard must be determined with an acceleration spectrum defined with procedures in the AASHTO code and appropriate seismic hazard maps. The design response spectrum developed with hazard map quantities and site factors is given in Figure 1. More details on the creation of this spectrum are in the code. From these values, the seismic zone is determined, which dictates the appropriate design forces. For example, if a bridge is determined to be located in a Zone 1 seismic area, which is a low seismic area, it must be designed to withstand a horizontal force not less than 0.15 times the vertical reaction due to permanent loads and live loads. This has increased significantly from the first provisions that had a maximum lateral force of 6% of dead load for any bridge. This edition provides great detail in terms of seismic load design for bridges and tailors design details to specific regions of the country.
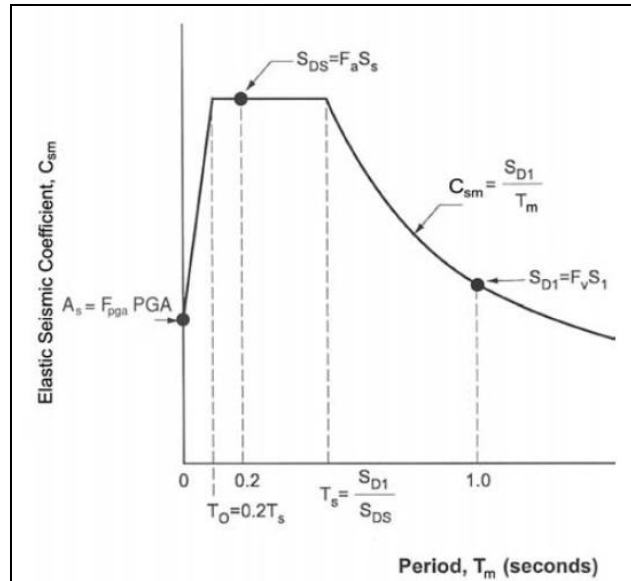
Figure 1: Design Response Spectrum developed with AASHTO procedure (AASHTO 2010).

2.1.1.2. Caltrans

Seismic design in the US has evolved significantly over the past 100 years, with most of the innovation in design coming after large earthquake events. In the United States, seismic design codes began to be developed after the 1906 San Francisco earthquake (FEMA, 2006). Seismic design concepts graduated from those based on wind loads and static force concepts, to dynamic design concepts using acceleration spectra. In recent history, the nonlinear behavior of components has been able to be modeled with computer analysis programs and verified with extensive lab tests. California has always been in the forefront of evolving seismic design in the US due to the high seismic activity in the state, with many universities playing key roles in testing and developing these new design concepts and ideas (FEMA, 2006).

The first seismic design provision in California for bridges was developed in 1940. The design criteria stated that bridges should be designed for a seismic force placed horizontally at the center of mass in any direction. The force was a percentage of the dead load which was determined by the design engineer. In 1943, and design criteria was more specific. It stated that the seismic force applied to the center of gravity of the weight of the structure should be between 2% and 6% of the dead load of the structure, depending

on the type of foundation. As was mentioned before, these criteria were soon adopted in the nationwide standards of AASHTO. In 1965, the criteria incorporated more characteristics of the bridge into the calculation of the seismic force. Eqn. (2.3) shows the formula for finding this force. The coefficient K represents the energy absorption of the structure, and is determined based on the bent system (wall, versus single and multi-column piers). The coefficient C represents the structure's stiffness, and is based on the natural period of vibration. The minimum force was 2% of the dead load of the structure, and the engineer was instructed to give special consideration to structures founded on soft soils, and structures with massive piers (Moehle, et al., 1995)

$$EQ = K * C * D$$

(2.3)

The 1971 San Fernando earthquake prompted major changes in the seismic bridge design code. For bridges in construction, lateral design forces were increased by a factor of 2 or 2.5. Design for new bridges then had to account for many new factors, including fault proximity, site conditions, dynamic response and ductile design for reinforced concrete structures. These changes were included in the 1974 seismic code for Caltrans (Sahs, et al., 2008). Practice in design continued to evolve to improve the reinforcement details of columns and to design for plastic shear in the column. From this era, the criteria for design provided more details for the proportions of the components that would lead to ductile response in the columns, and elastic response in other parts of the bridge (Moehle, et al., 1995). After the 1989 Loma Prieta earthquake, Caltrans decided to ask the Applied Technology Council (ATC) to review and revise their design criteria. However, the results were not completed nor implemented at the time of the 1994 Northridge earthquake. As a result, very little changes were made to the code until after the 1994 Northridge earthquake occurred (Sahs, et al., 2008).

Once the ATC completed its ATC-32 report for Caltrans, Caltrans incorporated nearly all of the recommendations made therein into its design code in 1996. Figure 2 shows how the seismic design spectra have changed throughout the years based on the

code provisions (Moehle, et al., 1995). The new recommendations included a capacity design approach to ensure flexural failure in the column, which would be made possible by carefully designing the joints, column geometry, footing connection, among other things (Sahs, et al., 2008).

Design Force / Weight
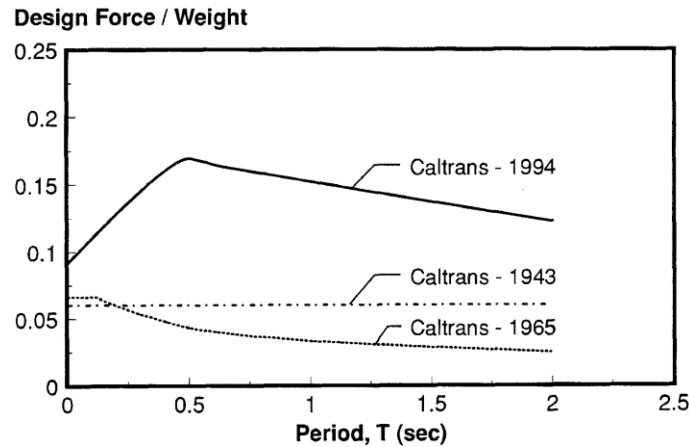
Figure 2: Caltrans design spectrum for a certain type of bridge(Moehle, et al., 1995).

Because the design concepts and codes were continually changing throughout the years, the design of structures and particularly bridges varied based on the period of design. Subsequently, each design period had its vulnerabilities to seismic forces (Sahs, et al., 2008). In general, bridges built in California before 1971 had the following design details: column shear reinforcement of #4 at 12", short set width at expansion joints, inadequate lap splices and development of longitudinal reinforcement in the footing. The potential vulnerabilities in bridges designed during that period are column shear failure, column longitudinal reinforcement pull-out, and unseating of expansion hinges. The 1971 San Fernando earthquake resulted in a major change in the seismic codes, and thus the bridge designs. Bridges built between 1971 and 1994 had closer spacing and improved column shear detailing, column longitudinal splices prohibited at maximum moment locations, short seat widths at expansion joint hinges, poor flare detailing, and inadequate joint reinforcement. The possible vulnerabilities of bridges designed during this time that were not retrofitted are column shear failure of plastic hinge regions, shear failure of

12

flared columns, and unseating of expansion joint hinges. Again, large earthquake events, including the 1989 Loma Prieta and 1995 Northridge earthquakes in California, forced major changes in seismic design of bridges. For bridges designed after 1994, new design details included long seats widths at expansion joints, improved flare column details, no lap splices in plastic hinge zones, shear reinforcement in footings, and joint reinforcement (Sahs, et al., 2008).

2.1.2 Japan

As one of the most seismically active countries in the world, the seismic design of bridges in Japan has been cultivated due to many catastrophic experiences during the last century (Unjoh, 2000). Since the Great Kanto Earthquake of 1923, over 3000 bridges have been damaged due to seismic loads, perpetuating the advancement of seismic design techniques in Japan. Seismic design of bridges in Japan began with the "Method of Seismic Design of Abutments and Piers", which was introduced in 1924. Since then, different seismic design practices have been implemented in Japan that involved updating the design of different components and how to apply seismic load to the structure. In 1971, comprehensive provisions for seismic design of bridges were given in the *Guide Specifications for Seismic Design for Highway Bridges*, after the damaging effects of the 1964 Niigata Earthquake triggered the need for updating the seismic design code. Topics addressed in this code included lateral force based on seismic zones, ground conditions, and design detailing. Since liquefaction was a major problem in that earthquake, an assessment of soil liquefaction was integrated into the design method. In 1980, those Guide Specifications were revised and integrated into the *Design Specifications of Highway Bridges* as "Part V: Seismic Design", and included a better way to predict soil liquefaction and to design foundations in liquefying soils (Kawashima, 2002). "Part V" was further updated in 1990 to include a ductility check of reinforced concrete piers,

provisions for soil liquefaction, and a prescription for dynamic response analysis (Unjoh, 2000).

The Hyogo-Ken Nanbu (Kobe) earthquake of 1995 revealed that there were still inefficiencies in the seismic design of bridges in Japan that needed to be addressed. Figure 3 shows the distribution of the design specifications used for the bridge piers that were a part of the national highway network. Most of the bridges that were damaged were built based on the 1964 or older Design Specifications (Kawashima, et al., 1997). The following month, the Ministry of Construction formed the Committee for Investigation on the Damage of Highway Bridges Caused by the Hyogo-Ken Nanbu Earthquake, which developed the "Guide Specifications for Reconstruction and Repair of Highway Bridge which Suffered Damage due to the Hyogo-Ken Nanbu Earthquake". These specifications were used in the rehabilitation of the damaged bridges as well as for the seismic design of new bridges and strengthening of existing bridges until the Design Specifications were revised (Unjoh, 2000). The revised version of the "Part V" of the *Design Specifications of Highway Bridges* was released in 1996, the main difference was the design procedure used in the new specifications included the ductility design method for design of bridges against effects of extreme low-probability ground motions, as well as the traditional seismic coefficient method which is for the design of the bridges against moderate earthquake ground motions (Kawashima, et al., 1997).

The current "Part V: Seismic Design" of the *Design Specifications for Highway Bridges* was released in 2002 (JPA, 2002). This section lists performance expectations of the bridges designed according to the code, summarized in Table 1 and Table 2. As is shown in the tables, a bridge is designed to perform a certain way based on the type of bridge it is, and the type of ground motion the bridge will experience. Class B bridges are those bridges that are important in the emergency response efforts of the region following an earthquake event, and include bridges in the national highway network and other urban expressways. Class A bridges are any other bridge not considered Class B.

14

Therefore, for an important bridge in the event of a large earthquake, the bridge should sustain no critical damage and be designed to ensure against unseating.
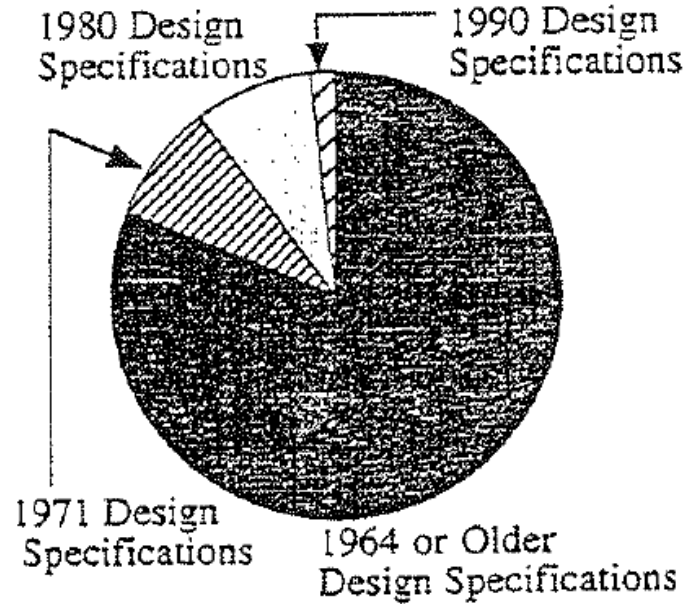
Figure 3: Design Specifications used in the design of bridges in the Hanshin Expressway **(Kawashima, et al., 1997)**.

Table 1: Seismic performance of bridges (JPA, 2002)

Seismic Performance	Seismic Safety Design	Seismic Serviceability Design	Seismic Repairability Design	
			Emergency Repairability	Permanent Repairability
Level 1: Keeping the sound function of bridges	To ensure the safety against girder unseating	To ensure the normal functions of bridges	No repair work is needed to recover functions	Only easy repair works are needed
Level 2: Limited damages and recovery	Same as above	Capable of recovering functions within a short period after the event	Capable of recovering functions by emergency repair works	Capable of easily undertaking permanent repair works
Level 3: No critical damages	Same as above	-	-	-

Table 2: Design earthquake ground motions and seismic performance of bridges (JPA, 2002)

Earthquake Ground Motions		Class A bridges	Class B bridges
Level 1 Earthquake Ground Motion (highly probable during the bridge service life)		Seismic Performance Level 1	
Level 2 Earthquake Ground Motion	Type I: Plate boundary type earthquake with a large magnitude Type II: Inland direct strike type earthquake like Hyogo-ken nanbu	Seismic Performance Level 3	Seismic Performance Level 2

With seismic performance clearly specified for new bridge designs, verification of seismic performance is needed, and the Seismic Design chapter in the *Design Specifications of Highway Bridges* prescribes some verification methods to ensure seismic performance of the design is met (JPA, 2002). First, limit states for the bridge and components must be established to accomplish each specific seismic performance level (SPL). The code gives guidelines as to how those limit states should be established. For example, limit states for structural members for SPL 1 should be determined such that the members behave within the elastic ranges. Table 3 shows the type of analysis acceptable for the verification of the limit states chosen for each SPL (Unjoh, et al., 2002). These tables give a broad summary of the ways the Japan seismic design code for bridges specifies bridge performance criteria and the methods used to enforce the criteria and ensure properly designed bridges.

Table 3: Applicable verification methods for seismic design performance (Unjoh, et al., 2002)

Dynamic characteristics / SPL to be verified	Bridges with simple behavior	Bridges with Multi-plastic hinges and not applicable of the energy constant rule	Bridges with limited applications of static analysis	
			With Multi-mode response	With complicated behavior
SPL 1	Static Verification	Static Verification	Dynamic Verification	Dynamic Verification
SPL 2/SPL 3		Dynamic Verification		
Example of bridges	Other than bridges shown to the right	Bridges that have: 1)Rubber bearings to distribute inertia force 2)Seismic Isolation 3)Rigid Frame 4)Steel columns	Bridges with: 1)Long natural periods 2)High piers	These types of bridges: 1)Cable-stayed and suspension 2)Arch 3)Curved

2.1.3. New Zealand

New Zealand is another country which has a long history of seismic activity. However, it was the San Fernando earthquake of 1971 that sparked interest in developing a seismic design of bridges in New Zealand due to the heavy damage caused by the earthquake (Park, 1997).The New Zealand National Society for Earthquake Engineering (NSZEE) gathered in 1978 to discuss procedures for the seismic design of bridges and produced a report of 12 technical papers in the Bulletin of the NZSEE. The report included design procedures based on the latest in seismic design techniques and developments in earthquake engineering. The recommendations for a seismic design approach from this group's report were then incorporated into the national bridge design specifications, *Bridge Manual*. The seismic loadings for bridges were taken from the standards for loadings for buildings and modified appropriately (Park, 1996). First introduced in 1994, the latest *Bridge Manual* is now in its 2nd edition and was released in 2003 (NZTA, 2003).

The main objective for seismic design in *Bridge Manual* is to produce bridges that maintain functionality and safety after a seismic event (Transit New Zealand, 2003). The performance goal of bridges designed with the *Bridge Manual* is for the bridge to be safe for emergency response after it experiences a design earthquake with a design return period, even though the bridge may suffer some damage. Other performance goals are for the bridge to sustain only minor damage during an earthquake event with a return period much less than the design return period, and for the bridge not to collapse during an event with a return period much greater than the design level. However, if the first performance goal is met, than the other two performance goals are assumed to be met with proper detailing (Transit New Zealand, 2003).

In the beginning, each structure is categorized based on the structural action expected under horizontal seismic loads. Structure categories include ductile structure, partially ductile structure, and elastic structure (Transit New Zealand, 2003). For each structural action group, the code prescribes a maximum displacement ductility factor, μ. The displacement ductility factor is defined as the ratio of the design displacement to the yield displacement of the center of mass of the structure. The maximum value for displacement ductility for any structure is six. Table 4 shows the ductility factors for each structural action group. Type I partially ductile structure has a plastic mechanism in only part of the structure up to the design displacement, while a Type II partially ductile structure forms a complete plastic mechanism with further displacement, although the load is unpredictable. The designer is responsible for ensuring the structure can meet the demands of the displacement ductility based on the structural action.

Designers must also take into consideration the site subsoil present in the design of the bridge, which corresponds to the appropriate response spectra to be used for the design earthquake hazard (Transit New Zealand, 2003). The response spectrum accelerations are applied to the structure based on three methods given in the code: equivalent static force analysis, modal analysis and inelastic time history analysis. The

code goes on to give instructions on how to address liquefaction, vertical acceleration, design methods for members, and design details of components. The *Bridge Manual* of New Zealand prescribes detailed ways to ensure the new seismic design of bridges will meet the objectives and performance goals set out by Transit New Zealand.

Table 4: Maximum allowable values of the design displacement ductility factor(Transit New Zealand, 2003)

Energy Dissipation System	μ
Ductile or partially ductile structure (Type I) in which plastic hinges form at the design load intensity, above ground or normal water level	6
Ductile or partially ductile structure, in which plastic hinges form in reasonably accessible positions	4
Ductile or partially ductile structure (Type I) in which plastic hinges are inaccessible or at a level reasonably predictable Partially ductile structure (Type II) Spread footings designed to rock	3
Hinging in raked piles in which earthquake load induces large axial forces	2
Locked in structure (T=0) Elastic structure	1

2.1.4. Europe

Many European countries have elevated risks of seismic activity, and several devastating earthquakes have struck the region, including earthquakes in Italy, Portugal and Greece (His12). Despite the long history of seismic activity in the region, interest in the development of a seismic design code is relatively recent (Elnashai, et al., 2008). For many years, different states held to their own design codes with varying degrees of seismic provisions for bridges. In 1975, there was a movement, made by the Commission of the European Community, to create a unified set of design codes, to reduce impediments to trade between countries and to homogenize the design codes of the region (CEN, 2002). These new codes would act as an alternative code for the Member

States of the European Union until they were adopted formally in all states. The first European codes, from this commission, appeared in the 1980s, but were hardly complete. Extensive research was conducted by different national sources in many labs throughout the member states, particularly in the field of earthquake engineering, to improve and expand the codes and make them comprehensive (Elnashai, et al., 2008). It is through this work that the current version of the European codes, *Eurocode 8*, has come to fruition.

The *Eurocode 8: Part 2* lists basic requirements for the seismic design of new bridges. One main requirement of the seismic design of bridges within the Member States is to avoid collapse after the design earthquake event and also allow for easy inspection and repairs after the event (Kolias, 2008). Another requirement is to minimize the amount of damage to secondary components of the bridge during events of high probability, though this requirement is assumed to have been met if criteria to accomplish the first requirement are followed.

Structures designed with this code are expected to have one of two behaviors during seismic loading: ductile behavior and limited ductile behavior (Kolias, 2008). Ductile behavior corresponds to values of the behavior factor between the range of 1.5 and 3.5, while limited ductile behavior has values of less than 1.5 for the behavior factor. The behavior factor is used to account for the nonlinear response for the structure and reduces the force determined from the linear analysis (CEN, 2004). Table 5 lists the maximum behavior factors associated with the different types of members of the bridge that are to be used in the linear analysis method described in the code.

Eurocode 8: Part 2 includes many prescriptions to accomplish the requirements mentioned above (Kolias, 2008). Criteria is listed for both linear and nonlinear analyses for ductile and non-ductile members, such as ensuring design rotation capacities are greater than the expected rotation demands. The design seismic action on the structures is determined based on an elastic design spectrum modified by such response indicators as the soil type and the behavior factor. The code specifies that several analysis types are

applicable for seismic design, and include linear analysis, modal analysis, static pushover analysis, and non-linear time history analysis. The code goes further to detail the design of structural members such as the joints, deck and foundation. *Eurocode 8: Part 2* is explicit and thorough in the detailing of the requirements to design a bridge that will perform satisfactorily under seismic loading.

Table 5: Maximum values of the behavior factor, q (CEN, 2002)

Type of Ductile Members	Seismic Behavior	
	Limited Ductile	*Ductile*
Reinforced concrete piers		
Vertical piers in bending ($\alpha_s \geq 3.0$)	1.5	3.5 $\lambda(\alpha_s)$
Inclined struts in bending	1.2	2.1 $\lambda(\alpha_s)$
Steel piers		
Vertical piers in bending	1.5	3.5
Inclined struts in bending	1.2	2.0
Piers with normal bracing	1.5	2.5
Piers with eccentric bracing	-	3.5
Abutments rigidly connected to the deck		
In general	1.5	1.5
Locked in structures	1.0	1.0
Arches	1.2	2.0

2.2. Caltrans Current Seismic Design Process

The current seismic design code available for bridges is the Caltrans Seismic Design Criteria (SDC) version 1.6 released in 2010 (Caltrans, 2010). The SDC specifies the minimum requirements for seismic design of bridges that go along with the performance goals for ordinary bridges. Within this document, it goes through the requirements for determining the demands and capacities of structural components, comparing the demand versus capacity, lists appropriate analysis methods of the structure, how to assess the seismicity of a site and the foundation performance, and details specifying design requirements to be met. Of particular interest to this project is the section dedicated to the design of the bridge. It has the requirements for frame design, superstructure, bent caps, joint design, bearings, columns and pier walls, foundations and

abutments. The first requirements are that the frame is balanced in terms of stiffness, mass and geometry. The SDC gives recommendations to follow to ensure a balanced frame, which is intended to increase the chance of the structure responding in the fundamental mode of vibration. This type of response may reduce the chance of producing a nonlinear response that cannot be modeled accurately. Balancing the fundamental periods between frames is also meant to reduce the relative displacements due to out-of-phase movements (Caltrans, 2010)

In the past, unseating of the deck from hinges or abutments was a source of major damage following large earthquake events. In the SDC, a minimum hinge seat width is specified as being greater than or equal to 24 inches to address that issue. The SDC lists equations used to determine the seat width of an internal hinge or abutment seat, which is based on thermal movement, prestressing effects, creep, and shrinkage in addition to earthquake displacements. Hinge restrainers are installed as a backup component at hinges to prevent unseating, but there is no method for design of these components, only guidelines. Pipe seat extenders can replace hinge restrainers if they provide vertical support beyond the hinge seat width. They are designed to withstand the induced moments under single or double curvature.

The Caltrans SDC goes on to list additional specifications to ensure proper performance at all bridge components. For bent caps, a section describes requirements for integral and non-integral bent caps. A section for superstructure joint design gives equations to ensure proper performance and proportioning of joints, and different requirements for t-joints and knee joints, as well as proper detailing for bent caps and joints. For the design of columns, not many directives are given. A suggestion is given to control the ratio of the column dimension to the superstructure depth to between 0.7 and 1.0. The SDC also gives the analytical plastic hinge length for different column types. Details for column flares were, mainly stating care should be taken to avoid a flare design

that would increase the seismic shear demand on the column. Other components addressed are bearings, foundation and pile performance, and abutment design.

As was demonstrated, current seismic design leaves little to be considered in terms of requirements for the capacity of many bridge components. Bridges designed today not only have to meet general bridge design requirements, but also have to make sure everything is designed to withstand an expected earthquake load. The flowcharts in Appendix A describe the steps that need to be taken to ensure a proper seismic design of a new bridge. The steps detailed in the flowchart are used by Caltrans design engineers to check the design of each bridge and ensure compliance with the SDC (Setberg, 2011). Each design check should be considered during the design process and after the design is complete. The design checks mostly deal with the relative stiffness of the structure, ductility of columns, and the structure displacement demand.

2.3. Closure

As is evident, the design provisions for bridges from around the world have many similarities and differences. All of the design codes have an objective for the design, one performance goal that must be met by following the provisions of the code. In California, Japan, and Europe, the objective is to design a bridge that will avoid collapse during a design earthquake event. In New Zealand, the objective is to maintain safety for emergency response vehicles after a design event. Each of the codes include design details of different components, criteria as to what analysis approach is allowed, design and response spectrum to determine seismic hazards, and specifications to account for varying local soil effects. These codes are consistently updated with new methods and techniques that arise in research or that address new issues that present themselves after major earthquakes. Through the years, these codes have improved to allow for a bridge design that is assumed to preserve life and provide safe passage for emergency response following an earthquake event.

With regards to the seismic design process in California, this chapter described the past and present bridge seismic design process along with important design checks to be employed during the design of the bridge. This process, however, does not provide the designer with critical information about specific performance of the bridge at a chosen design hazard level. It does not account for the uncertainty inherent in the capacity of the structure against collapse for a design event. Moreover, the current approach does not allow designers to determine the effects of design decisions on the performance of bridges. Fragility analysis determines the probability of a structure or system experiencing a seismic demand exceeding the structural capacity defined by a limit state (Hwang, et al., 2001). Fragility curves graphically show the performance of a bridge or bridge component at different ground shaking levels and at different damage levels. Thus, fragility analysis and fragility curves can be used to fill the gap of quantitative performance evaluation in the seismic design process. Later sections will describe how fragility can be used in the design process that will enable performance-based seismic design decisions.

CHAPTER 3

FRAGILITY ANALYSIS AND METHODS FOR BRIDGES

The hazard of earthquakes is widespread, as earthquakes occur several times daily in different locations of the world (USGS). Several earthquakes in the past have caused catastrophic damage due to the effects of earthquake ground motions, or the subsequent events of tsunamis, massive fires and landslides. There is very little scientists can do to predict future earthquakes and warn citizens to leave the area, which can be done with some other natural hazards. However, engineers can design and build structures to withstand an earthquake event or at least preserve the lives of those using the structures, as well as determine the expected the behavior of existing structures and lifeline networks during the event of an earthquake. In order to determine the expected performance of a structure during a seismic loading, earthquake engineers are able to use a tool called fragility analysis. Fragility analysis involves analyzing a structure to determine its preparedness to withstand certain ground motion intensities. This type of analysis has become extremely important in the earthquake engineering community in providing end users with information to assist in mitigating the effects of earthquake forces. Fragility curves have been developed and are used in earthquake-prone s to provide information about infrastructure performance and determine its expected performance during a likely earthquake, as well as assist agencies in making retrofitting decisions (Nielson, et al., 2007)(Shinozuka, et al., 2003)(Mackie, et al., 2005)(Padgett, et al., 2008).

Bridges are important to analyze because they serve as lifelines that connect roads and communities within a region, and are vital in an emergency situation because they allow disaster response teams to effectively travel to damaged areas. If several bridges are severely damaged during an earthquake, it could impede the recovery efforts tremendously and slow down the rescue and recovery process if emergency personnel

have to find alternative routes. Fragility analysis helps in pre-disaster planning because one can determine the probabilities of damage to any bridge due to a specified ground motion parameter and plan to lower the chances of severe damage to the bridge (via retrofit) or plan effective alternate routes in the case the bridge is damaged. Effective methodologies to create these fragility curves are constantly being researched. In this chapter, an overview of the evolution of fragility analysis is presented, as well as details of different approaches to develop a fragility curve of a structure. Following is a discussion on some of the methods used to estimate the fragility and how uncertainty is addressed in fragility analysis. Several applications and uses of fragility curves are given. The chapter concludes with an introduction to the bridges-specific fragility methodology that is presented in this thesis.

3.1. Background of Fragility Analysis and Methods

Seismic fragility curves are statistical functions that give the probability of exceeding a certain damage level or damage state as a function of a ground motion intensity measure. The fragility function can be written as $P[DS_i \mid IM=y]$, where $IM=y$ represents the ground motion intensity measure taking a particular value, and DS_i is the exceedance of the damage state in question. Fragility curves are tools used to assess and mitigate the effects of earthquake ground motions on structures, and their popularity was motivated by the development of earthquake loss models (Calvi, et al., 2006). Earthquake loss models were developed in response to the increasing losses in urban areas caused by earthquakes. One of the components of the loss model is the methodology to assess the vulnerability, or fragility, of a structure. The first seismic vulnerability assessment came in the 1970s in the form of damage probability matrices (DPM), developed using empirical methods that used past earthquake damage data. A DPM, shown in Table 6, displays the probability of a structure reaching or exceeding a damage state given a ground motion intensity, usually the Modified Mercalli Intensity (Cimellaro, et al., 2006).

26

Vulnerability curves, which came later, are very similar to DPMs. However they display the cumulative distribution of the probability of exceeding a damage state given a more continuous ground motion intensity measure, such as peak ground acceleration (Cimellaro, et al., 2006)(Calvi, et al., 2006). Many of the first fragility assessments were developed for nuclear power plant equipment and components because of the sensitivity of those structures to ground motions and the need for the contents to be protected from damage (Bandyopadhyay, et al., 1985)(Bandyopadhyay, et al., 1986). Today, more research has been done to create additional fragility methodologies and analysis types and to analyze many different structures, including bridges.

Table 6: Damage Probability Matrix (Cimellaro, et al., 2006)

Limit State	Modified Mercalli Intensity						
	VI	VII	VIII	IX	X	XI	XII
NONE	0.4						
SLIGHT	0.3	15.5					
LIGHT	9.3	84.5	88.4	28.9	1.4		
MODERATE			11.6	71.1	81.6	38.7	3.8
HEAVY					17.0	61.3	88.7
MAJOR							7.5
DESTROYED	--						
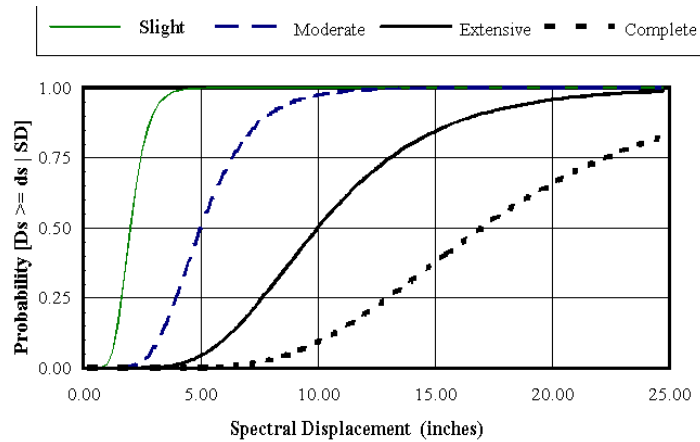
Figure 4: Fragility curves in HAZUS damage levels (FEMA, 2003).

There are four main approaches to developing fragility curves that are in use today, which are based on the origins of the damage data used in the generation of the curve. Early fragility curves were based on expert opinion (ATC, 1985) . In a literature review on the use of expert opinion in risk analysis, five basic principles were given that were meant to provide a consensus amongst the responses. The five principles are reproducibility of results, accountability of the sources of data, empirical control of an expert's assessments, neutrality of the expert's opinions to make sure they are consistent with the expert's actual views not swayed by any incentives, and finally, the principle of fairness employed to make sure that all opinions are regarded equally (Ouchi, 2004). These types of judgmental fragility curves are not limited to any particular damage or structural types; however the reliability of the information gained is difficult to quantify (Jeong, et al., 2007).

Empirical methods have been used to develop fragility curves in regions where extensive earthquake records are available, such as California and Japan (Nielson, et al., 2007) . Empirical curves are based on observed damage from past earthquakes. Shinozuka, et al, used empirical fragility curves in their analysis of Caltrans' bridges. Damage reports were used to establish the relationships between the damage states and the level of ground motion intensity. They used two-parameter lognormal distributions to develop the curves of the bridges which were broken up into several structural subsets, where each level subset was more homogeneous in content than the previous. Several methods were used to estimate the parameters, and the results compared well (Shinozuka, et al., 2007). These types of fragility curves tend to be the most realistic, but are very specific to a particular earthquake and structure and have limited applications (Jeong, et al., 2007).

Analytical methods are used to develop curves for bridges in regions where earthquake history records are not available, such as the Central and Southeastern United States (Nielson, et al., 2007) . Analytical curves are developed using distributions

simulated for an analysis of a structural model. Jeong and Elnashai proposed a new kind of analytical fragility framework by characterizing a response database and responses by fundamental values of stiffness, strength and ductility. In this way, they were able to avoid excessive analysis needed with traditional analytical fragility curves. The results were shown to be comparable with more rigorous analysis. Analytical curves are limited by computation efforts and may be calibrated to increase the accuracy by available observational data (Jeong, et al., 2007) .

Hybrid fragility curves combine data from different sources. These can be used to obtain more reliable curves because of the variety of sources of information (Jeong, et al., 2007) . Kappos, et al, developed a hybrid model combining a statistical approach and an analytical approach. They used existing damage data available for certain ground motion intensities, and supplemented that data with results of an inelastic dynamic analysis of structural models. This method made it possible to construct a damage probability curve in areas where limited empirical data is available. The use of analytical models in combination with empirical data allowed the author to construct more appropriate cost-benefit analyses. The authors also calibrated their models against data from a past earthquake, with which the models were consistent (Kappos, et al., 1998).

Fragility analysis and resulting curve definition has evolved throughout the years, from curves based on best engineering judgment and past damage data, to curves developed with simulated data and probabilistic formulations and a combination of many sources of data. The following sections will describe how uncertainty is addressed in the formulations used in the analysis and the different methods for estimating the fragility of structures.

3.2. Formulation of Fragility Estimation in Fragility Analysis

As discussed earlier in the chapter, the approach to fragility analysis and curves differs based on the type of structural response data that is available for the problem.

Beyond this initial decision on the analysis approach taken to complete the analysis, many more decisions await in order to complete a fragility analysis of a structure. One such consideration is the estimation of the fragility points. This section will highlight a few of the types of fragility estimation in use research literature for seismic fragility analysis.

3.2.1. Monte Carlo Simulation

Monte Carlo simulation techniques are used to generate random samples to simulate the uncertain behaviors of structures, materials and processes (Lemieux, 2009). While it is used often in seismic performance assessment to address the uncertainty in capacity and demand of a system and loading, some researchers have used the Monte Carlo method and simulation to directly develop fragility curves. Kafali and Grigoriu (2007) saw that the ground motion intensity measures used in recent studies may not be the best measures to use when performing fragility analysis and developing fragility curves for nonlinear systems. The authors thus proposed an alternative intensity measure based on two parameters, magnitude and distance from the seismic source, as a satisfactory intensity measure for nonlinear system. In their paper, this is demonstrated by assessing the performance of different oscillators and developing fragility surfaces with the proposed intensity measures. In order to develop those fragility surfaces, an algorithm developed using Monte Carlo Simulation was used. N samples of the ground acceleration process were generated from the seismic activity matrix defined for the region for each (m,r) pair. The system response was then calculated for each ground acceleration sample using a linear or nonlinear analysis method. Finally, the probability of failure for each (m,r) pair is approximated by taking the fraction of the number of structures whose response was greater than the limit state to the total number of samples. The fragility surface is created by plotting the approximated probability of failure on a 3D plot with magnitude and distance to source on the two horizontal axes, as shown in Figure 5. They

noted Monte Carlo method was more computationally expensive when creating fragility surfaces than with fragility curves where there was only one intensity measure to consider. Also, in comparing those fragility surfaces with ones created using the crossing theory, the authors noted that the crossing theory provided a more efficient method to developing fragility curves and was also accurate for systems with low fragilities.

(a)
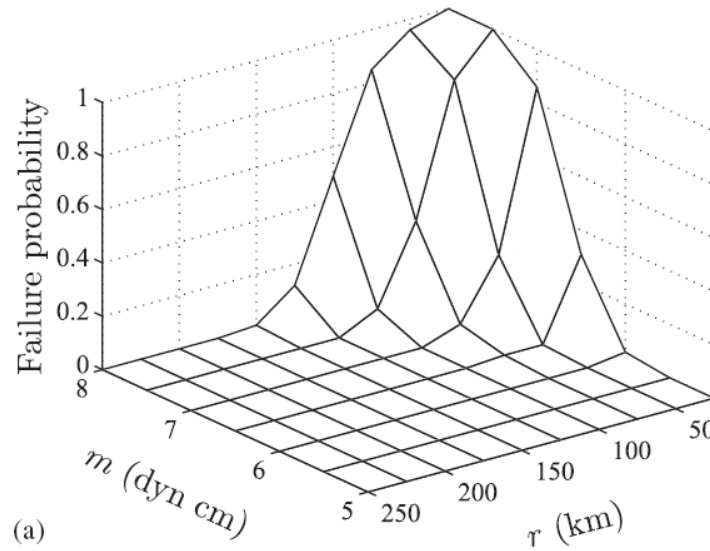
Figure 5: Fragility Surface for a linear system (Kafali, et al., 2007).

Lupoi, et al. (2004), developed a method to determine the seismic fragility of structures under nonlinear dynamic analysis. The probabilistic loading distribution would be established after the dynamic analyses and used along with a capacity model to solve the reliability problem of the structure. They propose a simple method of fragility analysis that addresses the aspects of reliability analysis, which include dependence between failure modes and uncertainty in the capacity of structures, among other things. The author arrives to Eqn. (3.1) to define the reliability problem. X in that equation includes all the basic variables of the problem along with capacity error and demand variability terms. The method presented by the authors was then compared to fragility estimates obtained by Monte Carlo simulation, the results of which are seen in Figure 6.

In comparing the proposed method results to Monte Carlo simulation results, he sets the simulation results as a standard to achieve or match, signaling the importance and reliability of Monte Carlo simulation techniques in fragility analysis.

$$P_f = Pr\left\{\bigcup_{j=1}^{n_c} \bigcap_{i\in I_{\in j}} C_i(x) \le D_i(x)\right\} \tag{3.1}$$
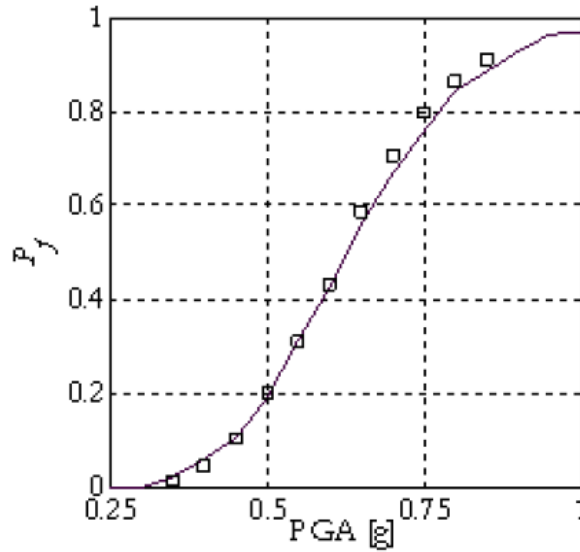
Figure 6: Comparison of results of fragility analysis with Monte Carlo (Lupoi, et al., 2004).

Smith and Caracoglia (2011) developed a method to creating fragility curves for tall buildings under turbulent wind loading. Wind loading, like seismic loading, carries uncertainty in loading like seismic loading, and in this case the authors created fragility curves based on similar principles in earthquake engineering to do a performance-based assessment of the structure. A Two-Step Monte Carlo Algorithm was presented that involved using Monte Carlo methods to compute power spectral density of the buffeting force and to derive statistical information on the response of the structure, while accounting for uncertainty in the loading. The authors conclude that the results of the proposed algorithm shows potential for future more realistic applications of the method

for computing fragility curves under wind loading. While Monte Carlo simulation techniques have been used to derive fragility curves and provides information on the uncertainty included in the analysis, some research suggest that the Monte Carlo technique may be too computationally expensive and not practical for real-life applications (Faravelli, 1989). Thus, there are other techniques in use for developing accurate and efficient fragility curves.

3.2.2. Lognormal Distribution

The use of the lognormal probability distribution is prevalent in probabilistic seismic analysis. It is used to describe the distributions of different material properties, define the parameters used in creating fragility curves, and in the determination of the fragility estimation itself with a two-parameter lognormal formula. Kennedy, et al. (1980), conducted a study in order to develop a rational approach to determining the earthquake-induced probability of failure for US nuclear power plants along the East Coast. The authors also quantified uncertainty of the parameters in the calculations by including confidence bounds with the fragility curves. In order to accommodate the case where limited damage test data was available to formulate fragility estimates and where engineering judgment would need to be applied, the authors developed a simplified procedure that required only three parameters: an estimate of the median ground acceleration capacity, and the logarithmic standard deviations of the lognormally distributed random variables that represent the inherent randomness about the median and the uncertainty in the median value. The authors justified the use of the lognormal distribution by stating studies have shown the distribution represents many structural materials and response variables well given the extreme tails of the distribution is not of a concern, adding that for probabilities greater than one percent the distribution can be used reasonably. The final fragility curve is described with these parameters using the standard Guassian cumulative function.

Goodman (1985) discusses the principle of maximum entropy for use in determining the best type of density function to formulate fragility estimations. The author discusses the distributions in use in research literature, and discloses that the lognormal distribution is better in structural fragility applications than a normal distribution, but there is still an issue with values in the extreme tails of the distribution. One way of addressing this issue is to confine the resulting fragility curve between minimum and a maximum acceleration values. The author concludes that the use of the lognormal distribution in fragility formulations is best when the failure parameter, usually a characteristic of the ground motion, is positive, using the principle of maximum entropy.

Hwang and Jaw (1990) present a probabilistic damage analysis procedure that can be used to develop fragility curves for different structures. The authors presented an analytical fragility analysis that includes the uncertainties present in structural modeling as well as earthquake ground motion modeling. The formulation presented to develop the fragility curves is that relates the structural response (S) and the structural capacity (R). Eqn. (3.2) shows the probability of failure as it relates to response and capacity. When the response and capacity are both lognormally distributed, the probability of failure can be defined with a two-parameter lognormal formulation, shown in Eqn. (3.3). The benefits of this approach are that the uncertainties can be included in the lognormal parameters, and that structural response is included in the fragility estimation.

$$P_f = P_F(R \leq S) = \int_0^\infty [1 - F_S(r)] f_R(r) dr \qquad (3.2)$$

$$P_f = \Phi \left[\frac{-ln\left(\frac{\mu_R}{\mu_E}\right)}{\sqrt{\beta_R^2 + \beta_E^2}} \right] \qquad (3.3)$$

Shinozuka, et al. (2003) used statistical analysis to present methods of developing empirical and analytical bridge fragility curves. The authors utilized a two-parameter lognormal distribution function that has been traditionally used in fragility construction

promulgated by risk assessment methods for nuclear power plants in the 1970's. The two parameters used in the calculation of the fragility curve represent the median and log-standard deviation of the curves for a particular damage state, and were estimated with the maximum likelihood method. Eqn. (3.4) shows the formula used to estimate the fragility, where c and ζ are the parameters to be estimated, and a is the ground motion intensity measure used in the formulation. The study presented by the authors presented two methods of parameter estimation, one of which being a method to simultaneously estimate parameters for a set of fragility curves with different damage states.

$$F(a) = \Phi\left[\frac{ln\left(\frac{a}{c}\right)}{\zeta}\right] \tag{3.4}$$

Nielson and Desroches (2007) also worked under the assumption that the structural response, or demand, and the capacity could be described with the lognormal distribution. The authors developed fragility curves for highway bridges with a component level approach, recognizing that most fragility curves of bridges were based on the response of the column only. They saw that neglecting to include other components in the fragility calculations could result in inaccurate bridge system level fragility. Using a relationship between the median demand (S_d) and ground motion intensity measure (IM) presented by Cornell, et al. (2002), allowed the authors to develop a probability distribution. Eqn. (3.5) shows the power model used to create the distribution, or probabilistic seismic demand model (PSDM). The PSDM along with the capacity distribution can be convolved and input into Eqn. (3.4) to develop analytical fragility curves. The authors' component level approach to creating bridge fragility curves show that the bridge system is more fragility than any individual component and that using only one component to represent the system fragility would result in an underrepresentation of the vulnerability.

$$S_d = aIM^b \tag{3.5}$$

The lognormal distribution and lognormal distribution functions have a significant influence in the research of fragility analysis. Lognormal distributions are often used to describe parameters, materials or structural responses that are then used in the fragility formulation. The use of two-parameter lognormal distribution functions are also prevalent in order to formulate the probability of failure based off of lognormally distributed demand and capacity variables. A major setback of using the lognormal distribution is inaccuracy of using values in the extreme tails of the distribution.

3.2.3. Logistic Regression

Logistic regression is used to find the best fitting model that describes the relationship between an outcome or response and a set of predictor variables (Kutner, et al., 2005). In fragility analysis, it is used as a way to calculate the probability that an event occurs, such as collapse or another limit state. Several researchers in the past have used this particular regression formula to calculate and create fragility curves. Basoz and Kiremidjian (1998) used logistic regression analysis in the creation of empirical fragility curves from damage data from the Loma Prieta and Northridge earthquakes in California. For their analysis, logistic regression was used to determine the effect of several independent variables, such as PGA values, span length of bridge, skew angle, soil type and design year among other attributes of the bridges. Analysis on the effect of these variables on the response variable was then conducted to determine the significance of each independent variable on the outcome of the model. The most significant variables were then used to group bridges in order to determine fragility curves based on the estimated PGA values due to the earthquake event. The authors produced empirical fragility curves in this manner for bridges damaged in the Loma Prieta and Northridge earthquakes based on different sub-categories and design attributes.

O'Rourke and So (2000)developed fragility curves for on-grade steel liquid storage tanks, which are important components in the lifeline systems of different liquids,

such as water and fuel. They developed fragility curves to represent the seismic vulnerability of the tanks that is needed in order to estimate the potential losses that could occur during an earthquake. The authors used logistic regression analysis to create the fragility relationships from existing damage data available from past earthquakes and observations. These empirical fragility curves were based only on the peak ground acceleration, and represented the probability that a damage state would be achieved or exceeded as a function of PGA. The authors used damage states that closely corresponded to the ones presented in HAZUS. In comparison to the fragility relationships developed by HAZUS, the authors' approach suggested that actual tank performance was better than indicated in HAZUS.

Baker and Cornell (2005) developed fragility curves with a vector-valued intensity measure instead of the traditional scalar intensity measure. They incorporate epsilon, an indicator of spectral shape, along with the spectral acceleration value in order to more accurately predict the responses of the structure they analyze. In order to more accurately predict the probability of collapse they use logistic regression. An indicator value is used to indicate the state of the structure, with 1 meaning the structure collapsed and 0 meaning it did not collapse. They suggest that in order to prevent unstable results from few data points in either extreme, the probability of collapse should be taken as a simple fraction of 1/n or 2/n for n records in question for 1 or 2 collapse data points. In reverse, they suggest using the converse for data sets with all data points representing a collapse state except for 1 or 2 data points.

Koutsourelakis (2010) presented a framework in which the seismic vulnerability of a structure can be estimated. The author uses a Bayesian framework in order to develop fragility curves regardless of the amount of data available to work with. The author uses logistic regression to estimate the fragility relationships of any structure in order to incorporate more characteristics of the earthquake ground motion, since no one measure of the seismic action can fully characterize any ground motion. This led to a

multi-dimensional fragility surface that can improve the accuracy in predicting damage for the structure. The earthquake intensity measures studied in the paper included peak ground acceleration, or root-mean-square intensity, Arias intensity, and the power of the excitation spectrum. Using the logistic regression analysis, the author discovered that the Arias intensity measure better predicted the structural damage than the PGA value or root-mean-square intensity measure.

These examples of logistic regression used in fragility estimation are just a few in a growing trend of exploring this useful regression tool in the realm of seismic vulnerability and loss estimation.

3.3. Uncertainty in Fragility Analysis

Uncertainty modeling and estimation in fragility analysis is an important topic that needs to be addressed in the analysis in order to ensure a reliable vulnerability of the structure. The risk due to uncertainty must be mitigated and kept within acceptable levels, as all uncertainty is impossible to eliminate. There are two types of uncertainty: aleatoric and epistemic. Aleatoric uncertainty includes factors that are inherently random, and usually cannot be avoided. Epistemic uncertainty comes from a lack of knowledge, and can be reduced depending on the amount and quality of information you introduce into the problem (Wen, et al., 2003). Both types must be considered when modeling or performing a fragility analysis. For a structural system analyzed under earthquake loads, uncertainty comes from the demand and capacity of the analysis (Ji, et al., 2007). The uncertainties from the demand on a system comes from the ground excitation, which includes the soil conditions, load path of the motions, and the random motions generated from the source of the quake. The uncertainty from the capacity of the system can emanate from the material and geometric uncertainty, where the properties of the designed structure and materials are considered random for the built structure. Figure 7shows the uncertainty sources in chart form.
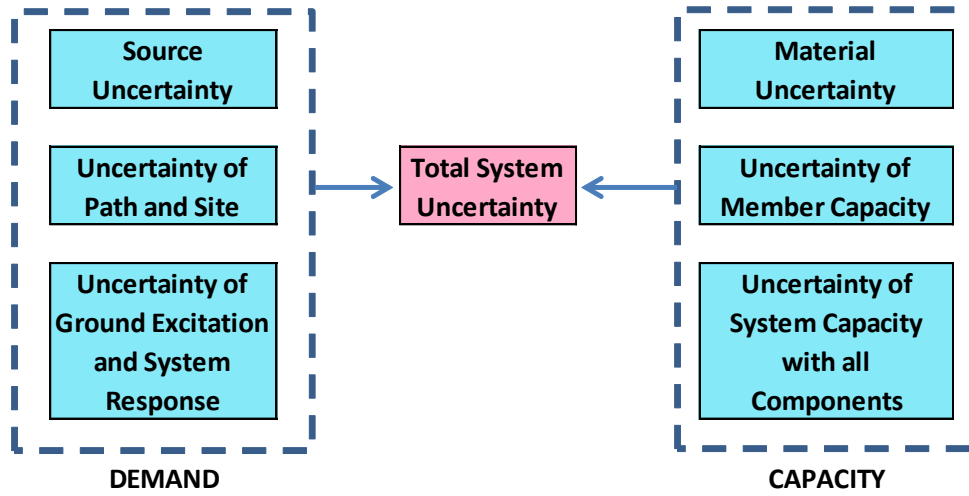
Figure 7: Chart of uncertainty found during analysis(Ji, et al., 2007)

Researchers have figured out ways to account for these uncertainties and mitigate the effects in their results. For the uncertainty in ground motions, it has been found that it is best to include many records of ground motions to cover as many frequencies and seismic energy levels as possible(Ji, et al., 2007). This is important for very complex structures, such as high-rise buildings, because these structures have many modes in which they respond to loading. The number of records needed to produce an accurate fragility analysis is not well defined (Cimellaro, et al., 2009), however it has been shown that the number of required records reduce as more constraint on the scaling and matching of accelerograms is applied (Hancock, et al., 2008).

From the capacity of the system, uncertainty can stem from the material properties used and the geometry of the structure. To account for the variability within the material strengths of a structure, it is common for a developer to model those strengths as random variables (Ji, et al., 2007)(Nielson, et al., 2007). Much of the variability can be taken from past research and experiments finding the distributions of material strengths. In his research of common bridge types, Nielson and DesRoches (2007) also took into account many other uncertainties in the modeling, including the

stiffness in abutment and foundation, and damping ratio. Those distributions also were found in past research.

Uncertainty can also come from damage states that one uses in developing fragility curves. HAZUS (2003) accounts for the variability of each damage state with a parameter β_{Sds} for structural components and β_{NSDds} for nonstructural components. The variability parameter for structural components, β_{Sds}, includes three contributors to variability; uncertainty in damage state threshold, variability in capacity properties of the building type, and variability in response due to variability of ground motion (demand). Eqns. (3.6) and (3.7) show how the parameter is formulated and how the parameter is included in the formula of fragility as addressing the issue of uncertainty in damage states.

$$\beta_{Sds} = \sqrt{\left(CONV[\beta_C, \beta_D, \bar{S}_{d,Sds}]\right)^2 + (\beta_{M(Sds)})^2} \tag{3.6}$$

$$P[ds|S_d] = \Phi\left[\frac{1}{\beta_{ds}} ln\left(\frac{S_d}{\bar{S}_{d,ds}}\right)\right] \tag{3.7}$$

With all of the uncertainty in the demand and capacity components of the fragility analysis, uncertainty of the fragility estimate itself is worth investigating and quantifying. Kim, et al. (2011), present an uncertainty analysis of the system fragility, which is an important step in seismic risk evaluation of a structure. Uncertainty analysis produces confidence intervals for fragility curves that provide the user an idea of the accuracy of the fragility estimation. Two methods were investigated, one utilizing Monte Carlo simulation where in order to draw an unbiased estimate of uncertainty, and sufficiently large sample size of random samples of component fragility is required. The other method utilizes the Latin Hypercube sampling method, indicating that the distribution of the system fragility is well distributed and thus requires fewer samples than the Monte Carlo method.

The inherent and random uncertainty present in many of the components of fragility analysis, including the final fragility curves, is critical to quantify and control. An understanding of the uncertainty is necessary for the successful application of the fragility curves to seismic risk mitigation strategies.

3.4. Introduction to Bridge Specific Fragility Method (BSFM)

One of the main products of this research is a methodology for fragility analysis of bridges that includes geometric design parameters in the creation of the probabilistic seismic demand model of the analysis problem. The fragility methodology presented in this thesis is a type of analytical fragility process rooted in a simulation based approach. Analytical bridge models will be analyzed with time history analyses using the Baker et al. ground motion suite (2011), a suite of ground motions that is applicable to a range of sites and structural properties. Once the analyses are done on the bridge models using the suite of ground motions, the responses of each bridge component are collected, and analysis on that data can be performed using the new fragility method of this report. A graphical overview of the typical analytical method is given in Figure 8.

One of the other main outcomes of this research is the implementation of a design support tool. Employing the aforementioned bridge specific fragility methodology, this tool is meant to be used by design engineers as a final design check for the seismic design of bridges. With this tool, an engineer can determine if their design meets certain standards of seismic load resistance based on a fragility analysis. To develop this tool for applicability to specific bridges under consideration, the fragility curves must be developed that are specific to the design bridge, as opposed to fragility curves developed for a general class of bridges. This would not be possible using the current method of developing a PSDM using a 2 parameter lognormal relationship between a response quantity and a ground motion intensity measure, as currently used by many researchers. Additional parameters relating to the specific bridge must be included. The details of this

41

fragility methodology, geometric design parameters and the design support tool will be fleshed out over the subsequent chapters.
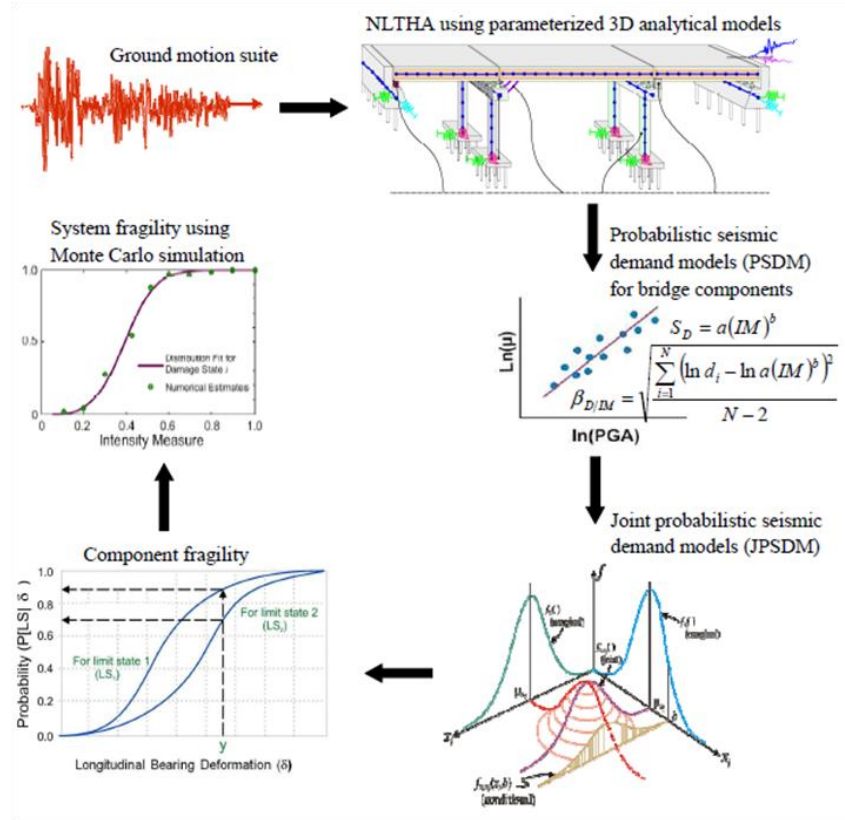
Figure 8: Graphical overview of analytical fragility analysis framework (Ramanathan, 2012).

CHAPTER 4

COMPONENT LIMIT STATES AND GROUND MOTION IN FRAGILITY ANALYSIS

The capacity model and selection of ground motion suite are important elements of the analytical fragility analysis method. The capacity model, consisting of limit states which define the quantitative threshold values for different damage conditions, is important to define specifically for the structure type and expectations of the performance of the structure. The ground motion suite is intended to be representative of the seismic hazards in the region of interest. The ground motion suite also adds variability to the responses of the analytical models necessary to provide accuracy to the fragility estimation. This chapter gives a history of limit states used in bridge fragility analysis as well as the Caltrans aligned limit states developed for this particular project. Then, an overview of the use of ground motions in fragility analysis is given, and the ground motion suite used in this thesis is presented.

4.1. Limit States

4.1.1. Bridge Damage States in fragility analysis

Damage states in fragility analysis are select levels of damage that a bridge system or component might experience during seismic loading. Figure 9 shows levels of damage a bridge column might undergo based on field observations after an earthquake event (Shinozuka, et al., 2003). Also called limit states, damage states are an important part of the capacity model used to develop fragility curves. Often, limit states are defined as discrete threshold quantities of a component response that corresponds to a physical damage condition (Mackie, et al., 2005).
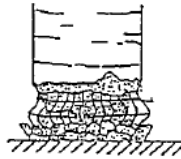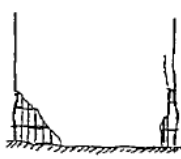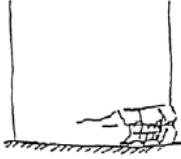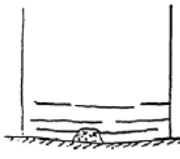
Damage State / Damage Mode	As	A	B	C	D
1. Bending Damage at ground level (This mode ultimately produces buckling of rebar, spalling and crushing of core concrete)	Damage through entire cross-section	Damage mainly at two opposite sides	Damage mainly at one side	Light cracking and partial spalling	No Damage

Figure 9: Description of States of Damage for Hanshin Expressway Corporation's Bridge Columns (Shinozuka, et al., 2003)

The damage states used in fragility curves have traditionally been the following four levels: Slight, Moderate, Extensive, and Complete (Table 7)(Choi, et al., 2004). The (N) damage level is usually not included in fragility analysis. These four categories apply to a particular component of the bridge being analyzed, such as the columns, footings, and abutments. Many fragility curves have focused on the response of one component, such as the drift of a column, to indicate the state of a bridge after an earthquake event. However, the responses of other major bridge components have emerged as significant elements in determining the fragility curve for the entire bridge (Nielson, et al., 2007);(Padgett, et al., 2008)(Shinozuka, et al., 2007). While including the effects of other component states on the bridge functionality is important, finding equivalent measures of loss due to damage between components is a challenge. For example, extensive damage in a column of a bridge may lead to a longer bridge closure and more repair costs than extensive damage in a bearing. This challenge is addressed later in this section with the discussion of Caltrans-aligned limit states.

To determine the damage level of a particular component, quantitative assessments may be in place for each component being inspected. For columns, it could be displacement or rotational ductility. For bearings, damage may be assessed by measuring the displacement of the bearing or deck from its original position. Often, the

44

engineer must rely on his or her judgment to visually inspect the components and relate a damage level based on experience and the description above. Therefore, if a bridge were inspected by different engineers, the results of the inspection and corresponding damage states may vary. Quantitative damage states directly affect fragility analysis, as they are used as the basis of the capacity model. Uniform damage states that are used for fragility analysis, particularly for specific regions of the country where bridge types and hazard levels are similar, could allow for uniformity and more confidence in the use of the resulting fragility curves.

Table 7: Damage States Commonly Used from Hazus (FEMA, 1997)

Damage States	Description
(N) – No Damage	No damage to a Bridge
(S) – Slight Damage	Minor cracking/spalling to abutment, cracks at hinges, minor spalling at column, or minor cracking to the deck
(M) – Moderate Damage	Moderate cracking and spalling at column, moderate settlement of approach, cracked shear keys or bent bolts at connection
(E) – Extensive Damage	Degraded column without collapse, some lost bearing support in connection, major settlement of approach
(C) - Complete Damage	Collapsed column, all bearing support lost in a connection, imminent deck collapse

4.1.2. Bridge limit states used in past research

Many different limit states have been used in probabilistic analysis of bridges in research. Elnashai, et. al, (2004) used displacement capacity of the bridge pier to define the limit states at slight, moderate, extensive and complete. Capacities were determine using static inelastic pushover analyses on a finite elements model of a bridge. Mackie, et. al (Mackie, et al., 2008), utilized maximum column drift damage states at four levels of damage, spalling strain to measure deck damage at three levels, and bearing damage with two levels of damage to perform a probabilistic evaluation on California bridges. These damage states, represented with median and dispersion value, are shown in Table 8 Table 9, and Table 10, and show that not all limit states fit into the mold of 4 levels as

described earlier. Shinozuka, et. al (Shinozuka, et al., 2003), developed empirical fragility curves based on damage data collected after the Northridge earthquake in California. Figure 9was used as the basis to define the damage states. The resulting fragility curves were then defined at levels such as "at least minor damage", "at least moderate damage", and so on. The bridge sample was divided in these damage states based on field observations and reports (Shinozuka, et al., 2003).

Table 8: Example of column damage states (Mackie, et al., 2008)

	Damage state limit description	λ	β
DS0	Negligible damage with initial cracking	0.23	0.30
DS1	Cover concrete spalling	1.64	0.33
DS2	Longitudinal reinforcing bar buckling	6.09	0.25
DS3	Column failure	6.72	0.35

Table 9: Example of deck damage states (Mackie, et al., 2008)

	Damage state limit description	λ	β
DS0	2% of spalling strain	0.00402	0.40
DS1	25% of spalling strain	0.00425	0.40
DS2	50% of spalling strain	0.00450	0.40

Table 10:Example of bearing damage states (Mackie, et al., 2008)

	Damage state limit description	λ	β
DS0	Bearing yield	0.076	0.25
DS1	Nearing failure	0.152	0.25

Many previous researchers focused on the response of the column to define the state of the bridge system. However, the response of other components in a bridge has been determined to have a significant effect in the development of fragility curves for bridges (Choi, et al., 2004)(Nielson, et al., 2007)(Padgett, et al., 2008). Damage states have been defined for components such as steel bearings, elastomeric bearings, and abutments (Choi, et al., 2004)(Nielson, et al., 2007). Component fragilities are found

analytically and have been combined into system fragilities using a first order series approach (Choi, et al., 2004) and by integrating failure domains of joint PSDMs with Monte Carlo Simulations (Nielson, et al., 2007)(Padgett, et al., 2008). Table 11 shows different damage states for certain bridge components. The damage states are defined with ranges of values for each component.

Table 11: Example of multiple bridge components and limit states (Choi, et al., 2004)

Damage State	Slight damage	Moderate damage	Extensive damage	Complete damage
Columns (μ)	$1.0< \mu<2.0$	$2.0< \mu<4.0$	$4.0< \mu<7.0$	$7.0< \mu$
Steel Bearings(δ, mm)	$1< \delta<6$	$6< \delta<20$	$20< \delta<40$	$40< \delta$
Expansion Bearings (δ, mm)	$\delta<50$	$50< \delta<100$	$100< \delta<150$	$150< \delta<255$
Fixed Dowels (δ, mm)	$8< \delta<100$	$100< \delta<150$	$150< \delta<255$	$255< \delta$
Expansion Dowels (δ, mm)	$\delta<30$	$30< \delta<100$	$100< \delta<150$	$150< \delta<255$

4.1.3. Caltrans Specific Bridge Limit States

As the fragility methodology presented here involves multiple components, one objective of the project is to compile compatible limit states that were specific to the Caltrans bridge inventory. Compatibility was needed in terms of similar damage and downtime consequences after an earthquake event. As this was not available in current literature, expert opinions from Caltrans design engineers and maintenance personnel combined with experimental test data of components were used to develop Caltrans specific limit states (Roblee, et al., 2011). Individual component damage thresholds and a method to determine the overall bridge system state based on primary and secondary component damage states were developed. One of the goals of developing this new damage state definition was to coordinate what inspectors see in the field with what engineers see in their analysis. Table 12 shows the component damage threshold (CDT) continuum. As is shown, every time a damage threshold is crossed, the component is expected to have a different level of visible damage, and thus a different repair strategy. Table 13 describes the Caltrans-specific bridge limit state definition framework. The bridge damage states are closely tied with the ShakeCast inspection priority levels. This

makes it easier to relate inspection criteria with engineering performance expectations. The chart also equates bridge damage states with traffic implications. Using the component continuum and bridge system damage states, the project team determined appropriate damage levels using engineering demand parameters that would be easily monitored during an analysis of a bridge model.

Table 12: Caltrans component level damage continuum.

Component Damage Thresholds	Component Level Damage Continuum			
	CDT-0	CDT-1	CDT-2	CDT-3
Component Damage Range	No Damage	Aesthetic Damage	Repairable Minor Functional Damage	Repairable Major Functional Damage	Unrepairable Damage – Component Replacement

Table 13: Caltrans bridge system damage states.

ShakeCast Inspection Priority Levels	None	Low	Medium	Medium-High	High
Bridge System States	*BSS-0*	*BSS-1*	*BSS-2*	*BSS-3*	*BSS-4*
Inspecting for possible ...	*No Bridge Damage*	*Slight Bridge Damage*	*Moderate Bridge Damage*	*Extensive Bridge Damage*	*Complete Bridge Damage*
Component Damage Range					
Primary Components	Below CDT-0	CDT-0 to CDT-1	CDT-1 to CDT-2	CDT-2 to CDT-3	Above CDT-3
Secondary Components	Below CDT-0	CDT-0 to CDT-2	Above CDT-2	NA	NA
Likely Immediate Post-Event Traffic State	Open to Normal Public Traffic – No restrictions	Open to Normal Public Traffic – No restrictions	Open to Limited Public Traffic – Speed/Weight/ Lane restrictions	Emergency Vehicles Only - Speed/Weight/ Lane restrictions	Closed (Until Shored/Braced) – Potential for Collapse
Traffic Operations Implications					
Closure/Detour Needed?	Very Unlikely	Very Unlikely	Unlikely	Likely	Very Likely
Traffic Restrictions Needed?	Very Unlikely	Unlikely	Likely	Very Likely	Very Likely - Detour
Emergency Repairs Implications					
Shoring/Bracing Needed?	Very Unlikely	Very Unlikely	Unlikely	Likely	Very Likely
Roadway Leveling Needed?	Very Unlikely	Unlikely	Likely	Very Likely	Very Likely - Detour

To relate bridge system performance with component performance, components are categorized into primary and secondary components. Primary components are those that create the risk of causing the bridge to collapse if they fail, indicated by surpassing the CDT-3 threshold. In conjunction with Caltrans engineers and bridge inspectors, two primary components were identified: columns and hinge openings (Roblee, et al., 2011). The failure of either of these components during an earthquake would likely lead to the collapse or inoperability of the bridge. Secondary components are defined as those components that affect the performance of the bridge following an earthquake event, but will not cause the bridge to collapse even at the highest component damage threshold. For this bridge type, that includes the displacement of the joint seals and the bearing displacement. The project team determined that bridges in the state inventory could have components with different properties based on the year that it was designed (Sahs, et al., 2008). Thus, there are several performance groups for each component. For example, under the column component, the different performance groups include a brittle column, strength degrading column, and ductile column. As the focus in this research is on newly designed bridges, only the performance groups associated with the latest design standards are considered for the limit states. In Table 14, the primary and secondary components used for the capacity model for this bridge-specific project along with the engineering demand parameter (EDP) of the components used and the CDT values are listed.

Table 14: Primary and secondary component and corresponding limit states.

	EDP* for CDT's	CDT-0	CDT-1	CDT-2	CDT-3	Lognormal Dispersion
Primary Components						
Ductile Column	Curvature Ductility ($\mu\varphi$)	1	4	8	12	0.35
Hinge opening, >24" seat joint at abutment, small gap	Joint displ (in)	1	3	14	21	0.35
Secondary Components						
Sealed Joints, type B	Joint displ (in)	1	n/a	n/a	n/a	0.35
Elastomeric Bearings	Joint displ (in)	1	n/a	4	n/a	0.35

4.2.   Ground Motions

4.2.1. Importance and Use of Ground Motions in Fragility Analysis

In developing analytical fragility analysis, the importance of selecting the appropriate ground motions is paramount. Kwon and Elnashai show that for different ground motion sets that had different characteristics, the resulting fragility curves varied greatly for the same structure, indicating careful consideration in ground motion selection for fragility analysis is very important (Kwon, et al., 2006). The characteristics of the input ground motion suite affects the outcome of fragility curves more than material variability or even limit state definition (Padgett, et al., 2008). Therefore, significant consideration is needed when selecting ground motions. Having variety in the characteristics of ground motions, such as frequency content, phase, and duration, is important as the structural response of a bridge can differ even between ground motions that have similar peak ground acceleration or peak ground velocity values (Karim, et al., 2001). When analyzing bridges, it is also important to choose ground motions applicable to the site location in which the bridge may be designed.

There are many things to consider when selecting a suite of ground motions for the dynamic analysis of structures. Earthquake loads represented by acceleration time histories have to be selected so that the seismicity of the region is accounted for and have to correspond to an expected or design earthquake in the region of interest (Katsanos, et al., 2010). In past research in earthquake engineering, different selection criteria have been used to select ground motions for analysis purposes (Katsanos, et al., 2010). These criteria include moment magnitude, distance from source of earthquake, soil conditions at the site, duration of the strong ground shaking, seismological features of the site, matching to defined target spectrum of the region, among other criteria. Important in the design process when a dynamic analysis of the structure is performed, acceleration time histories are selected that correspond to the design earthquake event prescribed in the

50

design code and represent the seismicity of the area. The most common parameters that represent earthquake motions are the magnitude and distance from the site to the rupture zone, known as the (M, R) pair. Many ground motion selection processes use this pair as the main criteria, however it has been reported that these characteristics of the ground motions used in dynamic analyses doesn't have a significant effect on some particular structural responses or post-damage index (Iervolino, et al., 2005). However, the (M, R) pair remains a common criteria used in choosing ground motions. Characteristics of the soil profile at the site of the structure are often considered in the selection of appropriate ground motion records. The soil profile can be represented by the shear-wave velocity of the first 30 m of soil at the site, denoted as $V_{s,30}$, or by site classifications based on soil categorization schemes (Katsanos, et al., 2010). Adding soil profile characteristics to the selection criteria may reduce the number of records available for use. The duration of time histories has also been used to select ground motions, however the duration of ground motions have been shown to affect energy-based damage measures more significantly than displacement-based response measures (Iervolino, et al., 2006). Another hindrance to duration as selection criteria is the many ways by which duration is defined. Nonetheless, duration is seen as a characteristic that is worth included in the selection process (Malhotra, 2003). These and other criteria have been used in the selection process of ground motions for seismic analysis, and also apply for generating synthetic ground motions that match the expected hazard of an area for regions where sufficient recorded motions are not available.

Research has shown that when analyzing bridges in order to perform fragility analysis, the selection of the ground motions will be dependent on the target of the analysis. For example, ground motions used for analysis may depend on the type of bridge, whether the analysis is for a class of bridges or for a deterministic bridge, the hazard in the region of the bridge, among other considerations. Shinozuka, et. al (2000), analytical bridge models that were representative of bridges in the Memphis area were

51

analyzed with generated time history records based on magnitude and epicentral distance pairs. A total of 80 generated time histories by Hwang and Huo were based off of scenario earthquakes in the area similar to an earthquake that occurred in the 19th century (Shinozuka, et al., 2000). Working with the same region, Nielson and Desroches (2007) also used synthetic ground motions when performing fragility analysis on highway bridges common to the Central and Southeastern United States. The suite of ground motions used in their analyses were chosen from bins generated by Rix and Fernandez-Leon, which included three different moment magnitudes and four hypocentral distances, were developed specifically for the soil profile typical in Memphis. As for research on bridges in California, a comparatively large database of real ground motion records are available to choose for analysis. Mackie and Stojadinović (2005) used a bin approach of choosing appropriate ground motion for the analysis of highway overcrossings. The bin approach involves choosing from bins that differentiate between earthquake records that have certain similarities, such as bins that separate near-field records from far-field records. Four bins of 20 ground motions each were obtained from the PEER Strong Motion Catalog and again the ground motions were separated and chosen based on magnitude and distance pairs for a particular soil type (Mackie, et al., 2005). From the work of these researchers, it is clear that magnitude, distance, and soil type are important to consider when choosing ground motions for use in fragility analysis of bridges. The following section details the characteristics of the ground motion suite chosen for the analysis of this research.

4.2.2. Suite Used In Bridge Specific Fragility Method

For the project for which this research was conducted, Caltrans has chosen to adopt the Pacific Earthquake Engineering Research Center (PEER) Transportation Research Program ground motions developed by Baker, et al. (2011). Their work focused on providing a new selection procedure that allows for better matching of target response

spectra quantities, as well as providing a standardized ground motion set that was applicable to many scenarios throughout California. These motions were not developed as structure-specific or site-specific, and so are applicable to many research needs and can be tailored to fit individual user needs through pre-processing (i.e. scaling of motions) or post-processing (i.e. finding regression relationships between response of models and ground motion measure) of the ground motion characteristics (Baker, et al., 2011). Baker, et. al, describe the algorithm they developed that was used to select ground motions for this project, which can select a set of ground motions that has response spectra with a specific mean and variance. Using the approach they outline in the report, four sets of ground motions are chosen for use in PEER research application, and are shown in Table 15. The first set, Set #1, broken up into two subsets (1a and 1b), consists of broad-band ground motions that would be expected for moderate strike-slip earthquakes at short distances at a soil site, with a shear wave velocity of 250 meters/second. The second set, Set #2, consists of broad-band ground motions that would be expected for moderate strike-slip earthquakes at short distances as well, except this time the ground motions were chosen for a rock site, with a shear wave velocity of 760 meters/second. The third set, Set #3, consists of ground motions that had strong velocity pulses occurring in the strike-normal direction, representing near near-fault ground motions. There is another set presented in their research specific to the site of a bridge in Oakland, CA, however, this set will not be used in the analysis presented in this dissertation.

Each set has 40 unscaled ground motions selected from the PEER Next Generation Attenuation (NGA) project database (Chiou, et al., 2008) to match the terms of the set. All 160 ground motions will be used unscaled as well as scaled by a factor of 2 in the final analyses for this project, as variability in ground motion characteristics was determined to be needed to account for the unknown site locations of designed bridges (Roblee, et al., 2011). The total number of ground motions used in the analysis of the

bride models was 320. Response spectra are shown for Sets 1a, 1b, and 2, and a histogram of peak ground velocities is shown for Set 3 in Figure 10 and Figure 11. Again, this suite of ground motions was chosen because of the flexibility in terms of the suite being structure-independent and site-independent, but also the ability to cater the ground motions to the specific project through pre-processing (i.e. scaling) or post-processing of the results of analysis. The suite was also created for the region that is applicable for the research presented here. The suite also covers a range of possible seismic action that could occur in the state of California. For these reasons, this suite was chosen for this research and the corresponding project.

Table 15: Characteristics of ground motions in PEER ground motion suite.

Set 1a	Broad-band motions, Magnitude 7, R=10 km, Soil site (V_{s30} = 250 m/s)
Set 1b	Broad-band motions, Magnitude 6, R=25 km, Soil site (V_{s30} = 250 m/s)
Set 2	Broad-band motions, Magnitude 7, R=10 km, Rock site (V_{s30} = 760 m/s)
Set 3	Pulse-like motions (strong velocity pulses in strike-normal direction)
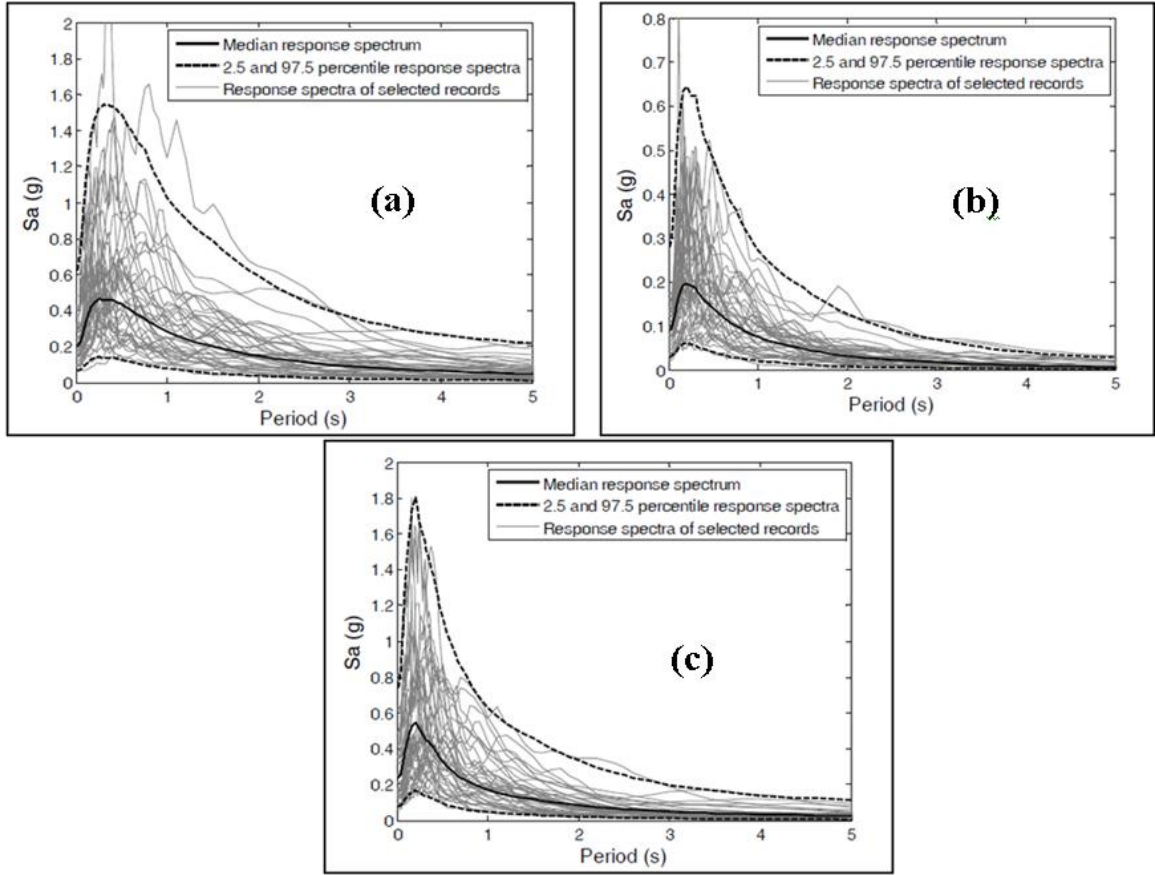
Figure 10: Response spectra for ground motions in sets (a)1a, (b) 1b, and (c) 2. **(Baker, et al., 2011)**
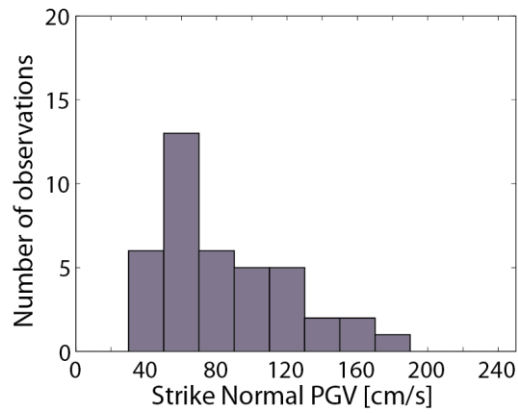
Figure 11: Peak ground velocities for ground motions in set 3 (Baker, et al., 2011)

CHAPTER 5

CALIFORNIA BRIDGE DESIGN DETAILS AND ANALYTICAL

MODELING OF CONCRETE BOX GIRDER BRIDGES

The research presented here provides a method of improving the seismic design process for California bridges. A method and tool were developed that allow a design engineer to determine the likely performance of a bridge design and the effects of design details on the predicted performance of the bridge. The Bridge Specific Fragility method and Design Support Tool presented in this thesis was developed with full consideration of the Caltrans design process. As the first iteration of this method and tool, one bridge type was targeted for the investigation of the effectiveness of the method, the Multi-Span Box Girder Bridge. This chapter describes the bridge type used to develop this new method and tool for the improvement of the bridge design process. Design characteristics and inventory data are presented about this bridge type. Finally, the details of the analytical modeling of the bridge components and systems are given. These analytical models were used to simulate the response of this bridge type to produce data for the prediction of response and formulation of fragility. More details about the fragility formulation will be given in later chapters.

5.1. Multi-Span Concrete Box Girder Bridge Class

5.1.1. Inventory Analysis of Bridge Types

The bridge type used to develop this iteration of the bridge specific fragility method and design support tool is the multi-span continuous (MSC) concrete box girder bridge. According to an inventory analysis of the bridge classes in California, this bridge class is the most common in California, making up 21% of the state bridge inventory. A

chart showing the bridge classes that comprise the California state bridge inventory is given in Figure 12. Further analysis of the inventory shows that most (~40%) of the MSC concrete box girder bridges have two spans, as shown in Figure 13. A bridge sample of modern (post year 2000) bridge plans revealed upwards of 70 bridges with these characteristics, which indicates that this bridge class is still being designed and constructed frequently in California
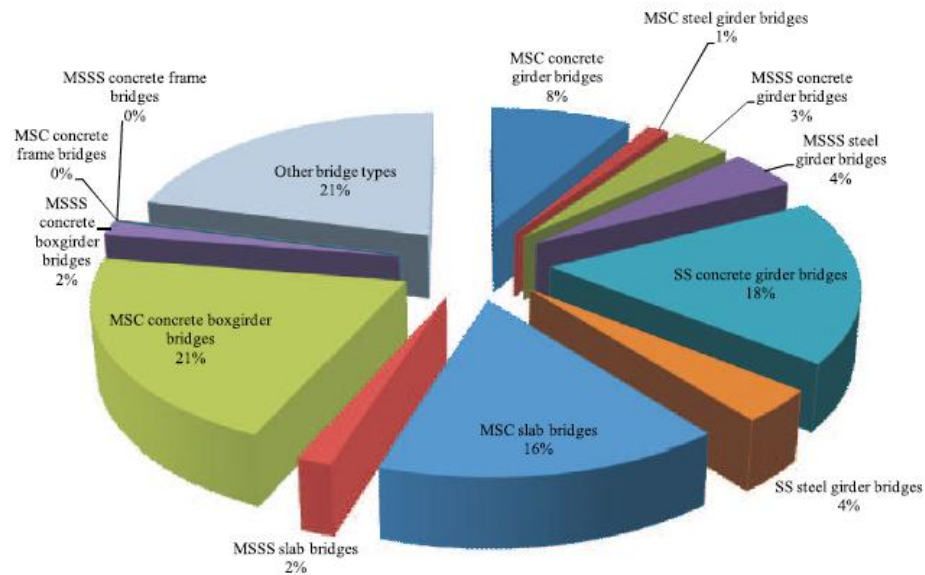
Figure 12: Pie Chart of California Bridge class inventory
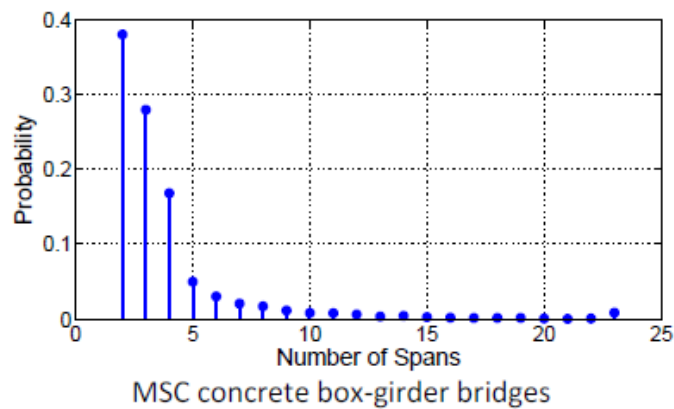
Figure 13: Statistics on the number of spans in box girder bridge class.

Based on this information from the inventory analysis, the MSC concrete box girder bridge type was chosen as the bridge type used to develop this design support tool and test the concept of bridge-specific fragility analysis in bridge design. The fragility methodology presented here is adaptable to encourage further work to develop the design support tool for additional bridge types and structure types in the future.

5.1.2. Sample of California Bridge Plans

Since the design support tool presented here was developed for use with new bridge designs, information about recently built bridges in this class needed to be obtained. Bridge plans were sampled from the California state inventory of brides in order to compile important details and characteristics of bridges built in California in the modern design era. All of the bridges sampled were constructed after the year 2000, because this is considered to be the modern design era which would employ the current design practices in use in Caltrans. Restrictions imposed when choosing bridge plans for the single frame bridges included a skew of less than 20 degrees and limiting the sample to brides with only two spans. These restrictions were used to narrow the type of bridge used in this analysis and for the bridge specific fragility method to be applicable.

These plans were analyzed and bridge data compiled for use in finite element bridge models developed for this project. Some of the properties of the bridges gathered from the bridge plans include span length, deck width, number of columns, column dimensions, reinforcement details, footing details, among others. For most of these properties, the minimum and maximum values from the sample were taken and used in the development of the finite element models in OpenSees. These properties and the ranges found from the analysis of the sample are listed in Table 16. These properties were varied randomly in the development of the bridge models to create statistically similar yet distinct bridges within this bridge class. Creating bridges in this manner addresses the differences found in the array of bridges in this bridge class as well as in the uncertainty

in the capacity of the structures due to uncertain construction detailing, among other reasons (Luco, et al., 2007).

Over forty bridge plans were surveyed for the single-frame two-span MSC concrete box girder bridge class. Table 16 displays the design details sampled and the ranges of the design details. All of the design details were not used directly in the analytical modeling of the bridges, as some details were determined using established distributions. That will be discussed later in this chapter. As is shown, the maximum span length varied widely between bridges, from 80 feet to nearly 190 feet. Many bridges in his class had multiple column bents, so bridge with more than one column were grouped together for the purposes of this research and analysis. Bridge with single column bents were grouped together, as these bridge types are assumed to behave differently (Ramanathan, 2012). The column heights, sampled as the minimum vertical clearance from the plans, varied between 16 feet to over 23 feet in height. The longitudinal and transverse steel content of the columns were noted for use in the column and concrete modeling. The maximum longitudinal steel content at 3.4% translates to about 44 #11 bars, while the maximum transverse content at 1.43% equaled #8 bars at 5 inch spacing. Details about the superstructure, such as the box girder dimensions from the typical section, were sampled. The thickness of the girders was consistent for most of the bridge at twelve inches. Most of the bridges had a seat type abutment with a seat width greater than 24 inches. The type and size of the footing beneath the columns was sampled, as well as the number and type of piles used in the footings. Some details were not ascertained from the bridge plans, such as the height of the abutment backwall and soil properties. These details were determined using probability distributions created from observations and experiments done in previous research. These details will be discussed further in a later section.

Table 16: Details gathered from the bridge plans of the California bridge plan sample

Bridge Section	Property Sampled	Minimum	Maximum
Deck Details	Max Span Length	976 in	2244 in
	Number of Boxes in Girder	3	15
	Width of bridge	495 in	1724 in
	Girder thickness	10 in	12 in
	Top deck thickness	7.3 in	9.1 in
	Bottom deck thickness	5.9 in	8.3 in
	Depth of Deck	45 in	90 in
Column Details	Minimum Vertical Clearance	201 in	281 in
	Number of Columns	1	6
	Spacing of columns (multi-column bents)	188.4 in	422.4 in
	Longitudinal Dimension	41.9 in	78.7 in
	Transverse Dimension	48 in	108 in
	Shape (Circle, oval, etc)		
	Flare or isolation details		
	Main Longitudinal reinforcement details and content	0.98 %	3.41 %
	Trans steel type (hoop or spiral)		
	Transverse reinforcement details and content	0.42 %	1.43 %
Bent Cap Details	Transverse Dimension	59.1 in	114.2 in
Footing Details	Footing Type (pile or spread)		
	Number of Piles (for pile footings)	9	20
	Type of pile		
	Area of Footing	11664 in^2	97472 in^2
	Depth of footing	36 in	63 in
Abutment Details	Abutment support type (pile or spread)		
	Abutment Seat Type		
	Abutment Seat Width	24 in	48 in
	Maximum Number of Piles	12	96
	Closest Spacing of piles	43 in	126 in
	Type of pile		

These bridge plan samples gave an accurate picture of the design details in use currently in the Caltrans bridge design practices. The design support tool was developed

to supplement the current seismic bridge design procedure with a tool designed to check the performance of the bridge. Having this information on the current design details is helpful not only in modeling the analytical bridge accurately, but in including relevant design details and parameters in the design support tool for Caltrans engineers to be able to use.

5.2. Analytical modeling of the bridge system and components

In order to build a database of bridge damage data, analytical finite element bridge models were constructed and analyzed with a suite of ground motions to gather bridge response data. This data was used for the bridge specific fragility design support tool. The Open System for Earthquake Engineering Simulation (OpenSees) is an open source software framework developed for use in earthquake engineering applications by the Pacific Earthquake Engineering Research Center (PEER). OpenSees is advanced in offering many different types of elements and nonlinear analysis to accommodate many structure and analysis types needed for research. This software program was used to develop and analyze finite element bridge models used in this project. The section describes the details of the modeling techniques used to simulate the behavior of the bridge components as well as the bridge system as a whole. Also, a description of model validation is given for the different bridge sub-classes.

Structure, component and material behavior of the bridges were carefully considered in the construction of the finite element bridge models in OpenSees. This part of the analytical fragility methodology is very important, since a better model, can lead to more realistic results [Nielson 2003]. Certain assumptions and modeling techniques have been employed in this research, and will be described in this section. Figure 14 shows a typical layout of the nodes and elements that define the bridge model. Following are brief descriptions of the modeling materials and elements used in the creation of the bridge models.
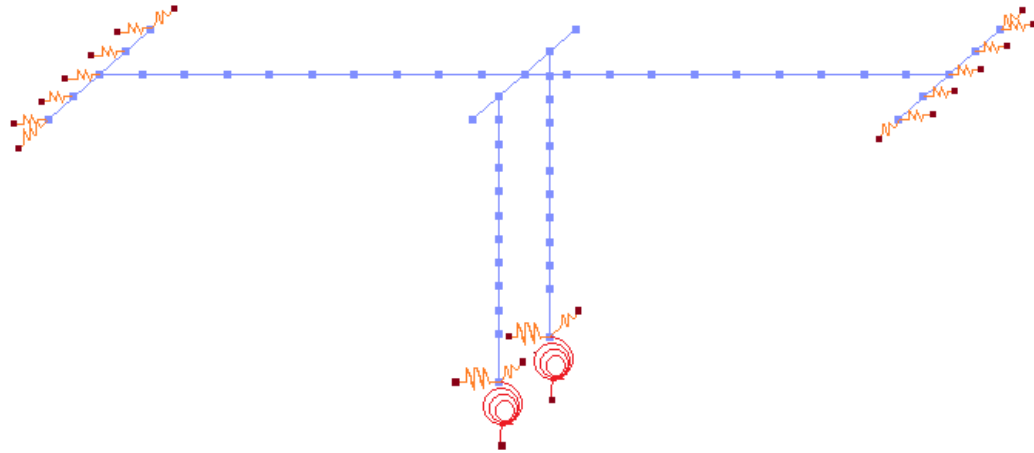
Figure 14: Typical layout of two span bridge modeled in OpenSees.

5.2.1. Component and material modeling

Each of the components of the analytical bridge model was developed to model the behavior of the actual component as closely as possible. In studying the bridge plan details, the geometry and design details were captured and translated to the appropriate finite element model properties. As part of a larger project sponsored by Caltrans, all material and component modeling was determined and developed with the design practices of Caltrans in mind, and was also kept constant between the different aspects of the project. The bridge columns, considered by many researchers to be the most vulnerable of components [Nielson 2003], were thoughtfully be modeled to match expected behavior. The columns of the analytical bridge models were modeled using nonlinear beam column elements in OpenSees. There are two types of nonlinear beam column element available for use in OpenSees, the force-based element and the displacement-based element. Both of these types of elements permit the distribution of plasticity throughout the element, allowing the possibility of an internal hinge to occur at any location along the element (Terzic, 2011). The displacement-based element was chosen for this research. The displacement-based approach follows traditional finite element analysis procedure in using section deformations to form the equilibrium

62

relationship (Terzic, 2011). Of consideration when using this particular element is that a finer mesh or more elements per member are required to improve accuracy of the analysis.

When modeling elements using the displacement-based beam column element, the cross section of the element must also be defined. A section describes the force-deformation response of the cross section of the beam (Mazzoni, et al., 2009). The cross sections of the columns were defined with fiber material elements, as shown in Figure 15. A fiber section is defined by a geometric configuration and broken into smaller regions of different shapes, or patches and layers. In this manner, fiber sections allow the different properties of unconfined and confined concrete to be specified, as well as the longitudinal steel properties. Properties of the unconfined and confined concrete strengths were derived from the theories of Mander et al. (1988), as shown in Figure 16. Mander et al.(1988) showed that the strength and ductility of confined concrete increased significantly as a result of the amount of transverse reinforcement used in a concrete column. The confined concrete strength is determined with Eqn. (5.1) for a concrete core confined with spiral or circular hoops. The strength of the reinforcing steel is determined based on the current standards for steel.

$$f_{cc}' = f_{co}' \left(-1.254 + 2.254\sqrt{1 + \frac{7.94f_l'}{f_{co}'}} - 2\frac{f_l'}{f_{co}'} \right) \tag{5.1}$$

$$f_l' = 0.5 k_e \rho_s f_{yh} \tag{5.2}$$

$$k_e = \frac{\left(1 - \frac{s'}{2d_s}\right)^2}{1 - \rho_{cc}} \tag{5.3}$$

$$\rho_s = \frac{4A_{sp}}{d_s s} \tag{5.4}$$
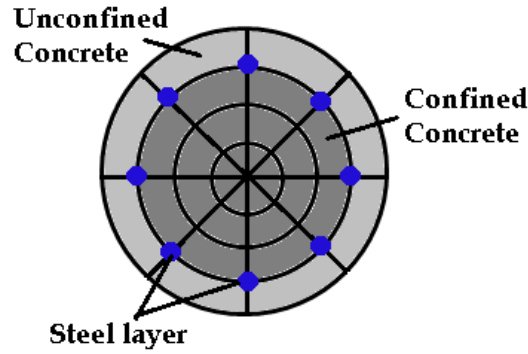
Figure 15: Fiber cross section of column element.
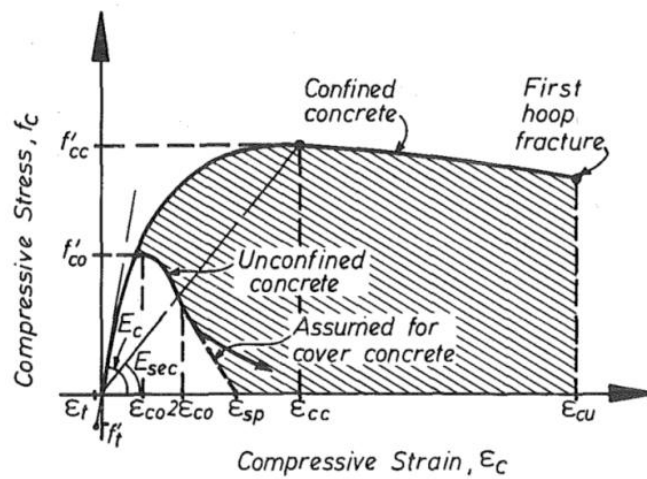
Figure 16: Stress-strain curve of confined and unconfined concrete (Mander, et al., 1988).

These calculated properties are then transferred to an OpenSees material model that best matches the expected behavior of the materials. For the concrete material model, the Concrete03 model is used, which includes the nonlinear tension softening of concrete as well as the compressive strength of the concrete as described earlier. The material model used to define the steel reinforcing bars is the Steel01 material model in OpenSees. This material model develops a bilinear steel material and option for introduced hardening into the model (Mazzoni, et al., 2009). Once aggregated, the different patches and layers of the fiber section, which are characterized by the appropriate material models, act together to simulate a resultant behavior, in this case, the reinforced concrete of the column.

The foundation support under the columns is considered part of the substructure system of the bridge. For this bridge type, only foundation systems with a pile cap and piles is considered, excluding any system that has only spread footings or one pile shaft supporting the columns. To characterize the response of the foundation system in the analytical mode, the behavior of the pile cap and piles under the columns of the bridge are represented by linear elastic translational and rotational springs. The translational springs include the stiffness of the piles as well as the pile cap. The stiffness of the pile cap is fixed at 30 kip/in, and the median stiffness of the piles in the model were randomly chosen as either 65 kip/in or 80 kip/in, per the standard pile stiffnesses used in modern bridges (Roblee, et al., 2011). The stiffness of the rotational springs would be calculated based on the pile arrangement and size of the footing. For the bridge models with multi-column bents, the columns are assumed to behave as though pinned at the base. Therefore, for these models, the rotational springs were taken as negligible to simulate a pinned connection at the footings. For bridge models with bents with only one column, the full rotational spring was modeled to simulate a fixed condition at the base of the column. The rotational springs acted about the X (longitudinal) and Z (transverse) axes. An illustration of the translational and rotational springs of the foundation is shown in Figure 17.
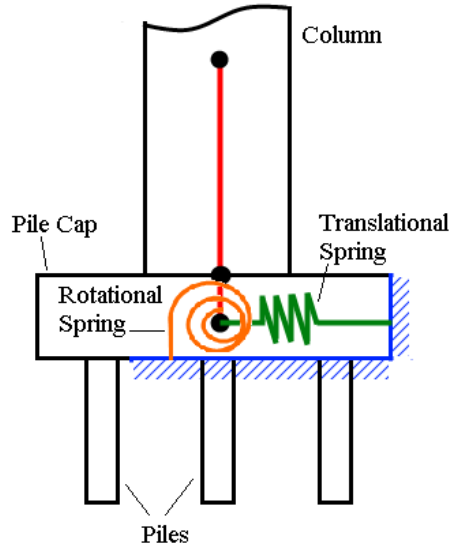
Figure 17: Illustration of translational and rotational springs at foundation nodes of model.

The role of abutment response on the overall response of the bridge system is recognized as important to capture in analytical modeling (Choi, 2002). Abutments often attract a significant amount of the seismic forces from an earthquake and affect the longitudinal response of the entire bridge system. The abutment behavior is characterized by the behavior of the supporting piles as well as the soil interaction from the soil behind the backwall of the abutment. To analyze this behavior, it is necessary to characterize both of the contributions to the overall behavior with appropriate material models.

Abutment piles and the soil behind the backwall of the abutment provide resistance against forces in the longitudinal and transverse directions of the bridge. In the longitudinal direction, there are two types of resistance provided by the piles and backfill soil: passive and active. The passive resistance is activated when the abutment backwall presses against the backfill soil, and the resistance is provided by the backfill soil and piles. Active resistance occurs when the abutment backwall pulls away from the backfill soil, and is provided by the piles only. In the transverse direction, only the stiffness of the piles contributes to the resistance at the abutment. The resistance in the transverse and

longitudinal directions at the abutment is modeled as springs represented by zero-length elements.

The abutment piles were represented by nonlinear springs that behaved in a hysteretic manner in the longitudinal and transverse directions, in tension as well as compression. The modeling technique of the piles as described by Choi (2002) is used in this research. The piles are assumed to have an ultimate deformation at one inch and an ultimate force as given by the type of pile. Yielding first occurs at 30% of the ultimate deformation and 70% of the ultimate force. This is assumed for the transverse direction as well as for the active and passive resistance in the longitudinal direction. Figure 18 shows the force-displacement response that is used to define the spring that models the behavior of the pile that supports the abutment.
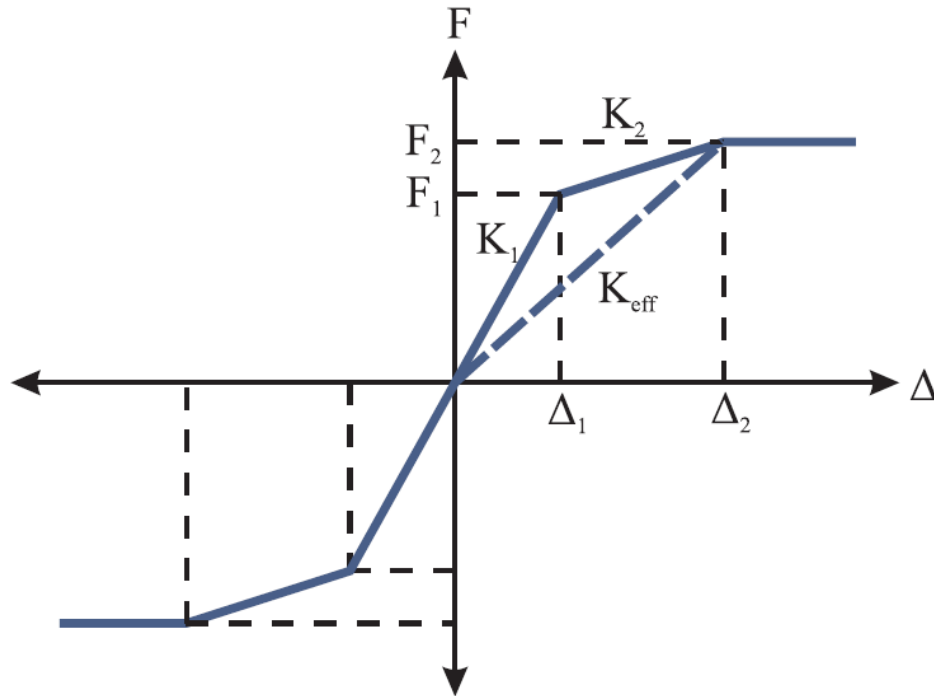
Figure 18: Force displacement response of pile behavior at abutment (**Ramanathan, 2012**).

The behavior of the backfill soil behind the abutment backwall was also represented by nonlinear springs using zero-length elements in OpenSees. The soil behind the abutment was represented by a hyperbolic gap material, based on the hyperbolic force-displacement model developed by Shamsabadi et al. (2007). Experimental tests of bridge abutment with backwalls of 5.5 feet height and cohesionless and cohesive soils led to the development of a closed form solution to describe the behavior of this material type. The behavior of the hyperbolic force displacement model is shown in Figure 19. The corresponding approximated equations of the response of the force and displacement given in this model are shown in Eqn. (5.5) for cohesive soils and Eqn. (5.6) for cohesionless soils, where H is the height of backwall of the abutment in feet, F is given in kips per foot of wall, and y is given in inches (Shamsabadi, et al., 2008). The soil behavior is assumed only to engage in the passive longitudinal direction, while the piles act in the passive and active longitudinal direction as well as the transverse direction. The hyperbolic gap material in OpenSees is based off of the ultimate passive resistance and the stiffness of the soil, and includes the option to define a gap length before the hyperbolic force-displacement model activates, shown in Figure 20 (Mazzoni, et al., 2009). The average soil stiffness behind the abutment was randomly chosen as either 50 kip/in or 25 kip/in per foot of backwall, which represents a granular soil or clay soil, respectively (Shamsabadi, et al., 2007).

$$F(y) \approx \frac{8y}{1+3y} H^{1.5} \tag{5.5}$$

$$F(y) \approx \frac{8y}{1+1.3y} H \tag{5.6}$$

$$K = \frac{0.5F_{ult}}{y_{ave}} \tag{5.7}$$

68
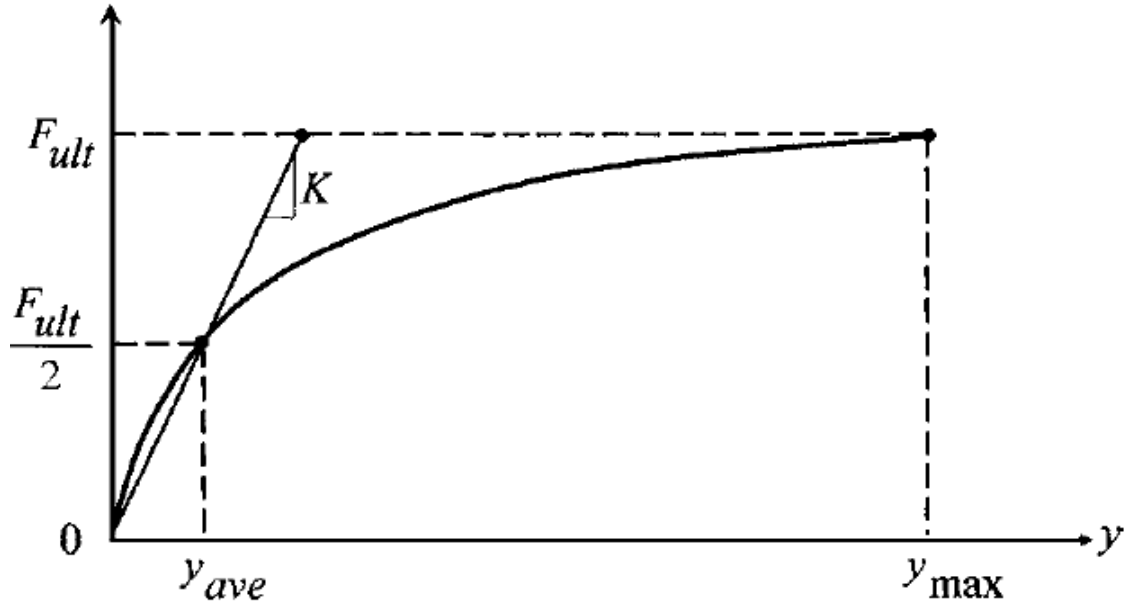
Figure 19: Hyperbolic force-displacement formulation (Shamsabadi, et al., 2007)
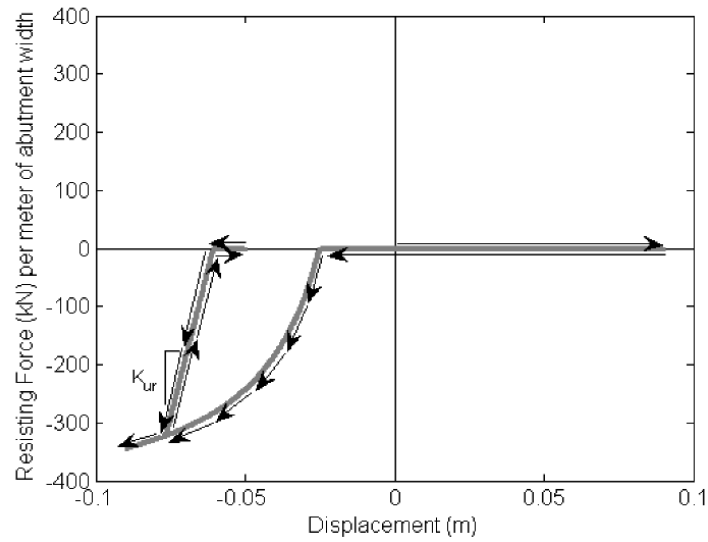
Figure 20: Hyperbolic gap material behavior (Mazzoni, et al., 2009).

The deck was modeled as an elastic beam column element, as the deck is assumed to remain elastic during earthquake loading (Nielson, et al., 2007). The deck has the properties of the cross section of the concrete box girder, including the area, moments of inertia, and elastic modulus. The deck is modeled as a centerline model with a linear

string of elastic beam elements representing the cross section of the deck. This was shown in Figure 14.

Pounding between adjacent decks at internal hinges and between the deck and abutment for bridges with seat-type abutments during an earthquake has been a source of major damage in the past (Muthukumar, 2003). Pounding in the past has lead to damage to other major components such as the column, abutments, shear keys, and other components. To model the effect of pounding between adjacent decks or the deck and the abutment backwall, impact elements are included in the bridge model. The contact element approach as described by Muthukumar (2003) was used to model the impact element. The element was modeled by a bilinear spring model with the option to define a gap before the spring activated. The stiffnesses of the springs were adopted from Nielson (2005).
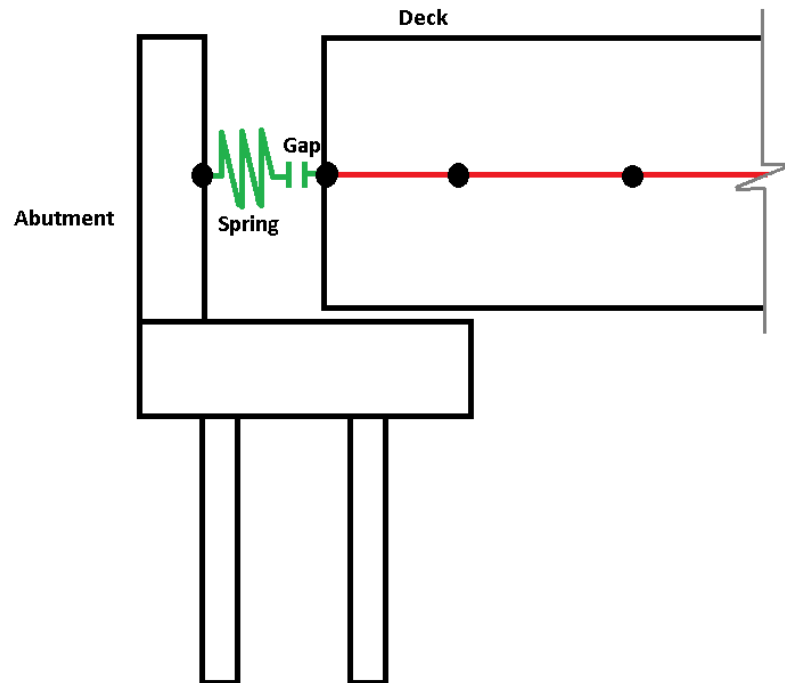
Figure 21: Illustration of impact element between abutment and deck nodes

Shear keys on bridges are meant to limit the transverse movement of the bridge deck and to transfer lateral forces to the abutment and wingwalls. Shear keys located at abutments are often designed as sacrificial elements that control the amount of seismic force experienced by the abutments to limit damage done during an earthquake. The shear keys are assumed to fail once the capacity is exceeded and they no longer provide lateral support One the shear keys fail, the substructure system is expected to provide support against transverse loads (Megally, et al., 2001). Shear keys could be located at abutments as internal or external shear keys or at in-span hinges. To model the behavior of the shear keys analytically, nonlinear springs modeling the force-displacement behavior are used at the nodes between the abutment and deck and between adjacent decks. The model presented by Megally, et al. (2001), based on experimental tests, is used in this research. Figure 22 shows the force displacement model assumed to represent the behavior of the shear keys. The capacity of the shear key is determined by calculating the shear capacity of the bent. The shear keys at the abutment is designed to resist seventy five percent of the capacity of the bent which is calculated based on the equation for shear capacity for the concrete and steel given in ACI 318 (ACI, 2008) shown in Eqn. (5.8-9).

$$V_c = \left(\sqrt{1 + \frac{N_u}{500 A_g}} \right) 3.5 \sqrt{f'_c} (0.8D^2) \tag{5.8}$$

$$V_S = \frac{A_v f_y (0.8D)}{s} \tag{5.9}$$
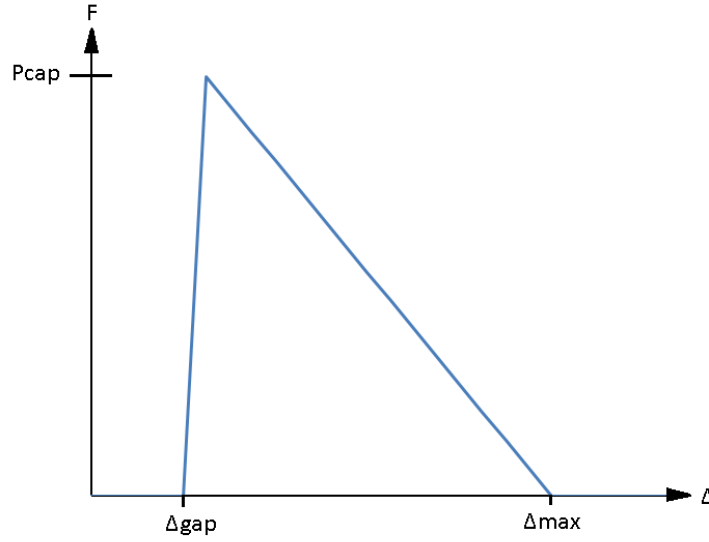
Figure 22: Force-displacement relationship used to model shear keys **(Shafieezadeh, 2011)**.

The bearing type used in this class of bridges is the elastomeric bearing pad, which is common in concrete bridges. This bearing type transfers horizontal loads by friction developed while sliding (Nielson, 2005). This component of the analytical bridges is modeled based off of the size of the bearing, coefficient of friction, and shear modulus. The elastomeric bearing pads that support the superstructure at the abutments and in-span hinges will be modeled with translational bilinear spring elements with an elastic-plastic material model in the transverse and longitudinal directions. The initial stiffness of the material is described with Eqn. (5.10), determined by the area of the pad, shear modulus, and thickness of the pad. The coefficient of friction, which is used to determine the yield force of the bearing, is modeled from an expression developed by Shrage (1981) relating the coefficient of friction to the normal stress.

$$k_{pad} = \frac{GA}{h} \tag{5.10}$$

$$\mu = 0.05 + \frac{0.4}{\sigma_n}, \sigma_n \text{ in MPa} \tag{5.11}$$

The bridge models that were developed for this project were parameterized to reflect the uncertainty in properties of the bridges. Distributions of geometric properties of the bridges, such as width of the deck and the number of foundation piles, were determined form an analysis of the sample of bridges described earlier. The distributions of some material properties, such as concrete and steel strength, are adopted from literature studies, while other parameters, such as the shear modulus of the bearing, were varied based on 50% and 150% bounds of the deterministic values of these parameters (Nielson, et al., 2007). These uncertainty parameters are listed in Table 17. Bridge properties whose values were dependent on uncertainty parameters are listed in Table 18. These distributions were developed from the analysis of the bridge plan sample of modern bridges. Parameters that were fixed for all of the bridge models are listed in Table 22. Random samples of these parameters based on the assigned distributions combined to form analytical bridge models used in this study. Along with the design parameters that will be instrumental to the development of bridge specific fragility method (to be introduced later), a set of bridge models will be produced that will encompass the range of modern bridge designs that may be found in the inventory.

5.2.2. Bridge system modeling

The entire bridge system model is composed of the individual component models previously described. All of the components are tied together, simulating real world conditions. For example, the superstructure and the column elements are connected with rigid elements, imitating the integral connection of the column and superstructure in this bridge type. Figure 23 shows the type of connections between the column and superstructure present in the bridge type modeled here.
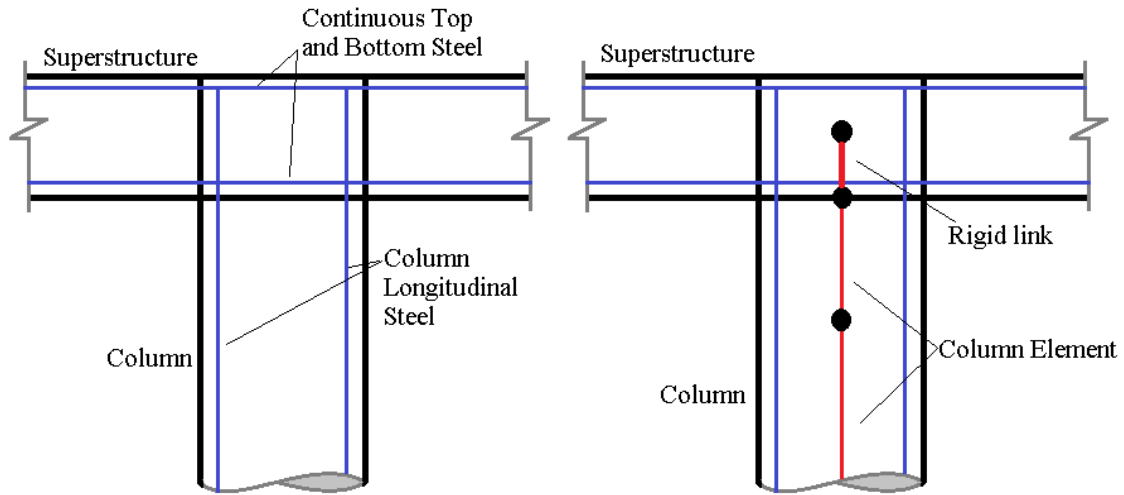
Figure 23: Joint connection between the column and superstructure of the MSC box girder bridge.

The column elements are tied to foundation springs by a rigid link also, modeling the way the column is anchored into the foundation mat. The way the column behavior is modeled at the footing as either pinned or fixed is modeled with the foundation springs as described earlier. The connection between the column and footing is shown in Figure 24 and Figure 25. Notice that the connections between the column base and the footing differs based on the number of columns at the bent, however the modeling strategy is similar. A rigid link connects the column element to the foundation support nodes, and the connection is simulated by the rotational springs at the foundation nodes.

The deck and abutment are connected by the bearing springs, simulating the deck sitting on the abutment seat on elastomeric bearing pads. In a similar manner, the other components in the analytical model are connected by springs and rigid links. The complete analytical bridge model is thus created for nonlinear time history analysis in OpenSees with the ground motion suite described in a previous chapter.
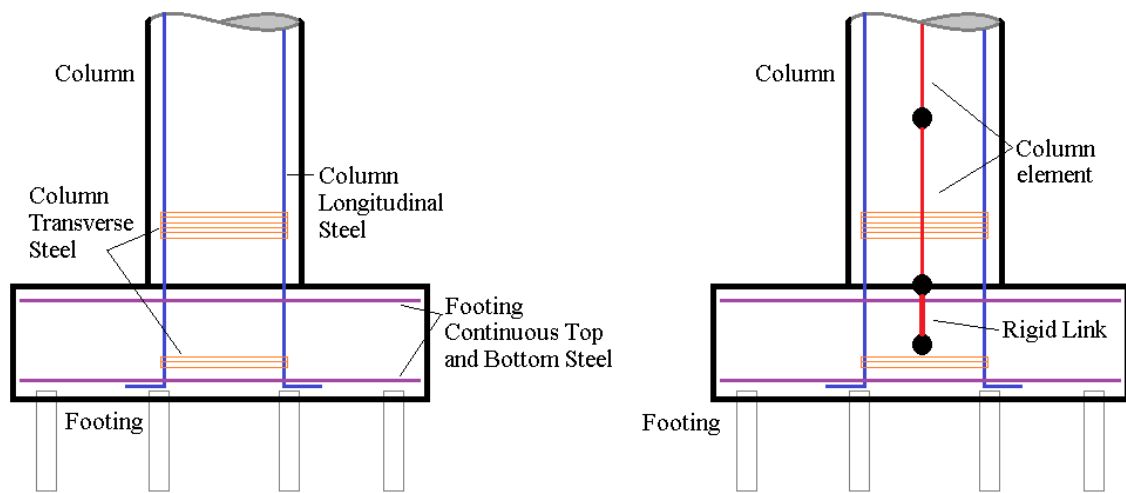
Figure 24: Connection between the column and foundation for single column bent bridges.
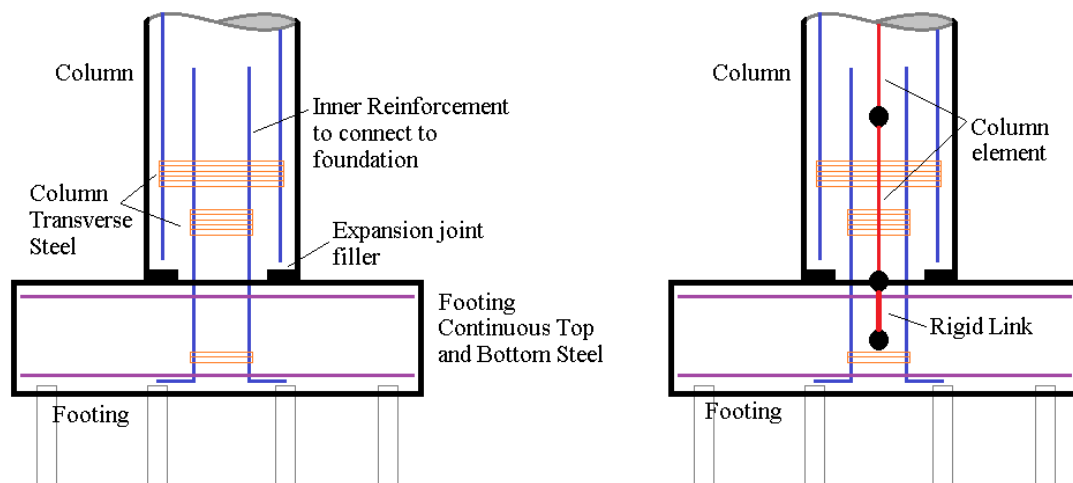
Figure 25: Connection between the column and foundation of bridges with multi-column bents.

5.2.3. Assumptions and Properties Defined Probabilistically Versus

Deterministically

The geometric and material properties of the analytical bridge models are determined from the sample of bridge plans surveyed for this research and from past research based on experimental data. Throughout the different analyses employed in this research, the details of the bridge models were determined with a parametric approach. This is because for analytical fragility analysis, it is advantageous to perform analysis on statistically similar but varied models to get a wide range of responses that reflect real world conditions. During parameterization, some properties will be set deterministically, while others will be determined probabilistically, depending on the goal of the analysis performed. The following describes generically which properties were determined deterministically based on educated assumptions, and which properties were determined probabilistically. Also detailed are some properties of the bridge type that were assumed true for the whole class to have a more homogeneous bridge class for analysis. Further details about how properties were determined are given in subsequent chapters in which the different analyses performed are described.

The bridge models that were developed for this project were parameterized to reflect the uncertainty in the properties of the bridges within the bridge class. Distributions of geometric properties of the bridges, such as width of the deck and the number of foundation piles, were determined form an analysis of the sample of bridges described earlier. The distributions of some material properties, such as concrete and steel strength, are adopted from literature studies, while other parameters, such as the shear modulus of the bearing, were varied based on 50% and 150% bounds of the deterministic values of these parameters (Nielson, et al., 2007). These uncertainty parameters are listed in Table 17. Bridge properties whose values were dependent on uncertainty parameters are listed in Table 18. These distributions were developed from the analysis of the bridge

plan sample of modern bridges. Parameters that were fixed for all of the bridge models are listed in Table 22. Random samples of these parameters based on the assigned distributions combined to form analytical bridge models used in this study. Along with the design parameters that will be instrumental to the development of bridge specific fragility method (to be introduced later), a set of bridge models will be produced that will encompass the range of modern bridge designs that may be found in the inventory.

In addition to these characteristics, additional details about the bridge type were controlled for the purpose of developing this design support tool. Figure 26 shows a typical configuration of the bridge type for which this version of the design support tool was developed. A seat type abutment, which was present in the majority of sampled bridge plans, was assumed to be standard for this tool. A multi-column or single-column bent in the bridge is also a requirement to use this tool, meaning a bridge design with a pier wall or other substructure configuration would not be applicable for this version of the tool. The footings under the columns, as well as the abutments, were assumed to be supported on piles. The skew angle of the bridges was assumed to be zero, and the bridges are modeled as straight.

These parameterized bridges, once analyzed in OpenSees with the ground motion suite chosen for this research project, provides the analytical data on the structural response of the bridges to seismic loads. This database of information is key in the analytical fragility analysis method, as the database is used to populate the model of the demand on the structure. Modeling the bridge accurately according to the modern design detailing used for this bridge class in California and according to the expected or observed behavior of the different materials and components is critical to moving forward to producing accurate and reliable fragility curves. This chapter shows the careful consideration applied to modeling the analytical bridge models to respond as closely to field observations as possible.

Table 17: Uncertainty parameters for parameterized bridge models for the multi-column bent bridge class

Uncertainty Parameters for Bridge Models			
	Distribution	**Parameter 1**	**Parameter 2**
Width of bridge (w)	Uniform	500 in	1600 in
Width of bent cap	Uniform	70 in	100 in
Concrete Strength	Normal	4.9 ksi	0.6 ksi
Steel Strength	Lognormal	4.27 ksi	0.072 ksi
Shear modulus of bearing	Uniform	0.1015 ksi	0.1668 ksi
Bearing pad coefficient of friction	Uniform	0.35	0.4
Pile Stiffness	Discrete Uniform	65 kip/in	80 kip/in
Number of foundation piles	Discrete Uniform	9, 12, 16	
Gap at abutment	Uniform	0 in	1.5 in
Soil Type	Discrete Uniform	1 (sand)	2(clay)
Abutment Backwall Height	Uniform	3.5 ft	8.5 ft
Angle of incidence of earthquake	Uniform	0	6.28

Table 18: Bridge properties that are dependent on Uncertainty Parameters for the multi-column bent bridge class

Property	Values
Number of girders	5, for w < 800 in
	9, for 800 in < w < 1200 in
	13, for w > 1200 in
Number of columns	2, for w < 800 in
	3, for 800 in < w < 1200 in
	4, for w > 1200 in
Number of abutment piles	Uniform between 12 and 24, for w < 800 in
	Uniform between 20 and 40, for 800 in < w < 1200 in
	Uniform between 30 and 80, for w > 1200 in
Soil Stiffness	50 kip/in for sand soil
	25 kip/in for clay soil

w=width of the bridge

Table 19: Fixed parameters for parameterized bridge models

Fixed Properties of Bridge models	
Longitudinal Steel Bar size	#11
Transverse confinement Steel size	#6
Diameter of Column	60 in
Cover depth of concrete	2 in
Thickness of girders	12 in

Table 20: Uncertainty parameters for parameterized bridge models for the single column bent bridge class

Uncertainty Parameters for Bridge Models			
	Distribution	**Parameter 1**	**Parameter 2**
Width of bridge (w)	Uniform	200 in	300 in
Width of bent cap	Uniform	70 in	100 in
Concrete Strength	Normal	4.9 ksi	0.6 ksi
Steel Strength	Lognormal	4.27 ksi	0.072 ksi
Shear modulus of bearing	Uniform	0.1015 ksi	0.1668 ksi
Bearing pad coefficient of friction	Uniform	0.35	0.4
Pile Stiffness	Discrete Uniform	65 kip/in	80 kip/in
Number of foundation piles	Discrete Uniform	9, 12, 16	
Number of abutment piles	Discrete Uniform	12	24
Gap at abutment	Uniform	0 in	1.5 in
Soil Type	Discrete Uniform	1 (sand)	2(clay)
Abutment Backwall Height	Uniform	3.5 ft	8.5 ft
Angle of incidence of earthquake	Uniform	0	6.28

Table 21: Bridge properties that are dependent on Uncertainty Parameters for the single column bent bridge class

Property	Values
Soil Stiffness	50 kip/in for sand soil
	25 kip/in for clay soil

Table 22: Fixed parameters for parameterized bridge models with single column bents.

Fixed Properties of Bridge models	
Longitudinal Steel Bar size	#11
Transverse confinement Steel size	#6
Diameter of Column	60 in
Cover depth of concrete	2 in
Thickness of girders	12 in
Number of girders	3
Number of columns	1
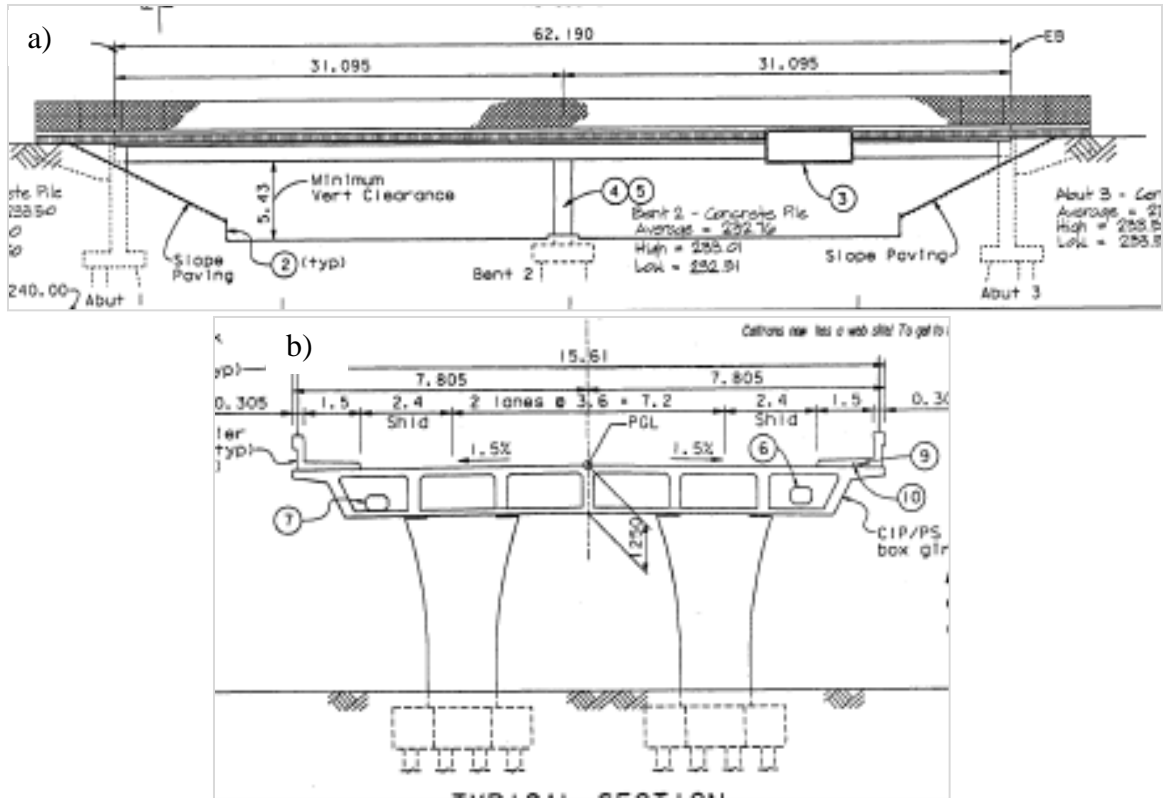
Figure 26: Typical configuration of two-span box girder bridge a) Elevation view, and b) Plan view.

5.2.4. Extracting Component Response Data from Analytical Models

The damage data generated with the analytical models and the nonlinear time history analyses populates the database of information used in the development of bridge-specific fragility method. In order to get the damage data, certain responses of the bridge model components were recorded during the analyses. In the Opensees platform recorders are used to monitor the response of specified elements or nodes of the model being analyzed. Recorders are used to track the response of a component throughout the entire loading sequence or they can be used to determine the minimum and maximum response values for the loading sequence. For elements, recorders can be used to record the force, deformation, stress, strain, or stiffness experienced at particular sections of the elements. For nodes, recorders can monitor the displacement, velocity, acceleration,

eigenvectors and reactions at those nodes (Mazzoni, et al., 2009). For this research, these node and element recorders are used to extract component response from the bridge models to use in the development of the bridge specific fragility method and to develop bridge-specific fragility curves.

For this project, the absolute maximum response quantity of each component was used as the response output of choice. Figure 27 illustrates the elements of the analytical bridge model that were used to find the demand data of each component used to develop the BSFM presented here. The maximum deformation response was recorded at the top and bottom elements of the column components to determine the demands of that component. As the column elements were modeled with beam-column elements, the deformation values that were recorded were the axial-strain curvature (Mazzoni, et al., 2009). This component response was directly applicable to the engineering demand parameter chosen for the column component response, which is used in the capacity model as column curvature ductility. The demands are converted to this engineering demand parameter by dividing the curvature recorded during the simulation by the yield curvature of the column model. For the abutment gap component, the deformation of the element used to model the bearing movement was used to determine the demand on that component. The bearing element was modeled as a spring with a zero-length element. The maximum deformation of that element was extracted, which is in the length units used to develop the model. In this case, the length units were inches. The same bearing response data was used to represent the responses of the secondary components, which were the joint seal movement and the bearing movement. This demand data is extracted from each simulation of all of the bridge models for use in developing the bridge-specific fragility method.
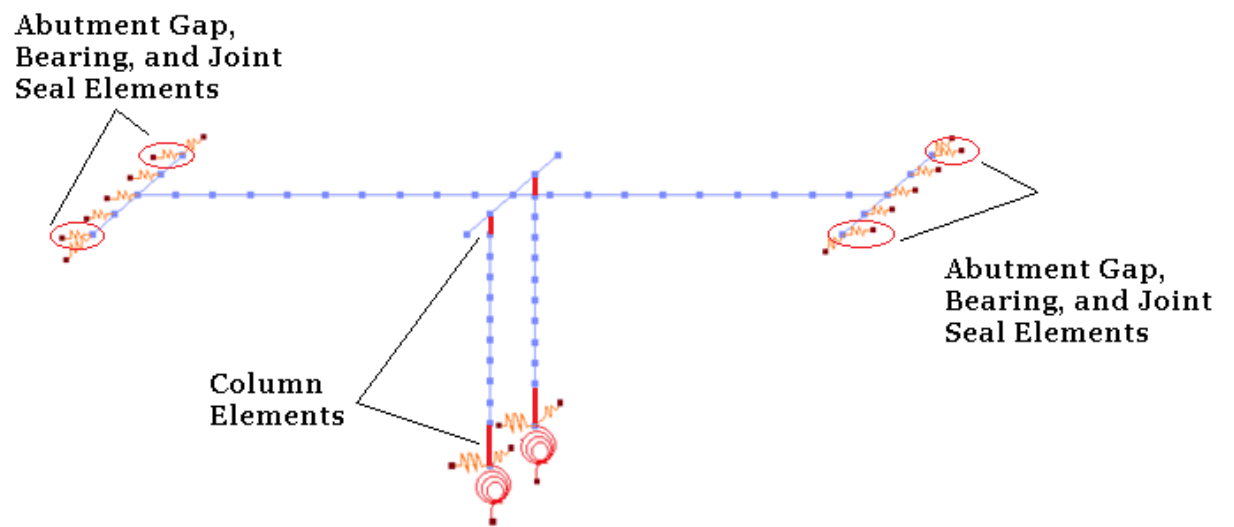
Figure 27: Figure illustrating the elements that are used to determine the demands of the different bridge components.

CHAPTER 6

SENSITIVITY STUDY OF BRIDGE DESIGN PARAMETERS

In the previous chapter, the analytical modeling of the two-span integral MSC concrete box girder bridge was detailed, including information on current design details of this bridge type in California. It was shown that many different components and design details are required to accurately model the bridge to produce reliable response data from analysis. Some of these parameters derived from the bridge plan sample have been designated as design parameters, the term used for the parameters that will be critical in developing bridge-specific fragility estimation. Design parameters, as used in this research, are those design details that the design engineers may have some control over, and those that have some impact on the response of the bridge to seismic loading. In this chapter, the design parameters explored in this thesis will be further explained, and sensitivity studies of the chosen parameters will be presented. The sensitivity studies acted as confirmation studies into the assumption that these parameters have a significant impact on determining the response of a bridge.

6.1. Introduction of Design Parameters

The method presented here for determining the bridge-specific fragility of a bridge design is based on incorporating the design aspects of the bridge into the method. The fragility methodology to be introduced in a later section requires design parameters as conditioning variables on the fragility equations and analysis. Thus, one need of this research was to find the design aspects which have the most effect on the responses of the different components of the two-span integral box girder bridge. Certain details were identified as possibly having a significant role in the design process as well as on the response of the bridge. This section will introduce these details, referred to as *design*

parameters, as well as the process used to determine whether these parameters in fact did affect the response of the two span integral box girder bridge type. The role of these parameters in the fragility methodology will be further explained in a later section.

The bridge design parameters chosen correspond to characteristics of the geometry of a bridge that were found to be important to monitor during the design process (Mackie, et al., 2005)(Caltrans, 2010), significant in the evolution of seismic design of bridges (Sahs, et al., 2008), as well as those suggested by the Caltrans project team (Roblee, et al., 2011).The five design parameters chosen for research are longitudinal steel ratio of the columns, the volumetric ratio of transverse steel in the columns, the aspect ratio of the column height to column diameter, the ratio of superstructure depth to column diameter, and the ratio of span length to column height. All of these parameters have different effects on the behavior and response of the bridge. Table 23 lists the design parameters used in this project and some of the effects on the seismic performance of a bridge. Illustrations of these characteristics are given in Figure 28 through Figure 30. The validity of assuming these parameters have a significant impact on the response of the bridge was tested with a sensitivity study described in this chapter.

Table 23: Description of design parameters used in this project.

Design Parameter	Symbol	Effect on Bridge Behavior
Longitudinal Steel Reinforcement Ratio of the Column	$LS = \rho$	A higher steel ratio stiffens and strengthens the column
Volumetric Ratio of Transverse Steel Reinforcement of the Column	$VR = \rho_s$	Determines the difference between unconfined and confined concrete strength, which determines the capacity of the component
Aspect Ratio – Column Height to Column Dimension Ratio	$AR = H/D$	Increasing this ratio makes the structure more flexible
Superstructure Depth to Column Dimension Ratio	$DepthDiam = t/D$	Increasing the depth makes the structure more stiff
Span length to column height ratio	$SpanHt = L/H$	Increasing the span length makes the structure more flexible
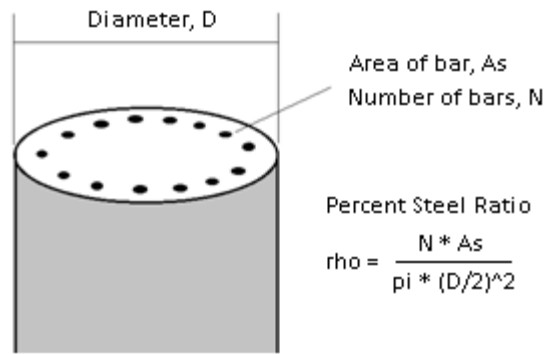
Figure 28: Illustration of the longitudinal steel ratio of the column.
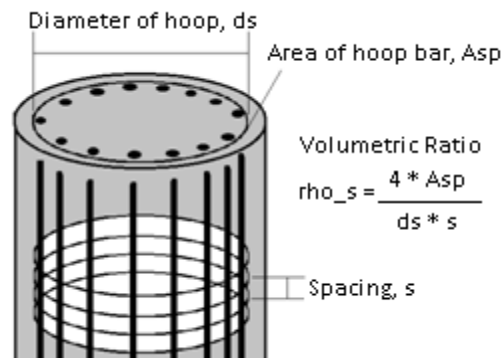
Figure 29: Illustration of the volumetric transverse steel content of the column.
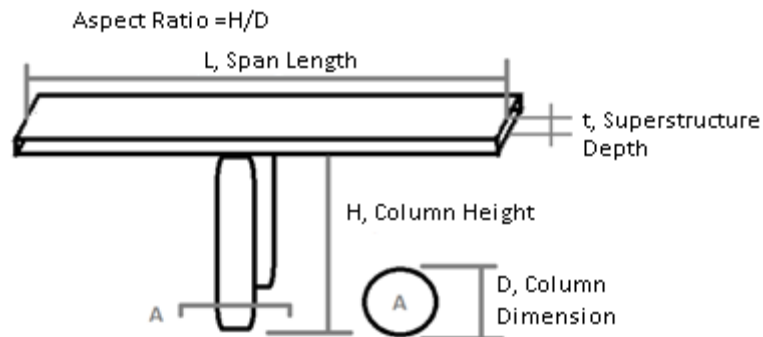
Figure 30: Illustration of the geometric ratios of the bridge.

From the bridge plan sample collected from the California state bridge inventory of this bridge type, information on the design parameters was gathered from each of the bridge plans. Histograms of the distributions of the parameters in the bridge plans are

shown in Figure 31. The red brackets on the histograms indicate the cut off for the ranges to be used in the development of the bridge models, the process of which will be detailed later. The minimum and maximum values found in the sample of bridge plans, as well as the adjusted minimum and maximum values based on consideration of outliers in the data are given in Table 24. In constructing the demand model using an appropriate design of experiment (DOE), these values will be varied according to the DOE to create bridge models that can be compared statistically. The creation of an appropriate DOE and construction of the demand model will be explained later. These ranges will also be used as upper and lower limits for the input parameters in the design tool, as the bridge models used to develop the tool were derived using these limits, so the tool would only be applicable for these ranges.

Table 24: Ranges of the design parameter values used in project

	AR	*LS*	*VR*	*SpanHt*	*DepthDiam*
Minimum	2.47	0.98%	0.42%	2.20	0.71
Maximum	11.35	3.41%	1.43%	10.29	1.43
Median	3.82	1.71%	0.93%	6.83	1.03
Adjusted Min*	**2.50**	**1.00%**	**0.50%**	**4.50**	**0.80**
Adjusted Max*	**6.00**	**3.00%**	**1.40%**	**9.50**	**1.30**

* Note: These adjusted values represent the actual ranges of the design parameters used in this research based on the limits shown in Figure 31.
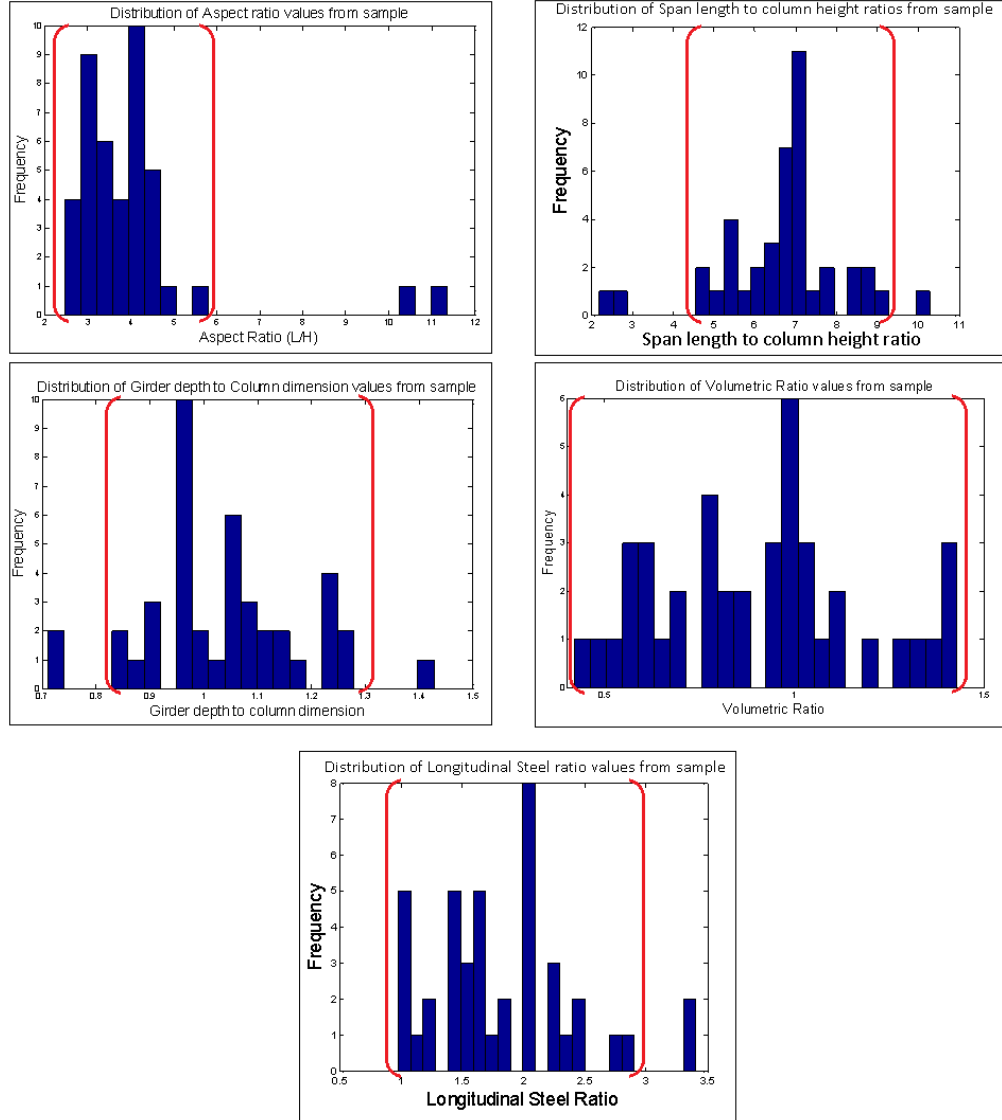
Figure 31: Histograms of the distributions of design parameters from bridge sample.

6.2. Deterministic Sensitivity Study

6.2.1. Motivation and introduction to sensitivity study

Presented here is the preliminary sensitivity study completed to determine the effects of varying different design parameters. This investigation was the primary step towards the end goal of developing the bridge specific design framework that incorporates bridge fragility into the design checking process. Finding the set of design

parameters that most affect the overall response of a bridge will lead into the next step of developing a multi-parameter fragility methodology or process that will develop individualized curves for a specific bridge input. There were many parameters to consider, including aspects of the bridge geometry, column reinforcement, and material properties. In this first sensitivity study, the effect of the five design parameters described previously on the response of the bridge was explored as the parameters were varied. The screening test used in this section is the "one-factor-at-a-time" approach, where each parameter is incrementally varied while the other parameters stay constant (Kutner, et al., 2005). This approach allows one to see the effect of each variable on the responses of the bridge individually. This section will highlight the base bridge model used in the study, the different bridge models developed based on the variations to the design parameters, and the results of the study.

6.2.2. Design parameters and Bridge models for deterministic study

The five design parameters in this study were longitudinal steel ratio of the columns, the volumetric ratio of transverse steel in the columns, the aspect ratio of the column height to column diameter, the ratio of superstructure depth to column diameter, and the ratio of span length to column height. All of these parameters have different effects on the behavior and response of the bridge. Table 23 listed some effects of these parameters on the behavior of a bridge, and illustrations of these characteristics were given in Figure 28 through Figure 30. To determine the range within which to vary the five design parameters incrementally, information on the properties of actual bridges was needed. For this study, these ranges were determined from a small sample of two span integral concrete box girder bridges from the Caltrans inventory designed after 1990. Table 25   lists the different bridges included in that sample, as well as each of the parameters for each bridge. Table 26 is a summary of these parameter and the ranges of the ratios used for this study.

Table 25: Summary of bridges in sample from Caltrans inventory and design parameters for each bridge for the deterministic sensitivity study.

Bridge Name	AR	LS	VR	SpanHt	DepthDiam
28th Street Overcrossing	3.14	1.2%	0.4%	7.20	0.84
Jackson Street OC (replace)	3.22	1.0%	1.4%	5.73	0.74
La Veta Ave OC (replace)	3.14	1.7%	0.8%	8.43	1.06
Mountain Ave OC	2.90	2.4%	0.7%	8.51	1.05
Nutmeg Street OC	3.07	2.1%	0.7%	7.12	0.84
Terwer Creek Bridge (replace)	3.59	1.1%	1.3%	5.73	0.81
First Street OC	5.02	1.7%	0.5%	4.38	1.19

Table 26: Design parameter ranges taken from bridge sample described above.

Design Parameter Ranges					
	AR	LS	VR	SpanHt	DepthDiam
Min	2.90	1.03%	0.42%	4.38	0.74
Max	5.02	2.42%	1.37%	8.51	1.19
Median	3.14	1.68%	0.73%	7.12	0.84

A base bridge model was chosen to be used as an original bridge on which all variations would be made and with which all comparisons would be made as to the effect of design parameters on the response of the bridge. The base bridge model was designed after an actual bridge in the California Department of Transportation bridge inventory, the Jackson St Bridge. It is a two span integral concrete box girder bridge with zero skew or curve, two columns at the integral bent, and a seat-type abutment. This bridge was chosen because it represented the design of many of the other bridges in our bridge sample during that design era. Figure 32 shows the plan and elevation views of the base bridge from bridge plans. In Table 27, the changes in each set of bridge models for each design parameter are shown. So for each bridge model, every other characteristic of the

bridge, including material properties, remained constant, and only the design parameter highlighted in the table was changed for each particular set of bridges. Each bridge model developed was analyzed using one set of 40 ground motions from the PEER ground motion suite, set 1a (Baker, et al., 2011) . In all, 880 OpenSees analyses were performed for this sensitivity exercise.

As described earlier, these bridge models were created and analyzed in OpenSees (Mazzoni, et al., 2009) . Figure 33 shows a typical layout of the nodes and elements that define the bridge model. The modeling of the bridge components and materials was based on the modeling techniques described in the previous chapter. Each model was subjected to 2 orthogonal ground motions at an incidence angle of zero input into defined support nodes. Recorders defined in OpenSees recorded the deformation, displacement, force or stress specified at particular elements or nodes along the bridge in order to find the response of the bridge system after the analysis. Responses were recorded at the top and bottom elements of the column component to find the maximum column curvature response. This component response was used as the measure of the effect of the variations on the response of the bridge for this sensitivity study, as column response is often used in this manner in other research involving fragility analysis (Hwang, et al., 2000)(Park, et al., 1985)(Choi, et al., 2004). These recorded responses are then compared with the corresponding ground motion intensity measure, and probabilistic seismic demand models were developed. Probabilistic seismic demand models (PSDMs) define the relationship between a component response and the ground motion intensity measure of interest that is used in the development of fragility curves. PSDMs will be further discussed later in the thesis. The PSDMs of the different sets of bridges can be compared to show the difference that each design parameter makes on the response of the bridge. After finding the PSDM, the capacity model can be introduced to develop the fragility curve of each bridge, which will further demonstrate the differences in response.

Figure 32: Base bridge model for sensitivity study, Jackson Street Bridge.

Figure 33: Typical OpenSees model setup for analysis in this study.
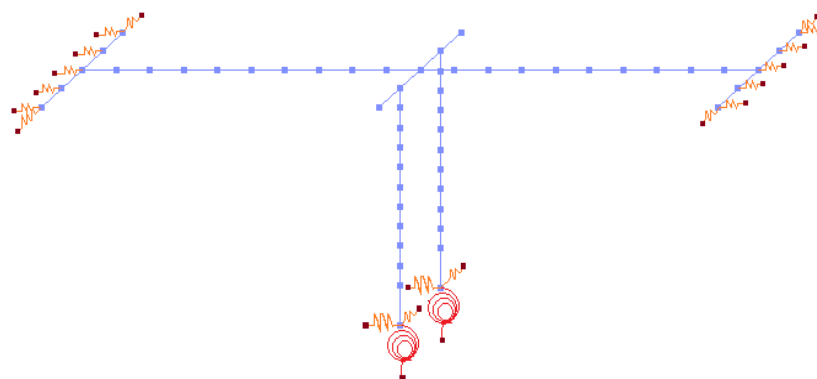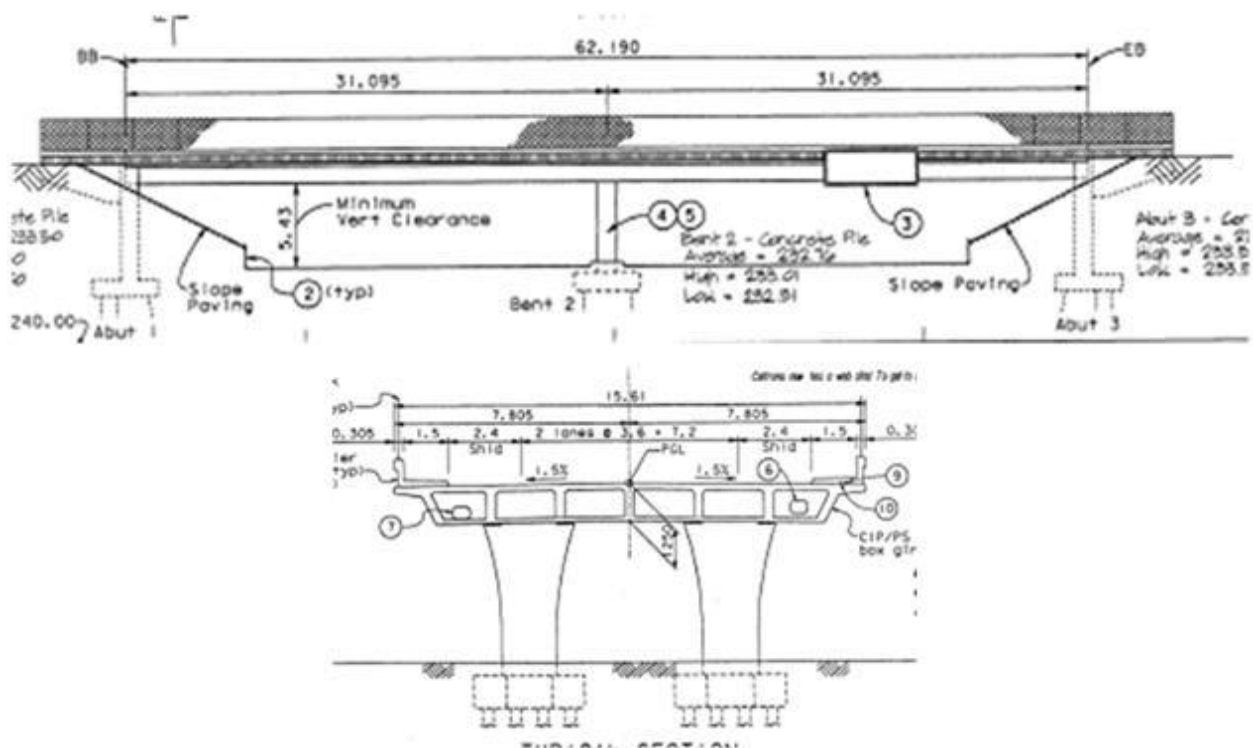
Table 27: Description of all bridge models and variations

Bridge Model	LS	AR	VR	DepthDiam	SpanHt
Original	1.03%	3.24	1.38%	0.74	5.72
A1	1.20%	3.24	1.38%	0.74	5.72
A2	1.50%	3.24	1.38%	0.74	5.72
A3	1.80%	3.24	1.38%	0.74	5.72
A4	2.30%	3.24	1.38%	0.74	5.72
B1	1.03%	2.73	1.38%	0.74	5.72
B2	1.03%	2.95	1.38%	0.74	5.72
B3	1.03%	3.41	1.38%	0.74	5.72
B4	1.03%	3.63	1.38%	0.74	5.72
C1	1.03%	3.24	0.40%	0.74	5.72
C2	1.03%	3.24	0.80%	0.74	5.72
C3	1.03%	3.24	1.00%	0.74	5.72
C4	1.03%	3.24	1.20%	0.74	5.72
D1	1.03%	3.24	1.38%	0.82	5.72
D2	1.03%	3.24	1.38%	0.94	5.72
D3	1.03%	3.24	1.38%	1.06	5.72
D4	1.03%	3.24	1.38%	1.14	5.72
E1	1.03%	3.24	1.38%	0.74	4.38
E2	1.03%	3.24	1.38%	0.74	5.21
E3	1.03%	3.24	1.38%	0.74	6.86
E4	1.03%	3.24	1.38%	0.74	7.68
E5	1.03%	3.24	1.38%	0.74	8.51

6.2.3. Results and discussion of study

The results of this sensitivity study shown here are the pushover curves of each of the bridge models and the PSDMs. Pushover curves show the capacity of the structure (Elnashai, 2001). The curve indicates the initial stiffness of the structure and the point of yielding, and the nonlinear behavior of the structure as a horizontal load is applied increasingly until a pre-determined stopping point. The pushover curves of the columns of the bridge for each design set are given in this section in Figure 34 through Figure 38.

As is shown, the pushover curves of models that varied longitudinal steel ratio and the ratio of column height to column diameter (aspect ratio) show significant changes as the parameter is changed. As the steel ratio is increased, the initial stiffness of the column increases and the columns are able to withstand greater loads before yielding. As the aspect ratio increases, or the height of the column increases, the columns get more flexible and lose strength. The other design parameters do not show as much influence is the steel ratio and aspect ratio on the pushover curve of columns. The volumetric ratio of the transverse reinforcement makes a small difference within the range of values tested. By increasing the superstructure depth to column dimension ratio, or the thickness of the superstructure, the column experiences an increase in ultimate load it can handle. The pushover curves for the different values of the span length to column height ratio show that not much difference is experienced in the capacity of the column until the two higher ratios are tested. Then, the column pushover curve shows an increase in the load carrying capacity of the column beyond the yield limit. The pushover curves offer a visual representation of the effect of the variation of these design parameters on the response of the bridges. The following PSDMs further illustrate the differences.
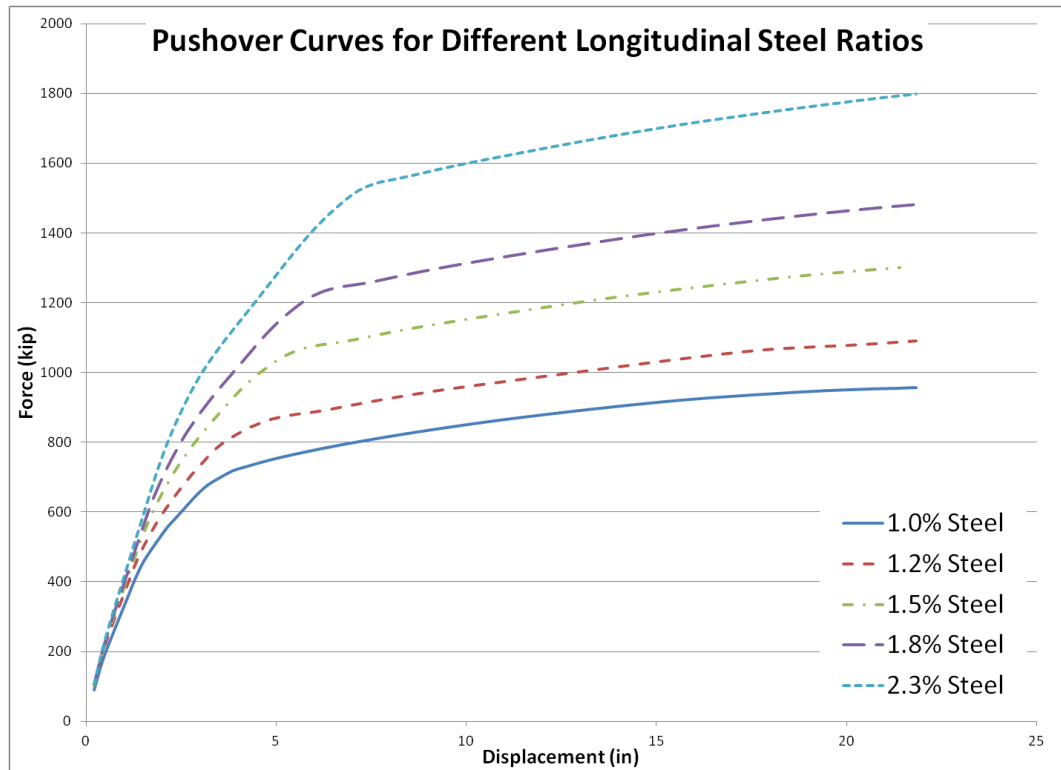
Figure 34: Pushover curves for different longitudinal steel ratios.
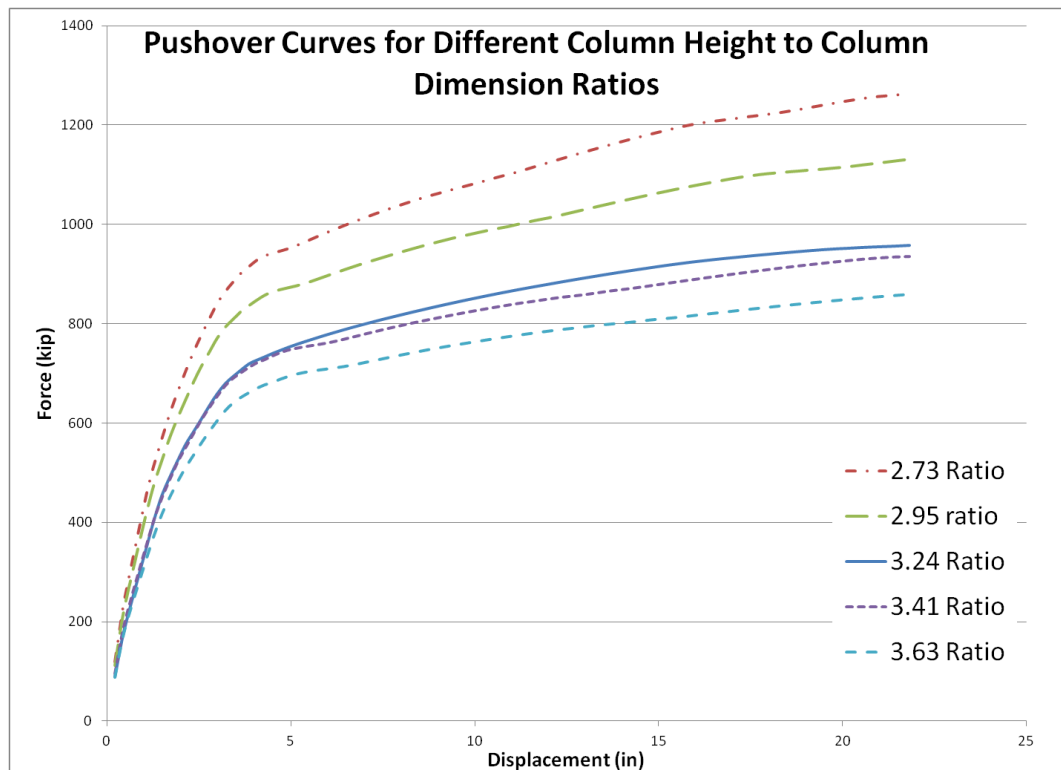
Figure 35: Pushover curves for different aspect ratios.

94
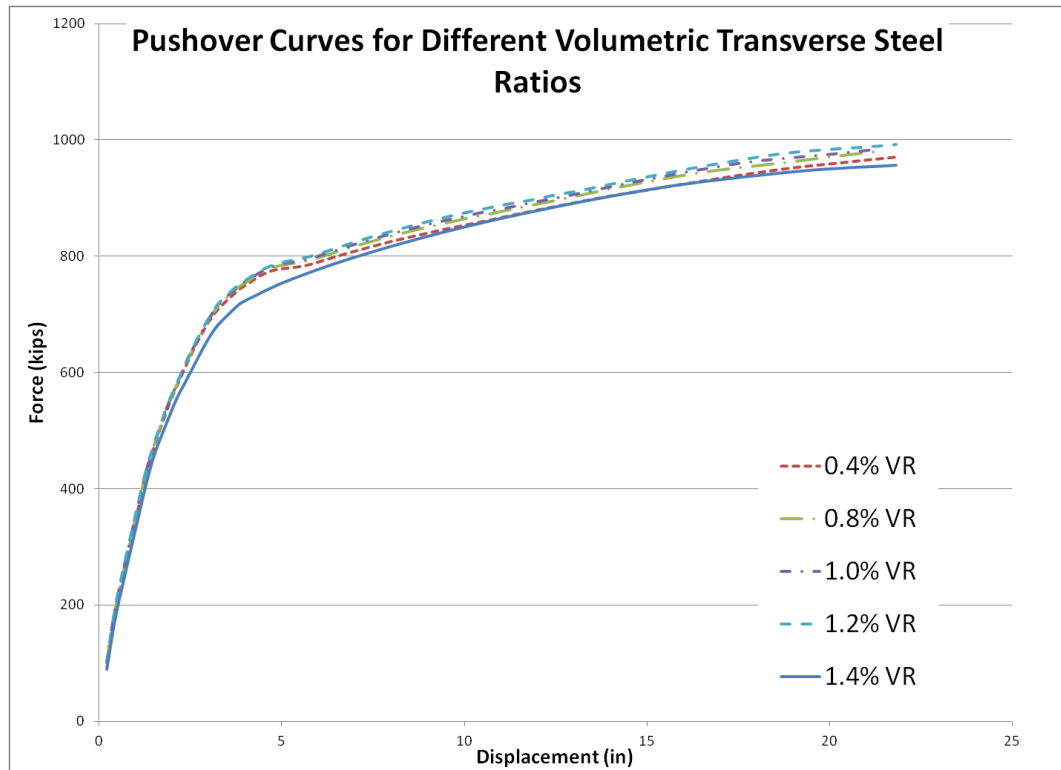
Figure 36: Pushover curves for different volumetric transverse steel ratios.
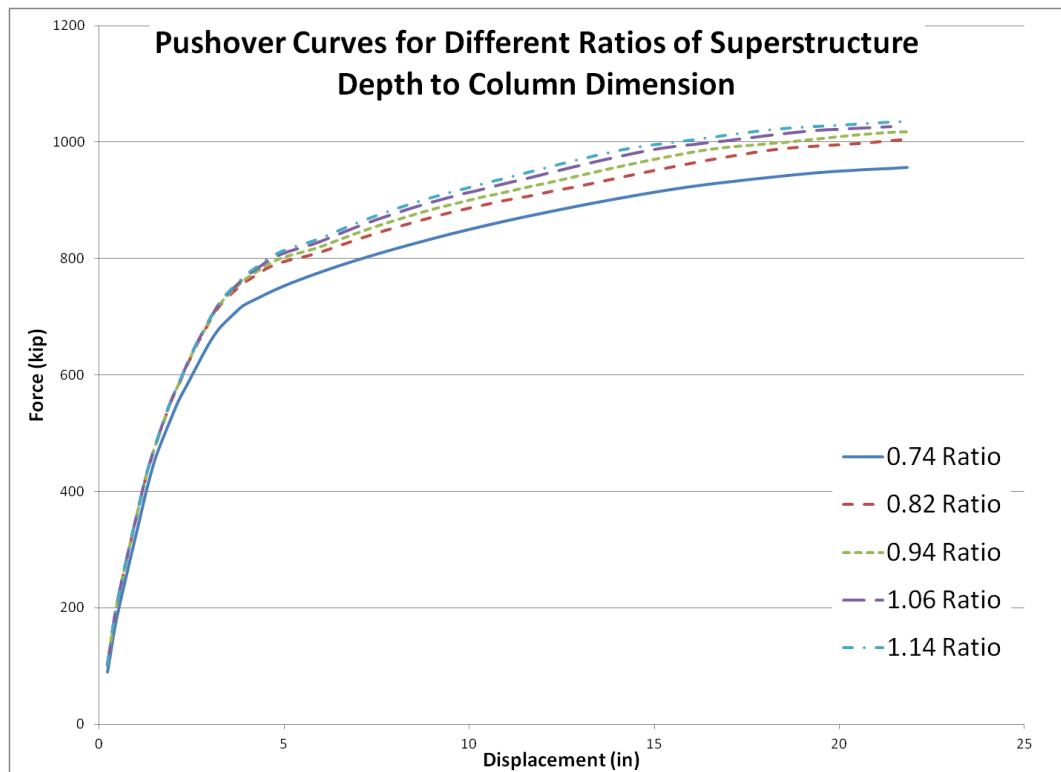
Figure 37: Pushover curves for different superstructure depth to column diameter ratios.

95
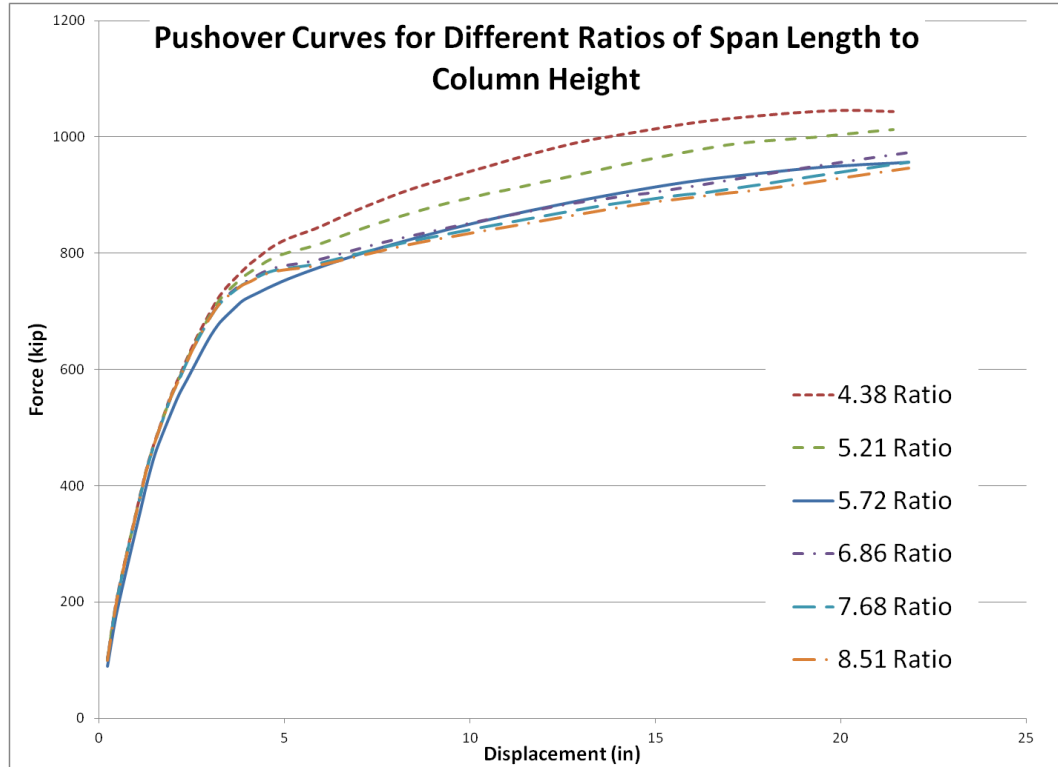
Figure 38: Pushover curves for different span length to column height ratios.

A probabilistic seismic demand model (PSDM) is a pairing of one demand measure (DM) and one ground motion intensity measure (IM) to develop a relationship that can be used to predict the demand on the structure. Intensity measures used for the development of PSDMs can vary; usually the criteria for choosing an IM includes an easy derivation from ground motion measurements, independence from ground motion characteristics, and good correlation with results from existing data (Mackie, et al., 2001). For this study, the Spectral acceleration at the fundamental period (SAFP) of the ground motions and the column curvature ductility were chosen to be the IM-DM pair used in the development of PSDMs for the response of the column. It is common to assume that the relationship of this type of PSDM can be approximated by a lognormal distribution (Choi, et al., 2004). Equation 1 shows the relationship between the IM and

96

DM used as the PSDM (Cornell, et al., 2002). The parameters of this relationship were determined with a linear regression that best fit all of the data from the analyses.

$$\ln(DM) = \ln(a) + b * \ln(IM) \tag{6.1}$$

When analyzing the PSDMs, the median values, slope and dispersion of the model were monitored, as these values are easily compared between models (Ramanathan, et al., 2010). Table 28 gives the intercept and slope of the regressed line, as well as the dispersion of the demand and R^2 values for each bridge demand model. Low dispersion and high R^2 values indicates a mode-less variation about the median demand (Padgett, et al., 2008) and a more accurate fit of the model in Eqn. (6.1) (Ramanathan, et al., 2010). A higher slope, or "b" value from the regression equation, indicates a higher dependence of the response variable on the intensity measure (Shafieezadeh, et al., 2011). The "a" value is used to determine the median of the fragility curves, and indicates the position of the fragility curve. Lower "a" values correspond to a higher median IM, and thus lower vulnerability of the component or bridge, at any limit state (Ramanathan, 2012).

As is shown in Table 28, many of the dispersion values, R2, and slopes are similar comparing the bridge models. The main differences are presented in the "a" values, which will distinguish the fragility curves of each model. These results are more clearly shown in PSDM plots, shown in Figure 39 through Figure 43. Visually, one can conclude that varying the span length to column height ratios had greater effects on the demand model than varying any of the other design parameters. The coefficients of the PSDMs for set E, which corresponds to the models with varying span length to column height ratios, reveal that the "a" values vary from 70% to 160% from the PSDM of the original bridge model. This is the highest variation of any of the design parameters tested. The coefficient "a" in Set E reveals that as the span length of column height ratio increases the vulnerability of the bridge increases significantly. The coefficients for Set A, which

corresponds to the models varied by the longitudinal steel ratio, show that the design parameter also has a significant effect on the PSDM of the bridge. The difference between the original bridge model and the model with the highest steel content is over 160%. The coefficient "a" also indicates that as the longitudinal steel increase, the vulnerability of the bridge decreases. Varying the volumetric ratio and aspect ratio seem to have the least effect on the demand models, with the maximum difference between the median values of the original bridge and the model with the lowest VR being around 16%. The coefficient "a" in Set C shows that as the volumetric ratio decreases, the vulnerability of the bridge increases slightly.

Fragility curves were developed with the closed form solution given in Eqn. (6.2). Limit states were introduced in a previous section, and the limit states for ductile column behavior were used. One such fragility curve is shown in Figure 44, which shows the different curves developed for the original bridge and each bridge in Set A at the Slight damage level. Many trends suggested by the PSDMs are also present in the fragility curves; therefore only one fragility curve is shown here. The high variability in the median values of the PSDMs for the set of models that varied the longitudinal steel ratios led to a wide variance in the fragility curves for the same limit state. Again, varying the volumetric ratio showed the least effect on the fragility curves. The trends shown in the PSDMs followed in the fragility curves.

$$P[Demand > Capacity|IM] = \Phi\left(\frac{\ln\left(\frac{S_d}{S_c}\right)}{\sqrt{\beta_{d|IM}^2 + \beta_c^2}}\right) \qquad (6.2)$$

Table 28: PSDM coefficients for Column Curvature Ductility vs. Spectral Acceleration at T1.

PSDM Regression coefficients

Model	a	b	R^2	Sigma
Original	0.519	1.300	0.590	0.721
A1	0.433	1.241	0.570	0.717
A2	0.299	1.229	0.589	0.683
A3	0.088	1.445	0.435	1.095
A4	-0.324	1.120	0.307	1.120
B1	0.263	1.236	0.547	0.750
B2	0.393	1.272	0.583	0.716
B3	0.518	1.288	0.606	0.691
B4	0.521	1.264	0.628	0.649
C1	0.602	1.260	0.605	0.677
C2	0.559	1.269	0.597	0.693
C3	0.532	1.268	0.591	0.702
C4	0.522	1.278	0.595	0.702
D1	0.397	1.228	0.572	0.709
D2	0.293	1.183	0.560	0.705
D3	0.215	1.154	0.554	0.684
D4	0.189	1.141	0.557	0.668
E1	-0.324	1.201	0.646	0.547
E2	0.057	1.148	0.538	0.704
E3	0.882	1.268	0.543	0.757
E4	1.176	1.283	0.584	0.718
E5	1.349	1.209	0.594	0.661
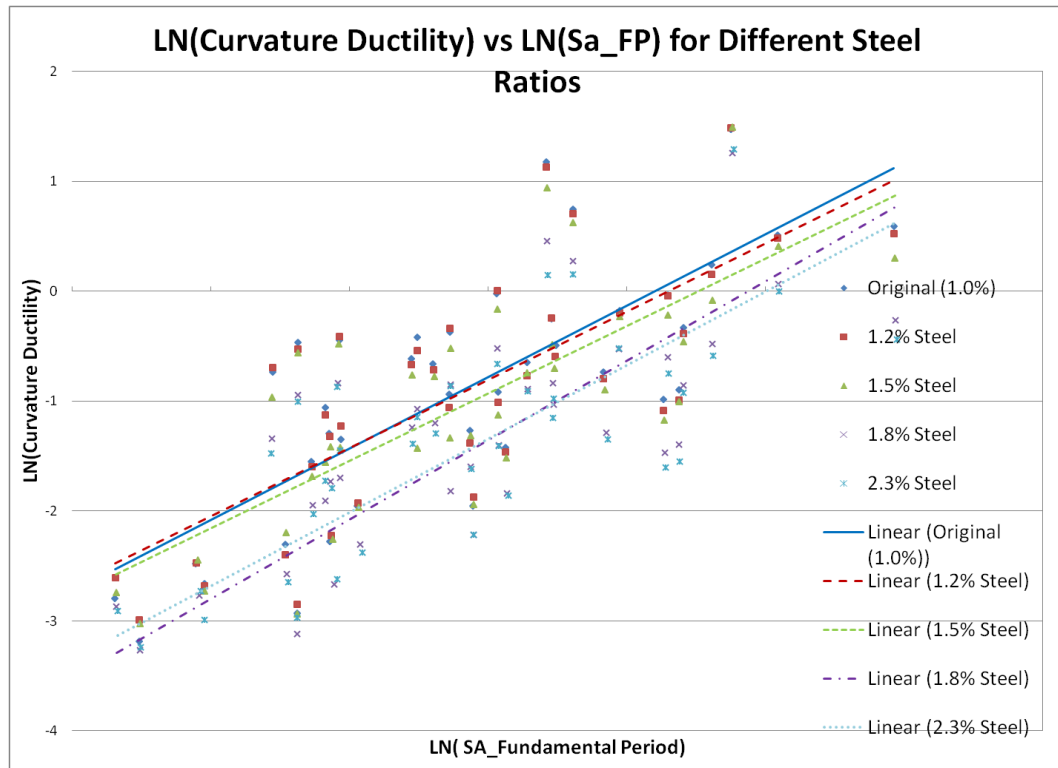
Figure 39:PSDM for different longitudinal steel ratios.
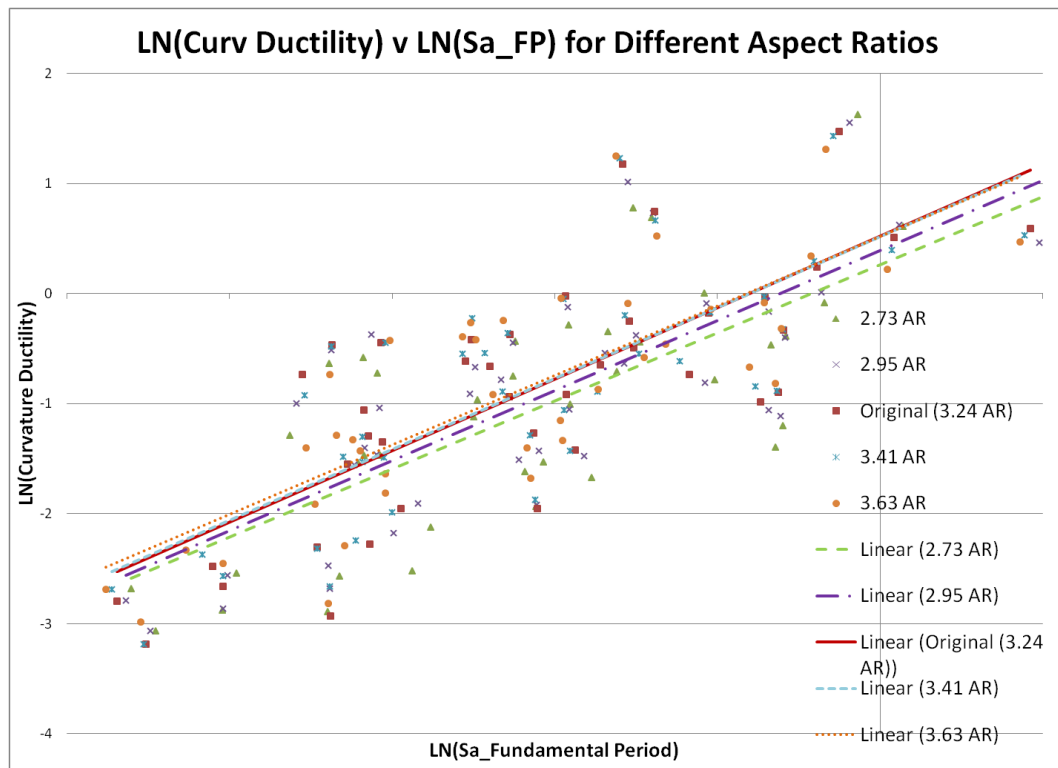
Figure 40:PSDM for different aspect ratios.
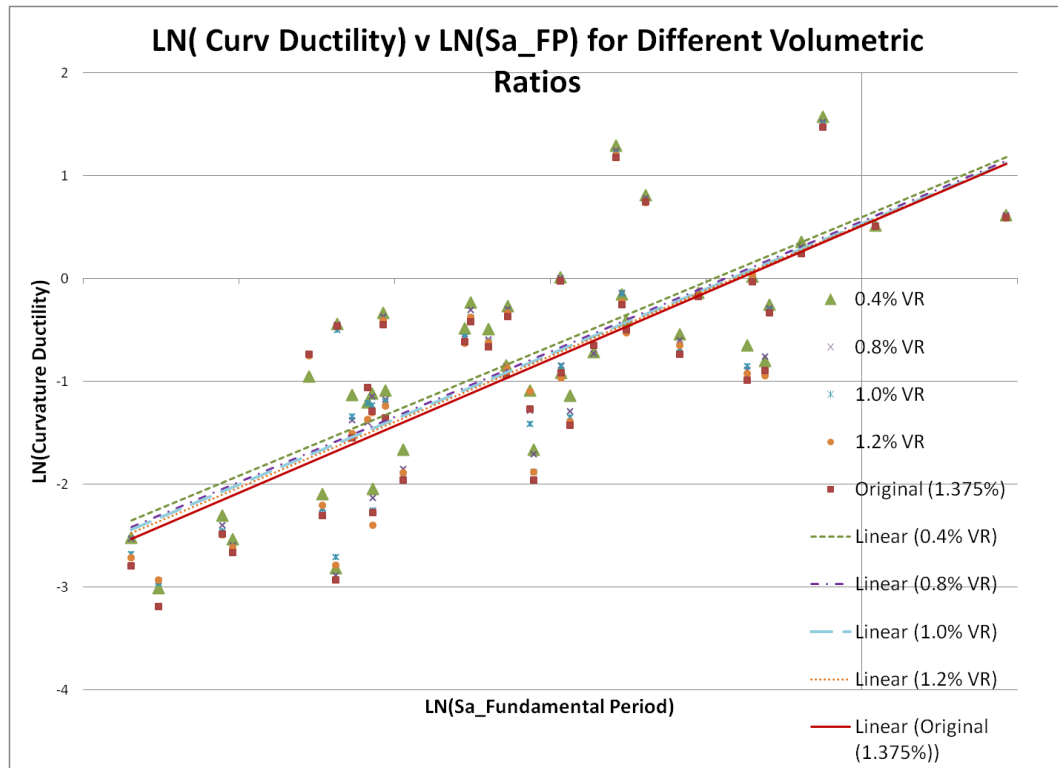
Figure 41:PSDM for different volumetric transverse steel ratios.
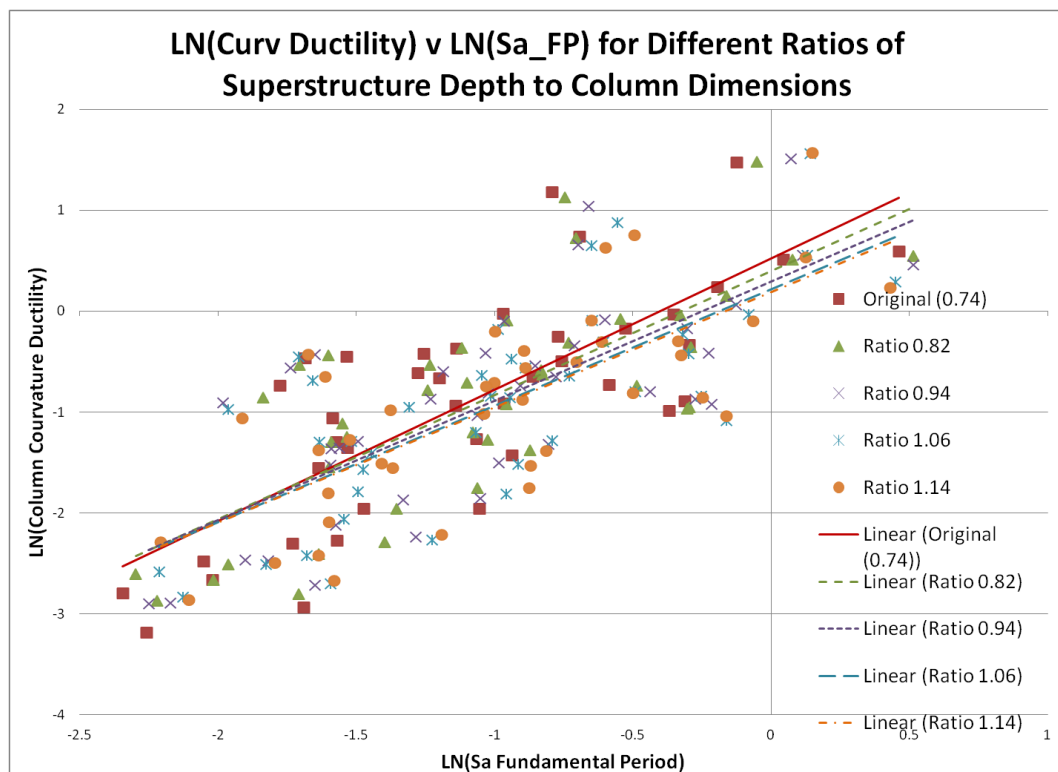
Figure 42:PSDM for different superstructure depth to column diameter ratios.
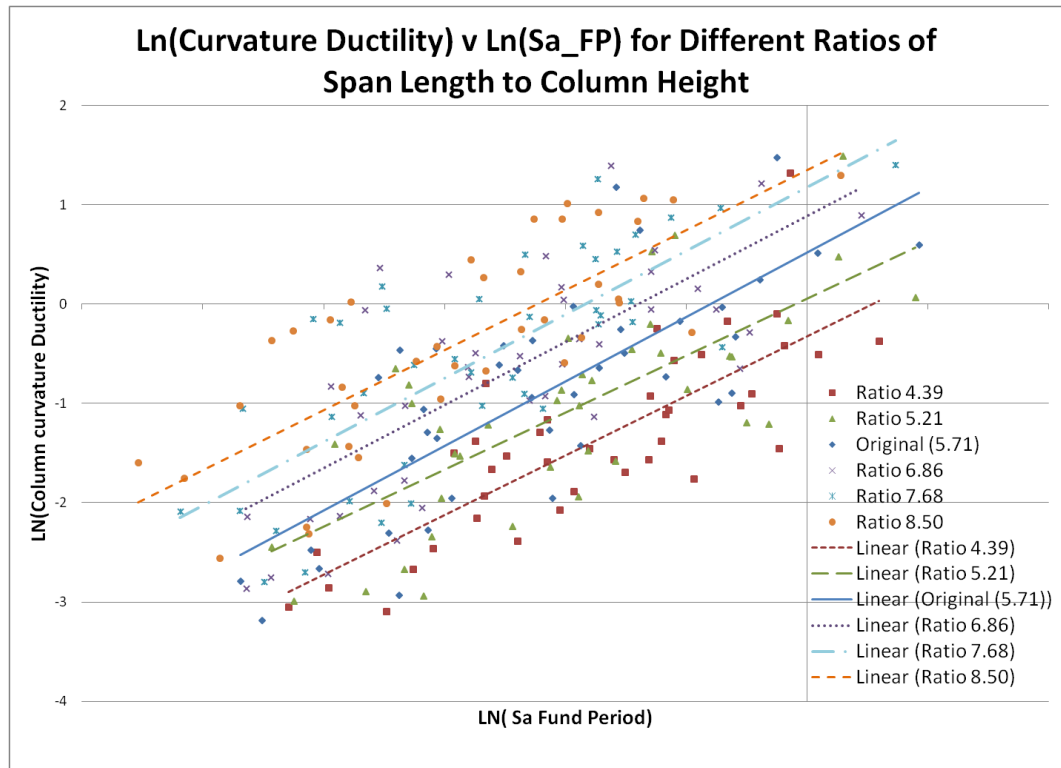
Figure 43:PSDM for different span length to column height ratios.
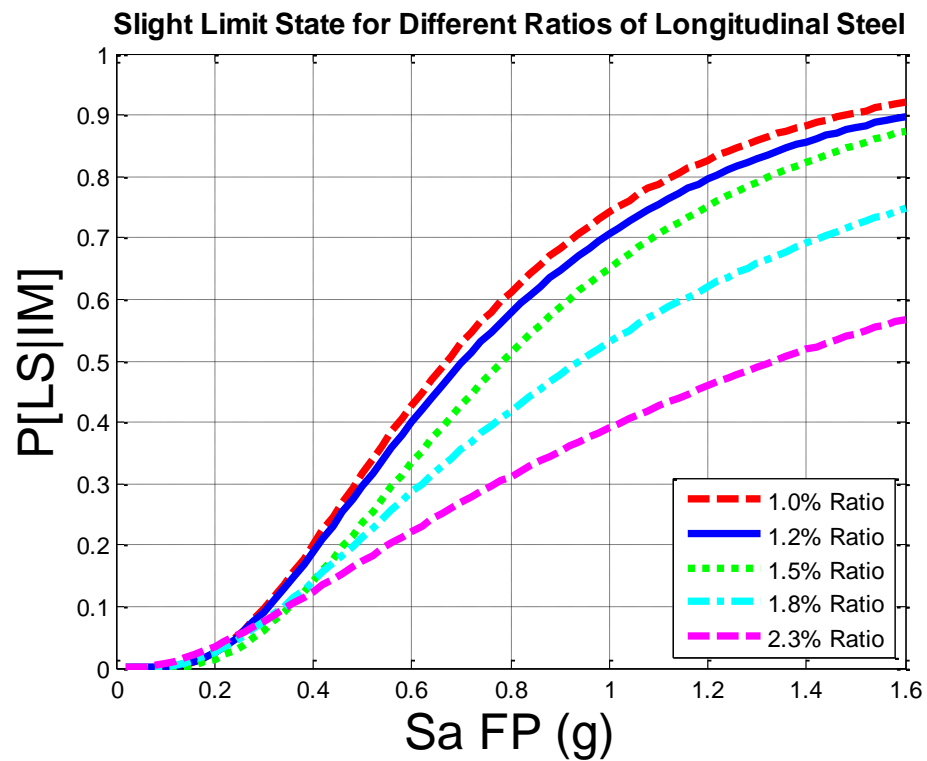
Figure 44: Fragility curve with different longitudinal steel ratios.

6.2.4. Conclusions

The pushover curves, PSDMs, and fragility curves developed from this sensitivity study show the effects of the proposed design parameters on the demand and the response of the bridge. The variation of all of the design parameters showed some effect on the response of the bridge, with some parameters showing more of an effect than others. In the pushover analysis of the columns, the percentage of longitudinal steel reinforcement in the column showed the greatest effect on the capacity of the bridge column, followed by the aspect ratio of column height to column diameter. The amount of transverse reinforcement in the column showed the least effect on the variation of the capacity of the column based on the pushover curve. In comparison, the probabilistic seismic demand model calculation and subsequent fragility curve generation revealed that the span length to column height ratio had the greatest effect on the performance of the bridge. After which the longitudinal steel ratio, the superstructure depth to column diameter ratio, and the aspect ratio showed a significant effect on the determination of the PSDM, in order of maximum difference in the "a" value. Again, the transverse steel ratio in the column had the least effect on the performance of the bridge, with the smallest difference between the original bridge results and the maximum difference. Based on the results, these design parameters appear to be good measures of the response of the bridge and should be included in the methodology presented here for bridge specific fragility. To further show that these parameters are well chosen for this task, a sensitivity study with a more statistical aspect is presented next.

6.3. Statistical Sensitivity Study using a Design of Experiment and ANOVA study

6.3.1. Introduction to statistical study

A more efficient method of conducting a sensitivity study, other than the one-factor-at-a-time approach, is using a statistical approach (Nielson, 2005). The "one-

factor-at-a-time" approach used in the previous section had many setbacks, including the inefficient manner of varying the parameters and the inability to determine how the changes in variables interact to affect the response of the bridge. For the statistical approach, a design of experiment (DOE) is chosen in order to systematically vary the design parameters in order to determine the effect of the parameters on the response variable. This approach also allows for the investigation of the interaction of the different parameters on the response variable (Nielson, 2005). In this section, a sensitivity study using the statistical approach will be presented. This section details the different design parameters included in the study as well as the tests done on the data produced from the DOE. For this statistical study, additional design parameters were included to test for the significance of the effect on the response of the bridge components. These additional parameters, described below, were added to investigate whether these parameters could give more information on the behavior of the components that would enhance the bridge specific fragility estimation.

6.3.2. Additional Parameters

The additional parameters introduced into this statistical study to gather more information on what affects the response of the bridge components that are monitored. In order to make the estimation of fragility as precise as possible for each bridge input, a parameter that is determined during the design of the bridge to have a significant effect on the response should be included in the bridge-specific method. In this section, the parameters investigated here in addition to the five mentioned earlier are the width of the bridge, the height of the backwall of the abutment, and the type of soil used as backfill behind the abutment backwall. The width of the bridge affects the period of the bridge by increasing the mass of the bridge with increased width. Since one of the fundamental modes of the bridge is transverse, the width of the bridge could play a large role in determining the period and subsequent response of the bridge. The height of the backwall

104

affects the stiffness of the abutment soil springs that are included in the analytical bridge model and contribute to the longitudinal response of the abutment. Thus, the backwall height is expected to affect the response of the abutment in the bridge model. The type of backfill soil affects the stiffness of the abutment soil springs as well, and is expected to affect the bridge response for similar reasons. These additional parameters are tested in this statistical sensitivity study in hopes of finding more parameters that can accurately predict the response of the bridge system for use in the bridge-specific fragility method.

6.3.3. Details of statistical study and Development of bridge models

A sensitivity study was completed to test the effects of varying the design parameters on the responses of key bridge components: column curvature ductility, abutment gap movement, longitudinal and transverse bearing deformation, and movement of the joint seals. This investigation was the final step toward finalizing the set of design parameters to be used in the bridge-specific fragility methodology presented later in this thesis. After the set of design parameters is defined, a multi-parameter fragility methodology can be implemented in order to produce individualized curves for a specific bridge design based on using the design parameters as conditioning variables in the fragility formulation. The five design parameters introduced earlier were varied in a statistical manner to create bridge models for analysis in order to quantify the effects of each parameter on the response of the bridge system and components.

The base bridge model from which all of the bridge models used in the study was built upon was based on median values of bridge characteristics, such as those listed in Table 17, excluding the design parameters in question. The base bridge is a two span integral concrete box girder bridge with zero skew or curve, two columns at the integral bent, and a seat-type abutment. Figure 32 depicts the plan and elevation views of a bridge from the California bridge plan survey that is similar to the base bridge developed for this study.

105

The sensitivity study was initially designed as a confirmatory experiment, in which the factors investigated have been suggested to be significant in previous studies (Kutner, et al., 2005). This is true for the first five design parameters, which were studied with a deterministic approach in the previous section. This experimental study will be used to confirm the importance of each factor in determining the response of different bridge components, as well as determine the importance of the additional design parameters introduced previously. A design of experiment (DOE) was developed in order to determine the effects of each individual factor, as well as interactions between them. A two-level full factorial design was chosen as the DOE of choice for this study. A two-level factorial experiment looks at each factor at two levels, usually the upper and lower bound of the range of the factor. This type of experimental design produces 2^k experimental runs, corresponding to the required number of unique bridge models for analysis, where k is the number of factors, or parameters, in the study. This type of experimental design is helpful in this type of screening study as it leads to the identification of the factors in the study with the most significance on the response variable from a larger set of factors to consider (Kutner, et al., 2005). With the additional parameters tested, the number of factors in the DOE is 8, and thus 2^8 (256) separate experimental runs along with the bridge models would need to be established. The DOE was created in MATLAB (2011). Table 29 shows part of the schedule of factors that correspond to the values of the design parameters that will be used to create bridge models for this sensitivity study. The [--] symbol indicates the minimum value, and the [+] symbol indicates the maximum value. The upper and lower bounds given in Table 24 were used as the minimum and maximum values of each factor from the bridge sample.

Each of the bridge models developed for each run from the DOE described earlier was subjected to 40 ground motions chosen from a suite of 160 broadband earthquake ground motions from the Pacific Earthquake Engineering Research Center (PEER) Transportation Research Program ground motions compiled by Baker, et al. (Baker, et

al., 2011). Further details of this ground motion suite, which is used in its entirety for the development of the design tool, can be found in a previous chapter. These 40 ground motions were chosen randomly from the 120 ground motions to ensure a variety of responses of the bridge models from each of the runs developed from the DOE. The peak ground acceleration (PGA) and spectral acceleration at one second values of these 40 chosen ground motions are shown in Figure 45. As is shown, the ground motion set encompassed a wide range of ground motion intensity levels, ranging from less than 0.05g to 0.5g in terms of PGA. The range is wider for the spectral acceleration at one second values.

Table 29: Part of design of experiment for the statistical sensitivity study.

Run	LS	VR	AR	SpanHt	DepthDiam	Width	BackwallHt	Soil
1	--	--	--	--	--	--	--	--
2	--	--	--	--	--	--	--	+
3	--	--	--	--	--	--	+	--
4	--	--	--	--	--	--	+	+
5	--	--	--	--	--	+	--	--
6	--	--	--	--	--	+	--	+
7	--	--	--	--	--	+	+	--
8	--	--	--	--	--	+	+	+
9	--	--	--	--	+	--	--	--
10	--	--	--	--	+	--	--	+
11	--	--	--	--	+	--	+	--
12	--	--	--	--	+	--	+	+
				Runs Continued…				
250	+	+	+	+	+	--	--	+
251	+	+	+	+	+	--	+	--
252	+	+	+	+	+	--	+	+
253	+	+	+	+	+	+	--	--
254	+	+	+	+	+	+	--	+
255	+	+	+	+	+	+	+	--
256	+	+	+	+	+	+	+	+
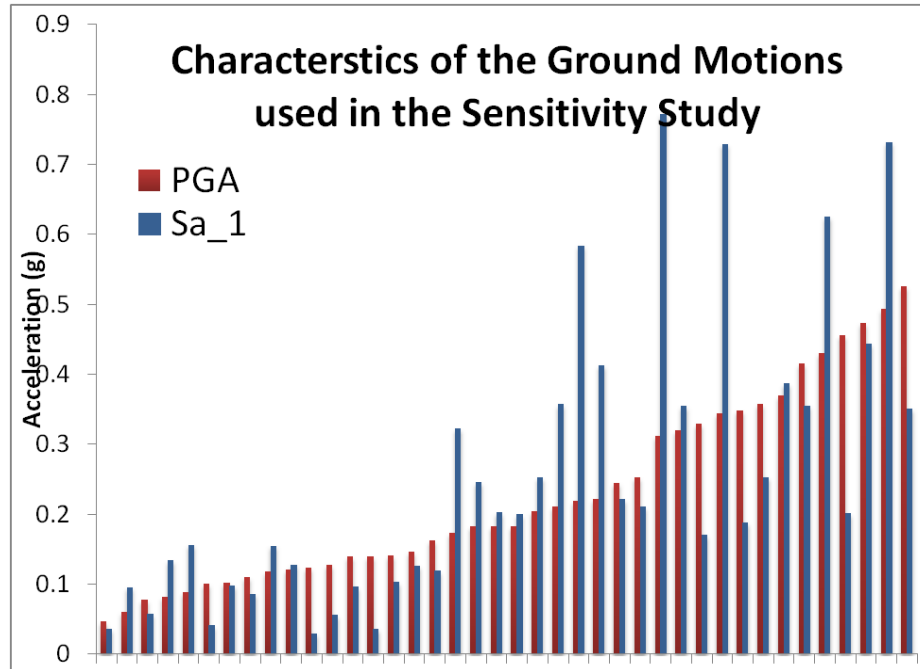
Figure 45: PGA and Sa_1 values of ground motions used in sensitivity study.

Finite element bridge models were created and analyzed in OpenSees (Mazzoni, et al., 2009). Figure 14 showed a typical layout of the nodes and elements that define the bridge model. These bridge models were analyzed using nonlinear time history analyses. Each model was subjected to two orthogonal ground motions at an incidence angle of zero input into the defined support nodes. Recorders defined in OpenSees recorded the deformation, displacement, force or stress specified at particular elements or nodes along the bridge in order to find the response of the bridge system after the analysis. Responses were recorded at the top and bottom elements of the column component to find the maximum column curvature response. Responses were recorded at the nodes of the abutment to find the maximum displacement of the deck from the abutment, as well as the movement of the abutment. Responses were also recorded at the nodes representing the bearing responses to determine the deformation of the bearing in the longitudinal and transverse directions. These recorded responses serve as the data used to determine the effect of the design parameters on the response of the bridge.

6.3.4. Results of the study

After all of the analyses were run in OpenSees, the recorded responses of the different bridge parameters were extracted to be used to determine the effect of the different design parameters on the component responses. The component responses monitored for this screening study are the column curvature ductility, movement at the abutment gap, transverse and longitudinal bearing deformation, and the movement at the joint seals. These components correspond with those introduced in the adopted capacity model for this research in a previous chapter. Different analyses are presented here to illustrate the results of the screening study. A visual representation of the results of the study is shown with box plots. Box plots are type of diagnostic measure that can visually show the distribution of a data set quickly (Kutner, et al., 2005). A box plot shows the median value of the data set, along with the first and third quartiles and any outliers of the data. Box plot can also indicate a significant difference of medians between two sets of data (2011). In Figure 46 through Figure 50, the box plots for the low (1) and high (2) of each design parameter (DP) tested for each of the component responses monitored. The numbering of the DP in each figure is as shown in Figure 46. A significant difference between the means of the two data sets is indicated by if the intervals around the median, shown by the ends of the notches, do not overlap (2011). As is shown in the figures, most of the design parameters showed a significant effect in the medians of the data indicated by the misalignments of the median values between the high and low parameter range values. DP-7 and DP-8 however do not seem to have significant effect on the determination of most of the component responses.
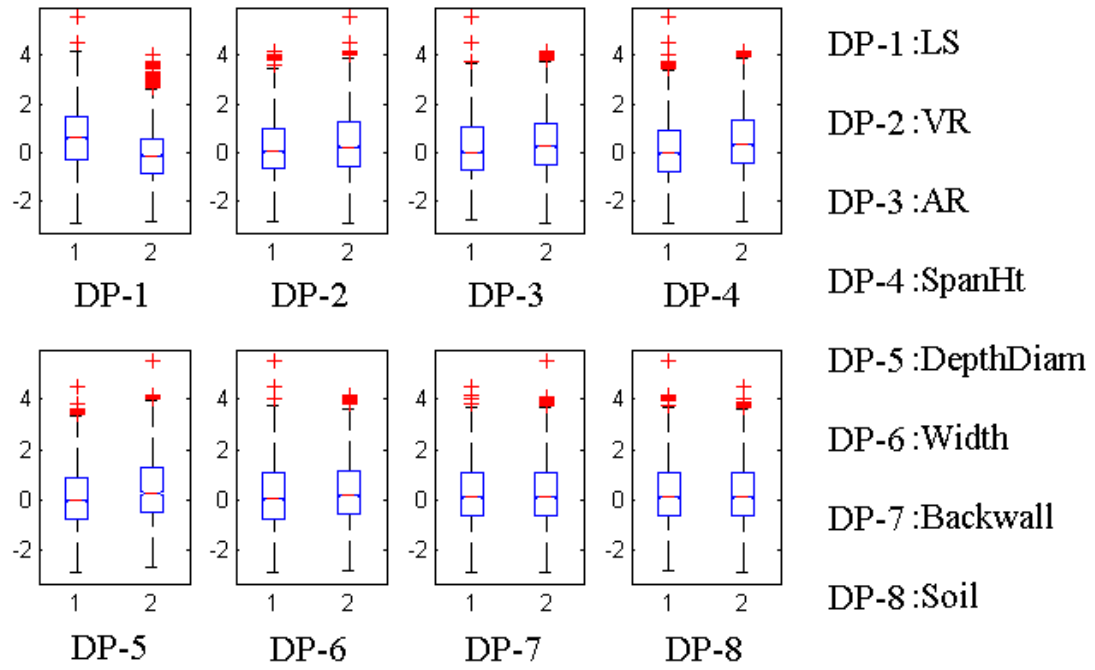
Figure 46: Box plot for the column response for the design parameters of the screening study.
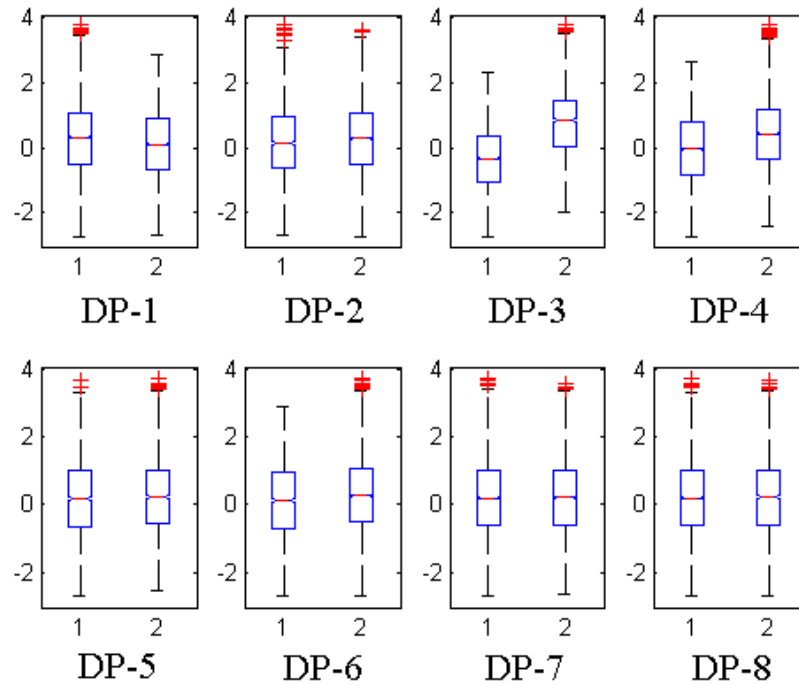
Figure 47: Box plot for the abutment gap response for the design parameters of the screening study.
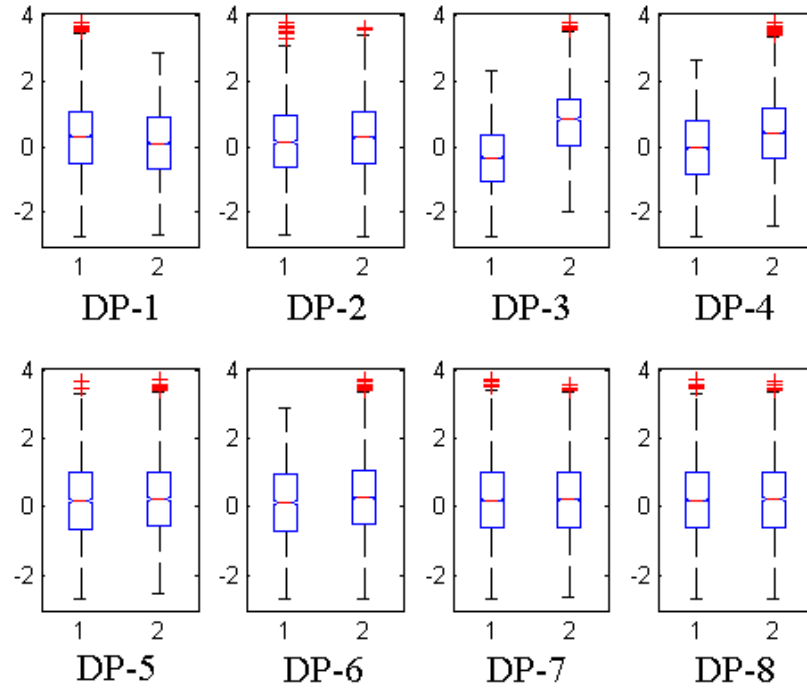
Figure 48: Box plot for the longitudinal bearing response for the design parameters of the screening study.
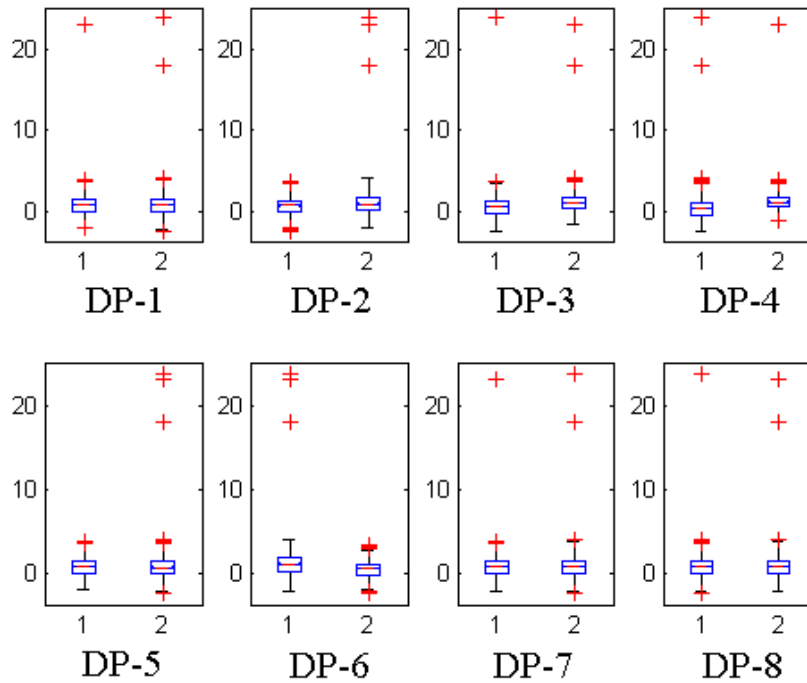
Figure 49: Box plot for the transverse bearing response for the design parameters of the screening study.
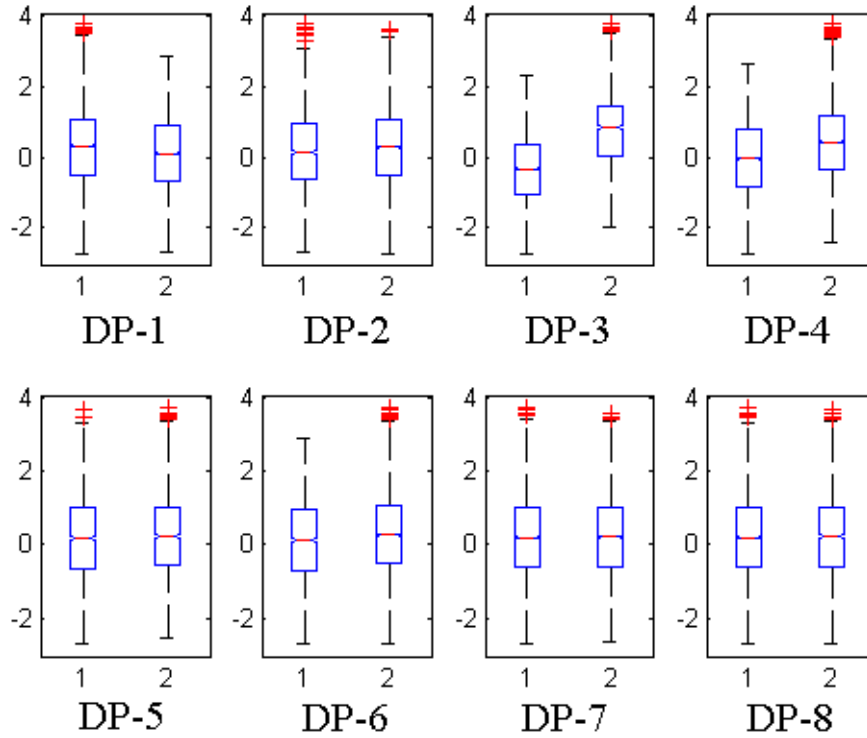
Figure 50: Box plot for the joint seals response for the design parameters of the screening study.

The other analysis performed to test the significance of the screened design parameters is the Analysis of Variance test. The different component responses were regressed against the design parameters to determine the significance of the parameters on the responses using Analysis of Variance (ANOVA) tests. JMP software and MATLAB were used to conduct ANOVA tests on the data from the analyses, which are presented in this section (2010) (2011). In conducting ANOVA tests, a hypothesis is considered and tested using the F-test (Kutner, et al., 2005). In this case, the null hypothesis (H_0) is that the coefficient (β_1) of a regression relationship between a component response (Y) and a design parameter (X) (see Eqn. 2) is equal to zero, and therefore there is no regression relation between the response variable and the design parameter. The hypothesis tests and F statistic is computed per Eqn. 3 for a single variable regression (Kutner, et al., 2005). MSR is the mean regression sum of squares,

MSE is the mean squared error of the regression, and [n-2] represents the number of degrees of freedom in the relationship. For this study, α is assumed to be equal to 0.05, which is a typical value used to test statistical significance. P-values are the probability of the calculated F statistic being greater than the $(1-\alpha)100$ percentile of the F distribution.

$$Y = \beta_0 + \beta_1 * X \tag{6.3}$$

$$
\begin{aligned}
&H_0 : \beta_1 = 0 \\
&H_a : \beta_1 \neq 0 \\
&F^* = MSR/MSE \\
&\text{If } F^* \leq F(1-\alpha; 1, n-2), \text{ conclude } H_0 \\
&\text{If } F^* > F(1-\alpha; 1, n-2), \text{ conclude } H_a
\end{aligned}
\tag{6.4}
$$

Table 30 shows the p-values from the ANOVA analysis of six different bridge component responses for each design parameter. Statistical significance in an ANOVA test is determined by the value of the p-value; if the p-value is less than the predetermined α level, then it shows that the factor being tested has a statistically significant effect on the response quantity according to the test. In this case, the p-value is the probability that $F^* > F(1-\alpha; 1, n-2)$, similar to that shown in Eqn. (6.4). Table 30 shows the ANOVA test completed from a regression of the design parameters against the untransformed component responses. Table 31 shows the result of the ANOVA tests for the same design parameters regressed against the component responses with a lognormal transformation. A lognormal transformation was used as the component responses will be transformed in the demand model described in the next chapter. As shown, almost every design parameter was found to be statistically significant in the prediction of one or more of the bridge component responses according to the ANOVA test and an α level of 0.05.

Table 30: P-values of the design parameters from ANOVA analysis

Parameter	Column Curvature Ductility	Movement of Abutment Gap	Longitudinal Bearing Deformation	Transverse Bearing Deformation	Movement of Joint Seals
LS	**0.0001**	**0.0001**	**0.0001**	0.6173	**0.0001**
VR	**0.0001**	**0.0001**	**0.0001**	0.1716	**0.0001**
AR	**0.0017**	**0.0001**	**0.0001**	0.6361	**0.0001**
SpanHt	**0.0001**	**0.0001**	**0.0001**	0.6113	**0.0001**
DepthDiam	**0.0001**	0.2788	0.2788	0.1803	0.2788
Width	0.7049	**0.0001**	**0.0001**	0.1715	**0.0001**
BackwallHt	0.7439	0.6750	0.6750	0.6302	0.6750
Soil	0.9858	0.6322	0.6322	0.6363	0.6322

Table 31: P-values of the lognormal transformation of the design parameters from the ANOVA analysis.

Parameter	LN of Column Curvature Ductility	LN of Movement of Abutment Gap	LN of Longitudinal Bearing Deformation	LN of Transverse Bearing Deformation	LN of Movement of Joint Seals
LS	**0.0001**	**0.0001**	**0.0001**	0.3024	**0.0001**
VR	**0.0001**	**0.0001**	**0.0001**	**0.0001**	**0.0001**
AR	**0.0001**	**0.0001**	**0.0001**	**0.0001**	**0.0001**
SpanHt	**0.0001**	**0.0001**	**0.0001**	**0.0001**	**0.0001**
DepthDiam	**0.0001**	**0.0016**	**0.0016**	**0.0001**	**0.0016**
Width	**0.0001**	**0.0001**	**0.0001**	**0.0001**	**0.0001**
BackwallHt	0.8407	0.6329	0.6329	0.5206	0.6329
Soil	0.6954	0.6415	0.6415	0.3362	0.6415

6.3.5. Conclusions

As is shown by the box plots and the ANOVA tests above, many of the design parameters tested exhibited a significant effect on the response of the bridge components monitored. Consistent with the findings of the deterministic screening described earlier in the chapter, the first five design parameters showed statistical significance in the resulting response of the bridge components. In Table 30, the ANOVA results show that the first five parameters had a significant effect on the column curvature ductility, while only the superstructure depth to column diameter ratio did not have a significant effect on the abutment gap, longitudinal bearing deformation and the movement of the joint seals. No

parameter affected the transverse bearing response. When looking at the effect of the design parameters regressed against the lognormal transformation of the bridge components, all of the first five design parameters were significant in determining the response of the five bridge components, except in the case of the transverse bearing movement.

Of the additional parameters tested, the width of the superstructure, backwall height of the abutment, and soil type, only the width of the superstructure showed a significant influence on the response of the bridge components. When regressed against the untransformed component response, the width affected the abutment gap, longitudinal bearing movement, and the movement of the joint seals, while it had a significant impact on all of the transformed component responses. This analysis leads to the final set of design parameters that will be used to develop the bridge-specific methodology to be fully detailed in the next chapter. Six design parameters will be used, with the width of the superstructure joining the first five design parameters. The process of incorporating these parameters into fragility analysis as well as using them to create bridge specific fragility curves will be detailed in the next chapter.

CHAPTER 7

BRIDGE SPECIFIC FRAGILITY METHOD

The main focus of this research was to find a way to incorporate fragility analysis into the bridge design process in order to determine the performance of the bridge and ensure compliance with design specifications. This objective could not be practically attained using the fragility methods and curves in use today, many of which are generalized for large bridge classes (Basoz, et al., 1999)(Nielson, 2005). While analytical fragility curves can be developed deterministically for specific bridges, current bridge-specific methods involve time-intensive bridge modeling, computer simulations and post-processing of data (Gardoni, et al., 2002) (Mackie, et al., 2007), which could be in addition to the analyses required for the initial bridge design. This may not be practical in the current bridge design process in use. While the BridgePBEE tool performs performance based earthquake engineering for new bridge designs and creates fragility curves, it also requires extensive computer simulations to determine the fragility curves (Lu, et al., 2011). From these observations, it was determined that fragility curves specific to a new bridge are needed for the use in the application of seismic design, specifically fragility curves or estimates that can be calculated or determined quickly by way of certain significant design parameters that affect the performance of the bridge.

In order to create these bridge-specific fragility curves, several options were considered. Current methods of developing fragility curves involve creating single parameter probabilistic seismic demand models (PSDM) that establish a two-parameter lognormal relationship between a component response quantity and a ground motion intensity measure. Because this demand model only conditions the response of the components on the ground motion intensity measure, the use of that method for the bridge-specific needs of this research project, fragility curves would have to be developed

for every possible configuration of the bridge type of this study. That would require a prohibitive amount of analyses; therefore, a different method of developing fragility must be used. Another option considered was the use of modification factors, which have been used in past research to modify fragility estimates based on bridge characteristics such as skew and soil effects (Mander, 1999). This approach would require the development of the fragility curves using a single parameter PSDM as previously described for the class of bridge studied, and develop modification factors to account for the variation of the design parameters to multiply with the fragility estimates. This option was not appealing as the simplification of the complex behavior of the bridge with modification factors was not deemed to be sufficient for this research. This idea was rejected as well.

The option that was chosen was to propose a new fragility methodology, which became the bridge-specific fragility method. The main concept of this option is that a parameterized fragility method would be developed that could produce fragility curves that are specific to the design bridge of the user. Recently, parameterized fragility curves have been developed for different structures and purposes (Seo, et al., 2012)(Ghosh, et al., 2012), but none have been developed targeting the design of new bridges and for use in the seismic design process. The other advantage of this method is that bridge-specific fragility curves can be produced without the need to create the curves deterministically with new simulations for each new bridge design. In creating the framework for this type of analysis, it was determined that design parameters relating to the specific bridge that affect the performance of the bridge must be included in the PSDM used in the new fragility method. In this chapter, the approach to develop demand models as a function of multiple design parameters is presented based on the concepts of metamodeling, so that the metamodels can be used in the bridge-specific fragility framework. Also, the new framework and methodology of developing bridge-specific fragility curves is detailed in this chapter. Examples of fragility curves will then be included for the single-frame multi-column concrete box girder bridge class and the single-frame single column

117

concrete box girder bridge class. A validation of the method is presented in comparison to other more established fragility analysis methods.

7.1 Key components of BSFM

The bridge-specific fragility method (BSFM) detailed in this chapter aims to incorporate fragility analysis into the seismic design process. A general overview of the method is shown in Figure 51. Steps to create bridge-specific fragility include creating a multi-parameter metamodel, performing nonlinear time history analyses on analytical bridge models, fitting the data from the analyses with the metamodel, convolving the demand and capacity models, and using logistic regression to calculate bridge-specific fragility.
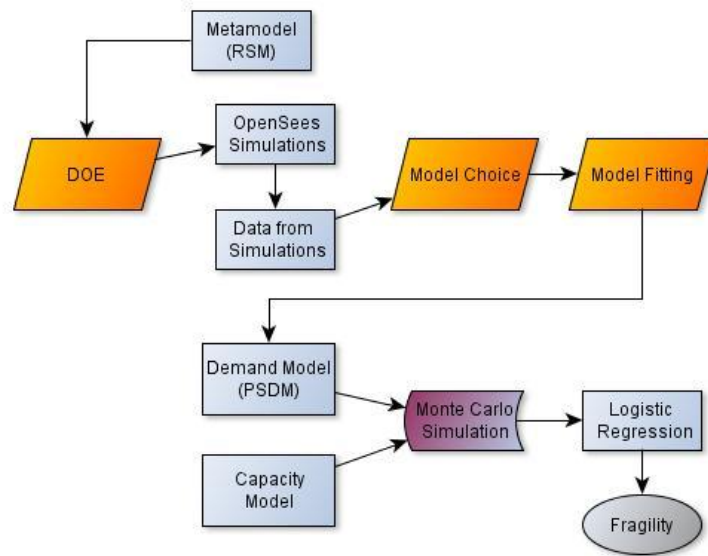
Figure 51: Steps to determining the fragility with the bridge-specific fragility method. Resulting fragility models can be readily applied to newly designed bridges.

As mentioned before, the bridge-specific fragility method involves aspects that are not found in traditional fragility methods. In this section, the key components of the method that separate it from other analytical fragility methods in use today will be described. This section will detail the multi-parameter seismic demand model, or bridge-specific probabilistic seismic demand model (PSDM), developed to include the design

parameters that enable the development of bridge-specific curves. This seismic demand model was developed based on the concept of metamodels, which will also be detailed. The use of logistic regression is also highlighted in this section. Logistic regression is used to calculate the fragility of the bridge using the bridge-specific design parameters.

7.1.1 Multi-Parameter Probabilistic Seismic Demand Model

<u>7.1.1.1 Introduction to Metamodels</u>

A metamodel is a "model of a model" (Simpson, et al., 2001). It is a statistical technique used to replace computationally expensive simulations with an approximation to the analysis. The metamodel represents or approximates the true nature of a computer analysis by estimating the response due to certain input variables with a closed form solution (Towashiraporn, 2004) . In Eqns. (7.1-3), the true relationship (7.1), the model of a model (metamodel) (7.2), and the true model with an error term (7.3) are presented, respectively. In the equations, *y* represents the response or predicted variable, *f(x)* is the true relationship between the predictor variables and response variable, *g(x)* and $\hat{y}$ represent the approximated model created by the metamodel, and *ε* represents the error between the true response and the predicted response. Metamodels are used to closely approximate the true relationship between predictor and response variables, and are useful in replacing computationally expensive computer simulations with appropriate analytical relationships (Ghosh, et al., 2012). Metamodels have been used in many engineering applications, to replace expensive computer simulations, such as for component optimization design as well as fragility analysis (Simpson, et al., 2001)(Towashiraporn, 2004).

$$y = f(x) \tag{7.1}$$

$$\hat{y} = g(x) \tag{7.2}$$

$$y = \hat{y} + \varepsilon \tag{7.3}$$

There are three steps to developing a metamodel. First, an experimental design must be chosen, followed by selecting a model to fit the data produced. Finally, the technique of fitting the data to the model must be decided. Different combinations of each of these steps have led to many approximation techniques found in research. The chart in Table 32 shows how different combinations of these three steps lead to established techniques.

The experimental design of the metamodel is very important to establish in order to make sure the set of computer experiments is efficient and will produce adequate data for the model. There are several experimental designs in place that are used for different scenarios. Types of designs include factorial designs, central composite designs, and space filling designs, among others. In Figure 52 and Figure 53, some of these designs are illustrated to show how the data and parameters are chosen. Each design has some statistical background and theory behind choosing such a design. It is important to determine the needs of the end product in order to choose the best experimental design (Simpson, et al., 2001). Before choosing a design, it is beneficial to do a pre-experimental plan, such as selecting a response variable and choosing the factors to input as variables, levels needs for each factor, and the range of the factors (Montgomery, 2009). Once these decisions are made, choosing a design becomes easier and can be aided by a statistical software program.

There are many models that can be used to fit the data after performing the experiments. The model choice will be tied to the design performed, as well as to the fitting of the model. Examples of different model choices include a polynomial model, network of neurons, and realizations of stochastic processes. Corresponding possible model fitting include least square regression, back propagation, and a best linear unbiased predictor, respectively (Simpson, et al., 2001).

Table 32: Different techniques for metamodels (Simpson, et al., 2001)

Experimental Design	Model Choice	Model Fitting	Sample Approximation Techniques
{Fractional} Factorial	Polynomial	Least Squares Regression	Response Surface Methodology
Central Composite	Splines		
Box-Behnken		Weighted Least Squares Regression	
D-Optimal	Realization of a Stochastic Process		
G-optimal		Best Linear Unbiased Predictor	Kriging
Orthogonal Array	Kernel Smoothing		
Plackett-Burman		Best Linear Predictor	
Hexagon	Radial Basis Functions		
Hybrid		Log-Likelihood	
Latin Hypercube	Network of Neurons		Neural Networks
Select By Hand		Backpropagation	
Random Selection	Rulebase or Decision Tree	Entropy	Inductive Learning
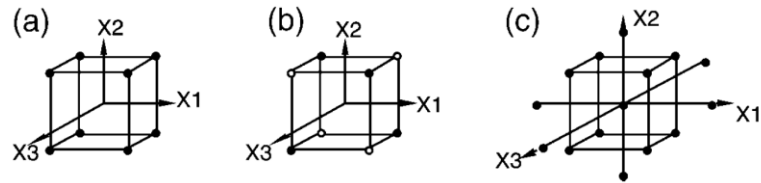
Figure 52: Basic three-factor designs. (a) 2^3 full factorial; (b) 2^{3-1} fractional factorial; (c) composite design (Simpson, et al., 2001)
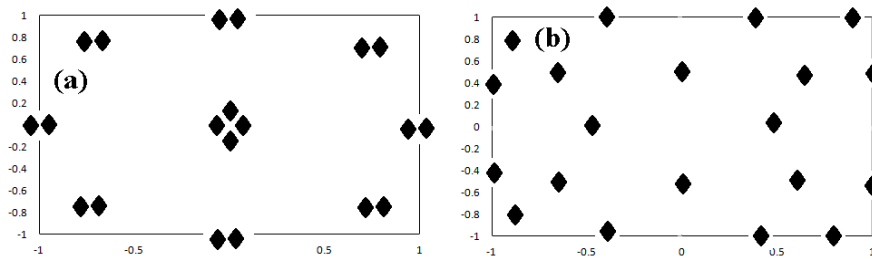
Figure 53: (a) 'Classical' and (b) 'Space filling' designs. (Simpson, et al., 2001)

The combination of an experimental design, model choice, and model fitting results in a complete metamodel. The neural networks method can be accomplished by selecting data by hand as a design of experiments, choosing a network of neurons model and fitting the data with back propagation. This method is used mostly for deterministic functions. Kriging often entails a D-optimal design, a realization of stochastic processes and a best linear unbiased predictor fit. This method is mostly used with computer codes that are deterministic and don't have a measurement error. Response surface methodology (RSM) usually combines a factorial design, polynomial model, and least squares regression (Simpson, et al., 2001). RSM has a history of application in chemical and processing fields (Myers, et al., 1989) as well as multiple engineering fields (Simpson, et al., 2001). RSM has also been used in civil engineering applications, particularly in the reliability assessment of structures (Yao, et al., 1996)(Franchin, et al., 2003)(Rajashekhar, et al., 1993). RSM is beneficial in this research as it facilitates the response of components to be approximated with a polynomial which can reduce the number of analysis needed to produce reasonably accurate results (Rajashekhar, et al., 1993). Traditional single-parameter fragility curves also utilize a form of response surface to create the PSDM that relate the component response with the ground motion intensity measure (Cornell, et al., 2002)(Nielson, et al., 2007). Therefore, for this project, the response surface methodology will be used to develop the bridge specific multi-parameter PSDM.

7.1.1.2 Generation of Bridge-Specific Probabilistic Seismic Demand Model using

Metamodels

As mentioned before, one of the objectives of this research is to create a fragility method that can create curves specific to a bridge design. To accomplish this, the concept of metamodels is utilized to develop a multiparameter bridge-specific fragility method. In this method, the response surface method (RSM) is used as the metamodel of

choice. RSM in general is a collection of tools in data analysis used to improve the knowledge of the effects of design variables on one or more response variables (Myers, et al., 1989). As is applicable to this research, it has been used for the purpose of facilitating the analysis of fragility (Towashiraporn, 2004)(Ghosh, et al., 2012) and for the use in reliability analysis (Rajashekhar, et al., 1993). It was chosen as the metamodel type for this research because of the recent promise it has shown for predicting structural response under seismic loading, and because it is a natural extension of current single parameter probabilistic seismic demand models used in traditional fragility analysis. Furthermore, this research demonstrates that RSMs provide good predictive models of the response of new bridges under seismic load with minimum error.

7.1.1.2.1 Design of Experiment

The first step in developing a metamodel is to choose a proper design of experiment (DOE) for the model. Several DOEs can be used in RSM, and all have different benefits. A common DOE used is the full factorial design, where the number of design points is determined by the factor levels desired and the number of factors considered (Simpson, et al., 2001). The number of design points becomes prohibitively large as the number of factors increases. For an experiment with 5 factors and 3 factor levels, the number of design points required would be 3^5, or 243 design points, or in this case, 243 distinct bridge models. For this project, that number is too large, considering these models will be analyzed with 160 ground motions, requiring a total of almost 40,000 analyses. Other DOEs to consider would be the fractional factorial design, central composite design, and Box-Behnken designs. Central composite designs (CCD) are two-level factorial designs that include center and star points (Simpson, et al., 2001). This type of DOE facilitates the production of second-order response surface model without necessitating the amount of data points for higher-order DOEs (Kutner, et al., 2005). Star points in the CCD are when all the factors are set at the mid levels except for one factor,

123

which is set at $\pm\alpha$, and they allow for the estimation of quadratic effects (Kutner, et al., 2005). The α level chosen depends on the desired DOE characteristics one wants to achieve. For example, the most common level is at ±1, called a face centered design. Other designs can be orthogonal, if the estimated coefficients are uncorrelated, or rotatable, where the variance of the fitted variables can be the same for any point in any direction (Kutner, et al., 2005). The α level thus affects the type of information one can determine from the DOE. An illustration of this type of design is given in Figure 52b. CCDs are beneficial because they incorporate a small number of additional design points that allow estimation of a second order response surface model. This design type has the advantage of including three levels of a factor, like a 3^k factorial design, without the expensively large number of treatments (Kutner, et al., 2005). For this project, a CCD was chosen for the DOE in this metamodel for the fragility method presented. The CCD used to create the single column bridge models is shown in Table 33 and for the multi-column bridges in Table 34. The central composite design DOE used for the bridges with single column bents is basically a two level fractional factorial design with 5 factors, like the one used for the sensitivity study of the design parameters, along with a center point, and 10 star points. The central composite design DOE used for the bridges with multi-column bents is a two level fractional factorial design with 6 factors, along with a center point, and 13 star points. The design parameters were defined in Table 23. In the case of these DOEs, the +1, -1, and 0 values correspond to the maximum, minimum, and median values of the design parameters as determined from a bridge plan survey, as shown in Table 24.

After the design of experiment has been chosen, the bridge models can be created for analysis. For each of the patterns in Tables 33 and 34, 160 parameterized bridge models were realized with the design parameters as specified for that pattern. The process of the creation of parameterized bridge models was introduced in an earlier section. These parameterized bridge models are then analyzed with the full suite of unscaled

PEER ground motions (Baker, et al., 2011) described earlier, totaling 160 ground motions. Response quantities are then extracted from the analyses, such as the column, bearing and abutment responses, to be used as input into the metamodel in the form of response surface models and create the multiparameter demand model.

Table 33: Design of Experiment for multiparameter demand model for single column bents.

Run	Pattern	LS	VR	AR	SpanHt	DepthDiam
1	+−+++	1	-1	1	1	1
2	++−++	1	1	-1	1	1
3	000a0	0	0	0	-1	0
4	−++−−	-1	1	1	-1	-1
5	0000A	0	0	0	0	1
6	++−−−	1	1	-1	-1	-1
7	++++−	1	1	1	1	-1
8	−−−−−	-1	-1	-1	-1	-1
9	00000	0	0	0	0	0
10	+−−+−	1	-1	-1	1	-1
11	−−+−+	-1	-1	1	-1	1
12	+++−+	1	1	1	-1	1
13	0000a	0	0	0	0	-1
14	0A000	0	1	0	0	0
15	−++++	-1	1	1	1	1
16	000A0	0	0	0	1	0
17	−−−++	-1	-1	-1	1	1
18	+−−−+	1	-1	-1	-1	1
19	+−+−−	1	-1	1	-1	-1
20	−−++−	-1	-1	1	1	-1
21	−+−−+	-1	1	-1	-1	1
22	00000	0	0	0	0	0
23	00A00	0	0	1	0	0
24	a0000	-1	0	0	0	0
25	0a000	0	-1	0	0	0
26	00a00	0	0	-1	0	0
27	−+−+−	-1	1	-1	1	-1
28	A0000	1	0	0	0	0

Table 34: Design of experiment for multiparameter demand model for multi-column bents.

Run	Pattern	LS	VR	AR	SpanHt	DepthDiam	Width
1	+++++−	1	1	1	1	1	-1
2	++−−+−	1	1	-1	-1	1	-1
3	A00000	1	0	0	0	0	0
4	+++−++	1	1	1	-1	1	1
5	−+−−++	-1	1	-1	-1	1	1
6	−−++−+	-1	-1	1	1	-1	1
7	−−−−+−	-1	-1	-1	-1	1	-1
8	−+++−−	-1	1	1	1	-1	-1
9	−+++−	-1	1	1	-1	1	-1
10	−−+−++	-1	-1	1	-1	1	1
11	0A0000	0	1	0	0	0	0
12	−+−−−−	-1	1	-1	-1	-1	-1
13	−+−+−+	-1	1	-1	1	-1	1
14	00a000	0	0	-1	0	0	0
15	+−+−−+	1	-1	1	-1	-1	1
16	+−++++	1	-1	1	1	1	1
17	+−+−+−	1	-1	1	-1	1	-1
18	00000A	0	0	0	0	0	1
19	+−−−++	1	-1	-1	-1	1	1
20	++−+++	1	1	-1	1	1	1
21	000000	0	0	0	0	0	0
22	00A000	0	0	1	0	0	0
23	000A00	0	0	0	1	0	0
24	+−−−−−	1	-1	-1	-1	-1	-1
25	+−++−−	1	-1	1	1	-1	-1
26	+−−++−	1	-1	-1	1	1	-1
27	+++−−−	1	1	1	-1	-1	-1
28	0000a0	0	0	0	0	-1	0
29	000a00	0	0	0	-1	0	0
30	−−−+−−	-1	-1	-1	1	-1	-1
31	++−+−−	1	1	-1	1	-1	-1
32	−++−−+	-1	1	1	-1	-1	1
33	00000a	0	0	0	0	0	-1
34	−+−++−	-1	1	-1	1	1	-1
35	−−−−−+	-1	-1	-1	-1	-1	1
36	+++++	1	1	1	1	-1	1
37	a00000	-1	0	0	0	0	0
38	−−−+++	-1	-1	-1	1	1	1
39	+−−+−+	1	-1	-1	1	-1	1
40	−++++++	-1	1	1	1	1	1
41	−−+++−	-1	-1	1	1	1	-1
42	0000A0	0	0	0	0	1	0
43	−−+−−−	-1	-1	1	-1	-1	-1
44	0a0000	0	-1	0	0	0	0
45	++−−+	1	1	-1	-1	-1	1

7.1.1.2.2 Model Choice and Model Fitting

The next steps in developing the metamodel are model choice and model fitting. A common model choice for this type of analysis in developing response surfaces is a general linear regression model (Towashiraporn, 2004)(Ghosh, et al., 2012). Model types stemming from this regression model include first order models, polynomial models of second order, models with transformed variables, and models with interaction terms. A regression model can also combine these different elements and still be considered a linear regression model (Kutner, et al., 2005). Examples of a first order model, a second order model, and a model that includes interaction terms between the variables that were explored for this project are as shown in Eqns. (7.4-6). The fitting of the model, which includes determining the regression coefficients of the chosen model, can be accomplished with a regression model such as the least squares regression approach or the step wise least squares regression approach (Kutner, et al., 2005).

$$E[Y] = \beta_0 + \sum_{i=1}^{n} \beta_i X_i \tag{7.4}$$

$$E[Y] = \beta_0 + \sum_{i=1}^{n} \beta_i X_i + \sum_{i=1}^{n} \beta_i X_i{}^2 \tag{7.5}$$

$$E[Y] = \beta_0 + \sum_{i=1}^{n} \beta_i X_i + \sum_{i=1}^{n} \sum_{j=1,i<j}^{n} \beta_{ij} X_i X_j \tag{7.6}$$

Where $X_1 \dots X_n$ are the different design variables and $\beta_0 \dots \beta_n$ are the regression coefficients used to estimate the response quantity Y. In order to choose the best model to use for this research, the merits and benefits of the models should be weighed. The first order model is mainly used as a starting point to determine the characteristics of the explanatory variables on the response variables. The first order regression model will produce a plane as the response function or the response surface (Kutner, et al., 2005), and for data that has low curvature the first-order model can be used (Simpson, et al., 2001). If the response surface is not well captured by the first model regression model, then other models can be used to better fit the data, such as a second-order polynomial model that includes quadratic terms and interaction terms, or polynomial models with

transformed variables (Simpson, et al., 2001). As a strategy for determining the best regression model to use for a response surface, different models should be compared by studying certain diagnostics on the model, the model should be refined to get a better fit, and the best tentative model should then be validated based on different factors (Kutner, et al., 2005). The following describes this strategy in choosing the model to be used for the multi-parameter PSDM for this research.

The first step was to investigate the first order linear model to determine if any additional elements needed to be added to the model using statistical diagnostics. The response variable used in this section is the column response represented by the column curvature ductility, and the predictor variables are the five design parameters used for the single-column bent bridge type and the ground motion intensity measure peak ground acceleration (PGA). The column response is just one of the component responses that are monitored in this research and which were discussed in Chapter 4. General conclusions about the form of metamodel to be used for the multi-parameter PSDM will be based off of the conclusions on the model for the column response. Figure 54 shows the scatter plot of the residuals against the predicted value of the model based on a first order regression of the 6 design parameters and PGA against the response of the column. This residual plot is useful in determining if there is any curvature in the data or non-constant error variance (Kutner, et al., 2005). Figure 55 shows a normal probability plot for the residuals of the regression model, which would show any departure from normalcy of the distribution of the error of the model. A scatterplot matrix is also useful in determining the nature of the relationships between response and predictor variables, and is shown in Figure 56. The scatterplots for the predictive variables against the response variables are linear because of the nature of how the data was generated through the use of a DOE. These diagnostic figures show that the first-order regression model may not be the best model, as the normal probability plot showed a great deviance from a normal distribution in the error values in the higher values of the residuals. The residual plot showed that a

128

few outliers in the data may play a role in the determination of the model. The scatterplot matrix showed that no strong relationship existed between the response variable and any other variable.
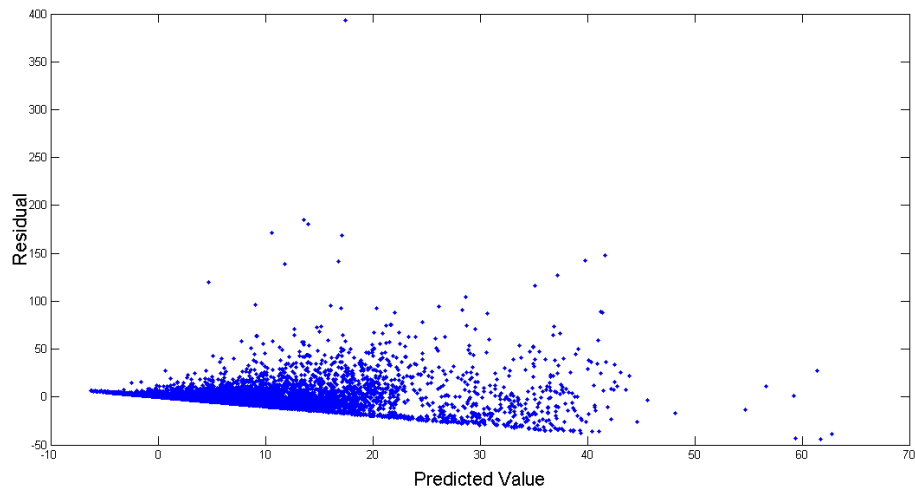
Figure 54: Residual plot of linear first order regression model
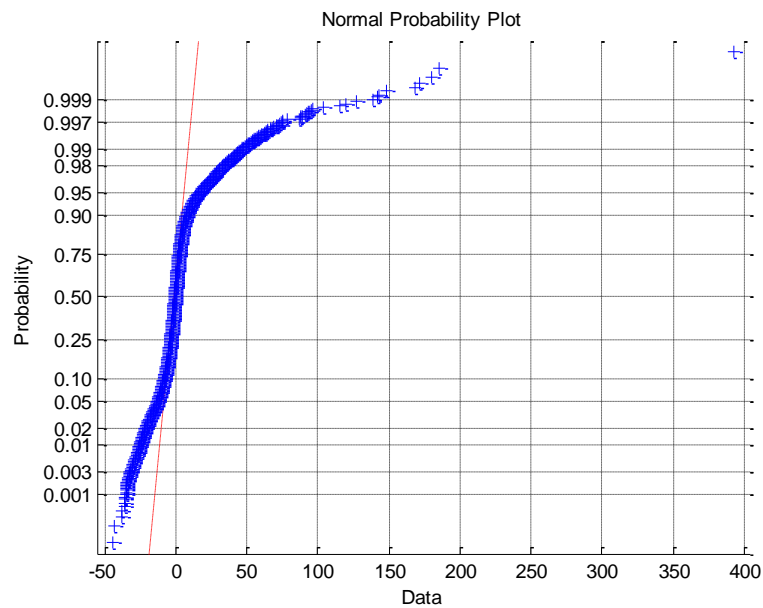
Figure 55: Normal probability plot for the residuals of the first order model.
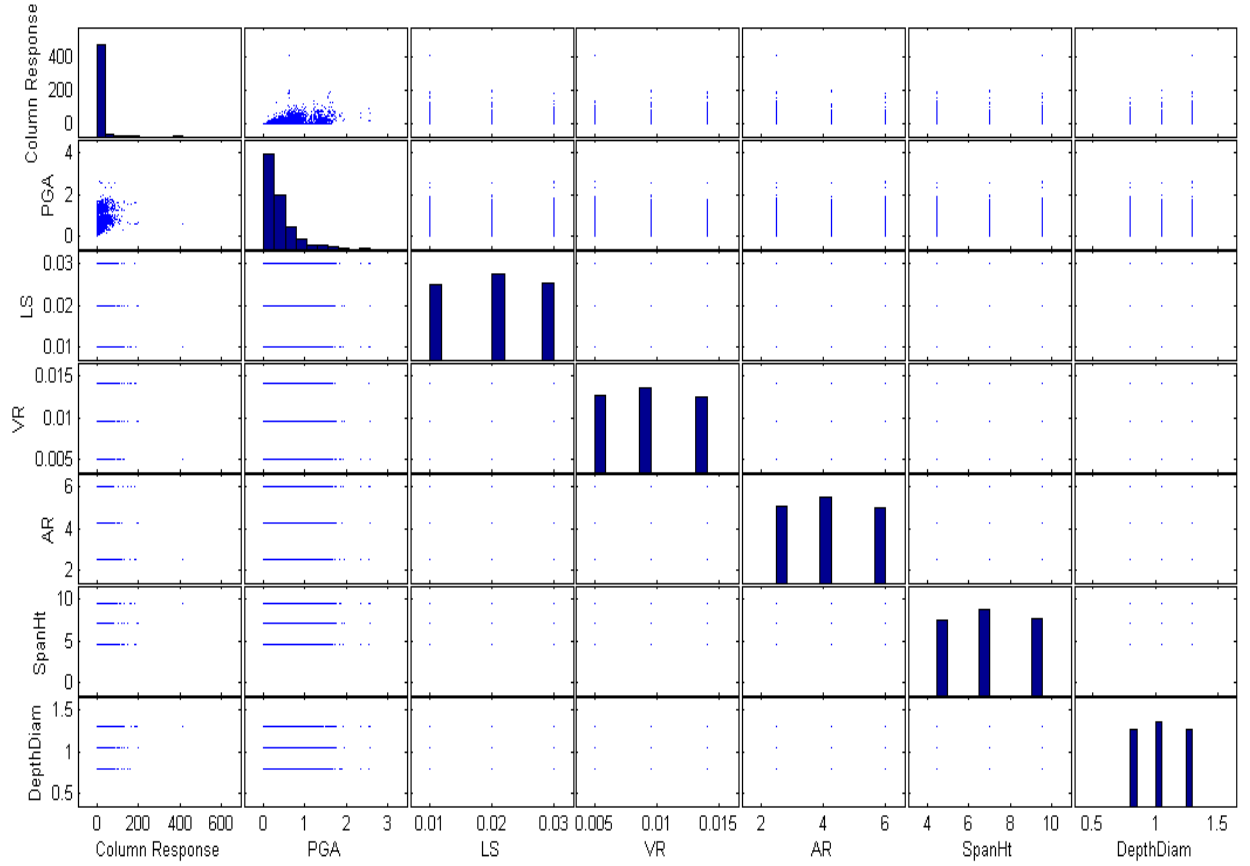
Figure 56: Scatterplot matrix of all variables in the model.

To improve the model, changes were implemented to the model to see if a better model could be found, starting with transformations. As is common in other fragility applications, the response variable and the ground motion intensity measure is transformed in the lognormal space to produce a better relationship between the two (Cornell, et al., 2002). This relationship is shown in Eqn. (7.7), where *Y* is the component response variable, *IM* represents the ground motion intensity measure, and *a* and *b* are regression coefficients found when regressing the response variable against the available damage data. The lognormal transformation is used for the metamodel to determine if the model can be improved. Figure 57 and Figure 58 show that the residuals and the correlation between variables indicate a better fitting model with the transformation. Also explored were models with added second-order terms such as quadratic terms and

130

interaction terms. These models are not shown here as those models didn't offer much benefit over the transformed model based on the diagnostics used in this section. Based on all of these diagnostics on the different regression models that could be used in this instance to represent the statistical determination of the response of different bridge components for the multi-parameter PSDM, the equation adopted here is shown in Eqn. (7.9), which is a linear first-order regression model with transformations on the response variable and the ground motion intensity measure in the natural logarithmic space.

$$\ln(Y) = a + b\ln(IM) \tag{7.7}$$

$$Y = a(IM)^b \tag{7.8}$$

$$\ln(Y) = \beta_0 + \beta_1(\ln(IM)) + \beta_2 X_1 + \beta_3 X_2 + \beta_4 X_3 + \beta_5 X_4 + \beta_6 X_5 \tag{7.9}$$
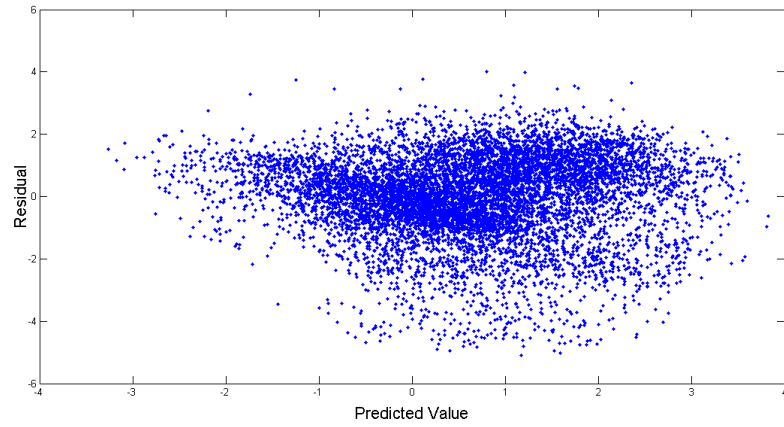
Figure 57: Residual plot of model with transformations.
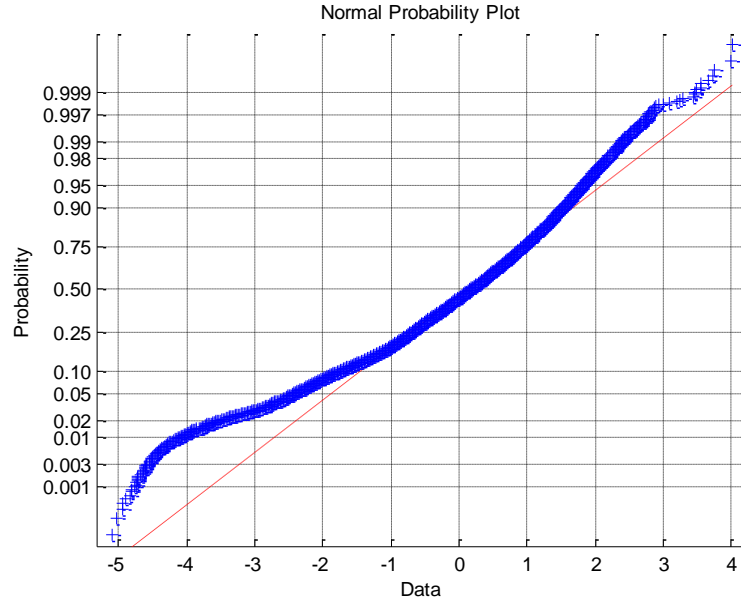
Figure 58: Normal probability plot for the residuals of the model with transformations.

In conjunction with choosing the correct model, the way in which the model is fit is has to be considered. Model fitting of regression models within the Response Surface Method has most commonly been achieved using the least squares regression method (Simpson, et al., 2001). Least squares regression estimation is accomplished by finding the coefficient of regression that minimize the sum of squared deviations (Kutner, et al., 2005). This is the method used for this research in determining the multi-parameter PSDM. This entire process of determining appropriate regression coefficients will be done for each response quantity of interest, such as column response, abutment gap displacement, and bearing response. These multiparameter PSDMs are similar to the traditional PSDM given in Eqn. (7.7), developed by Cornell, et al (Cornell, et al., 2002). The main difference is that the fragility of the response quantity will now be conditioned on the ground motion intensity measure as well as the other design variables, resulting in fragility curves developed specifically for a bridge with the conditioning design variable quantities. This fragility can be expressed in the probability statement in Eqn. (7.10).

These component PSDMs will be used in the fragility method as the demand model to be convolved with a capacity model. This will be discussed later in the chapter.

$$P[Fragility] = P[Demand > Capacity(LS_i) | IM, x_1, x_2, ..., x_n] \tag{7.10}$$

7.1.2 Logistic Regression used to determine fragility

The combination of the capacity and demand models will also differ from the traditional single variable fragility analysis. Commonly, a closed form equation has been used to integrate the capacity and demand models in analytical fragility analysis at the component level (Shinozuka, et al., 2000)(Nielson, et al., 2007). When these models follow a lognormal distribution, the fragility curve can be found with Eqn. (7.11) (Hwang, et al., 2001), where S_d is the median value of the structural demand, S_c is the median value of the structural capacity, $\beta_{d|IM}$ is the logarithmic standard deviation of the demand, and β_c is the logarithmic standard deviation of the capacity.

$$P[Demand > Capacity | IM] = \Phi\left(\frac{\ln\left(\frac{S_d}{S_c}\right)}{\sqrt{{\beta_{d|IM}}^2 + {\beta_c}^2}} \right) \tag{7.11}$$

For this bridge specific fragility method, the capacity and demand models will be compared using Monte Carlo simulation and logistic regression. The chart in Figure 51 shows the steps to creating fragility curves with this method. If the probability of exceeding a damage level varies from 0 to 1 only, and is a never decreasing function, then any cumulative distribution function can be used to develop fragility curves (Koutsourelakis, 2010). In this method, a logistic distribution and regression, which has been used to find fragility surfaces in research before, is used instead of the lognormal distribution used in previous research (Koutsourelakis, 2010)(Towashiraporn, 2004).

This logistic regression provides the form of the cumulative distribution function that describes the parameterized bridge failure probability given multiple input parameters.

Monte Carlo simulation and its applications in fragility analysis were discussed in Chapter 3. In this fragility method, Monte Carlo simulation is used to generate random samples from the distributions of the demand and capacity models in order to compare the sampled points from the demand and capacity models and calculate the probabilities of failure for each component and limit state. The capacity model was described in Chapter 4 as the limit states for primary and secondary components defined by engineering demand parameter values at four CDT levels and dispersion. The capacity models are described by a lognormal distribution. The demand model is the multi-parameter PSDM developed using the Response Surface Method shown in Eqn. (7.9). To compare the capacity model with the demand model with Monte Carlo simulation, the design parameters in the demand models are randomly generated to enter into the multi-parameter PSDM, which creates realizations for the demand model, and the capacity of the component is randomly generated based on the lognormal distribution. Thus for each run in the Monte Carlo analysis, the realizations randomly simulated from the demand and capacity models are compared. During this process, the number *1* is assigned to a realization where the demand is greater than the capacity, representing a "failure", and the number *0* is assigned when the capacity is greater than the demand. These binary results from the Monte Carlo simulation are assembled into vectors for each component. These resultant vectors are then regressed against a matrix of the original design parameters using a logistic regression to find regression coefficients, α_i, seen in Eqn. (7.12). This procedure will lead to the fragility of each bridge component, calculated with the logistic regression formula, where the α_i values come from the regression analysis and the x_i values are the design parameters to be defined by the specific bridge design.

To find the fragility of the bridge system, a series system assumption is adopted to combine the results of the components. The series system assumption specifies that for

each simulation, if any of the components within a system fails, then the entire system has failed (Melchers, 1999). This is a common assumption that is adopted in bridge fragility analysis (Padgett, et al., 2008)(Ramanathan, 2012). For each realization, the results from each component are compared, and if at least one of the components failed, the number *1* is assigned for the system, and if none of the components failed, then the number *0* is assigned to the system analysis. These new binary results are stored in a vector and regressed against a matrix of design parameters with a logistic regression to find a set of regression coefficients for the system fragility. Again, Eqn. (7.12) is used to define the probability of failure for the bridge system at each limit state.   An illustration of this process is given in Appendix B.

$$P(Fragility) = p_f = \frac{e^{(\alpha_0 + \alpha_1 X_1 + \cdots + \alpha_k X_k)}}{1 + e^{(\alpha_0 + \alpha_1 X_1 + \cdots + \alpha_k X_k)}} \qquad (7.12)$$

The results of the Monte Carlo simulation using the response surface metamodels and logistic regression are given in Appendix C. The results include the logistic regression coefficients of the probability of failure equation for the primary and secondary components and bridge system. Those results will be used in the design support tool to produce bridge specific fragility curves. Eqn. (7.12), with the coefficients found from the Monte Carlo simulation process included, becomes the fragility equation that is used to estimate the fragility of the bridge and components, and directly correlates to the fragility equation shown in Eqn. (7.10). Substituting the design parameters in for the X_i in Eqn. (7.12), the probability of failure equation becomes Eqn. (7.13) for multi-column bridges (MCB), and Eqn. (7.14) for single-column bridges (SCB).

$$p_f(MCB)$$

$$= \frac{e^{(\alpha_0 + \alpha_1 \ln(IM) + \alpha_2 LS + \alpha_3 VR + \alpha_4 AR + \alpha_5 SpanHt + \alpha_6 DepthDiam + \alpha_7 Width)}}{1 + e^{(\alpha_0 + \alpha_1 \ln(IM) + \alpha_2 LS + \alpha_3 VR + \alpha_4 AR + \alpha_5 SpanHt + \alpha_6 DepthDiam + \alpha_7 Width)}}$$

$$(7.13)$$

$$p_f(SCB) = \frac{\text{e}^{(\alpha_0 + \alpha_1 \ln(IM) + \alpha_2 LS + \alpha_3 VR + \alpha_4 AR + \alpha_5 SpanHt + \alpha_6 DepthDiam)}}{1 + \text{e}^{(\alpha_0 + \alpha_1 \ln(IM) + \alpha_2 LS + \alpha_3 VR + \alpha_4 AR + \alpha_5 SpanHt + \alpha_6 DepthDiam)}}$$

$$(7.14)$$

As the fragility will be based on more than one parameter, the result would be a multi-dimensional fragility surface or cloud, generated by the points produced by the logistic regression equation, instead of the traditional 2-dimensional curve developed in current fragility methods (Nielson, et al., 2007)(Shinozuka, et al., 2000). To graphically show the cloud in two or three dimensions, one would have to deterministically define all but one or two parameters and vary the remaining one or two parameters of interest within a range in order to graph the 2-dimensional fragility curve or 3-dimensional fragility surface. The design tool does just that; it takes the bridge design inputs from the user as deterministic values, and varies the ground motion intensity measure within a pre-determined range in order to develop the 2-dimensional fragility curves that is most familiar to engineers. Thus, this fragility methodology was developed in order to facilitate the implementation of bridge-specific fragility analysis that would produce fragility curves in this common form of 2-dimensional curves.

7.2 Fragility Analysis of Bridges

This section will illustrate the method for the bridge type studied in this research, the two-span concrete box-girder bridge. The bridge was further distinguished by the number of columns at the bent, with the fragility method applied to this bridge class with multi-column bents and single column bents separately. The fragility curves presented in this section will be shown for the bridges at the median values of the design parameters found from the bridge plan survey described earlier. In the next chapter a more detailed illustration is presented of the use of the bridge-specific fragility method implemented within the design support tool commissioned by Caltrans for this research.

7.2.1 Multi-Column Bent Bridge Class

The following describes the fragility curves developed with the bridge-specific fragility method for the multi-column two span concrete box girder bridge class. A description of this bridge type was given in a previous chapter. Table 35 shows the median values of the design parameters that correspond to different geometric properties of the bridge that were used to develop the curves shown in this chapter. These properties are input into the logistic regression equations shown in Eqn. (7.12) that produce the fragility points. To develop fragility curves that mirror the curves commonly found in practice, a range of the ground motion intensity measure is inserted into the equation instead of specific points, then the individual points generated at each ground motion intensity measure point are connected to create a smooth curve. Fragility curves with the spectral acceleration at one second (Sa1) ground motion intensity measure, which is commonly used in fragility analysis, and suggested by Caltrans engineers to use for this project (Roblee, et al., 2011), are shown in this chapter. Fragility curves with peak ground acceleration (PGA) are shown in Appendix D, as PGA is also commonly used by engineers in traditional fragility curves (Shafieezadeh, et al., 2011).

Table 35: Median values of design parameters for use in illustrated fragility curves.

Design Parameter	Median value
Longitudinal Steel Ratio, LS	2.0%
Volumetric Ratio for Transverse Steel, VR	0.95%
Aspect Ratio, Column Height over Column Diameter, AR	4.25
Span length to Column Height Ratio, SpanHt	7.0
Depth of Deck to the Column Diameter Ratio, DepthDiam	1.05
Width of the Bridge Deck, Width (in) (only for Multi-column Bent bridge class)	1000

The fragility curves shown in Figure 59 are shown for each of the limit states encompassed in the capacity model of the analysis, and include the bridge components monitored in this research to determine the condition of the bridge. They include the

column curvature response and the abutment gap displacement response as the primary components. The bearing movement and the displacement of the joint seal are shown as the secondary components. Primary and secondary components were discussed in earlier sections. The fragility curve for the bridge system state is also included in the figures. The process by which the logistic regression coefficients were determined to create the regression equations used in this analysis was described in an earlier section. The results of the multi-parameter PSDM developed using the Response Surface Method, logistic regression analysis and resultant regression coefficients are all presented in Appendix C for the MCB bridge class and the SCB bridge class. Additional fragility curves showing each of the component fragility at the four different damage states are also given Appendix D.

Fragility Curves for all Components for Limit State1 For MCB

Fragility Curves for all Components for Limit State2 For MCB

Figure 59: System and component level fragility curves for the multi-column bent box girder bridge class at four damage states.

Table 36 summarizes the attributes of this fragility analysis with the median fragility estimates of each of the bridge components as well as the bridge system fragility. The median fragility estimate is a common measure of a fragility curve that is often used to help characterize the entire curve, especially when the fragility analysis is based on demand and capacity models that are lognormally distributed (Mackie, et al., 2007). The median fragility is the value of the ground motion intensity measure that corresponds to a probability of 50% of reaching the limit state in question. The lower the median fragility, the more vulnerable that particular component is to reaching the indicated damage state. As indicated in the figures, the bridge system is always as vulnerable or more vulnerable than any of the contributing components, as is the nature of a series system. As is shown, the performance of the column controls the performance of the bridge system for the lower bridge system state where both the primary and secondary components contribute to the bridge system fragility. The trend continues at the higher bridge system damage states, where only the primary components contribute to the fragility. At these higher damage states, the abutment gap response is not as vulnerable as the column response. So for this bridge class, it is clear that the column is the most vulnerable component of the bridge in regards to checking the bridge performance at the collapse damage state.

Table 36: Median fragility estimates for the multi-column bent bridge class.

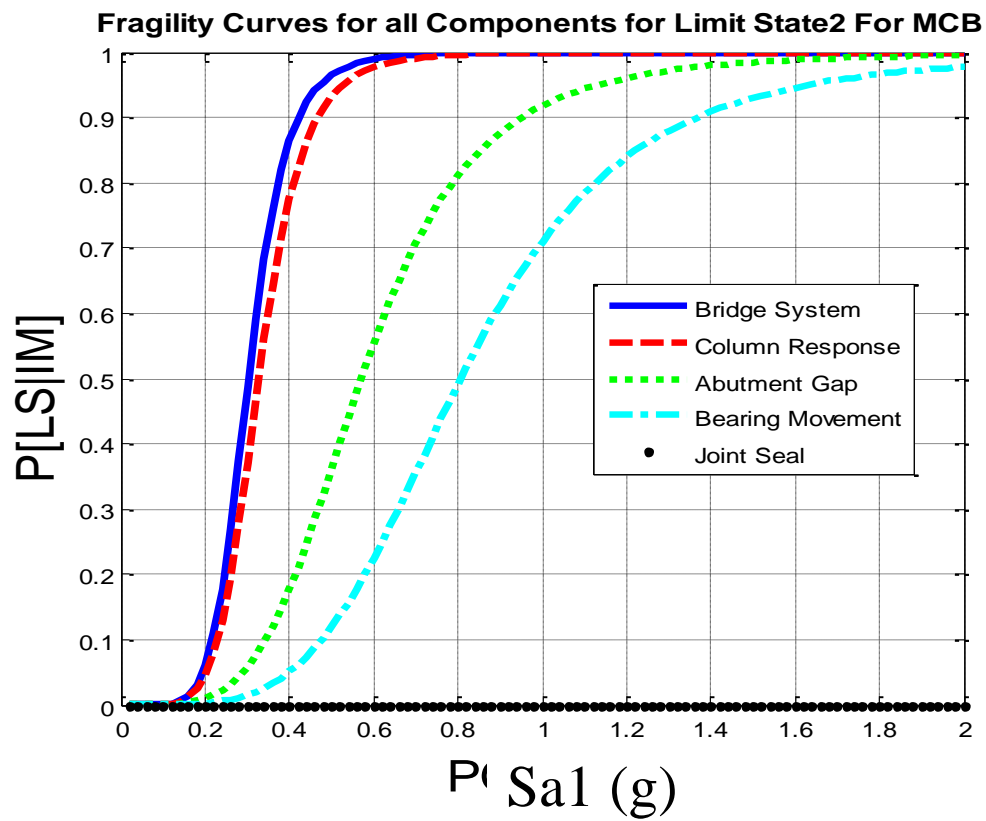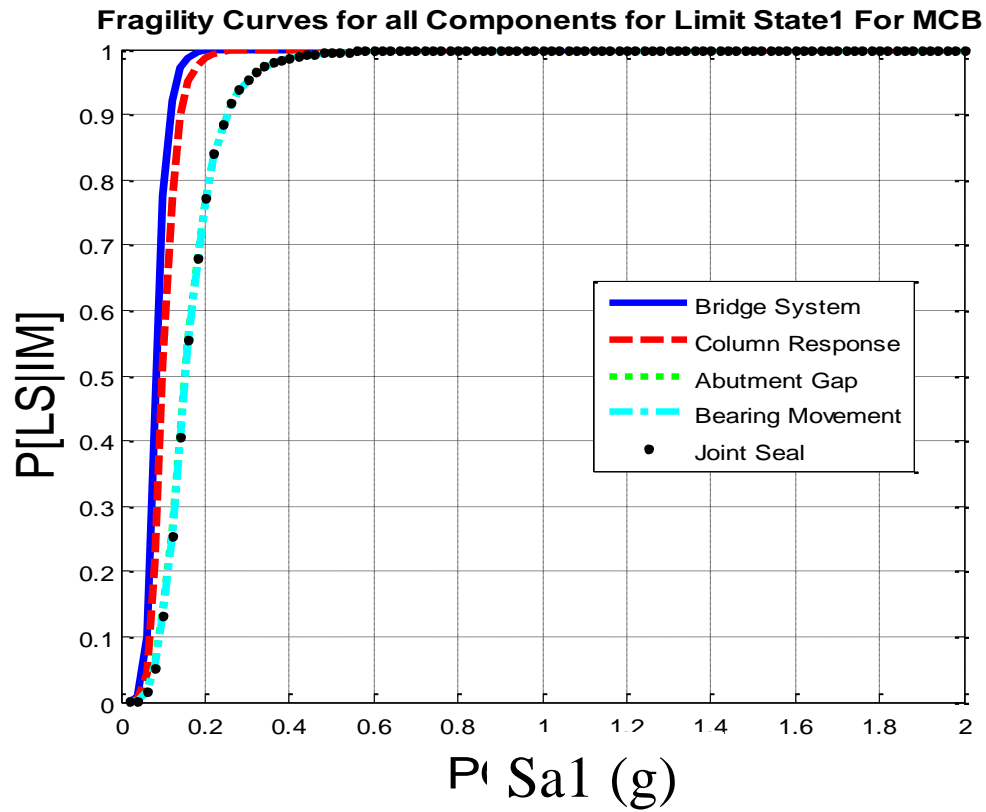| Bridge Component	Median Fragility – Spectral Acceleration at 1.0 sec (%g)			
	LS-0	LS-1	LS-2	LS-3
Bridge System	0.0830	0.3025	0.5910	0.8165
Column	0.0990	0.3270	0.5910	0.8165
Abutment Gap	0.1520	0.5710	3.2110	4.2945
Bearing	0.1530	0.8070	N/A	N/A
Joint Seal	0.1520	N/A	N/A	N/A

7.2.2 Single-Column Bent Bridge Class

The following describes the fragility curves developed with the bridge-specific fragility method for the single-column two span concrete box girder bridge class. A description of this bridge type was given in a previous chapter. Table 35 showed the median values of the design parameters that correspond to different geometric properties of the bridge that were used to develop the curves shown in this chapter. These properties are input into the logistic regression equations shown in Equation (7.12) that produces the fragility points for the single-column bridge class. Fragility curves were developed in the same way as those shown previously for the multi-column bent bridge class.

The fragility curves shown in Figure 60 are shown for each of the limit states that was included in the capacity model of the analysis, described in an earlier chapter. The fragility curves include the bridge components monitored in this research to determine the condition of the bridge, similar to those included for the multi-column bent bridge class. The process by which the logistic regression coefficients were determined to create the regression equations used in this analysis was described in an earlier section. The results of the multi-parameter PSDM developed using the Response Surface Method for the single-column bent bridge, logistic regression analysis and resultant regression coefficients are all presented in Appendix C. Additional fragility curves showing each of the component fragility at the four different damage states are also given Appendix D.

Fragility Curves for all Components for Limit State1 For SCB

Fragility Curves for all Components for Limit State2 For SCB
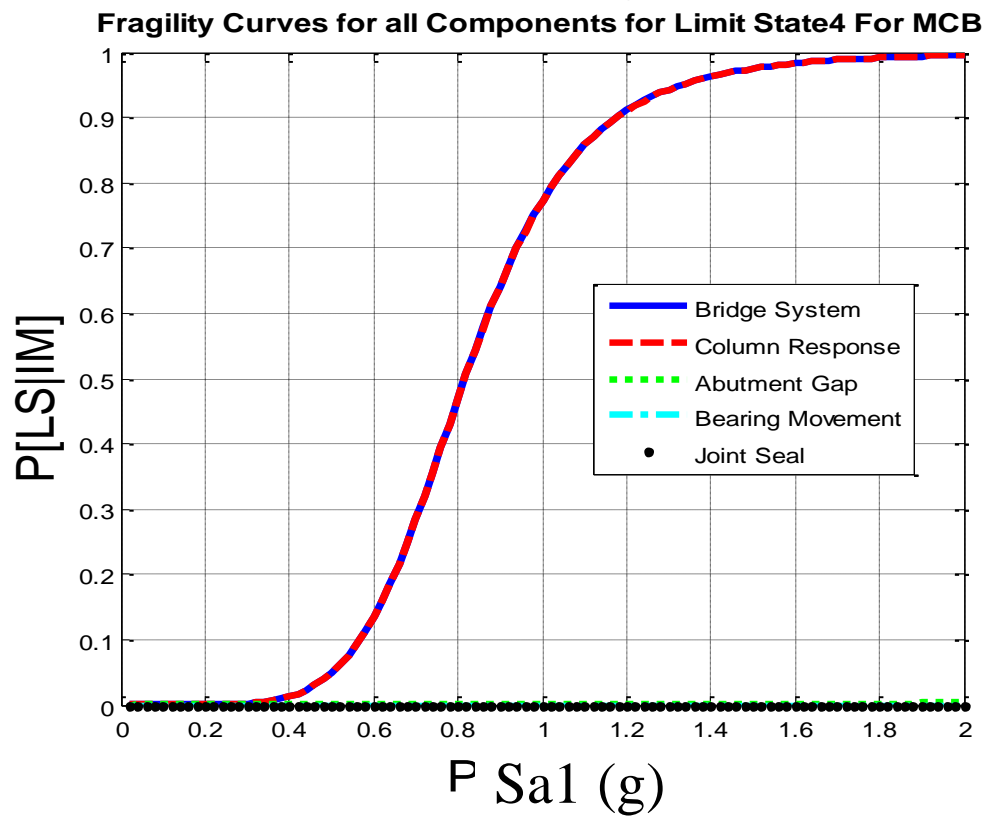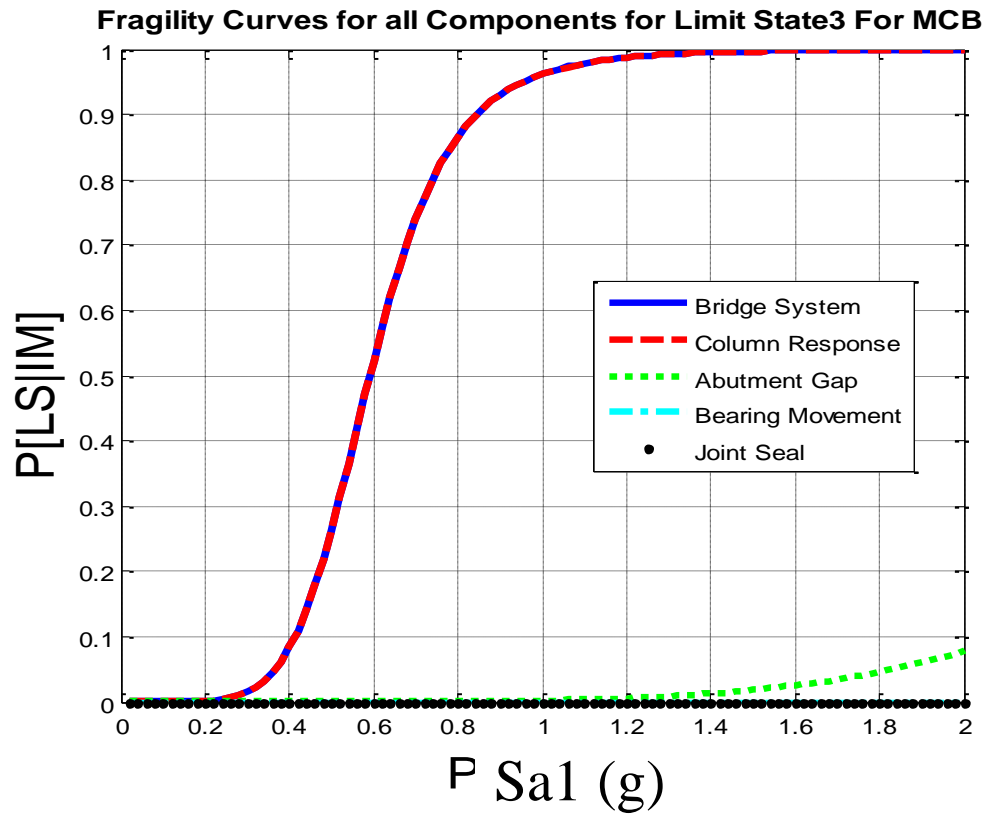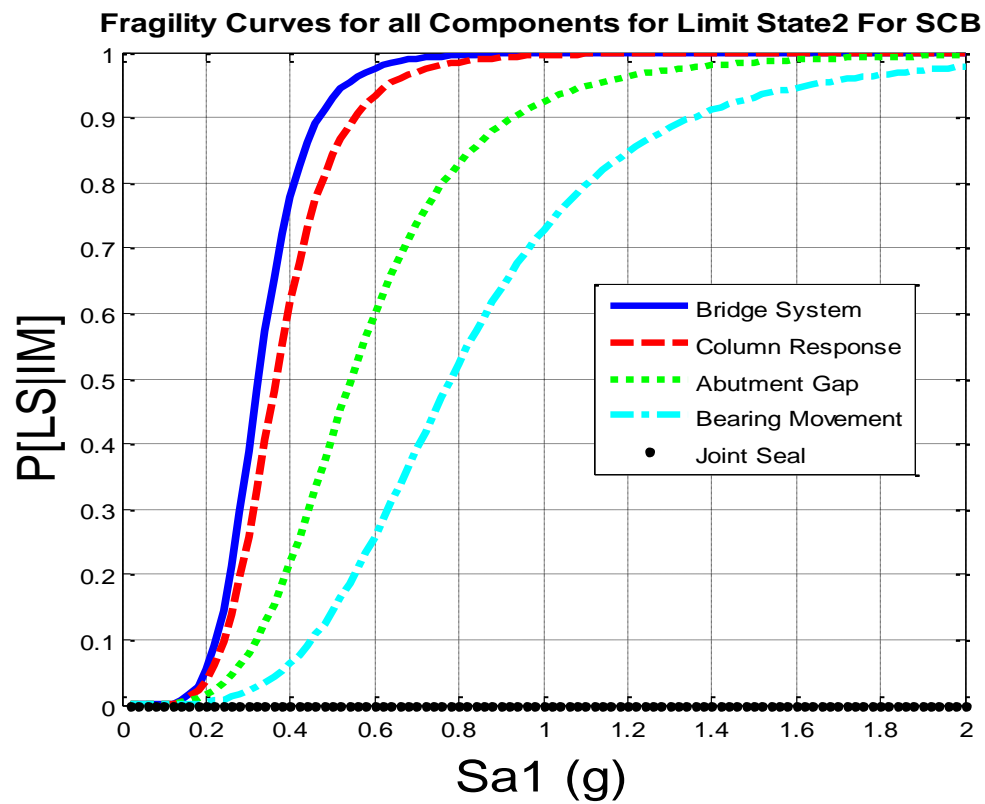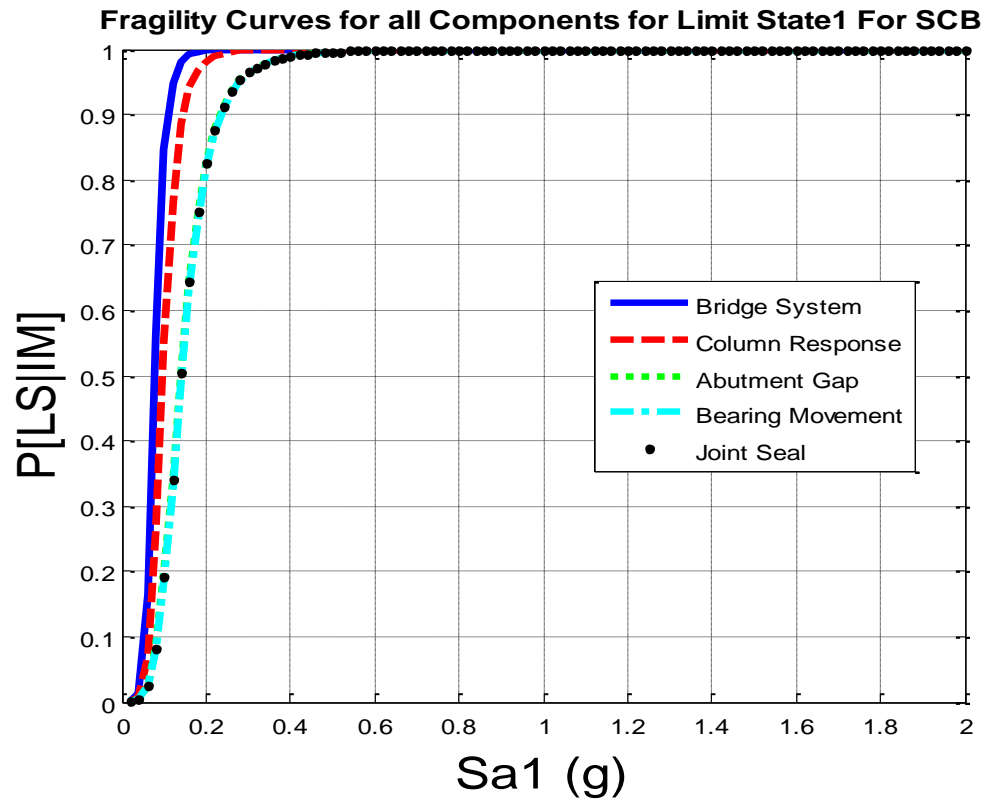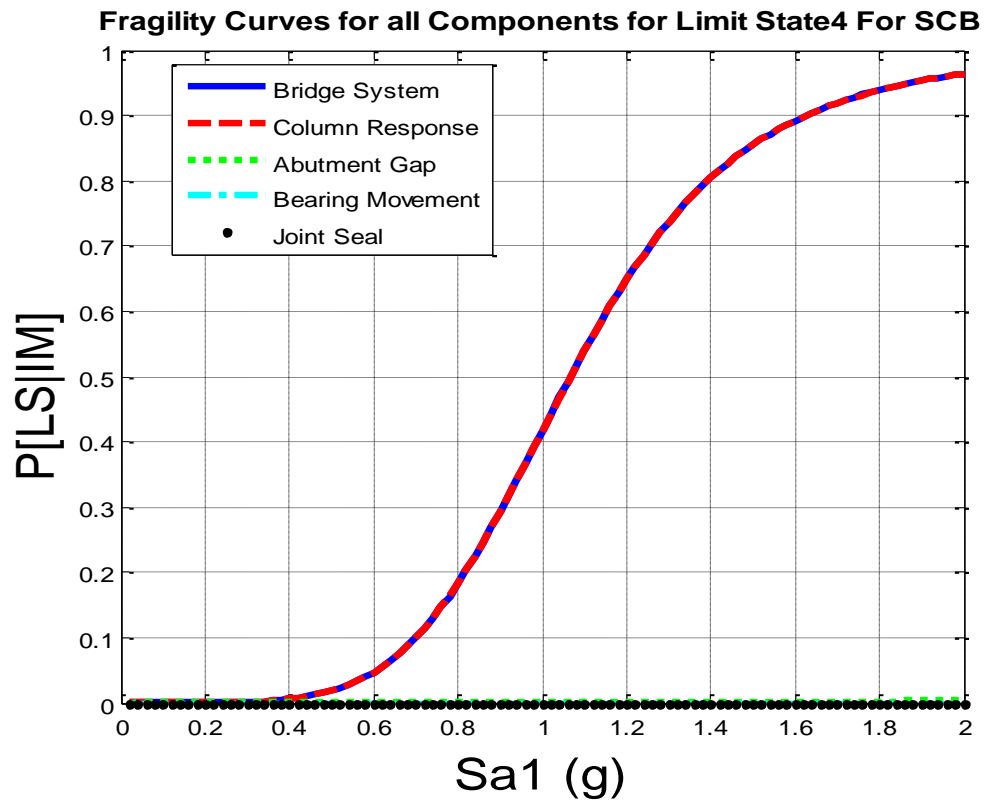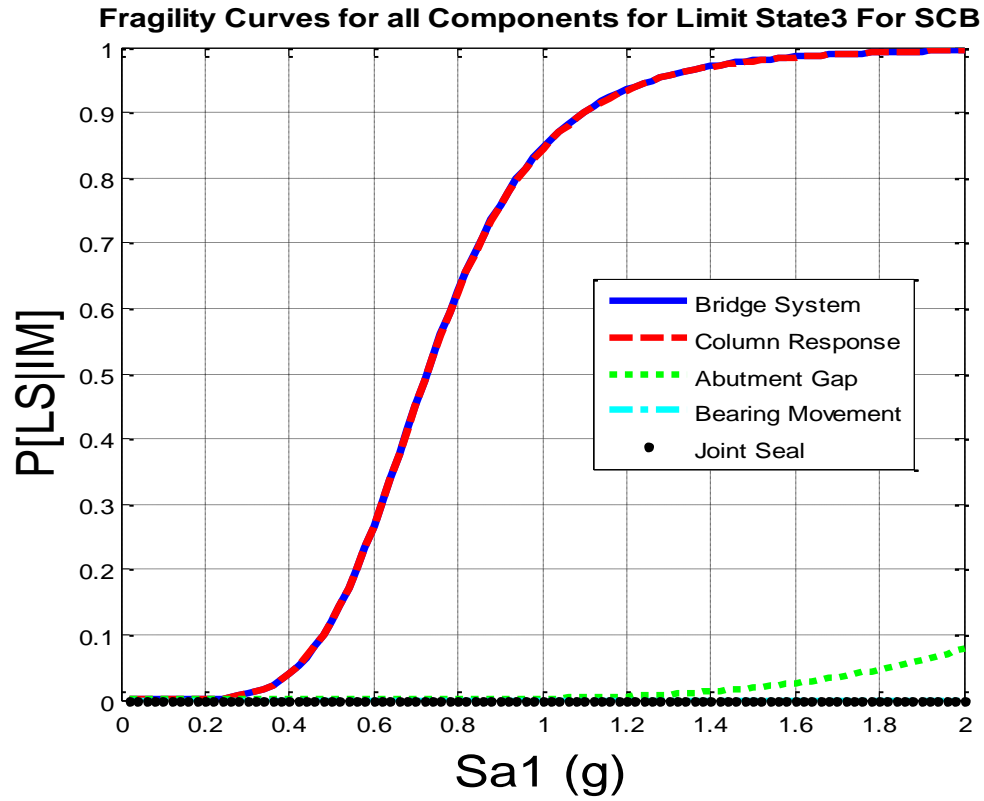
Figure 60: System and component level fragility curves for the single-column bent box girder bridge class at four damage states.

Table 37 summarizes the attributes of this fragility analysis on the single-column box girder bridge class with the median fragility estimates of each of the bridge components as well as the bridge system fragility. The results of this fragility analysis are similar to that of the multi-column bridge class, where the performance of the column controls the performance of the bridge system for all of the bridge system damage states. For this bridge class, the column response is again the component that contributes the most to the determination of the fragility performance of the bridge system.

Table 37: Median fragility estimates for the single-column bent bridge class.

Bridge Component	Median Fragility – Spectral Acceleration at 1.0 sec (%g)			
	LS-0	LS-1	LS-2	LS-3
Bridge System	0.0770	0.3235	0.7260	1.0665
Column	0.0965	0.3655	0.7265	1.0665
Abutment Gap	0.1395	0.5445	3.1980	3.9510
Bearing	0.1410	0.7815	N/A	N/A
Joint Seal	0.1400	N/A	N/A	N/A

In comparison to the median fragility estimates for the multi-column bridge class, Table 38 shows how each component and each limit state fares among the bridge classes. For example, if the median fragility estimate for the column component and LS-1 is lower in the single-column bridge class, the cell in the table will be marked with SCB, indicating that component is more vulnerable than in the other bridge class. As is shown, the single-column bent bridges are more vulnerable at the lowest damage state than the multi-column bent bridges. However for the higher damage states, the response of the column system in multi-column bent bridges is shown to be more vulnerable than that of the single-column bent bridge class. This result reinforces the decision to distinguish

145

between the bent types when analyzing the box girder bride class for this research. This section described the fragility analysis possible with this method using multi-parameter demand models and logistic regression analysis to determine the fragility points; the following will compare this method to previous fragility analysis methods used in bridge fragility analysis.

Table 38: Details for the most vulnerable bridge class for each bridge component.

Bridge Component	Most Vulnerable Bridge Class in Each Category			
	LS-0	LS-1	LS-2	LS-3
Bridge System	SCB	MCB	MCB	MCB
Column	SCB	MCB	MCB	MCB
Abutment Gap	SCB	SCB	SCB	SCB
Bearing	SCB	SCB		
Joint Seal	SCB			

7.2.3 Extension of Bridge Specific Fragility Estimation in Risk-based Design

In the Pacific Earthquake Engineering Research Center (PEER) performance based earthquake engineering (PBEE) framework, there are several steps taken to perform a risk assessment on the structure being designed. These steps include hazard analysis, structural analysis, damage analysis, and loss analysis (Moehle, et al., 2004). In building codes such as ATC 58 and ASCE/SEI 7-10, the trend of risk based design is replacing other methods of design (Applied Technology Council, 2012). A structure would be designed to meet a performance goal of X% probability of failure in Y years and would be dependent on the importance of the structure (Applied Technology Council, 2012). This method of risk-based design in building design can be extended to bridge design, and the bridge-specific fragility method provides a basis for determining the risk of the bridge by providing bridge-specific fragility information that can be used

to determine the risk of the bridge. Eqn. (7.16) shows how to estimate the total probability of failure or the annual risk of the bridge collapsing using fragility information and a hazard curve of a particular locale (Cornell, et al., 2002). $H_D(d)$ refers to the hazard curve which provides the mean annual frequency of a hazard, or ground motion level, occurring at the specified site. $P[C \leq D|D=d_i]$ is the probability of the structural response exceeding a set limit state threshold conditional on a particular ground motion intensity, characterized by the fragility estimate produced by the bridge-specific fragility method. This relationship will determine the probability of collapse for a bridge given a specific hazard exposure using bridge-specific fragility estimation.

$$H_D(d) = P[D \geq d] = \sum_{all\ x_i} P[D \geq d|S_a = x_i]P[S_a = x_i] \qquad (7.15)$$

$$P_{PL} = P[C \leq D] = \sum_{all\ d_i} P[C \leq D|D = d_i]P[D = d_i] \qquad (7.16)$$

An example of extending the use of the bridge-specific fragility method into a risk-based analysis and design approach is given below. The fragility estimates, which are shown in the fragility curves in Figure 59 and Figure **60**for the single-column bent bridge and multi-column bent bridge classes, are used to find the total probability of the bridge experiencing the collapse limit state for a specific hazard. The location of Los Angeles, CA, was chosen as the location to determine the hazard. Hazard curve information can be found on the U.S. Geologic Survey (USGS) website which has a web application that provides access to hazard curves generated for the 2008 National Seismic Hazard Mapping Project (NSHMP) (USGS). Figure 61 shows the hazard curves for Los Angeles, CA, for the peak ground acceleration ground motion as well as the ground motion for structures with 0.2 second and 1.0 second periods.
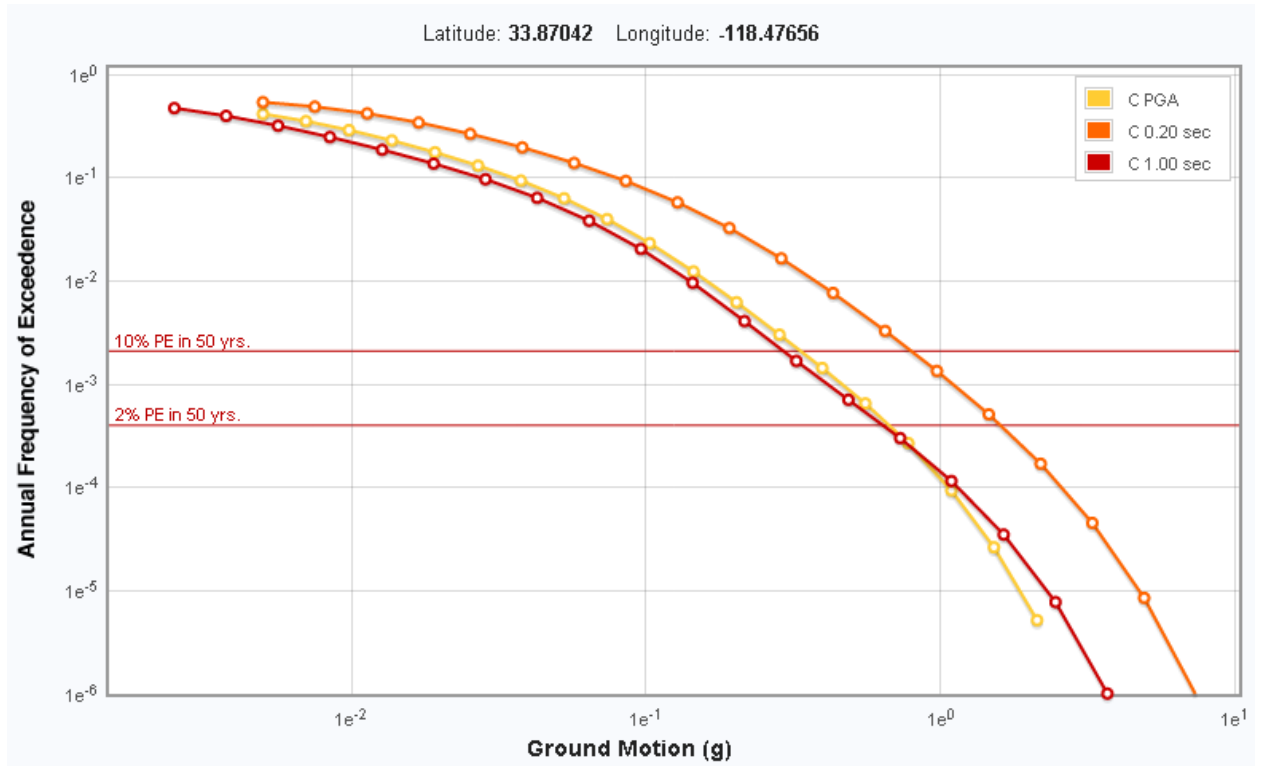
Figure 61: Hazard curves for Los Angeles, California, for PGA, Sa_1.0 and Sa_0.2 for soil type C
(USGS).

Taking this hazard information and combining with the fragility information found previously, Eqn. (7.16) is used to produce the total annual probability of collapse for the bridge structure. The calculated total probability of collapse for the bridge system of the single-column bent bridge class and multi-column bent bridge class are shown in Table 39 and Table 40. In those tables, *D=di* stands for the ground motion intensity measure value, in this case peak ground acceleration (PGA), *AFE* is the Annual Frequency of Exceedence of some limit state, and *Fragility* is the bridge-specific fragility estimate at that particular PGA level. The fragility estimates were determined using the design parameters listed in Table 35. As is shown, the estimated annual probability of collapse due to the seismic hazard in Los Angeles and the fragility of the structure is 0.0034% annually for the single-column bridge, and 0.0064% for the multi-column bridge. With this information, bridge designers must decide if this risk for their bridge

148

design is acceptable based on specific project criteria or based on engineering judgment. In this way, the bridge-specific fragility method can be used not only to produce bridge-specific fragility curves, but can be used as a basis for risk-based design analysis of bridges.

Table 39: Calculation of total probability of failure of a single-column bent bridge in Los Angeles based on peak ground acceleration ground motion levels.

D=di	AFE (Hazard)	Fragility	AFE*Fragility
5.00E-03	3.57E-01	3.39E-13	1.21E-13
7.00E-03	2.97E-01	2.19E-12	6.49E-13
9.80E-03	2.35E-01	1.41E-11	3.31E-12
1.37E-02	1.77E-01	9.02E-11	1.59E-11
1.92E-02	1.26E-01	5.85E-10	7.36E-11
2.69E-02	8.49E-02	3.79E-09	3.21E-10
3.76E-02	5.50E-02	2.42E-08	1.33E-09
5.27E-02	3.45E-02	1.57E-07	5.42E-09
7.38E-02	2.12E-02	1.01E-06	2.14E-08
1.03E-01	1.25E-02	6.42E-06	8.02E-08
1.45E-01	6.75E-03	4.27E-05	2.88E-07
2.03E-01	3.27E-03	2.75E-04	9.00E-07
2.84E-01	1.36E-03	1.76E-03	2.41E-06
3.97E-01	4.76E-04	1.12E-02	5.32E-06
5.56E-01	1.36E-04	6.80E-02	9.21E-06
7.78E-01	3.14E-05	3.19E-01	1.00E-05
1.09E+00	6.16E-06	7.52E-01	4.63E-06
1.52E+00	1.15E-06	9.50E-01	1.09E-06
2.13E+00	1.48E-07	9.92E-01	1.46E-07
		Annual Probability of Failure	**0.0034%**

Table 40: Calculation of total probability of failure of a multi-column bent bridge in Los Angeles based on peak ground acceleration ground motion levels.

D=di	AFE	Fragility	AFE*Fragility
5.00E-03	3.57E-01	3.18E-14	1.14E-14
7.00E-03	2.97E-01	2.60E-13	7.72E-14
9.80E-03	2.35E-01	2.13E-12	5.00E-13
1.37E-02	1.77E-01	1.72E-11	3.05E-12
1.92E-02	1.26E-01	1.42E-10	1.78E-11
2.69E-02	8.49E-02	1.17E-09	9.89E-11
3.76E-02	5.50E-02	9.43E-09	5.19E-10
5.27E-02	3.45E-02	7.77E-08	2.68E-09
7.38E-02	2.12E-02	6.36E-07	1.35E-08
1.03E-01	1.25E-02	5.10E-06	6.38E-08
1.45E-01	6.75E-03	4.32E-05	2.91E-07
2.03E-01	3.27E-03	3.53E-04	1.15E-06
2.84E-01	1.36E-03	2.86E-03	3.91E-06
3.97E-01	4.76E-04	2.27E-02	1.08E-05
5.56E-01	1.36E-04	1.60E-01	2.17E-05
7.78E-01	3.14E-05	6.08E-01	1.91E-05
1.09E+00	6.16E-06	9.27E-01	5.71E-06
1.52E+00	1.15E-06	9.90E-01	1.13E-06
2.13E+00	1.48E-07	9.99E-01	1.47E-07
		Annual Probability of Failure	**0.0064%**

7.3 Validation of Bridge-Specific Fragility Method

There has been much research in the area of bridge fragility analysis based on different methodologies and objectives of research. Some of this research on bridge fragility analysis was discussed earlier in a previous chapter. The current fragility information in use by Caltrans are the fragility curves used in HAZUS (2011) which were developed by Basoz and Mander (1999). These fragility curves were developed using a capacity-spectrum approach, and was based on the limited information in the National Bridge Inventory (NBI). These curves and other that have applications in fragility analysis in California have used different approaches in terms of gathering

damage data, and formulating the fragility estimation. This section will compare the present research of the bridge-specific fragility method with other research that has been developed and accepted into use in the past. The section will seek to find commonalities between the new method and the other established methods and results, as well as determine the main differences between them. This section will also highlight some advantages of the BSFM over other fragility methods and results in the realm of application to the seismic design of bridges.

7.3.1 Single Parameter Analytical Fragility Curves

The Caltrans project for which the research was conducted had another component that presented updated the fragility curves that Caltrans could use in different applications, such as post-event response, retrofitting decisions, and the like (Ramanathan, 2012). These fragility curves were designed based on detailed sub-bins of California state bridges, include distinction between design eras, bent types, and abutment type. These curves are meant to replace the current fragility curves in use, the HAZUS curves mentioned previously, for Caltrans applications as these curves would be more specific to the California bridge inventory and thus more reliable and accurate (Ramanathan, 2012).

The method in which these next generation fragility curves followed a more traditional approach to fragility analysis as compared to the method proposed in this research. The next generation fragility curves were based on an analytical method that utilizes the lognormal distribution to develop a relationship between a component response and the ground motion intensity measure and create a single parameter PSDM. The relationships used in this type of analysis were described earlier in the chapter with Eqn. (7.7). This method also uses a Monte Carlo simulation to convolve the demand and capacity models and determine the component fragility models. A joint PSDM of the component fragilities were then used to create the system fragility models, also

incorporating a Monte Carlo simulation. For more information on this method, see the thesis by Ramanathan (2012). This section will present a comparison between the traditional single parameter fragility method and the bridge-specific fragility method.

Using the aforementioned analytical fragility technique with the data generated for this research project, fragility curves were created to compare with the fragility curves created with the bridge-specific fragility method. To compare the two methods, the median values of the design parameters were used in the bridge-specific fragility curves to simulate curves that could applied to the whole bridge class. This is done because the analytical fragility curves generated with the traditional method are meant to be used in this way, as curves that can be used for any bridge in a particular bridge class. The median values of the design parameters were shown in Table 35. The two types of fragility curves were then plotted on the same plot to directly compare the results of the methods. Figure 62 through Figure 65 show system and component fragility curves for the traditional (indicated by MC) analytical method and the bridge-specific fragility (BSF) method. As for the trends of which component has the most impact on the system fragility, it is the column component for both methods. This is the case for each bridge damage state. For the first damage state, the component fragility of the joint seal contributes more to the system fragility than the rest of the components for the traditional fragility method, while in the BSF method, the abutment seat, bearing and joint seal each have the same fragility response. In the next bridge damage state, BSST-1, the contributions of each component to the bridge system fragility is more clearly seen, as the column attributes most of the fragility in each method, followed by the abutment seat then the bearing response. In the highest two damage states, the column is shown to be the component that drives the fragility of the bridge system in both of the bridge fragility methods. These fragility curves show that both methods lead to similar trends in terms of which components drive the bridge system response. Discussion about the respective fragility estimations of both methods is forthcoming.

152
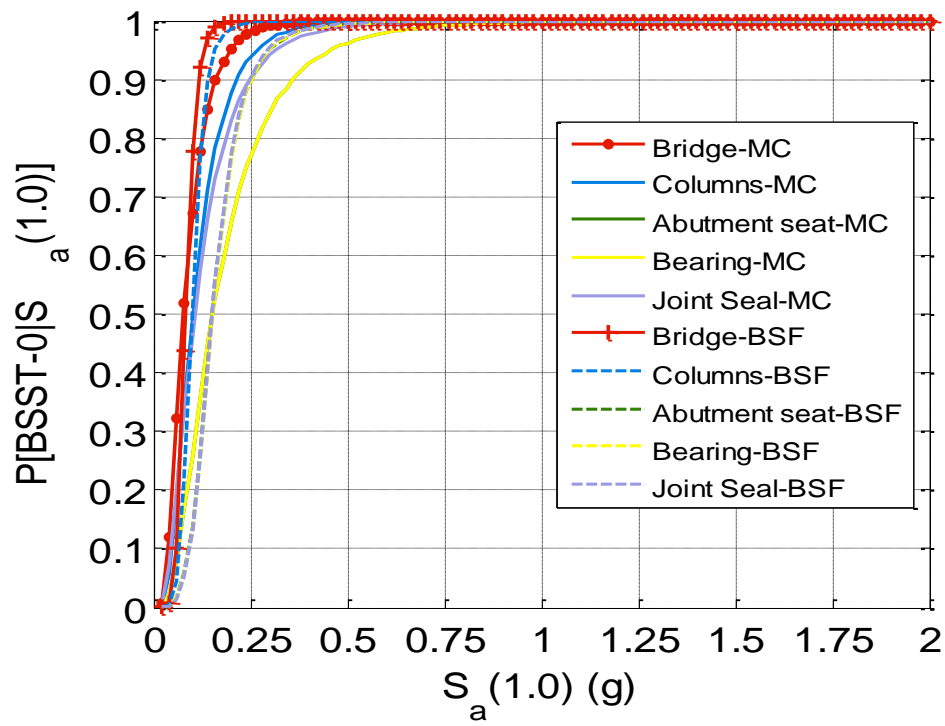
Figure 62: Comparison of MC and BSF fragility curves in the BSST-0 damage state.
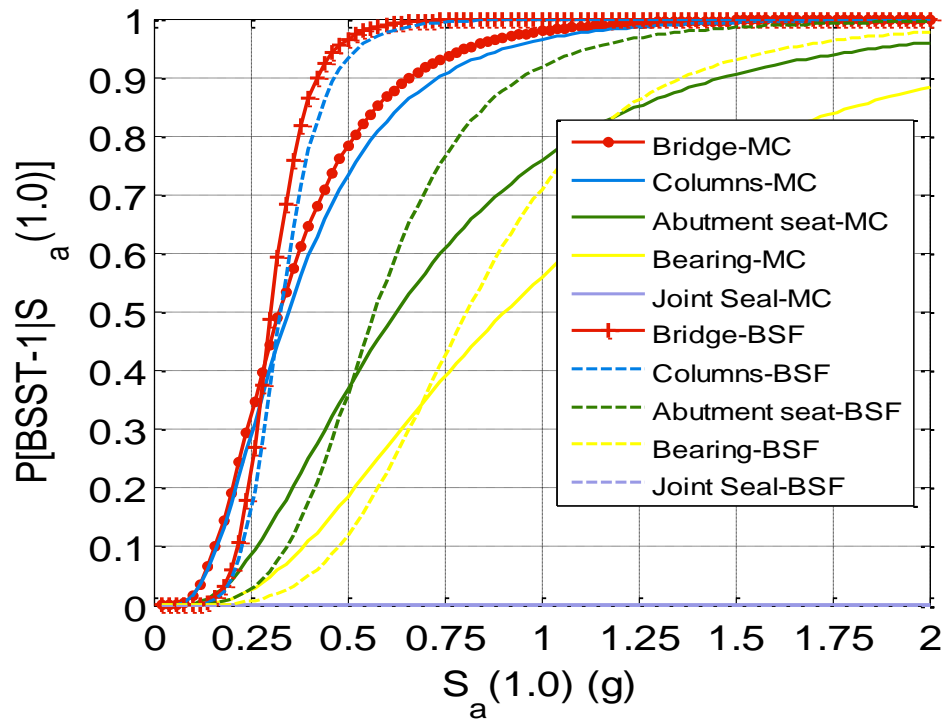
Figure 63: Comparison of MC and BSF fragility curves in the BSST-1 damage state.
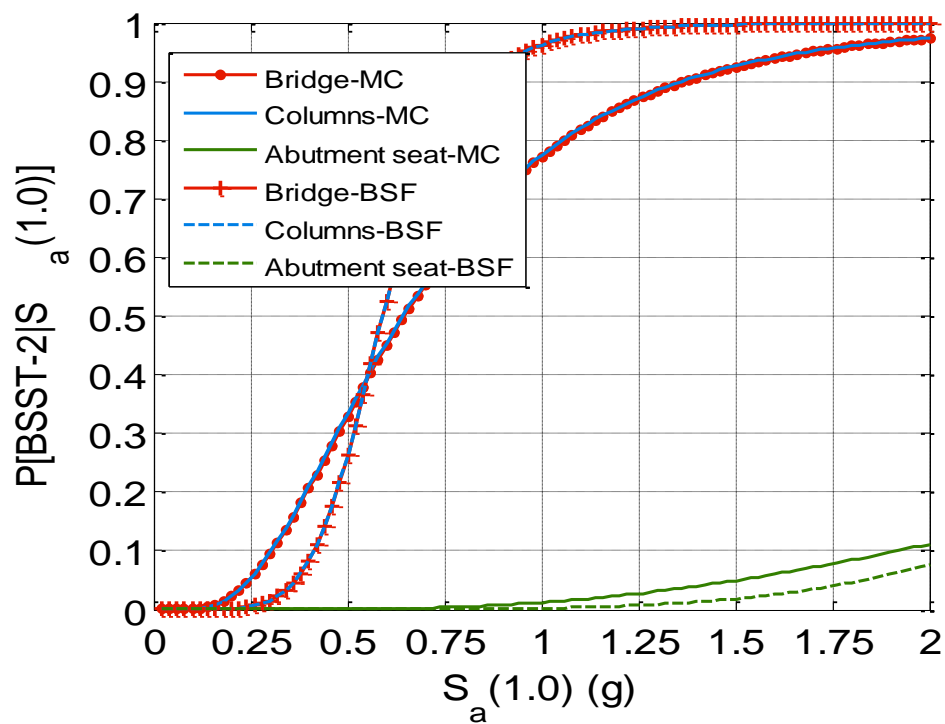
Figure 64: Comparison of MC and BSF fragility curves in the BSST-2 damage state.
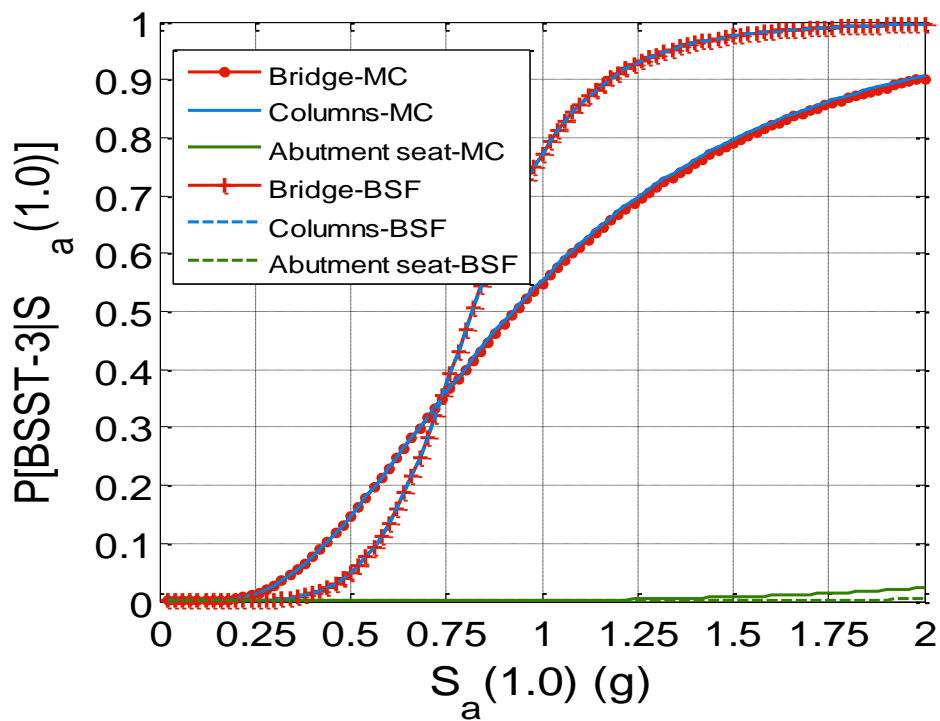
Figure 65: Comparison of MC and BSF fragility curves in the BSST-3 damage state.

The median and dispersion values of a fragility curves developed with the analytical method used here as a comparison is important in characterizing the fragility of a component or bridge system. Figure 66 shows how median and dispersion values are used to describe the fragility curve in only two values. It is shown that by increasing the median of the curve, the curve shift to the right and indicates a less vulnerable bridge. By increasing the dispersion value, the curve rotates about the median of the bridge, and is a measure of the amount of uncertainty of the curve (Mackie, et al., 2001). The calculation of the dispersion used here to compare the methods is shown in Eqn. (7.17). The value β_{FC} represents the dispersion of the fragility curves, while β_R represents the uncertainty in the structural capacity, which is given as the dispersion from the capacity model, while β_S represents the uncertainty of the structural response, given as the lognormal standard deviation of the demand model (Nielson, et al., 2007). The dispersion from the capacity model was given in an earlier chapter. These dispersions presented here are normalized by the "slope" of the PSDM, or the regression coefficient of the ground motion intensity measure, as is practiced in the MC fragility method. As is clear in Figure 62 through Figure 65 as well as in Table 39, both methods being compared have median fragility values that compare well for the bridge system as well as the component fragilities. Visually, it is evident that the two methods have different dispersion values and the dispersion values in Table 39 show that the BSF fragility curves have less dispersion about the median of the curve than the MC curves. This may be due to the fact that the BSF curves contain more information about the bridge in the multi-parameter PSDM and subsequently the regression equation is better fit to the data, compared to the MC method which only uses the ground motion intensity measure to regress against the component responses to create the PSDM.

$$Dispersion = \beta_{FC} = \sqrt{\beta_R{}^2 + \beta_S{}^2} \qquad (7.17)$$
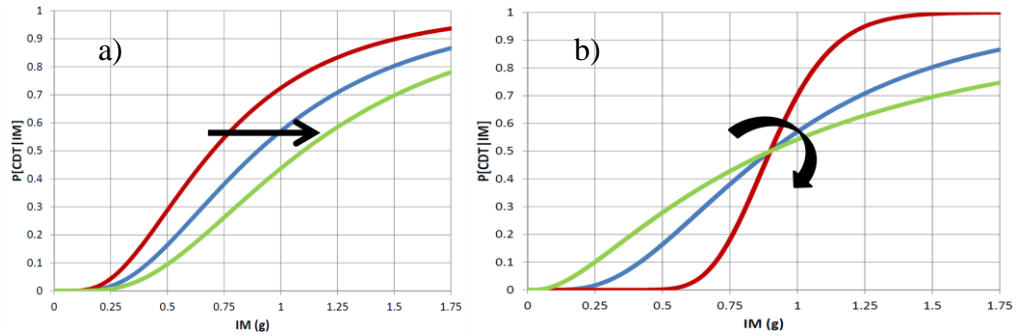
Figure 66: Effects of changes in fragility characteristics a) median, and b) dispersion.

Table 41: Comparison of fragility characteristics of the BSF and MC methods.

Bridge Component	Median Fragility – Spectral Acceleration at 1.0 sec (%g)				Dispersion
BSF Method	LS-0	LS-1	LS-2	LS-3	β
Bridge System	0.0830	0.3025	0.5910	0.8165	
Column	0.0990	0.3270	0.5910	0.8165	0.4371
Abutment Gap	0.1520	0.5710	3.2110	4.2945	0.4678
Bearing	0.1530	0.8070	N/A	N/A	0.4678
Joint Seal	0.1520	N/A	N/A	N/A	0.4678
MC Method	LS-0	LS-1	LS-2	LS-3	β
Bridge System	0.0780	0.3240	0.6470	0.9300	
Column	0.1010	0.3470	0.6430	0.9230	0.5860
Abutment Gap	0.1530	0.6260	4.4980	7.5580	0.6660
Bearing	0.1530	0.9050	N/A	N/A	0.6660
Joint Seal	0.1060	N/A	N/A	N/A	0.6660
	Percentage difference between methods				
	LS-0	LS-1	LS-2	LS-3	β
Bridge System	6.02	-7.11	-9.48	-13.90	
Column	-2.02	-6.12	-8.80	-13.04	-34.08
Abutment Gap	-0.66	-9.63	-40.08	-75.99	-42.38
Bearing	0.00	-12.14	N/A	N/A	-42.38
Joint Seal	30.26	N/A	N/A	N/A	-42.38

In conclusion, the two methods are shown to predict similar trends in terms of which components control the response of the bridge. The median values of the fragility curves are comparable across system and component levels of fragility. The dispersion

values suggest that the BSF method allows for less uncertainty in the fragility estimation due to the inclusion of additional information about the bridge and components.

7.3.2 Comparison with other analytical fragility curves

In this section, the bridge-specific fragility method is compared to other fragility analysis methods used for applications to bridges in California. There have been many different fragility curves that have been developed for application to specific bridges (Zhong, et al., 2008)(Mackie, et al., 2005), and for bridge classes or bins (Basoz, et al., 1999)(Ramanathan, 2012)(Shinozuka, et al., 2007). In this section the fragility analysis results done by some of the aforementioned researchers will be compared with the results from the bridge-specific fragility method.

Table 42 includes the median fragility estimates of the fragility curves from the work done by the fragility estimates used in HAZUS, Ramanathan, Mackie and Stojadinovic, and the results of the BSF using the median values of the design parameters. The work of Basoz and Mander (1999) has been used for years in Caltrans as the fragility estimation used in HAZUS (2011) and subsequently in the ShakeCast platform used by Caltrans that is part of their post-event assessment capability (Lin, et al., 2008). These fragility curves have been used as comparison in other papers on fragility analysis (Mackie, et al., 2007)(Ramanathan, 2012), therefore the work done by these researchers could be considered a standard by which to compare one's work. The fragility median values associated with this research work are noted as HAZUS. Ramanathan developed a new set of fragility curves for use by Caltrans meant to replace the current fragility relationships used in HAZUS (2012). He generated analytical fragility curves using an approach similar to that used in the work of Nielson and DesRoches for bridges in the central and southeastern United States (Nielson, et al., 2007). He created fragility curves for the most common types of bridges in California based on an extensive inventory analysis, including the bridge type analyzed in this research, the two-span

157

continuous concrete box girder bridge. The fragility median values associated with this research work are noted as KR. Mackie and Stojadinovic have produced research on fragility in the context of bridges in California for use in risk assessment and performance based engineering (Mackie, et al., 2005)(Mackie, et al., 2001). The fragility curves being compared in this section are based on the new design of a similar bridge type as the one analyzed in this research, a reinforced concrete highway overpass bridge, although the superstructure of the bridges could vary from box girder to I-girders or culverts. The fragility median values associated with this research work are noted as PBEE.

Table 42: Fragility median values of different fragility analysis methods.

Fragility Method	Median Fragility – Spectral Acceleration at 1.0 sec (%g)				Percentage difference from the BSF estimates			
	LS-0	LS-1	LS-2	LS-3	LS-0	LS-1	LS-2	LS-3
BSF	0.08	0.32	0.73	1.07				
HAZUS	0.60	0.90	1.30	1.60	-679	-178	-79	-50
KR	0.09	0.57	1.44	2.06	-17	-76	-98	-93
PBEE	N/A	0.5	0.72	1.82		-55	1	-71
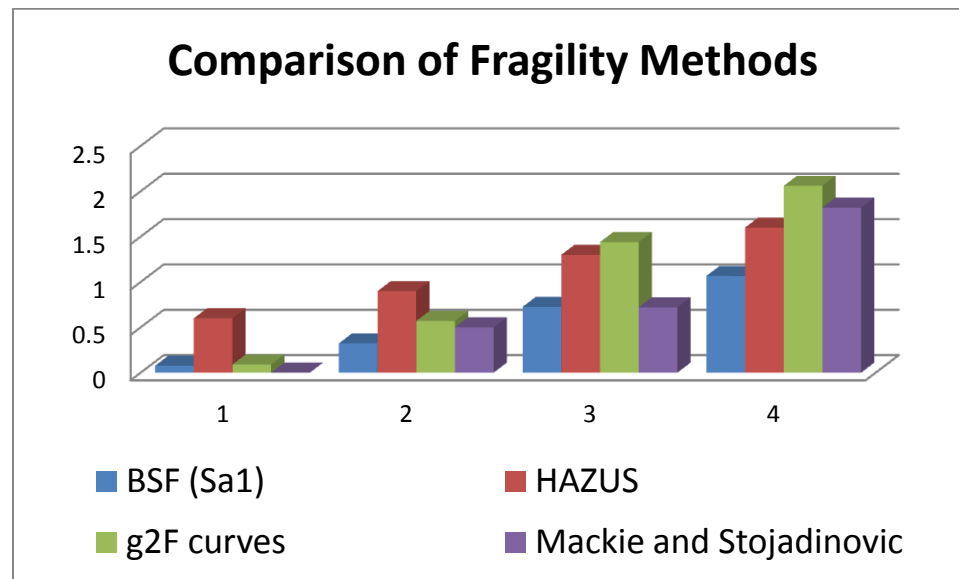
Figure 67: Comparison of different fragility analysis results with the bridge-specific results.

The median fragility estimates of the aforementioned are compared visually with the results from the bridge-specific fragility method. The bridge type compared here is the two-span single column bent bridge. The fragility information gathered from work Mackie and Stojadinovic was given in spectral acceleration at the fundamental period, instead of spectral acceleration at 1.0 second, but since most of the bridges used in this research had fundamental period within the range of 0.5 to 1.5, this was allowed. The limit states definitions may also not exactly align in the comparison. As is shown in Figure 67, the median fragility of the work of Ramanathan (KR) was the highest of the methods shown for the highest damage states, showing that that particular method estimated a bridge more robust than the other methods. The median fragility of the bridge-specific fragility method was the lowest, indicating that this particular work estimated a bridge that was more vulnerable than the others for each of the damage states. The BSF method fragility median values compared well with the work of Mackie and Stojadinovic, which may be because both analyses included in these research endeavors included additional information on the geometric design properties of the bridges in the analysis. HAZUS curves have in the past been criticized for being based on the NBI inventory bridge characteristics, which may not be able to fully describe and correctly sub-bin the different bridges types in California. This may the reason why HAZUS estimates seem to overestimate the fragility in the lower damage states. Overall, the fragility results of the BSF method seem to agree with the results of past fragility analysis research, and differ in some ways as well. The results of the BSF show that the fragility may be overestimated in some cases by other analysis techniques, perhaps due to the generalization that occurs in creating fragility curves for entire bridge classes instead of specific to single bridge.

159

7.4 Closure

In this chapter, the bridge specific fragility method (BSFM) was fully detailed and explored. The key components of the BSFM were enumerated, which include the multi-parameter probabilistic seismic demand model, and the logistic regression used to calculate the fragility estimates. The results of the analysis from following the bridge-specific framework are then presented in the form of regression equations that give fragility point estimates. Examples of the types of fragility curves one can generate with the final regression equations are then given based on median values of design parameters. Finally, the validation of the method is discussed. The method is first compared against formulating fragility curves based on a Monte Carlo simulation approach common in literature. The results of that comparison revealed that the methods predicted similar trends of component response and influence on the system response of the bridge. Also, the median values of both methods compared well. Further comparisons were given between the BSF method and other fragility analyses from past research are given. The results of that comparison shows that the BSF predicts lower median fragility values than the compared methods, indicating the BSF predicts bridges that are more vulnerable than those predicted in other methods.

CHAPTER 8

BRIDGE SPECIFIC DESIGN SUPPORT TOOL

One of the main deliverables of this research to the Caltrans project was a Bridge-Specific Design Support Tool utilizing the bridge-specific fragility analysis method described in the previous chapter. This tool implements the analysis method in an easy-to-use format for Caltrans engineers to determine the performance of their new bridge design. With the information given in the tool, the engineer can check their bridge design to determine if design criteria and goals were met with their design. It can also be used to determine if their bridge design can be made more efficient by adjusting the design parameters to see the effect of the changes on the performance of the bridge. Not only will the tool give the Caltrans information on the probability of bridge collapse for the Design Hazard as specified in the Seismic Design Criteria (SDC) used for seismic bridge design in California, but the engineer can also check the bridge performance at other damage levels and hazard levels. The design support tool, which is detailed in this chapter, was created for ease of use by the engineer and has all of the analyses of the previous chapter included to create fragility curves. This chapter will describe the implementation of the bridge-specific fragility methodology in the tool and the format of the tool. Then examples of the use of the tool will be given using existing bridges and with an example of design checks of a new bridge design with the SDC.

8.1. Format of Tool

The design support tool presented here was developed on the platform of Microsoft Office Excel 2007 (2007). This platform was chosen because of the common availability of the software to most computer users, and in particular the engineers at Caltrans. This platform also offered ease of developing the tool by using the built in

functions and chart development capabilities. Along with the Excel framework, the built-in Microsoft Visual Basic functionality was used to create macros. Macros are code that is stored in the workbook in order to automate some tasks, essentially shortcuts to tasks done in Excel (Microsoft). The following will describe the setup of the tool, and how it was designed for usage by Caltrans bridge engineers as a design support tool.

The bridge specific design support tool is presented in a Microsoft Macro-enabled Excel worksheet. As stated earlier, the spreadsheet utilizes Visual Basic macros in order to produce the bridge specific fragility curves, so the user would need to enable Macros content on their individual Excel programs. The design tool includes hidden and protected sheets in which the data from the logistic regressions for the fragility curves are placed in order to ensure the integrity of the analyses. The previous processes described earlier of the generation of the multi-parameter PSDM and the logistic regression to obtain fragility information, were completed and verified before incorporating the results into the design tool as reported in the previous chapter. The only sheets that the user would be concerned with are the Information sheet and the sheet entitled "Bridge Specific Fragility – XXX", where the XXX stands for whichever ground motion intensity measure the user chooses for the fragility analysis, such as PGA or spectral acceleration at 1 second (Sa_1). Separate worksheets could be provided for different ground motion intensity measures, depending on the analyses available with different ground motion measures. The user would only need to input the design parameters, which were discussed earlier, into the sheets and choose the appropriate macros activated by buttons included in the tool to generate the fragility curves of choice. There are optional input boxes where the user can input upper and lower bounds of the design parameters to see the effects of the variation of the design parameters on the fragility estimate of the bridge design. The output of the design support tool include system fragility curves, component fragility curves, the estimated fundamental period of the bridge, and specific fragility estimates for a given hazard level. A screenshot of the input page is given in Figure 69.

When the tool is first opened, the user will be presented with an information sheet that details the process of using the tool, as well as contact information if there are issues or questions with the tool. The message is shown in Figure 68. The user should note a warning that may be displayed about enabling Macros content in Excel, and the user should choose to activate Macros for use of this tool. The next tab gives the limit states used for the creation of the fragility curves. These values were given in Table 14, and cannot be changed by the user.

The user will then move on to the input page to develop fragility curves. Figure 69 shows a snapshot of the input page of the tool where the user would input the design parameters of his bridge. Input should only be placed in blue boxes. Red boxes will display output, and all other boxes should not be modified. The ratios of the bridge, which were described in the design parameter section of this thesis, are calculated from the input variables within the tool and checked for compliance with the boundaries of this project. The boundaries are based on the ranges of the design parameters used in the metamodels that defined the analytical bridge models that created the damage database used in the development of the PSDM.

Welcome to the Bridge Specific Fragility Design Tool for Caltrans! This tool is in Beta mode and can only be used for 2 span integral concrete box girder bridges with 2, 3, or 4 columns and seat type abutments. If this is not your bridge, these results may not be accurate!

To begin, please start by inputting your design parameters, as listed. Input boxes are blue. Be sure to check your units! If you wish to include upper and lower bounds on your design parameters to determine the effect of the parameters on the fragility of your bridge, you may do so. Make sure to include bounds on all of the parameters. Even if you only want to see the effect of one design parameter, make sure to duplicate the design parameters for the bounds of the other parameters.

After inputting your design parameters, you will be able to choose different output for your bridge. There are buttons which will produce fragility curves for the system and component level of the bridge, an estimate of the fundamental period, as well as fragility information at specific hazard levels. Output boxes are in red. If you make any changes to any parameters and want to compare the fragility curves, be sure to save the curves before producing a new one.

If there are any issues with this design tool, please contact the developer, Jazalyn Dukes, at jdukes6@gatech.edu. Enjoy!

Figure 68: Introduction message for design support tool.

Bridge-Specific Fragility

CT Design Support Tool

Please input your design parameters:

	Design		Lower Bound	Upper Bound
			Optional Input:	
Longitudinal Steel Ratio	1.64	%	1	2.4
Volumetric Transverse Steel Ratio	0.59	%	0.59	0.59
Column Height	18.1	feet	18.1	18.1
Column Diameter	54	in	54	54
Span Length	122.1	feet	122.1	122.1
Deck Depth	59	in	59	59

Your Fragility Curves and more options:

Check your Ratio Bounds:

		Status!
Longitudinal Steel Ratio	0.0164	OK!
Volumetric Transverse Steel Ratio	0.0059	OK!
Aspect Ratio	4.0222	OK!
Span Length to Column Height	6.75	OK!
Deck Depth to Column Diameter	1.0926	OK!

Figure 69: Input page for design support tool.
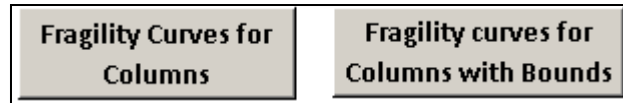
Figure 70: Buttons to produce fragility curves for column component.

8.2. Implementation of BSFM into Tool

It was determined that the best way to present the bridge-specific fragility method to Caltrans engineers for use as a way to check the performance of a new bridge design was to create a tool that included the finalized equations from the analyses of analytical bridge models. This design support tool will allow the design engineer to skip all of the analyses required for traditional analytical bridge fragility method, and get the end product of fragility analysis instantaneously for their specific bridge design. For this version of the tool presented here, the equations are formulated specifically for the type of the bridge and type of ground motion intensity measure used in the analysis. For each ground motion intensity measure considered, the coefficients of the equation, presented in Chapter 7, that determine the fragility will change. For this reason, separate worksheets were presented that were based on the specific ground motion intensity measure used in the fragility estimation.

As the regressions and determination of the bridge- specific fragility equations were determined per the procedure described in the previous chapters, the tool simply houses the equations and provides the vehicle for bridge designers to easily create bridge-specific fragility curves. The sheets in the tool are protected from modification so the integrity of the analysis can remain intact. The limit states used in the calculation of the fragility estimates and curves are also pre-determined, as mentioned in a previous chapter, and unable to be modified by the user. In future versions, the option to modify the limit states to address changing design standards or adjust to the criteria for particular bridge designs may become available. The fragility curves are created automatically with the activation of the built-in macros and are formatted specifically for ease of reading and

interpreting. The fragility curves are color-coded to correspond with the ShakeCast inspection levels used by Caltrans in post-event evaluations (Lin, et al., 2008). Since the limit states used in the analyses were designed to match those inspection levels, the results of these curves are more easily interpreted by the Caltrans design engineer who has knowledge on the meaning of the ShakeCast inspection levels. In this manner, the bridge-specific fragility method was implemented into the design support tool. The following illustrates use of the tool with an example using existing bridge information and an example illustrating the design checks used on a new bridge design in Caltrans along with the design support tool as the final design check.

8.3. Design support tool example with an existing bridge

This section will describe an example of the use of the design support tool with an existing bridge, demonstrating the results one can get and the comparative analysis possible with this tool. The example bridge chosen for analysis is California state bridge Willow Avenue Overcrossing, designed in 2002 and constructed in 2005. In Figure 69, the input parameters of the example bridge are shown. Figure 71 and Figure 72 show the elevation and typical section views of this bridge. This 2-column bridge has 1.64% longitudinal steel, 0.59% transverse steel per column, 18.1 foot columns with a 54 inch diameter, a 123 foot maximum span length, and 59 inch depth of the superstructure. A summary of the design parameters of this bridge is shown in Table 43. In the optional input section, the effect of the longitudinal steel ratio on the performance of the bridge is investigated by providing lower and upper bounds for the steel ratio at 1.0% and 2.0%, and keeping the other parameters constant.

166

Table 43: Design parameters of existing bridge, Willow Avenue Overcrossing Bridge.

Design Parameters	Abbrev.		Acceptable Ranges for Multi-Column Bridges	
			Minimum	Maximum
Longitudinal Steel Ratio	LS	1.64%	1.00%	3.00%
Volumetric Ratio	VR	0.59%	0.50%	1.40%
Aspect Ratio	AR	4.02	2.5	6.0
Span Length to Column height ratio	SpanHt	6.8	4.5	9.5
Deck Depth to Column diameter ratio	DepthDiam	1.09	0.8	1.3
Width	Width	58.0	40	125
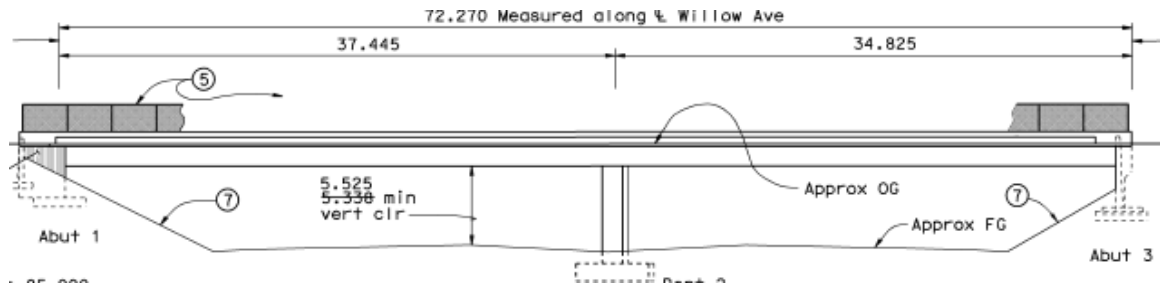
Figure 71: Elevation view of the Willow Avenue Overcrossing Bridge.
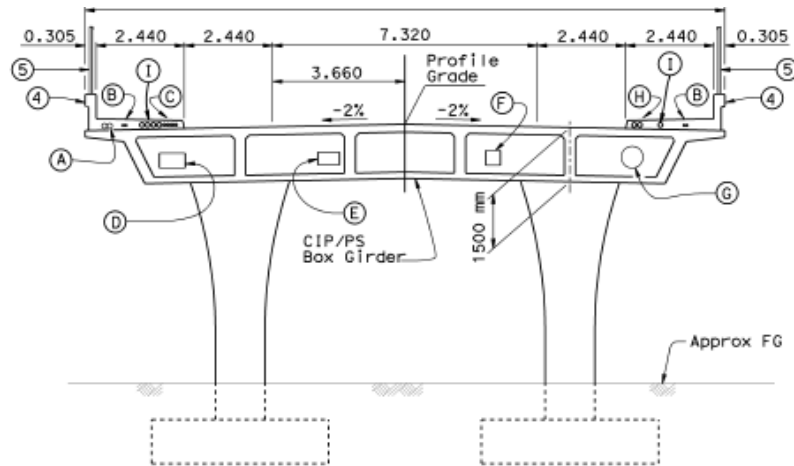
Figure 72: Typical Section of the Willow Avenue Overcrossing Bridge.

The fragility curves based on the ground motion intensity measure, PGA, for the example bridge for the column components are given in Figure 73 and Figure 74. The fragility curves for the bridge system as well as the other primary and secondary components are given in Appendix E. The first figure shows the fragility curves for the

four component damage threshold (CDT) values for the column component based on the design parameters of the design bridge. The colors of the curve correspond to the ShakeCast inspection priority levels as described earlier. The second figure includes the fragility curves of the upper and lower bounds to show the effect of changing the design parameters, in this case the longitudinal steel ratio, on the fragility of the bridge. Table 44 shows the percent savings and gains made by choosing the upper or lower bounds of the longitudinal steel ratio. Based on the criteria for their specific bridge design project, the user can then decide which value of steel content works best for that particular project. The table shows that the user would increase the probability of the highest damage level (CDT-3) occurring by 237% if the lower longitudinal steel ratio was used instead of the original percent steel, and could reduce the probability of failure by around 60% if the amount of longitudinal steel was increased to 2.0% from 1.64% at a PGA of 0.5 g. The user can also find specific fragility points for any hazard level, as shown in Table 45, where LS-# corresponds to appropriate CDT or BSST limit state. The user inputs the desired hazard level into the blue box and the different fragility points are displayed for the system level fragility as well as the component fragility information.

This procedure can continue with the other design parameters, by changing the bounds and design parameter inputs, to get the fragility information needed to gather useful performance based information on the user's bridge design to make more informed design decisions backed by probabilistic fragility analysis results. Using this tool to do comparative analysis can result in a better understanding of the performance of the bridge as well as more efficient and safer bridge designs.
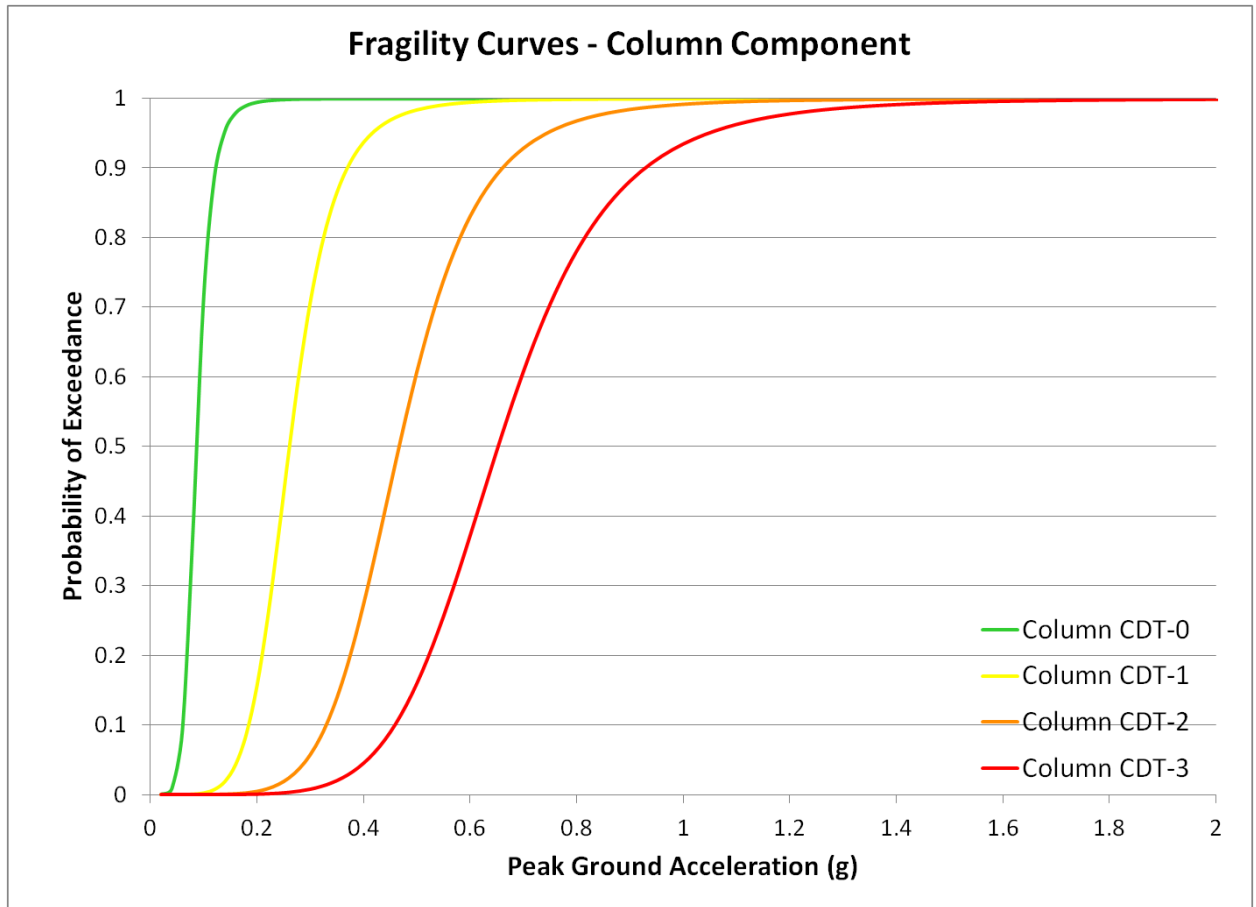
Figure 73: Bridge specific fragility curves for column components at all damage levels.
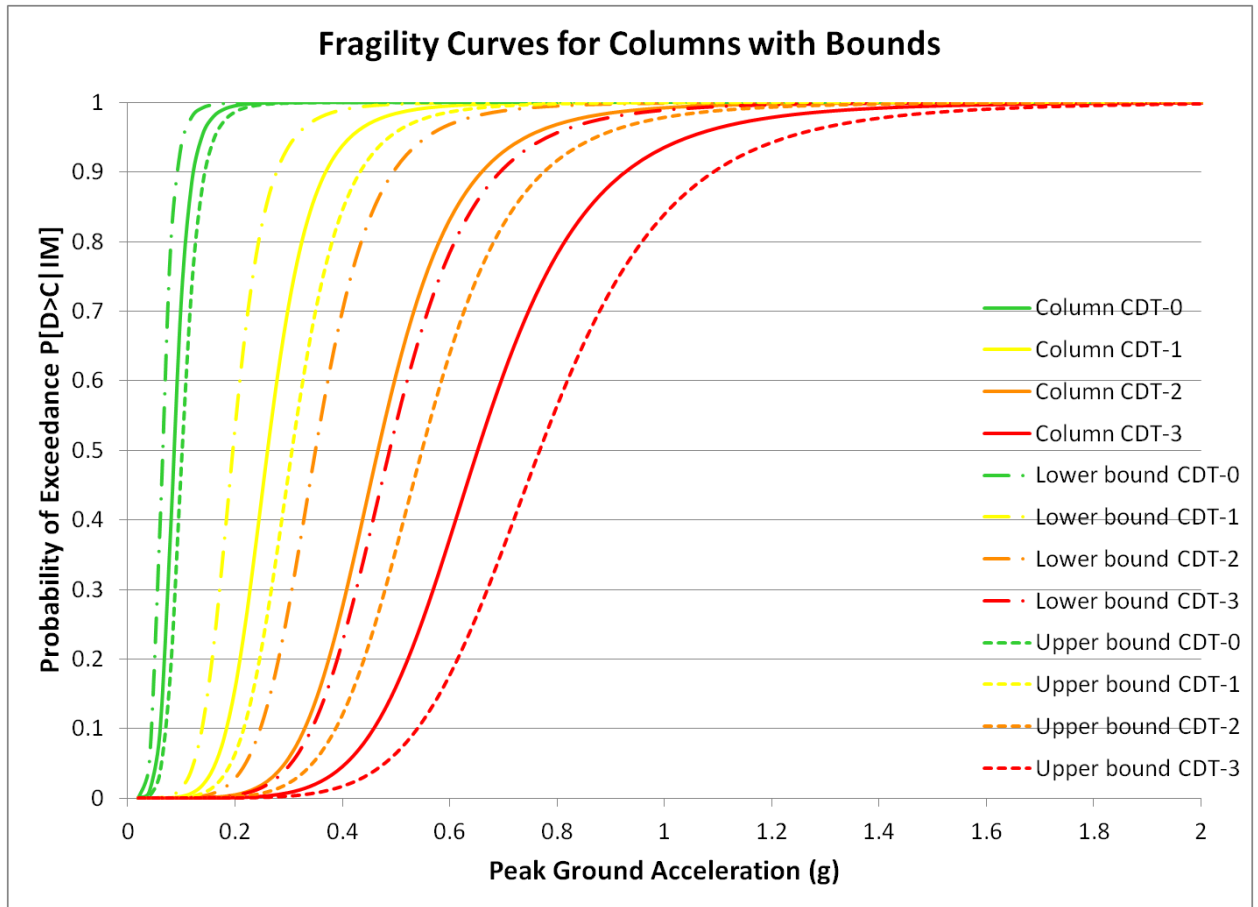
Figure 74: Bridge specific fragility curves for column components with upper and lower bounds.

Table 44: Comparison of fragility values at 0.5g of PGA at upper and lower bounds of the longitudinal steel content for the column component.

	Original (1.64%)	Lower bound (1.0%)	Percent Diff	Upper Bound (2.0%)	Percent Diff
CDT-0	1.000	1.000	0.0%	1.000	0.0%
CDT-1	0.984	0.997	1.4%	0.957	-2.7%
CDT-2	0.608	0.905	49.0%	0.357	-41.2%
CDT-3	0.160	0.537	236.5%	0.064	-59.8%

Table 45: Specific hazard level fragility information.

Peak Ground Acceleration (g)	0.5			
Specific Fragility estimates:	**LS-0**	**LS-1**	**LS-2**	**LS-3**
System	100.0%	98.9%	59.2%	16.0%
Column Component	100.0%	98.4%	60.8%	16.0%
Gap at Abutment Component	99.7%	45.2%	0.0%	0.0%
Bearing Component	99.7%	16.2%	0.0%	0.0%
Joint Seal Component	99.6%	0.0%	0.0%	0.0%

8.4. Design Check Example with SDC

This section will illustrate checking the new design of a bridge in California using the design checks in place in the Caltrans seismic design process and also the design support tool. As was mentioned in a previous chapter, the current seismic design process is very thorough in terms of setting requirements for checking the capacity and demand of many bridge components. Bridges designed today not only have to meet general bridge design requirements, but also have to make sure everything is designed to withstand an expected earthquake load. The flowcharts in Appendix A describe the procedures that need to be taken to ensure a proper seismic design of a new bridge, as detailed by a Caltrans bridge engineer (Setberg, 2011). Each design check should be considered during the design process and afterwards. The design checks mostly deal with the relative stiffness of the structure, ductility of columns, and the structure displacement demand. The design support tool will be used as the final design check to determine the performance of the bridge, it's compliance with the requirements of the SDC, and the performance of the bridge in other limit states.

The new bridge design will be determined as followed. All of the design properties and parameters that were included in the building of the analytical models for the fragility analysis will be determined randomly with a MATLAB code (2011). The geometric properties will be checked to ensure that the bridge fits within the ranges determined from the Caltrans bridge plan analysis and that the resulting bridge design is

realistic. The details of the bridge design determined in this matter are shown in Table 46 and Table 47.

Table 46: Geometric Properties of example bridge design.

Geometric Properties of the design bridge	Units	
Span Length	(ft)	144.
Column Height	(ft)	27.6
Deck Width	(ft)	41.7
Number of cells in girder	(Num)	5
Wall thickness	(in)	12
Deck Depth	(in)	67.6
Number of Columns	(Num)	2
Column Diameter	(in)	60
Abutment Backwall Height	(ft)	7.71
Concrete Strength	(ksi)	5.19
Steel Strength	(ksi)	79.1

Table 47: Design parameters of the example bridge design.

Design Parameters	Abbrev.		Acceptable Ranges for Multi-Column Bridges Minimum	Maximum
Longitudinal Steel Ratio	LS	1.17%	1.00%	3.00%
Volumetric Ratio	VR	1.04%	0.50%	1.40%
Aspect Ratio	AR	5.52	2.5	6.0
Span Length to Column height ratio	SpanHt	5.23	4.5	9.5
Deck Depth to Column diameter ratio	DepthDiam	1.13	0.8	1.3
Width	Width	41.7	40	125

The following describes the process of checking the bridge design for compliance with the Caltrans seismic design criteria as specified in the SDC. The calculations for these design checks are included in Table 50 in Appendix A. The first design check is that of balanced stiffness, as shown in Figure 76 of Appendix A. This check requires that the stiffness of the bents of the bridge system are close enough so there would not be an issue of unbalanced responses to an earthquake loads, which may lead to complex nonlinear response, increased damage in the stiffer bents, and possible column torsional

response (Caltrans, 2010). Details on balanced stiffness requirements are found in Section 7.1.1 of the SDC. As the bridge type only has one frame and one bent, the only stiffness to check are the stiffness of the two columns in the bent. The design check specifies that adjacent columns within a bent need to have stiffness within 75% of the other, shown in Eqn. (8.1). As the columns in this bridge are similar, the stiffness of the columns would be equal. Based on this the bridge passes this design check.

$$\frac{k_i}{k_j} \geq 0.75 \tag{8.1}$$

The second design check is that of the local member ductility capacity, shown in Figure 77 of Appendix A, and is quantitatively shown in Eqn. (8.8). This design check is referenced in the SDC in section 3.1.4.1 as the Minimum Local Displacement Ductility Capacity for each ductile member in the bridge. This requirement is to ensure adequate rotational capacity in the plastic hinge regions of the ductile member (Caltrans, 2010) . In order to find the ductility capacity of the ductile members of the bridge, in this case, the columns at the bent, several steps must be taken. Eqns. (8.2-7) show the parameters that must be calculated from the properties of the bridge, including the plastic hinge length of the column (L_p), plastic curvature capacity (ϕ_p), plastic rotational capacity (θ_p), plastic displacement capacity (Δ_p), yield displacement of column at the formation of plastic hinge (Δ_y), and the displacement capacity (Δ_c). Some quantities, such as the yield curvature (ϕ_y) and ultimate curvature (ϕ_{ult}), were determined from the section analysis software called CONSEC (Matthews, 2005). The final displacement ductility (μ_c) of the ductile members for the example bridge is 10.7, exceeding the minimum ductility capacity as specified in the SDC, therefore the bridge passes this design check.

$$L_p = \max\{0.08L_{eff} + 0.15f_{ye}d_{bl}, 0.3f_{ye}d_{bl}\} \tag{8.2}$$

$$\phi_p = \phi_u - \phi_y \tag{8.3}$$

$$\theta_p = L_p\phi_p \tag{8.4}$$

$$\Delta_p = \theta_p \left(L_{eff} - \frac{L_p}{2} \right) \tag{8.5}$$

$$\Delta_y = \frac{L_{eff}^2}{3} * \phi_y \tag{8.6}$$

$$\Delta_c = \Delta_y + \Delta_p \tag{8.7}$$

$$\mu_c = \frac{\Delta_c}{\Delta_y} > 3 \tag{8.8}$$

The next design check is that of the displacement ductility demand, shown in Figure 78 of Appendix A, and quantitatively shown in Eqn. (8.11). This requirement is described in Section 2.2.4 of the SDC. The displacement ductility demand describes the post-elastic bending of the ductile member (Caltrans, 2010). This value is calculated by first determining the period of the frame or structure using Eqn. (8.9). The mass and stiffness values were calculated in a previous design check. Then, the spectral acceleration at that period (a) is determined using ARS curves. To find this value, seismic loading details were taken from an actual bridge from the California bridge plan survey, the Jackson Street Bridge in Riverside County, California. This bridge was designed for a Magnitude 7.25±0.25 earthquake at a site with a Soil Profile D and peak rock acceleration of 0.4 g. The ARS value for this information, along with the period calculated previously is 0.69 g. The demand is then calculated using Eqn. (8.10). The resulting ductility demand is found to be 2.3, which is less than the maximum allowed of 5. Thus the bridge passes this design check.

$$T = 2\pi \sqrt{\frac{m}{k}} \tag{8.9}$$

$$\Delta_D = \frac{m \cdot a \cdot g}{k} \tag{8.10}$$

$$\mu_d = \frac{\Delta_d}{\Delta_y} \leq 5 \text{ for multi column bents} \tag{8.11}$$

The next design check is that of the global displacement criteria, shown in Figure 79 of Appendix A, and shown in Eqn. (8.12). The global displacement criteria is given in Section 4.1.1 of the SDC, listed as a Performance Criteria for the bridge design. The SDC

mentions that care should be taken to compare the two values as calculated along the same local axis to ensure the proper comparison. In this example, the displacement demand of the ductile member (Δ_{dg}) is taken as the same as calculated in the previous design check, and the displacement capacity (Δ_c) is the same as was determined in the local member ductility capacity design check. As the demand at 2.3 is less than the capacity at 10.7, the example bridge passes the design check.

$$\Delta_{dg} < \Delta_c \qquad (8.12)$$

The final design check is that of the load-displacement, or P-Δ, effect, shown in Figure 80 of Appendix A. This requirement is found in the SDC in Section 4.2. This design check is to determine if the lateral displacements caused by the axial load on the ductile member, or column, can be ignored, and further non-linear analysis to determine the effects can be skipped (Caltrans, 2010). To check this requirement, Eqn. (8.13) is used. The dead load on the column (P_{dl}) and the displacement demand (Δ_{dg}) was calculated in the previous design check. The plastic moment (M_p) was determined with the CONSEC software. The ratio as shown in Eqn. (8.13) for the example bridge was calculated as 0.001, much less than the limit of 0.20, therefore this bridge passes this design check, and P-Δ effects can be ignored in this design.

$$\frac{P_{dl}*\Delta_{dg}}{M_p} \leq 0.20 \qquad (8.13)$$

The example design bridge developed here has passed all of the design checks used by Caltrans engineers. The assumption is that by following the procedures set out in the SDC and designing the bridge to meet the design checks, then the bridge should be able to meet the performance objective of the SDC, which is to prevent collapse of the bridge in the case of a Design Earthquake Hazard (Caltrans, 2010). In order to quantify that performance to give the design engineer a better indication of the performance and efficiency of the bridge design, the design support tool (DST) presented in this research will be used. The design parameters will be entered into the DST to create bridge-specific

fragility curves and determine specific fragility estimates at the Design Hazard level to determine the probability of collapse of the bridge, as well as information on other damage levels.

The bridge system fragility curves of the design example bridge are shown in Figure 75. As was the case for the previous fragility curves, the curves are color-coded to match the inspection levels used in the post-event assessment tool, ShakeCast (Lin, et al., 2008). Table 48 contains the specific fragility points for the design example bridge at a peak ground acceleration of 0.5g. As is shown, the probability of collapse of the system, which is the fragility estimate at the highest damage state, BSST-4, is 24.3% for this bridge. Depending on the specific project criteria, this probability of collapse may not be acceptable for this design. The engineer must then modify the design in order to meet the criteria of the project. The tool can also be used for that purpose as well.
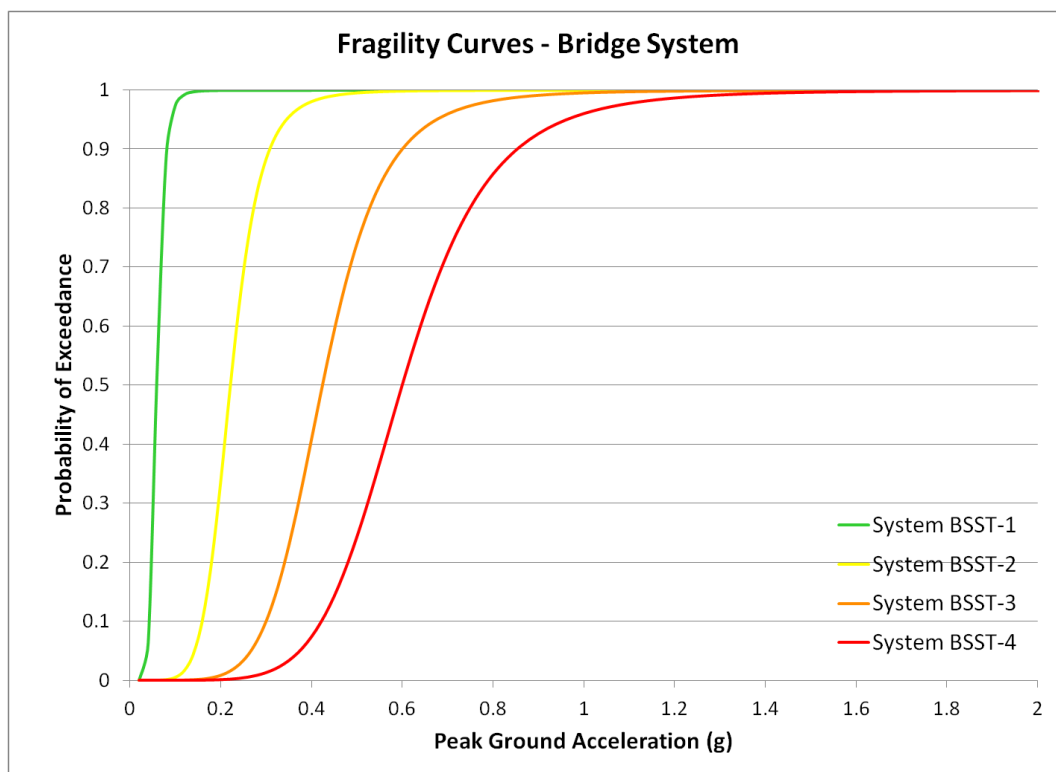

Figure 75: Bridge system fragility curves for design example bridge.

Table 48: Fragility estimates for bridge components and system of design example at PGA of 0.5g.

Peak Ground Acceleration (g)	0.5			
Fragility estimates:	**LS-0**	**LS-1**	**LS-2**	**LS-3**
System	100.0%	99.6%	74.0%	24.3%
Column Component	100.0%	99.1%	74.9%	24.3%
Gap at Abutment	99.9%	72.6%	0.0%	0.0%
Bearing Deformation	99.9%	38.3%	0.0%	0.0%
Joint Seal Component	99.9%	0.0%	0.0%	0.0%

In order to determine the necessary changes to the design in order to get the performance the engineer wants for the bridge design, a comparative analysis can be performed within the design support tool. With the comparative analysis, the engineer can look at one or more design parameters to adjust in order to get the performance the engineer needs for their design. Table 49 shows the comparative analysis one can perform under this circumstance. For example, if the Design Earthquake Hazard for this bridge is a peak ground acceleration of 0.5 g, and the acceptable probability of collapse at that hazard level is 10% or less, then the engineer knows the criteria to meet with the modifications to their design parameters, and can check compliance with the design support tool.

Table 49: Comparative analysis of design example bridge to find design to meet criteria.

Peak Ground Acceleration (g)	0.5
Fragility Estimates:	**BSST-4**
Original Design	24.3%
LS 1.5%	11.2%
LS 1.8%	**5.1%**
VR 1.4%	23.8%
AR 6.0	21.6%
SpanHt 4.5	18.4%
DepthDiam 0.9	22.4%
Width 55	27.1%
LS 1.5%, SpanHt 4.5	**8.2%**
LS 1.8%, SpanHt 4.5	**3.7%**

From the analyses done in the tool shown in Table 49, it is shown that several modifications can actually help the engineer design their bridge to move closer to meeting the project criteria. Recall, the original design parameters of the design example bridge are given in Table 47. Increasing the longitudinal steel content in the columns of the bridge significantly reduces the fragility of the bridge at that damage state. If the steel content was increased to 1.8%, the bridge would be able to meet the project criteria by reducing the probability of collapse to 5.1%. Varying the other design parameters also impact the fragility of the bridge, although to a lesser degree. Increasing the volumetric transverse steel ratio in the columns, increasing the aspect ratio by increasing the column height, decreasing the span length to column height by decreasing the span length, and decreasing the deck depth to column diameter by decreasing the deck depth all decreased the probability of collapse of the bridge. Increasing the width of the bridge actually increased the fragility of the bridge, thus that variation of that design parameter is not desirable. It is then shown that by combining changes to different parameters, one can also obtain the desired performance from the bridge design. If the engineer increases the longitudinal steel content of the columns to 1.5% and increase the span length to column height ratio to 4.5, then performance criteria of that bridge design can be met. Further comparative analysis of this type can be performed with this tool, which can assist the design engineer to better understand the performance of the bridge, and the impact of the different geometric design aspects of the bridge on the response of the bridge. The use of this bridge in the seismic design process can thus lead to better, more efficient bridge designs.

8.5. Closure

This chapter described the Design Support Tool that was developed as the vehicle for presenting the bridge-specific fragility method to Caltrans engineers. This tool was developed for ease of use and comprehension. It has automated the process of developing

the fragility curves of new bridge designs by using macros in the Excel worksheet of the design support tool. This chapter presented the format of the tool, as well as examples of using the tool. The first example showed how using information from an existing bridge from a bridge plan can result in bridge-specific fragility curves as well as information on a comparative analysis that can be completed to determine the effects of varying the design parameters on the performance of the bridge. The second example showed how the DST can be integrated into the final design checks used by Caltrans engineers. The example went through the procedure of checking the new bridge design with the design checks as outlined by a Caltrans engineer, then using the DST as the final design check to quantify the performance of the bridge. Using these design checks in conjunction with each other can ultimately lead to the safest and most efficient bridge design possible. This chapter shows how the bridge-specific fragility method can be used in a practical way for bridge designers and how the DST can lead to a better understanding of the performance of new bridge designs and more efficient designs.

CHAPTER 9

CONCLUSIONS AND FUTURE WORK

9.1 Summary and Conclusions

The seismic bridge design process of California details the minimum requirements of a bridge design that will result in a structure that should be able to withstand the Design Seismic Hazard (DSH) level without collapse. However, the process does not include a way to determine the expected performance of the bridge at the DSH level or at other hazard levels. This research introduced a bride-specific fragility method and accompanying performance-based design support tool into the Caltrans design process that provides probabilistic fragility information that describes the performance of the bridge at different hazard levels. The support tool also gives insight into the effect that different design decisions can have on the performance of a bridge. The results for this method and tool are presented here for a common bridge type in California: the two-span integral concrete box girder bridge.

In order to accomplish the aforementioned objectives, a new fragility method was developed that incorporates bridge design details into the fragility estimation. Design details that were included in the new fragility method were those that, in research and experience, were found to have a significant effect on the response of the bridge during an earthquake. The significance of the effects of the design details, or design parameters, on the bridge responses was tested in sensitivity studies, and the results agreed with the assumption that the set of design parameters investigated would have significant effects on the response of different bridge components.

The fragility method presented here is a type of analytical fragility method. One of the main components of the typical analytical fragility method that was modified for use in this project was the demand model. The traditional probabilistic seismic demand

model (PSDM) had to be modified to accommodate design parameters as input variables, creating a multi-parameter PSDM. The multi-parameter PSDM facilitates the development of bridge specific fragility curves. Because the multi-parameter PSDM uses specific bridge design details, the resulting fragility analysis can be specific to a new bridge design with those design details as inputs in the fragility estimation.

Results from the bridge-specific fragility method were compared with fragility curves developed by an analytical fragility analysis method that was described as the traditional fragility method. The BSFM fragility curves were developed by using the median values of the design parameters in the regression equations to simulate curves that represented the entire bridge class. The traditional curves were created with the method described by Ramanathan (2012), and used the data generated in this research from the analytical bridge models described in Chapter 5. The results showed that both methods predicted similar trends in terms of which components controlled the overall bridge system fragility estimating. The median values of the fragility curves compared well, although the shapes of the curves differed. This may be attributed to the fact that BSFM curves contain more information about the bridge in the fragility calculation, thus reducing the uncertainty in the curves as compared to the traditional curves. Results from BSFM fragility curves were also compared to the results from fragility curves developed in past research on bridge fragility, including the curves used in HAZUS and curves developed by Ramanathan that are intended to replace the HAZUS curves in Caltrans fragility applications (2012). The BSFM fragility curves were again developed by entering the median values of the design parameters in the regression equations. Past research was chosen that included analysis on a similar bridge type to the one used in this research. The comparisons show that BSFM predicts a more vulnerable bridge in all of the limit states as compared to the other fragility curves, including HAZUS curves. One possible explanation for these results could be that additional information from the bridge design parameters included in the fragility estimation allowed the prediction of a more

181

vulnerable bridge than the other methods. There could also be discrepancies based on the vulnerability introduced into the fragility estimation from the ground motion suites used, the way the bridge models were designed, and the how the limit states were defined in each of the different cases which were compared.

The bridge specific design tool was created to be a supplemental analysis tool and a final design check for the Caltrans bridge designer. The design support tool makes use of the results of the bridge-specific fragility methodology, which consists of the multi-parameter demand model, the capacity model developed for California bridges, and logistic regression to develop bridge-specific fragility curves for the user. The design support tool was created to be user-friendly and easy to use, with options for the user to extract only the information most useful to them in the forms of fragility curves or point estimates. The user can get fragility information for the bridge system, as well as for individual primary and secondary components. It includes different options to display fragility curves and also gives the user the opportunity to access fragility estimations at particular hazard levels in terms of a ground motion intensity measure values like peak ground acceleration. In this way, engineers can directly determine the probability of collapse at the Design Seismic Hazard level of their design and decide whether the bridge meets the performance specifications for their particular project. If the design does not meet the performance requirements, the tool allows the engineer to adjust the design parameters to find a design that meets the requirements. The tool allows for comparative analysis of design parameters because of the included option of entering upper and lower bounds of the design parameters. This allows the user to visually see the effect of different design decisions on the performance of the bridge. In this way, the DST assists design engineers in making better informed design decisions, as the engineer can directly see the impact of the variation in the design parameter values on the performance of the bridge. This tool will be a useful and accessible way to generate probabilistic fragility information on new bridge designs as well as add a much needed performance-based

design aspect into the Caltrans seismic design process. It should be noted that because of the objective of the research, the use of the design tool has a limited application in terms of the type of bridge for analysis and the range of the design parameters for which the tool can be used. This is to ensure that the bridge-specific fragility information produced by the method and tool is applicable to the specific bridge design of the user.

Throughout the thesis, the case for bridge-specific fragility analysis was built, demonstrated and defended. The BSFM is adaptable and customizable to the bridge type and other details that may be desired by users. The results of the BSFM have been shown to be comparable with existing fragility curves and methods. The DST is easy to use and provides a needed service to design engineers. It was also shown that this tool can be easily adopted into the seismic design process used by Caltrans as a design check after the design of the bridge has been completed and passes the other design checks. This tool can be used as the final check to give design engineers needed performance information on their design to ensure that the design meets the specified criteria of non-collapse at the design hazard level. It also gives fragility information at other hazard levels and limit states as well. Furthermore, this work has been presented to Caltrans design engineers and accepted as a promising tool that can be expanded within the design program after initial testing of the tool by design engineers. The results of this research are part of a feasibility study into fragility methods and applications that may be expanded into full use by Caltrans in the future. If Caltrans design engineers find this tool useful, are comfortable with the way it works as a design check, and are confident with the results given by the method and tool, then this method and tool can be developed for other bridge classes for expanded use in new seismic bridge design. In all, this method and tool presented in this thesis have shown that fragility analysis has a place in the future of the seismic design process of Caltrans.

9.2 Research Impact

This study presented a bridge-specific fragility framework that can be used to develop fragility curves that are specific to a particular bridge design based on important design parameters for one common bridge type in California. The following are major contributions of this research to the field of fragility analysis and seismic bridge design:

- This research presented a better understanding of the effects of certain design parameters on the response of different bridge components within a probabilistic framework. The sensitivity studies including in this work as well as the BSFM fragility curves show how each of the design parameters included in this research affect the response and performance of the components of the two-span concrete box girder bridge.

- The capacity model, which focused on aligning the limit states to directly correlate to ShakeCast inspection levels, and to specific traffic and closure implications, can be useful in future applications of such a capacity model. Limit states that directly align with traffic, loss, or closure implications are more useful in the practical application of fragility curves.

- In this research, properties of the bridge such as the longitudinal steel ratio and the span length to column height ratio were determined to have a significant impact on the prediction of the response of bridge components for the two-span concrete box girder bridge. These findings show that consideration of the design properties of bridges should be included in the estimation of response models, such as the demand models used in fragility analysis.

- The multi-parameter PSDM developed in this study utilized design parameters in addition to the ground motion intensity measure to predict the response of bridge components. This form of demand model introduced design parameters

184

into the fragility estimation of bridges. The results of the PSDM regression models showed a model that fits the data very well, with a better fit than a PSDM that only considered the ground motion intensity measure, indicating that this demand model is an improvement over the traditional PSDM.

- The bridge-specific fragility framework is one of the major contributions from this research. The bridge-specific fragility method was developed to create fragility curves specific to the design of a bridge, and to be used in the design process of bridges. This framework allows fragility analysis to be directly relevant in the design process of new bridges, by facilitating the creation of fragility curves that are tailored to the specific design details of the bridge design. The method eliminates the need to follow the traditional fragility analysis method to create bridge-specific fragility curves for each new bridge design, which requires extensive computer simulations and post-processing. The BSFM has the advantage of creating bridge-specific fragility curves based on regression equations that require the input of design details of the new bridge design, and does not require new computer simulations and analysis for each bridge design.

- The BSFM adds the ability to produce performance-based analysis into the seismic design process. The results of the analysis can be used to determine the probabilistic performance of the new bridge design based on the design details of the bridge. The results can be used by the design engineer to show that the bridge has met the performance criteria set forth by the SDC and other project criteria.

- The design support tool allows the user to directly access fragility curves and fragility estimation through the vehicle of the easily accessible platform, Microsoft Excel. The tool is user-friendly and gives the design engineer clear results in the form of fragility curves distinguished by components, as well as

185

specific fragility points that correspond with a particular hazard level. This facilitates access to the probability of failure or collapse of the bridge at the Design Seismic Hazard level which gives the engineer quantitative information as to the performance of the bridge and the ability of the design to meet the performance criteria set forth in the SDC.

- The ability to directly quantify the expected performance of a new bridge design with fragility analysis within the design process is a major impact into the fields of seismic bridge design and fragility analysis. Prior to the work presented here, there was no application of fragility analysis in the seismic design process for bridges. Fragility analysis also has not been used to quantify the expected performance of bridges while yet in the design phase. This research introduces fragility analysis into the seismic design process and allows for the quantification of the expected performance of different bridge components and the bridge system during the design process.

- Once the bridge-specific fragility method and tool presented here are implemented into the seismic design process and used as a final seismic design check, the bridges designed and constructed will be safer as a result of the ability to check the expected performance of the design. The DST gives design engineers access to performance information specific to the design details of the new bridge design and the ability to affirm that the bridge design meets or exceeds specified design performance criteria. Additional benefits to the design of bridges that will be built using the BSFM and DST include more cost effective and efficient bridge designs. The ability to determine the effect of each design parameter change on the fragility estimation of bridge components and bridge systems allows the designer to find optimal combinations of the design parameters that will still satisfy the seismic design requirements for the specific design. Thus, the BSFM and DST have the

potential to improve the quality, value and effectiveness of future bridge designs in California and wherever this method is adopted.

- An important impact of the research presented here is the acceptance of this method and tool by Caltrans design engineers. As part of the project for which this research was conducted, a final report and presentation were given to a team of Caltrans design engineers who would be most impacted by this method implemented into the design process. The work was embraced with enthusiasm and optimism as to the future use of this method and tool in the Caltrans seismic design process.

9.3 Recommendations for Future Work

There are several areas in which the research presented in this thesis could be extended. The following describe some of those areas.

- This study looked at the potential of bridge-specific fragility analysis for one bridge type in California: the two-span continuous concrete box girder bridge with single column bents and multi-column bents. Future work can focus on expanding the use of the method and tool to other bridge types common in California. Work can begin by extending the tool to include other bridge types within the multi-span continuous concrete bridge class, such as multi-frame bridges with in-span hinges. Other common types of bridges in California include the multi-span T-girder bridge class, multi-span I-girder bridge, and slab bridges. In order to expand the DST to other bridge types, the entire bridge-specific fragility framework must be followed, as described in Appendix B, for each bridge type, and the regression equations necessary to create bridge-specific fragility curves should be created. Once the regression equations are developed for each bridge type through the framework, they can be entered into the DST for use by design engineers.

187

- The metamodel chosen for this tool was the Response Surface Method to create the multi-parameter PSDM. Future work can explore other metamodels that may be used for the multi-parameter PSDM to determine the best fit of the data and best prediction of response. There are several other metamodels in use today that are used to predict response based on various input variables (Simpson, et al., 2001). Metamodels involving Neural Networks or Multivariate Adaptive Regression Splines (MARS) are possible avenues that future research could explore to identify a better predicting PSDM, if applicable.

- Comparison of the BSFM curves to the traditional fragility curves and comparisons with other fragility curves that were developed for similar regions, bridges, and ground motion intensity measures also revealed some similarities and differences between the resulting curves. Another step that should be done to further validate the BSFM is a Monte Carlo validation. A Monte Carlo simulated fragility represents a better basis for comparison of a fragility estimate due to its being closest to the "ground truth" (Ghosh, et al., 2012). In order to validate the proposed method, hundreds of simulations would be analyzed for a deterministic bridge model within a limited range of peak ground acceleration (PGA) intensities. The proportions of the simulations that "failed" or exceeded the limit state threshold would estimate the true fragility for the bridge or component at that PGA level. Future work should include this type of validation of the BSFM to determine how well the BSFM estimates the "true" fragility of a specific bridge.

- The platform used to present the BSFM to design engineers was through the DST developed in Microsoft Excel. While this platform was determined to be accessible and readily available for most potential users, an independent platform might be useful and more efficient. The potential future software

program could have options to choose the bridge type, design parameters used in estimation, ground motion intensity measure for fragility estimations, and other parameters before creating the fragility curves. Thus, separate Excel sheets would not be necessary for each different bridge type for which bridge-specific fragility is available; they could all be housed in one program. In this way, an independent program could lead to more flexibility while analyzing bridges.

- This BSFM and DST were designed specifically for California bridge types for use by Caltrans design engineers. Future research could extend this framework and methodology to other agencies and seismic regions across the country, and even across the world. There is great potential for this tool to be adapted and modified to address the different concerns faced by different agencies and regions and for the engineers and decision makers to have a tool such as this to help with decision making and performance based engineering. The concepts used to develop this BSFM could even be expanded for use of other structure types, such as buildings, and hazard concerns, like hurricane hazards or wind hazards.

APPENDIX A

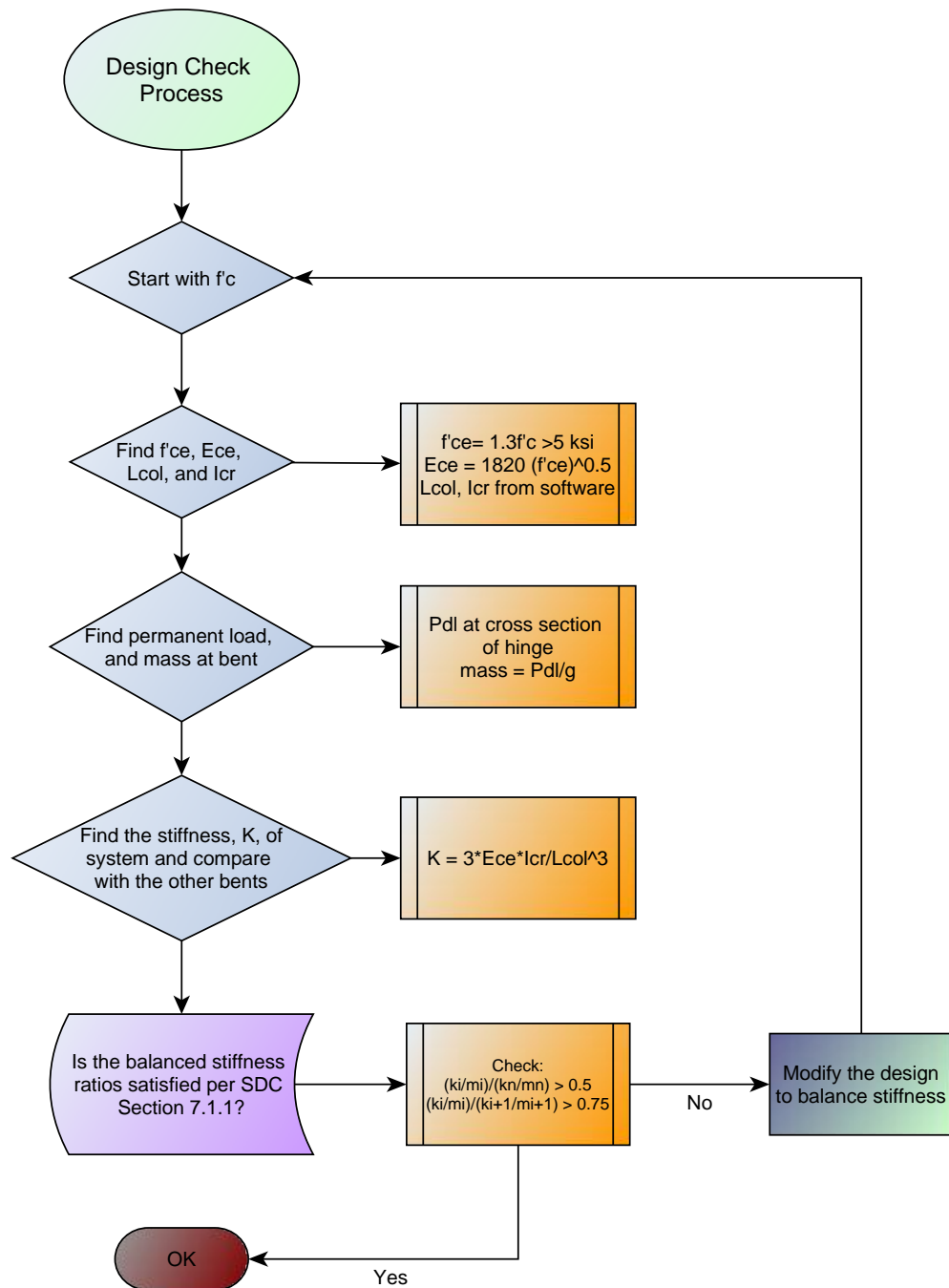# FLOWCHARTS OF DESIGN CHECKS FOR CALTRANS SEISMIC

DESIGN CRITERIA

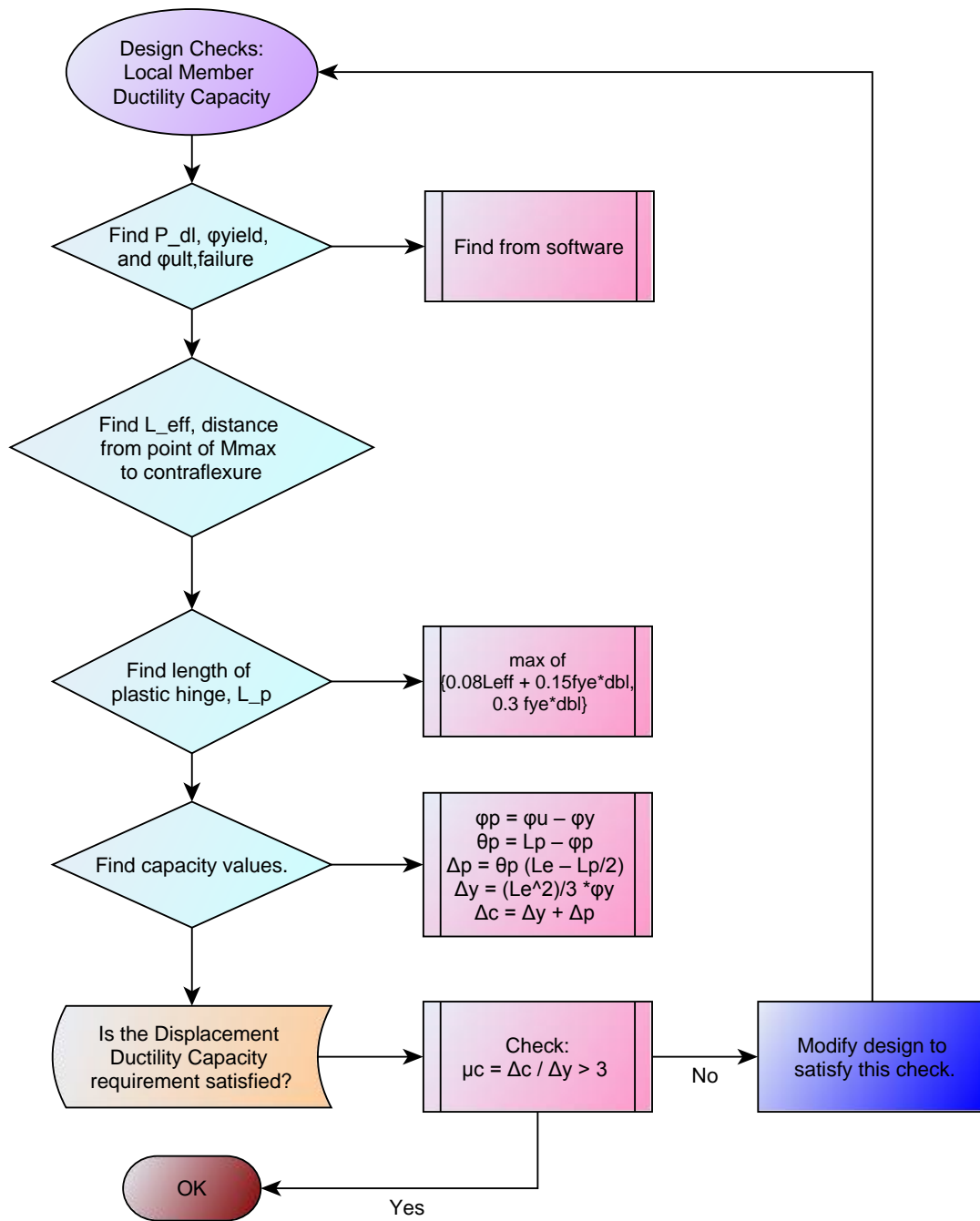Figure 76: Balanced stiffness check for new bridge design.
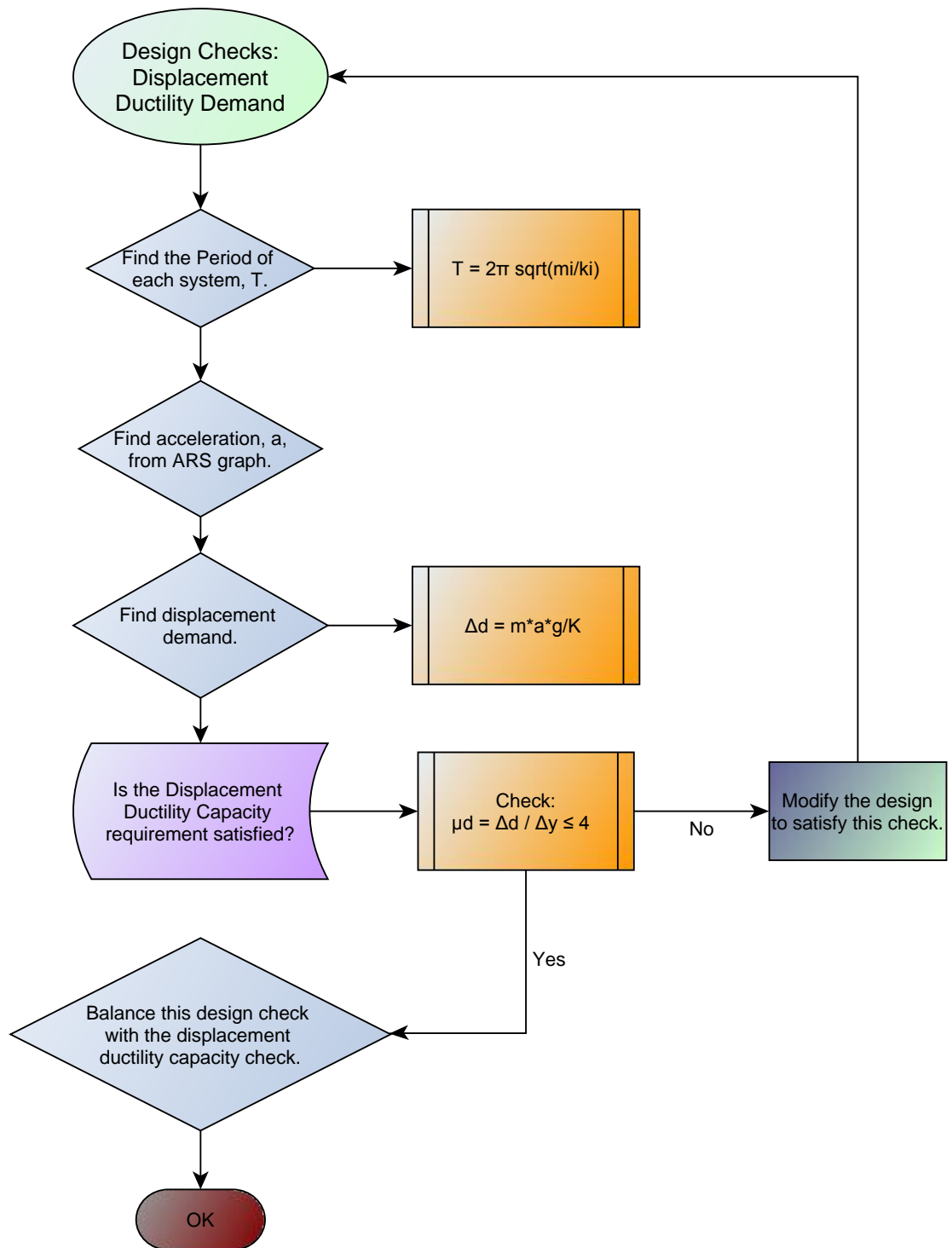
Design Checks: Local Member Ductility Capacity

Find P_dl, φyield, and φult,failure

Find from software

Find L_eff, distance from point of Mmax to contraflexure

Find length of plastic hinge, L_p

max of
{0.08Leff + 0.15fye*dbl, 0.3 fye*dbl}

Find capacity values.

$φp = φu − φy$
$θp = Lp − φp$
$Δp = θp (Le − Lp/2)$
$Δy = (Le^2)/3 *φy$
$Δc = Δy + Δp$

Is the Displacement Ductility Capacity requirement satisfied?

Check:
$μc = Δc / Δy > 3$

No

Modify design to satisfy this check.

OK

Yes

Figure 77: Local member ductility capacity design check.

Figure 78: Displacement ductility demand design check.
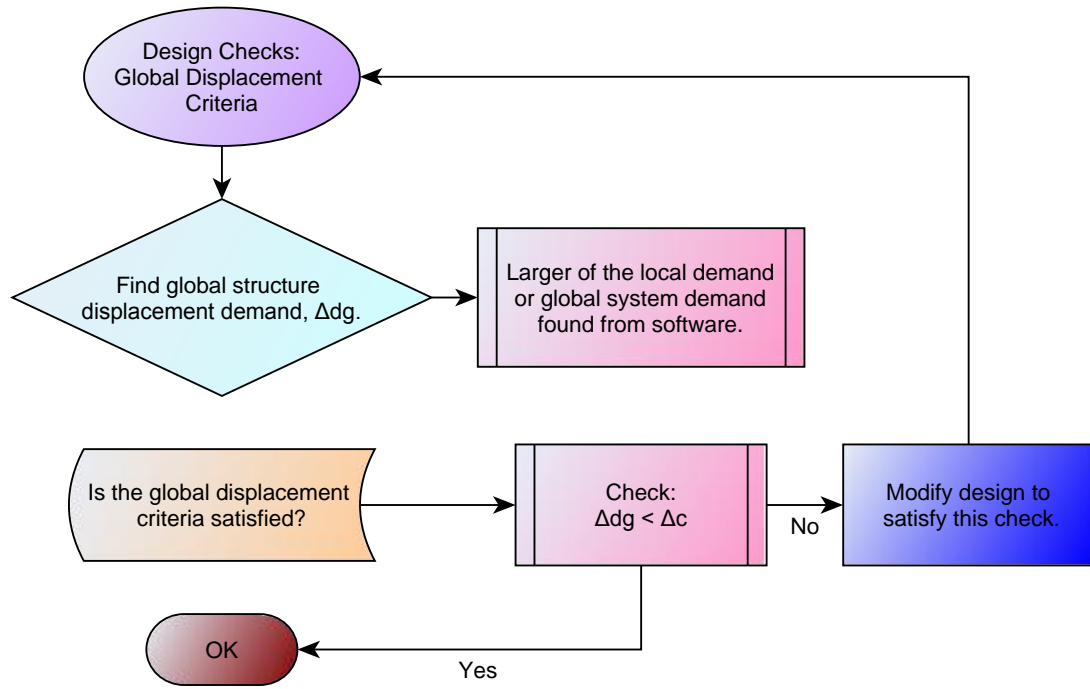
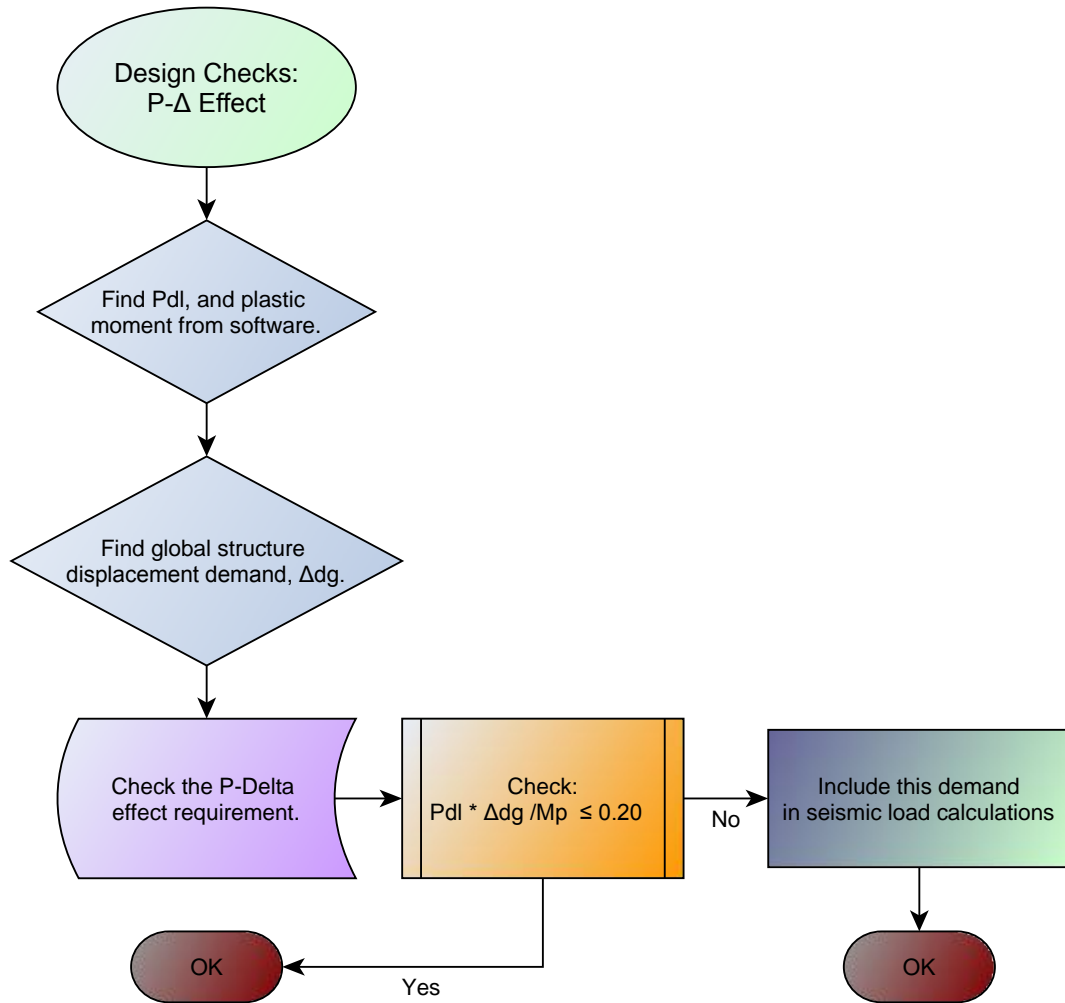Figure 79: Global Displacement Criteria design check.

Figure 80: Load-displacement (P-Δ) effect design check.

Table 50: Design Check calculations from example in Chapter 8.

A. Balanced Stiffness			
f'ce	6.7535	**OK!**	
Ece	4729.724453	ksi	
Lcol	331.02	in	
Icr	2.21E+05	in4	from software
Pdl	1527.707231	kips	
Mass	3.953693662	kip-sec2/ft	
K	172.6426133	kip/in	
B. Local Member Ductility Capacity			
Pdl	1527.707231	kips	
φyields	7.41E-05		from software
φultimate	5.86E-04		from software
Leff	27.585		
Lp	20.4		
φplastic	5.12E-04		
θplastic	1.04E-02		
Δplastic	0.181631436		
Δyield	1.88E-02		
Δcap	2.00E-01		
μcap	10.6673259	**OK!**	
C. Displacement Ductility Demand			
T	0.950839852	sec	
accel	0.69343058	g	from ARS curve
ΔD	0.04261207		
μD	2.27E+00	**OK!**	
D. Global Displacement Criteria			
Δdg<Δcap		**OK!**	
E. P-Delta Effect			
Mp	7837.1	kip-ft	from software
Ratio	0.000692207	**OK!**	

APPENDIX B

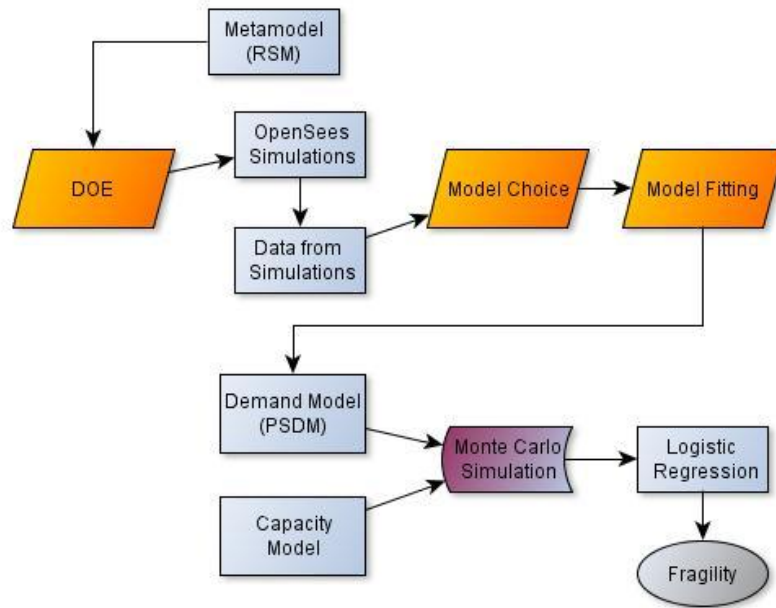# BRIDGE SPECIFIC FRAGILITY FRAMEWORK

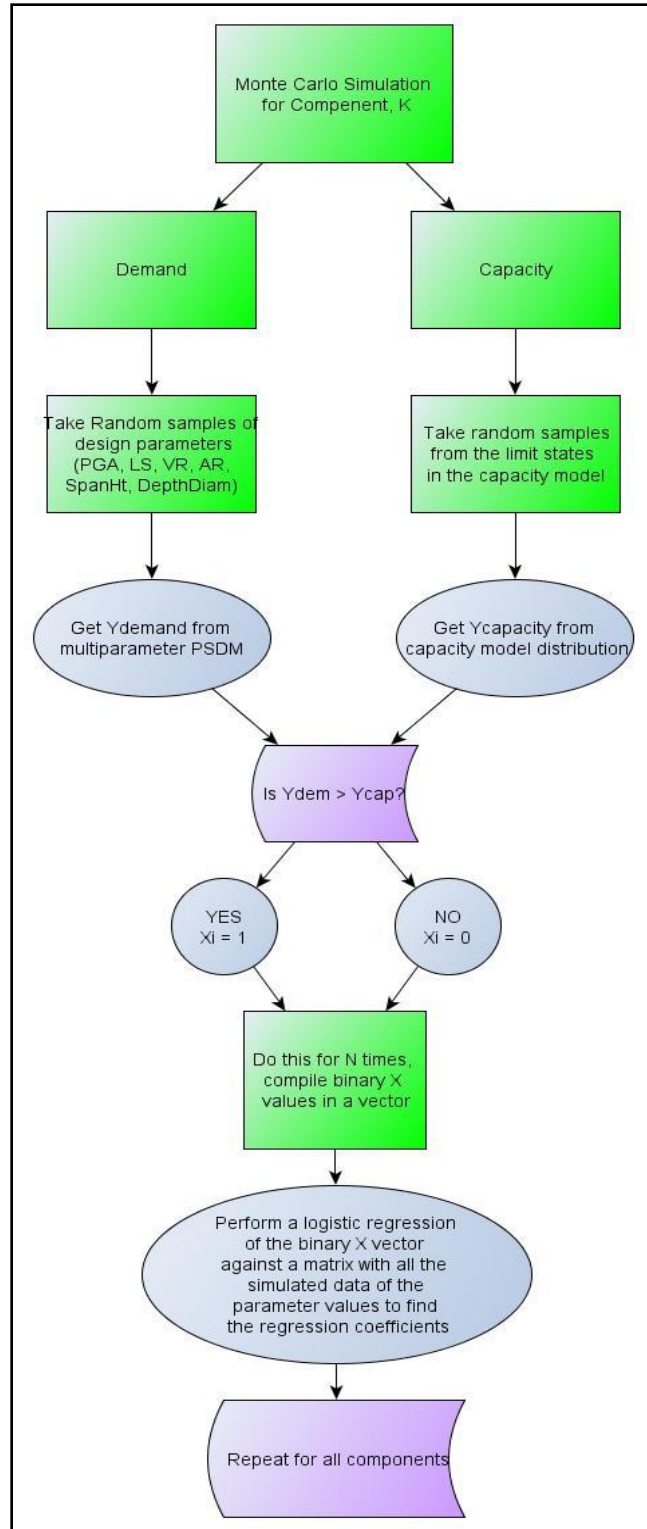Figure 81: General overview of the bridge-specific fragility framework.

Figure 82: Monte Carlo simulation used to compare demand and capacity models and find logistic regression coefficients for components.
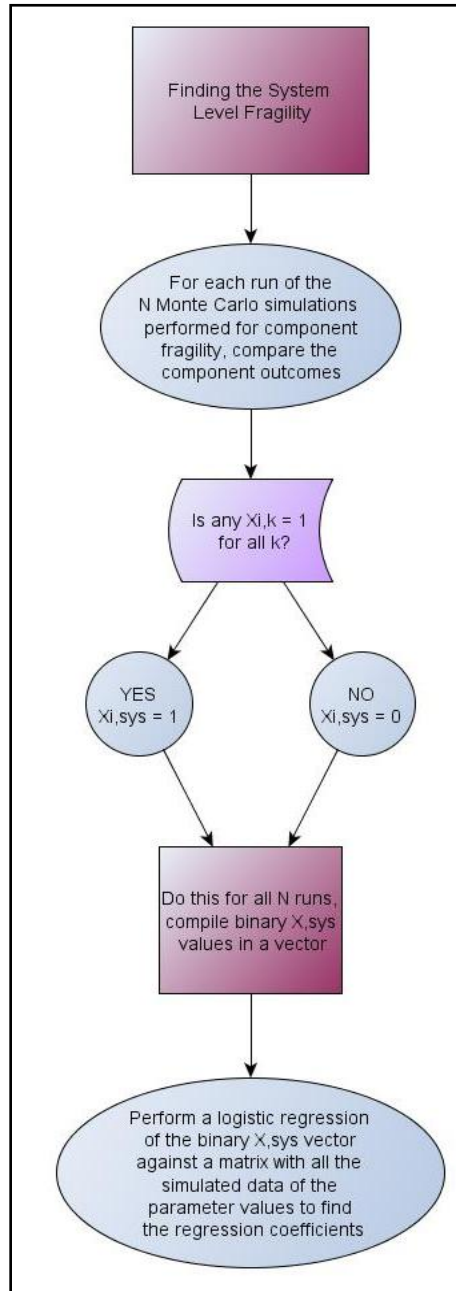
Figure 83: Series method to determine the system level logistic regression coefficients and fragility estimation.

APPENDIX C

RESULTS OF BRIDGE SPECIFIC FRAGILITY METHOD

This section contains the results of the bridge-specific fragility method analysis on the bridge models described in an earlier chapter. Here, the regression coefficients of the multi-parameter probabilistic seismic demand model are shown for each component in the single-column bent and multi-column bent bridge classes for two ground motion intensity measures, spectral acceleration at one second and peak ground acceleration. The coefficients of the logistic regression equations that calculate the fragility estimation are also given in this Appendix.

C.1   Multi-parameter PSDM coefficients

$$\ln(Y) = \beta_0 + \beta_1(\ln(IM)) + \beta_2 LS + \beta_3 VR + \beta_4 AR + \beta_5 SpanHt + \beta_6 DepthDiam$$

Table 51: Regression coefficients for multi-parameter PSDM for single-column bent bridges.

	R2	Sigma	β0	β1	β2	β3	β4	β5	β6
Sa 1									
Column	0.880	0.161	2.426	1.029	-53.51	-0.117	0.092	0.100	-0.026
Gap at Abutment	0.831	0.125	0.503	0.805	-0.577	-0.105	0.132	0.041	0.234
Bearing Movement	0.831	0.125	0.503	0.805	-0.577	-0.105	0.132	0.041	0.234
Joint Seals	0.831	0.125	0.503	0.805	-0.577	-0.105	0.132	0.041	0.234
PGA									
Column	0.720	0.376	2.615	1.084	-53.66	0.325	0.091	0.101	-0.021
Gap at Abutment	0.632	0.272	0.627	0.834	-0.692	0.235	0.132	0.042	0.238
Bearing Movement	0.632	0.272	0.627	0.834	-0.692	0.235	0.132	0.042	0.238
Joint Seals	0.632	0.272	0.627	0.834	-0.692	0.235	0.132	0.042	0.238

$$\ln(Y) = \beta_0 + \beta_1(\ln(IM)) + \beta_2 LS + \beta_3 VR + \beta_4 AR + \beta_5 SpanHt + \beta_6 DepthDiam + \beta_7 Width$$

Table 52: Regression coefficients for multi-parameter PSDM for multi-column bent bridges.

	R2	Sigma	β0	β1	β2	β3	β4	β5	β6	β7
Sa 1										
Column	0.797	0.379	2.784	1.181	-53.8	-0.15	0.025	0.095	0.099	1E-4
Gap at Abutment	0.796	0.174	0.522	0.836	-1.65	0.175	0.170	0.025	0.203	0.000
Bearing Movement	0.796	0.174	0.522	0.836	-1.65	0.175	0.170	0.025	0.203	0.000
Joint Seals	0.796	0.174	0.522	0.836	-1.65	0.175	0.170	0.025	0.203	0.000
PGA										
Column	0.617	0.716	2.943	1.208	-53.7	-1.21	0.022	0.095	0.099	1E-4
Gap at Abutment	0.585	0.355	0.615	0.844	-1.58	-0.58	0.168	0.025	0.203	0.000
Bearing Movement	0.585	0.355	0.615	0.844	-1.58	-0.58	0.168	0.025	0.203	0.000
Joint Seals	0.585	0.355	0.615	0.844	-1.58	-0.58	0.168	0.025	0.203	0.000

C.2   Logistic Regression Coefficients

$$p_f(SCB) = \frac{e^{\alpha_0 + \alpha_1 \ln(Sa_1) + \alpha_2 LS + \alpha_3 VR + \alpha_4 AR + \alpha_5 SpanHt + \alpha_6 Depthdiam}}{1 + e^{\alpha_0 + \alpha_1 \ln(Sa_1) + \alpha_2 LS + \alpha_3 VR + \alpha_4 AR + \alpha_5 SpanHt + \alpha_6 Depthdiam}}$$

Table 53: Logistic Regression Equation coefficients for single column bridge class for spectral acceleration at one second.

Component	Limit State	a0	a1	a2	a3	a4	a5	a6
	BSS-1	11.50	6.33	-165.9	-5.83	0.88	0.50	0.79
	BSS-2	4.03	6.04	-210.1	-8.42	0.72	0.48	0.59
	BSS-3	1.92	5.32	-276.5	11.42	0.47	0.50	-0.29
System	BSS-4	-0.29	5.28	-269.7	4.66	0.45	0.50	-0.16
	CDT-0	13.05	5.40	-278.6	-0.01	0.48	0.49	-0.32
	CDT-1	5.18	5.38	-274.2	-2.50	0.47	0.52	0.04
	CDT-2	1.95	5.29	-276.5	11.61	0.47	0.50	-0.29
Column	CDT-3	-0.29	5.28	-269.6	4.80	0.45	0.50	-0.16
	CDT-0	2.65	4.32	-0.81	-10.72	0.70	0.24	1.26
	CDT-1	-2.96	4.16	-3.23	-7.06	0.70	0.20	1.14
	CDT-2	-12.34	5.24	-8.60	-6.12	0.83	0.27	1.02
Gap at Abutment	CDT-3	-19.95	6.79	-37.63	-47.48	1.22	0.36	3.01
	CDT-0	2.62	4.25	-9.46	-5.41	0.71	0.24	1.21
	CDT-1	-4.65	4.06	-3.56	5.27	0.66	0.22	1.30
	CDT-2	-102.6	0.00	0.00	0.00	0.00	0.00	0.00
Bearing Movement	CDT-3	-102.6	0.00	0.00	0.00	0.00	0.00	0.00
	CDT-0	2.11	4.34	-3.31	11.61	0.76	0.22	1.50
	CDT-1	-102.6	0.00	0.00	0.00	0.00	0.00	0.00
Joint Seals	CDT-2	-102.6	0.00	0.00	0.00	0.00	0.00	0.00
Movement	CDT-3	-102.6	0.00	0.00	0.00	0.00	0.00	0.00

Table 54: Logistic Regression equation coefficients for single column bridge class for PGA.

Component	Limit State	a0	a1	a2	a3	a4	a5	a6
	BSS-1	13.93	6.99	-167.6	39.35	0.84	0.47	0.53
	BSS-2	5.26	6.30	-216.9	4.15	0.72	0.48	0.41
	BSS-3	2.47	5.61	-274.6	-1.40	0.51	0.53	-0.05
System	BSS-4	0.42	5.55	-273.1	4.56	0.48	0.54	-0.15
	CDT-0	14.77	5.82	-296.6	7.24	0.47	0.49	-0.33
	CDT-1	6.71	5.76	-290.2	-1.54	0.49	0.53	-0.21
	CDT-2	2.50	5.59	-274.7	-1.89	0.50	0.53	-0.06
Column	CDT-3	0.43	5.54	-273.2	4.73	0.48	0.54	-0.15
	CDT-0	2.87	4.46	4.80	5.55	0.70	0.23	1.47
	CDT-1	-2.46	4.34	-3.96	0.31	0.68	0.21	1.33
	CDT-2	-11.22	5.06	-5.30	11.41	0.77	0.21	1.28
Gap at Abutment	CDT-3	-16.69	6.56	-1.99	-7.08	0.94	0.26	2.29
	CDT-0	2.96	4.43	1.64	7.67	0.73	0.21	1.42
	CDT-1	-3.96	4.26	-3.44	-2.03	0.68	0.21	1.30
	CDT-2	-102.6	0.00	0.00	0.00	0.00	0.00	0.00
Bearing Movement	CDT-3	-102.6	0.00	0.00	0.00	0.00	0.00	0.00
	CDT-0	3.40	4.44	-5.72	-7.60	0.70	0.22	1.37
	CDT-1	-102.6	0.00	0.00	0.00	0.00	0.00	0.00
Joint Seals	CDT-2	-102.6	0.00	0.00	0.00	0.00	0.00	0.00
Movement	CDT-3	-102.6	0.00	0.00	0.00	0.00	0.00	0.00

$$p_f(MCB)$$
$$= \frac{e^{(\alpha_0+\alpha_1 \ln(IM)+\alpha_2 LS+\alpha_3 VR+\alpha_4 AR+\alpha_5 SpanHt+\alpha_6 DepthDiam+\alpha_7 Width)}}{1 + e^{(\alpha_0+\alpha_1 \ln(IM)+\alpha_2 LS+\alpha_3 VR+\alpha_4 AR+\alpha_5 SpanHt+\alpha_6 DepthDiam+\alpha_7 Width)}}$$

Table 55: Logistic regression equation coefficients for multi-column bent bridges for spectral acceleration at 1 second.

Component	Limit State	a0	a1	a2	a3	a4	a5	a6	a7
System	BSS-1	13.52	6.72	-173.9	-42.29	0.67	0.38	1.14	0.00
	BSS-2	6.51	6.62	-242.5	6.69	0.46	0.44	0.65	0.00
	BSS-3	3.56	6.15	-281.0	-2.13	0.14	0.48	0.64	0.00
	BSS-4	1.49	6.04	-276.4	3.73	0.16	0.48	0.49	0.00
Column	CDT-0	14.92	6.19	-283.1	-32.30	0.09	0.51	0.64	0.00
	CDT-1	7.18	6.17	-284.3	6.30	0.18	0.49	0.47	0.00
	CDT-2	3.56	6.14	-281.0	-1.76	0.13	0.48	0.64	0.00
	CDT-3	1.49	6.03	-276.5	3.82	0.16	0.48	0.49	0.00
Gap at Abutment	CDT-0	2.79	4.36	-8.04	-5.56	0.84	0.16	1.00	0.00
	CDT-1	-2.97	4.31	-8.78	8.05	0.86	0.13	1.08	0.00
	CDT-2	-11.97	5.23	-17.13	0.63	1.03	0.14	1.00	0.00
	CDT-3	-19.46	7.06	6.73	-38.0	1.50	0.21	2.16	0.00
Long Brg Movement	CDT-0	2.88	4.42	-9.33	-7.99	0.87	0.12	1.16	0.00
	CDT-1	-4.51	4.18	-7.86	1.87	0.88	0.13	1.08	0.00
	CDT-2	-102.6	0.00	0.00	0.00	0.00	0.00	0.00	0.00
	CDT-3	-102.6	0.00	0.00	0.00	0.00	0.00	0.00	0.00
Trans Brg Movement	CDT-0	2.88	4.42	-9.33	-7.99	0.87	0.12	1.16	0.00
	CDT-1	-4.51	4.18	-7.86	1.87	0.88	0.13	1.08	0.00
	CDT-2	-102.6	0.00	0.00	0.00	0.00	0.00	0.00	0.00
	CDT-3	-102.6	0.00	0.00	0.00	0.00	0.00	0.00	0.00
Joint Seals	CDT-0	3.16	4.50	-9.19	-0.95	0.90	0.14	0.98	0.00
	CDT-1	-102.6	0.00	0.00	0.00	0.00	0.00	0.00	0.00
	CDT-2	-102.6	0.00	0.00	0.00	0.00	0.00	0.00	0.00
	CDT-3	-102.6	0.00	0.00	0.00	0.00	0.00	0.00	0.00

Table 56: Logistic regression equation coefficients for multi-column bent bridges for PGA.

Component	Limit State	a0	a1	a2	a3	a4	a5	a6	a7
	BSS-1	13.71	6.93	-184.5	26.57	0.77	0.35	1.35	0.00
	BSS-2	6.97	6.66	-234.1	0.97	0.37	0.44	1.01	0.00
	BSS-3	4.48	6.34	-284.6	-0.65	0.15	0.49	0.51	0.00
System	BSS-4	2.37	6.24	-282.7	-7.47	0.11	0.50	0.49	0.00
	CDT-0	14.85	6.27	-282.3	56.56	0.09	0.46	0.65	0.00
	CDT-1	8.20	6.33	-282.2	-6.08	0.08	0.49	0.75	0.00
	CDT-2	4.49	6.34	-284.7	-0.41	0.15	0.49	0.50	0.00
Column	CDT-3	2.37	6.24	-282.8	-7.40	0.11	0.50	0.48	0.00
	CDT-0	3.72	4.53	-10.18	-16.55	0.86	0.13	1.05	0.00
	CDT-1	-2.52	4.36	-6.58	-4.03	0.86	0.13	1.14	0.00
Gap at	CDT-2	-11.10	5.13	-11.00	-16.27	0.95	0.14	1.12	0.00
Abutment	CDT-3	-18.81	6.63	-13.54	23.72	1.38	0.24	2.32	0.00
	CDT-0	3.04	4.52	-9.19	-6.93	0.90	0.15	1.23	0.00
	CDT-1	-4.01	4.27	-9.54	-3.53	0.87	0.14	1.07	0.00
Long Brg	CDT-2	-102.6	0.00	0.00	0.00	0.00	0.00	0.00	0.00
Movement	CDT-3	-102.6	0.00	0.00	0.00	0.00	0.00	0.00	0.00
	CDT-0	3.04	4.52	-9.19	-6.93	0.90	0.15	1.23	0.00
	CDT-1	-4.01	4.27	-9.54	-3.53	0.87	0.14	1.07	0.00
Trans Brg	CDT-2	-102.6	0.00	0.00	0.00	0.00	0.00	0.00	0.00
Movement	CDT-3	-102.6	0.00	0.00	0.00	0.00	0.00	0.00	0.00
	CDT-0	3.46	4.52	-4.94	-9.41	0.91	0.11	1.01	0.00
	CDT-1	-102.6	0.00	0.00	0.00	0.00	0.00	0.00	0.00
	CDT-2	-102.6	0.00	0.00	0.00	0.00	0.00	0.00	0.00
Joint Seals	CDT-3	-102.6	0.00	0.00	0.00	0.00	0.00	0.00	0.00

APPENDIX D

MEDIAN SYSTEM AND COMPONENT FRAGILITY CURVES

FROM BSFM

In Chapter 7, fragility curves based on the median values of the design parameters were given for spectral acceleration at one second for each of the limit states. In this appendix, similar fragility curves are given, expect with the peak ground acceleration as the ground motion intensity measure. Also, fragility curves for each of the primary and secondary components studied in this research are given that show all the limit states on one graph, for both peak ground acceleration (PGA) and spectral acceleration at one second (Sa1). All of these fragility curves are presented for the multi-column bent bridge and the single-column bent bridge class.

D.1 Multi-Column Bent Bridge Class

Fragility Curves for all Components for Limit State1 For MCB
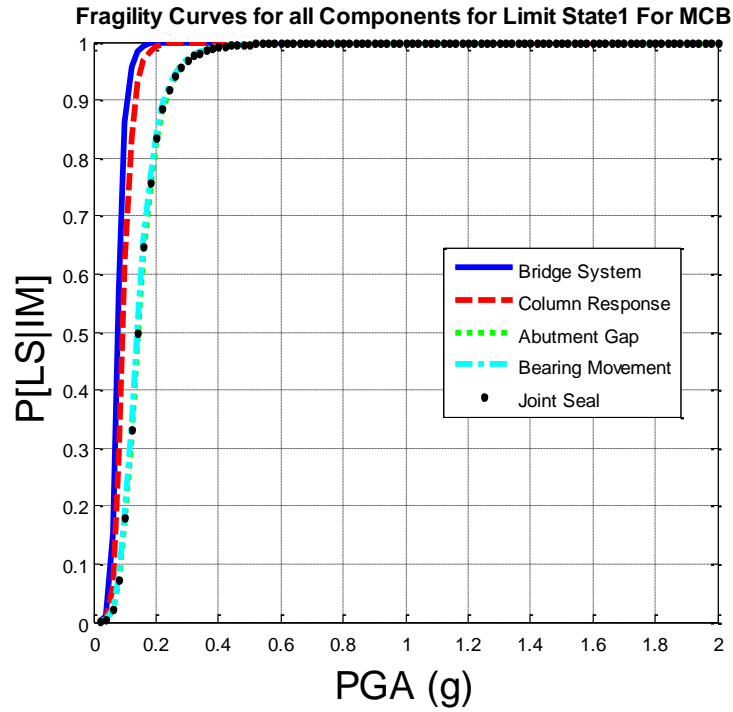
Figure 84: System and component level fragility curves at the first damage state, with PGA.

Fragility Curves for all Components for Limit State2 For MCB
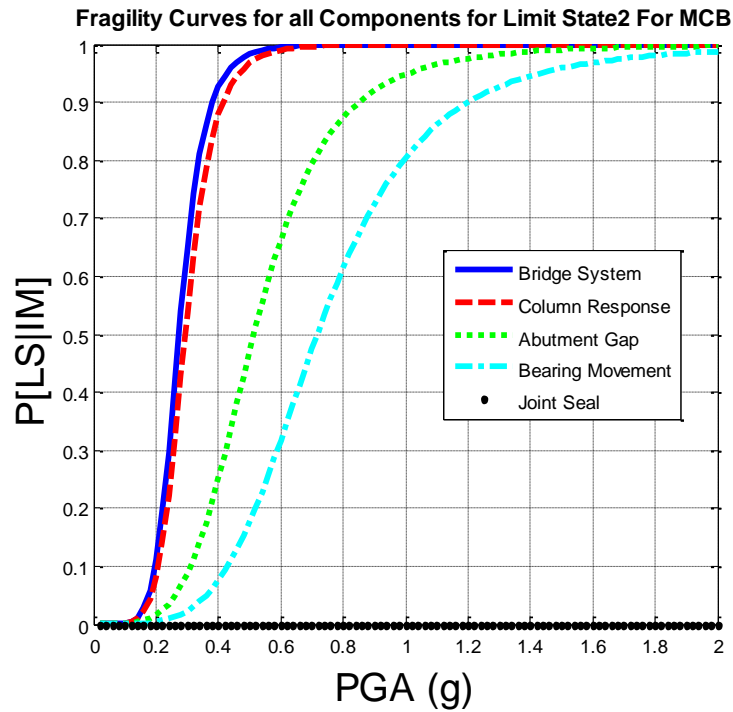
Figure 85: System and component level fragility curves at the second damage state, with PGA.
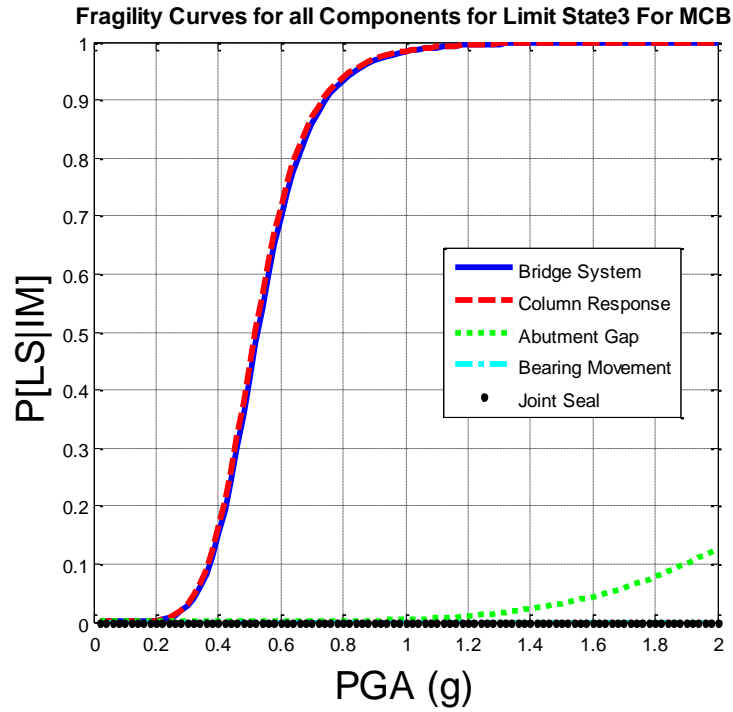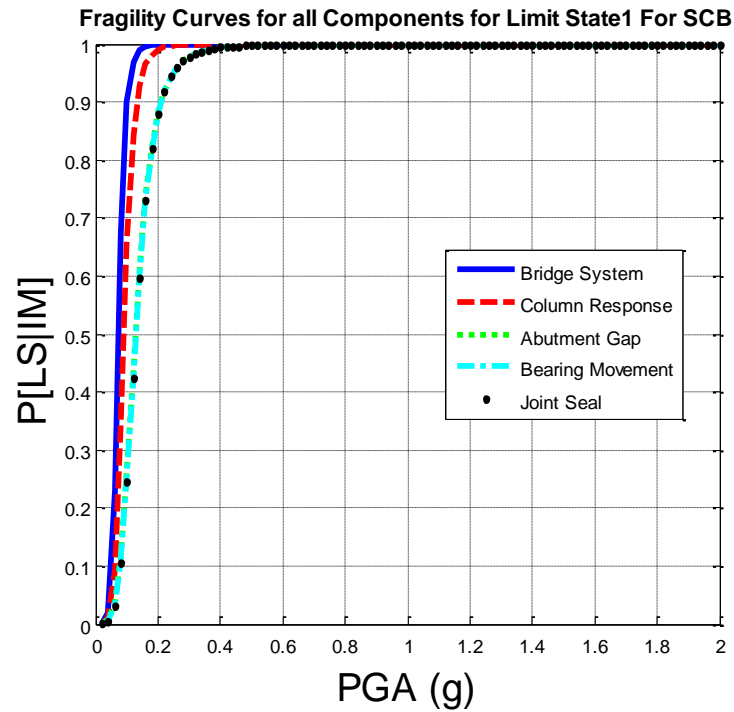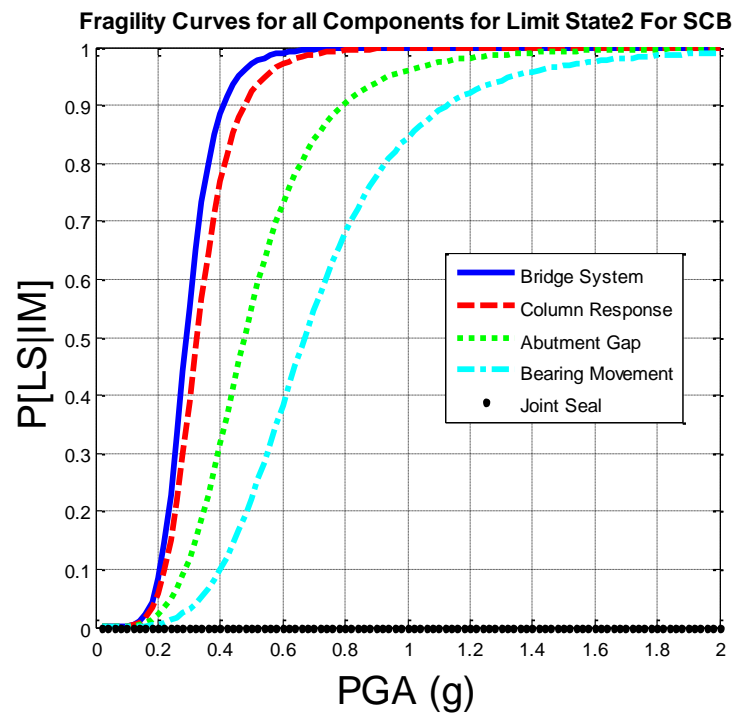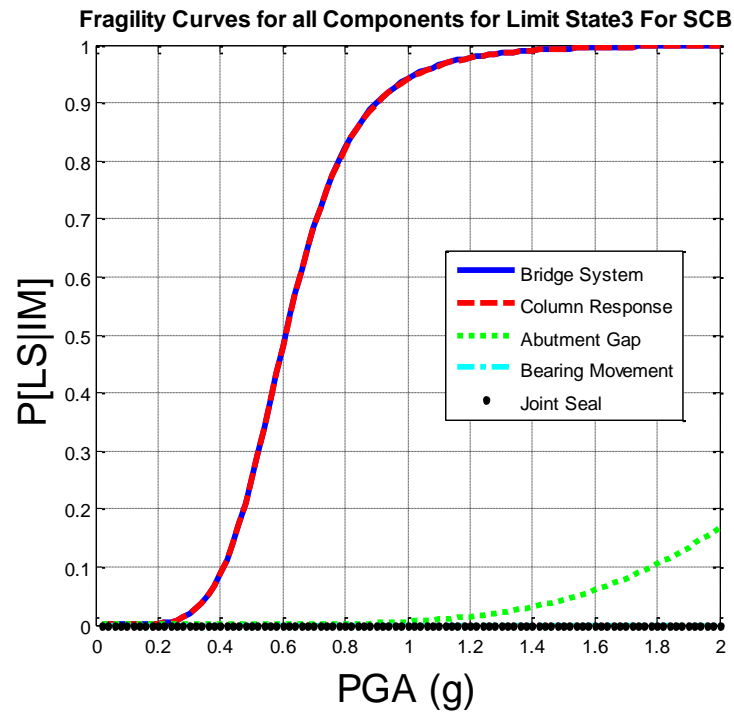
Figure 86: System and component level fragility curves at the third damage state, with PGA.
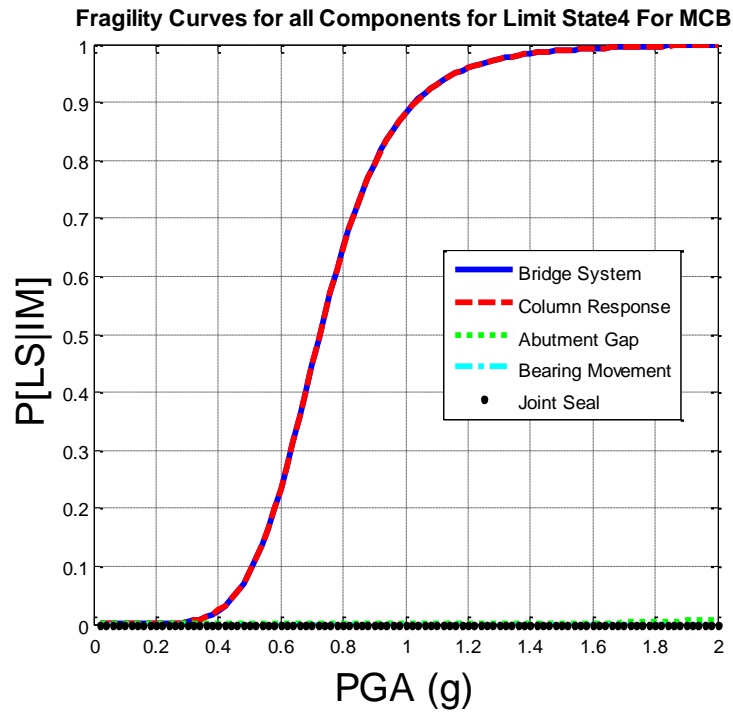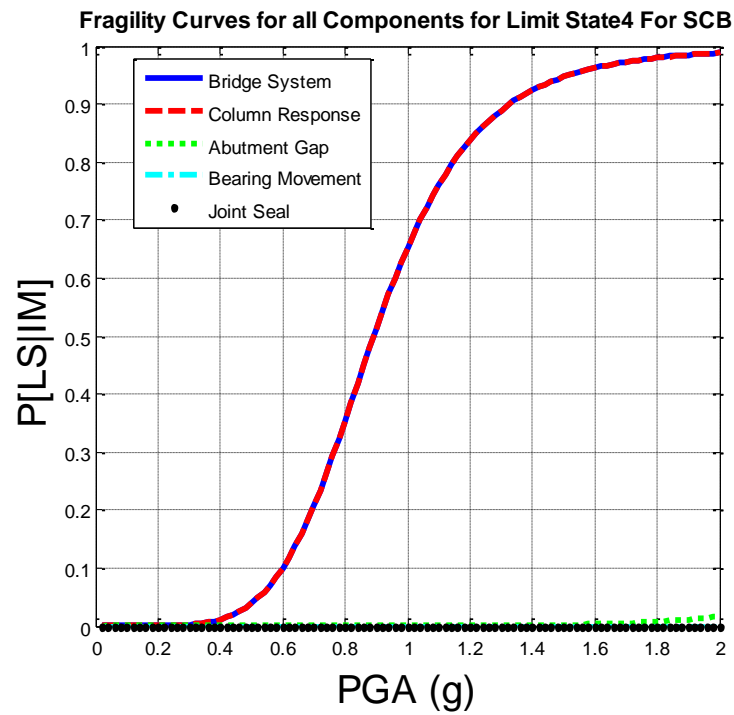

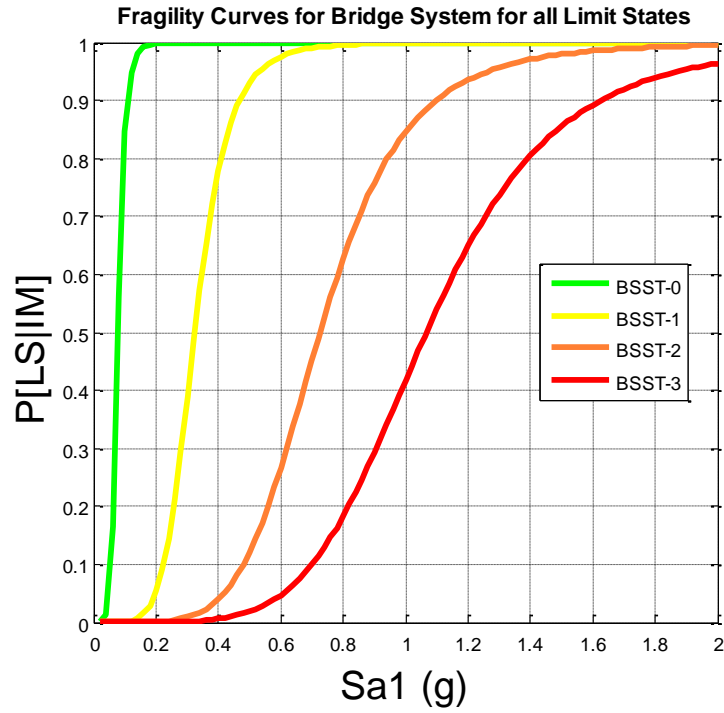Figure 87: System and component level fragility curves at the fourth damage state, with PGA.
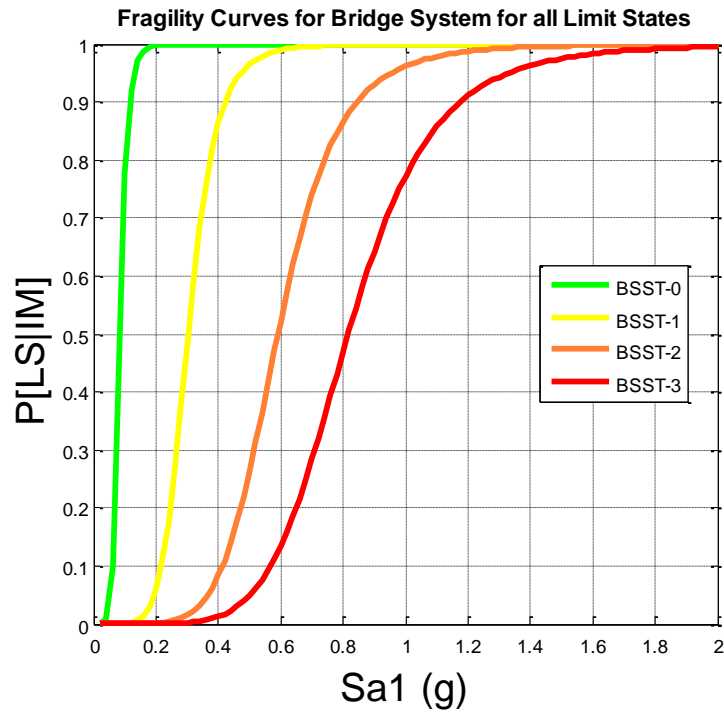
Figure 88: System level fragility curves for all damage states, with Sa1.
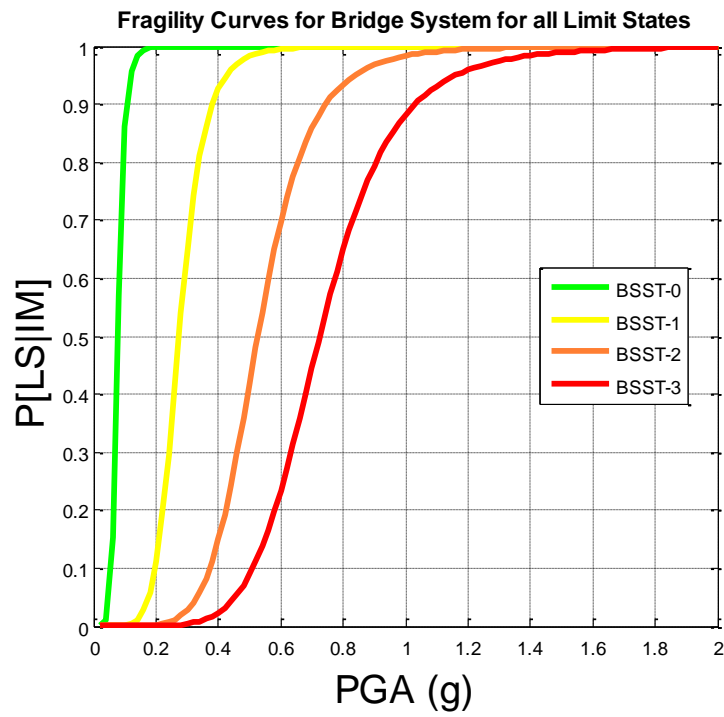
Figure 89: System level fragility curves for all damage states, with PGA.
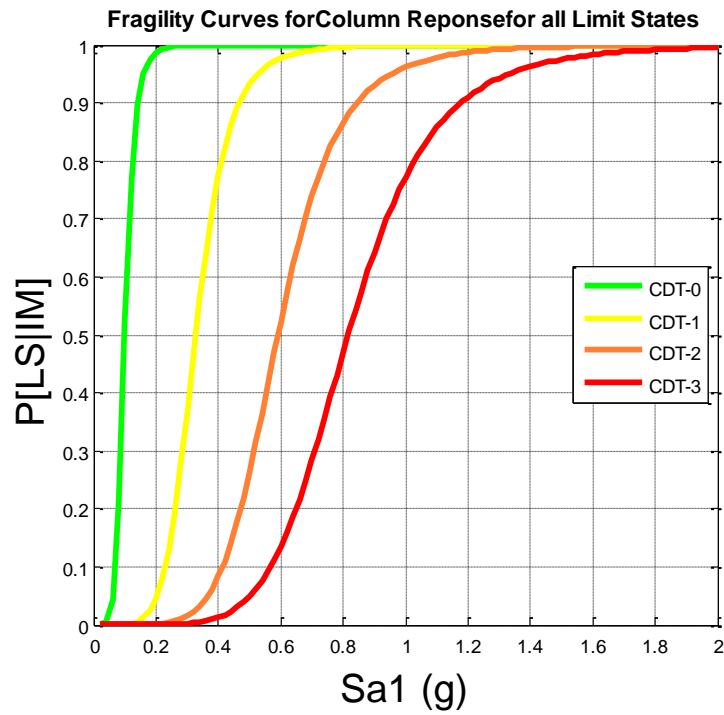
Figure 90: Fragility curves for the column component response at all damage states, with Sa1.
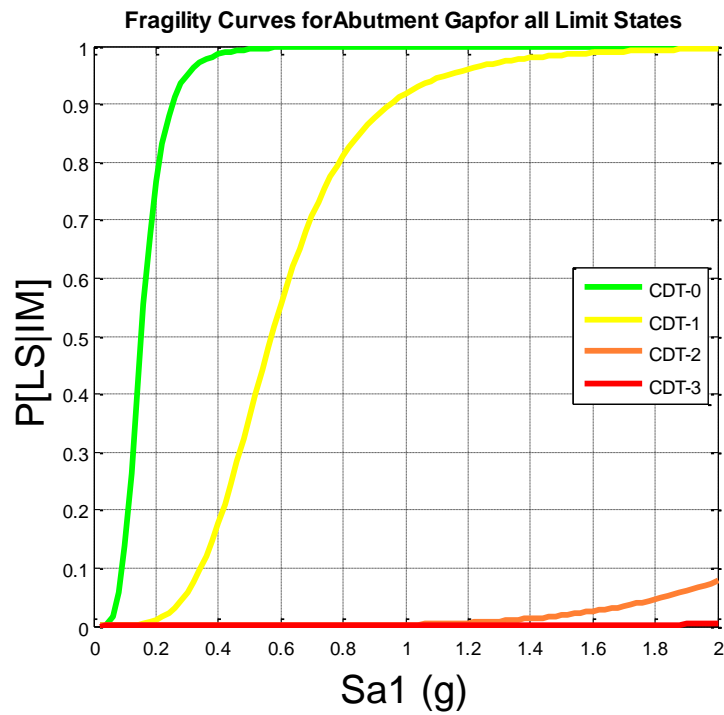
Figure 91: Fragility curves for the abutment gap component response at all damage states, with Sa1.
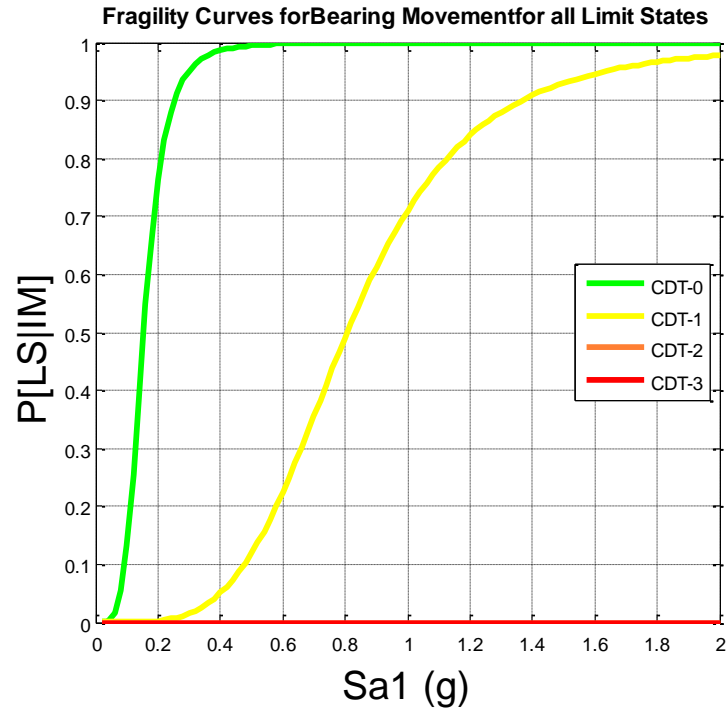
Figure 92: Fragility curves for the bearing component response at all damage states, with Sa1.
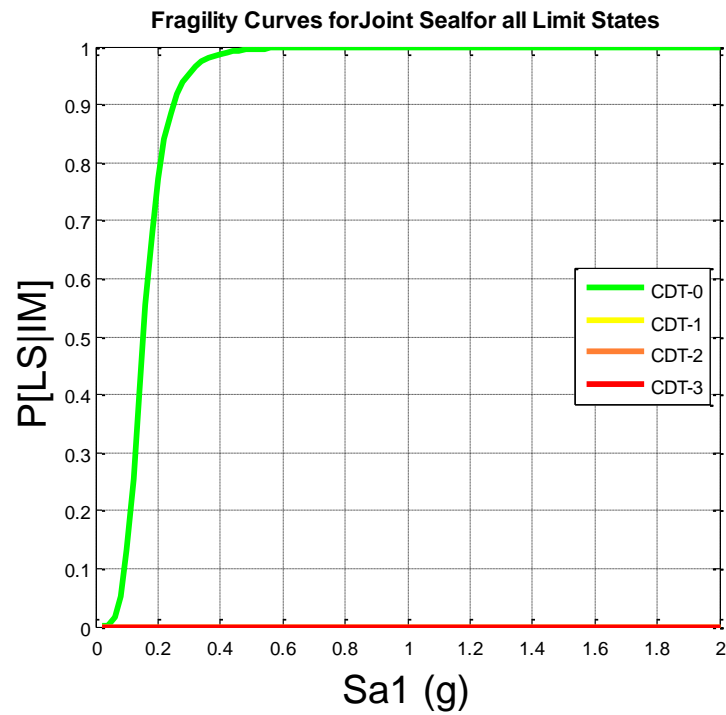
Figure 93: Fragility curves for the joint seals component response at all damage states, with Sa1.
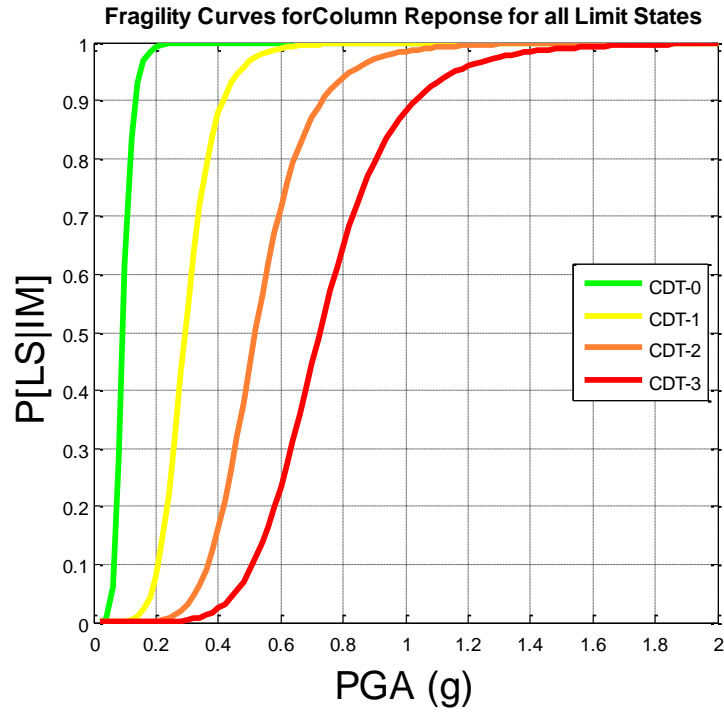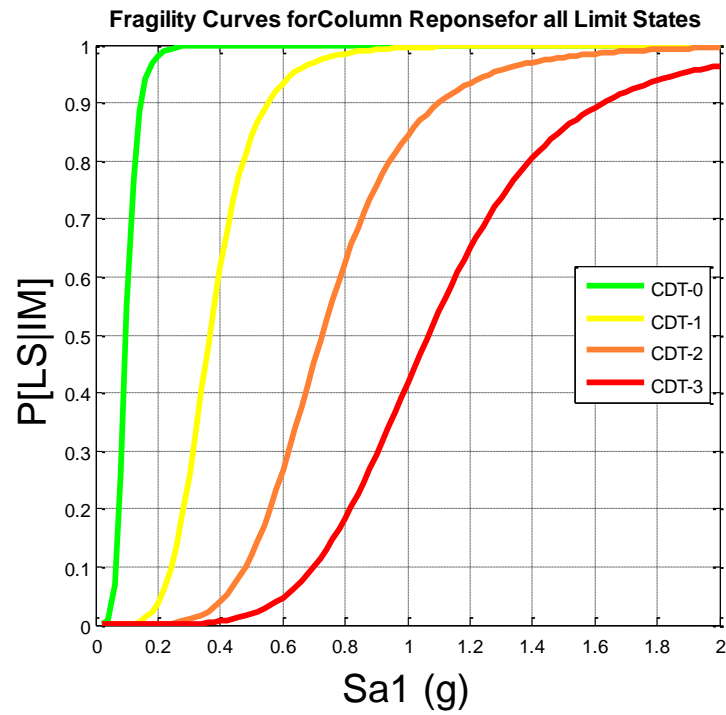
Figure 94: Fragility curves for the column component response at all damage states, with PGA.
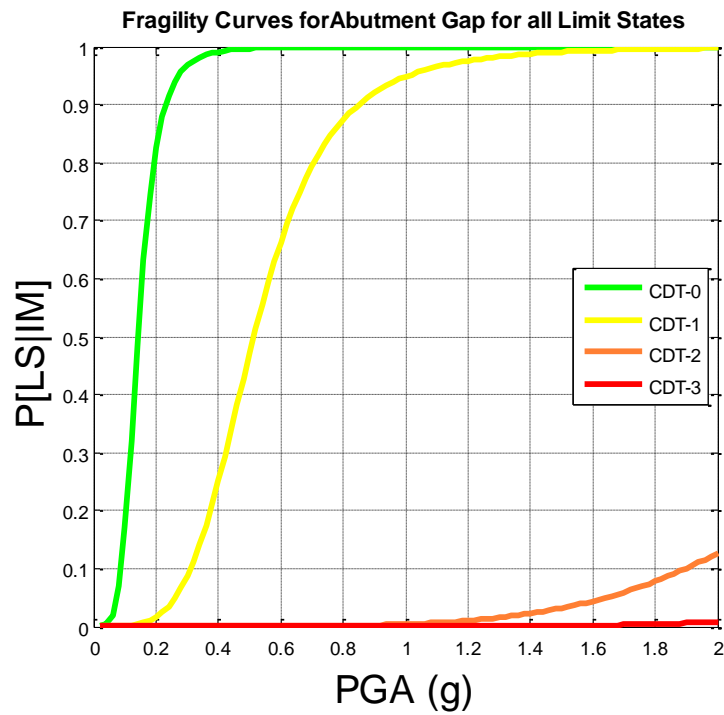
Figure 95: Fragility curves for the abutment gap component response at all damage states, with PGA.
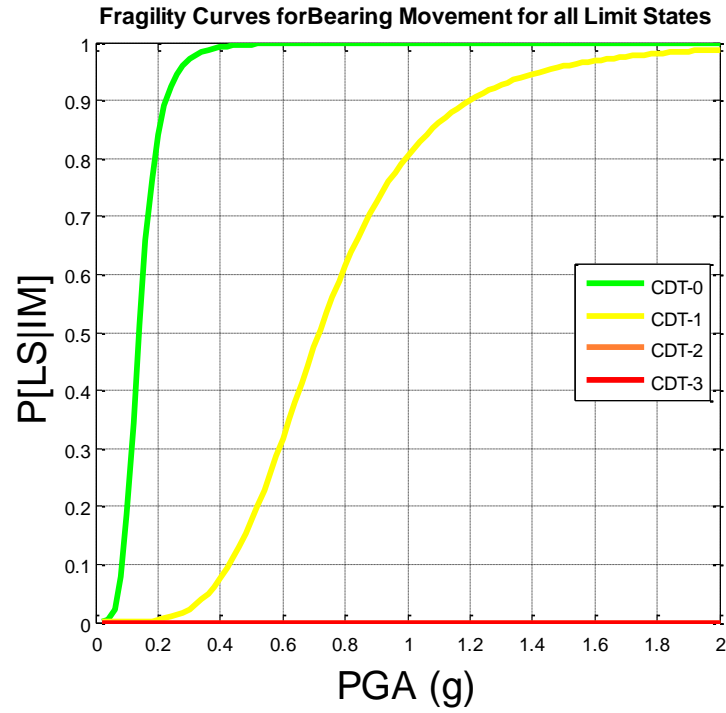
Figure 96: Fragility curves for the bearing component response at all damage states, with PGA.
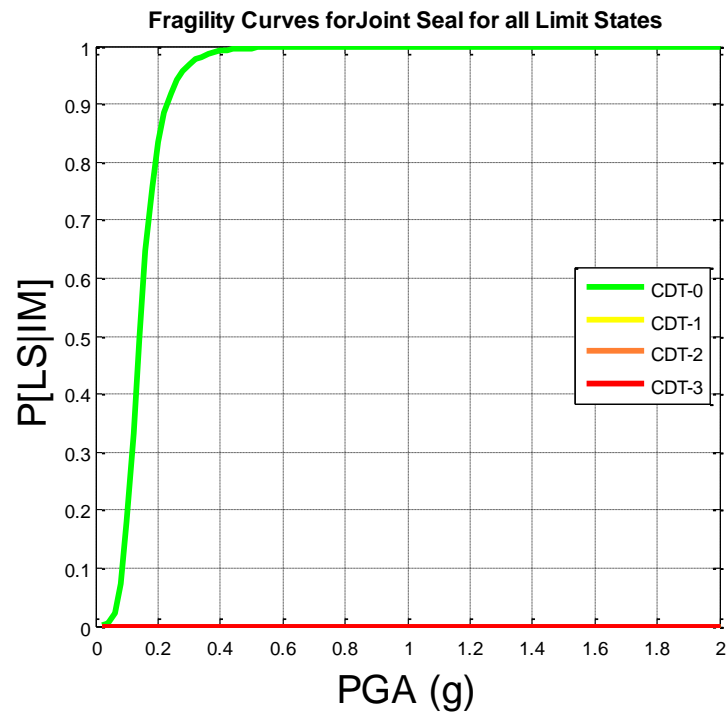
Figure 97: Fragility curves for the joint seals component response at all damage states, with PGA.

D.2 Single-Column Bent Bridge Class

Figure 98: System and component level fragility curves at the first damage state, with PGA.

Figure 99: System and component level fragility curves at the second damage state, with PGA.

Figure 100: System and component level fragility curves at the third damage state, with PGA.

Figure 101: System and component level fragility curves at the fourth damage state, with PGA.

Figure 102: System level fragility curves for all damage states, with Sa1.
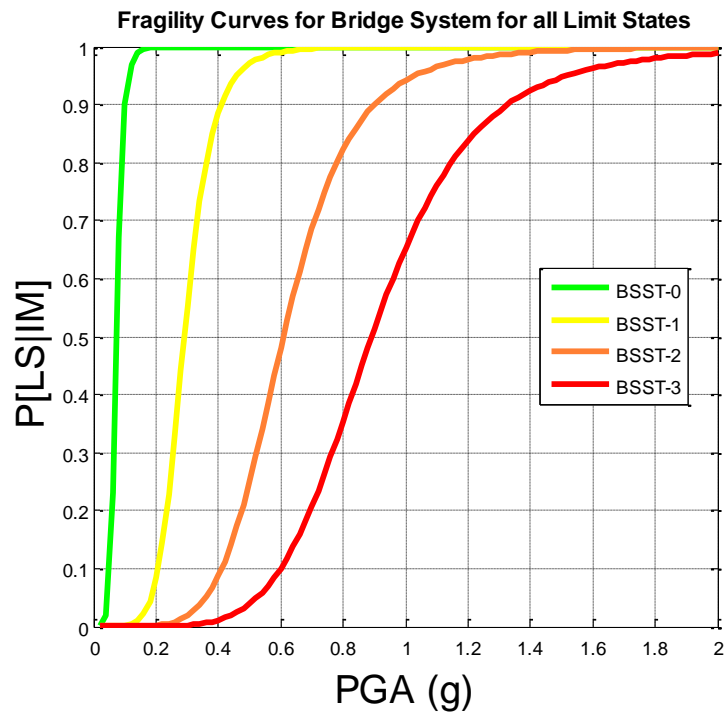
Figure 103: System level fragility curves for all damage states, with PGA.

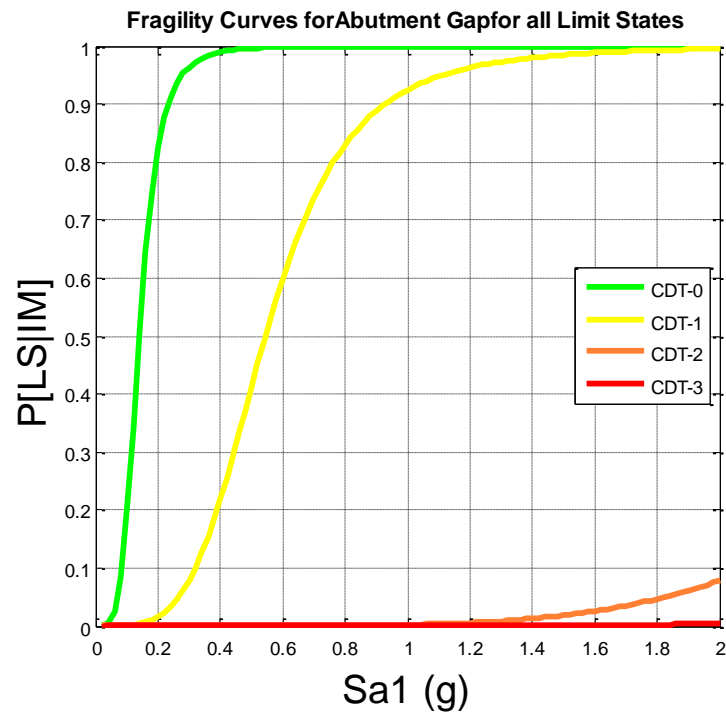Figure 104: Fragility curves for the column component response at all damage states, with Sa1.

Figure 105: Fragility curves for the abutment gap component response at all damage states, with Sa1.
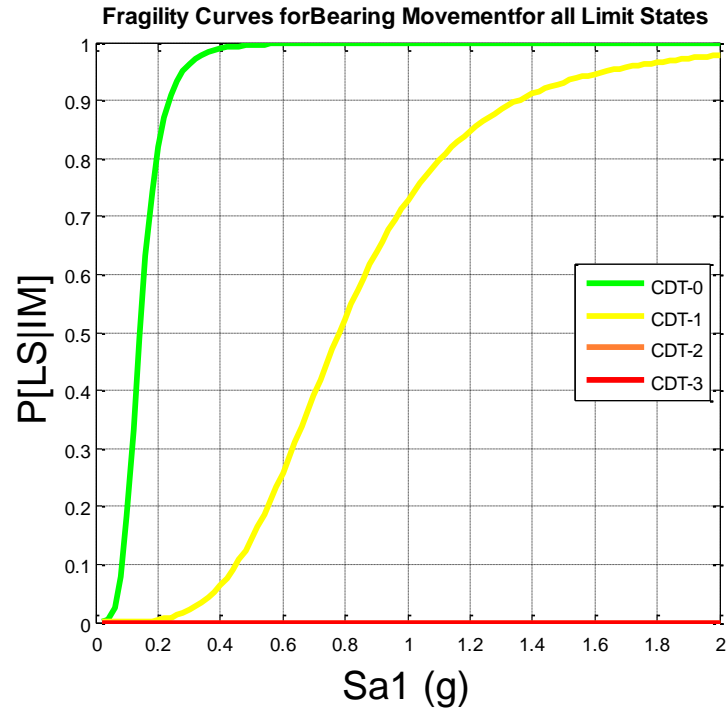
Figure 106: Fragility curves for the bearing component response at all damage states, with Sa1.
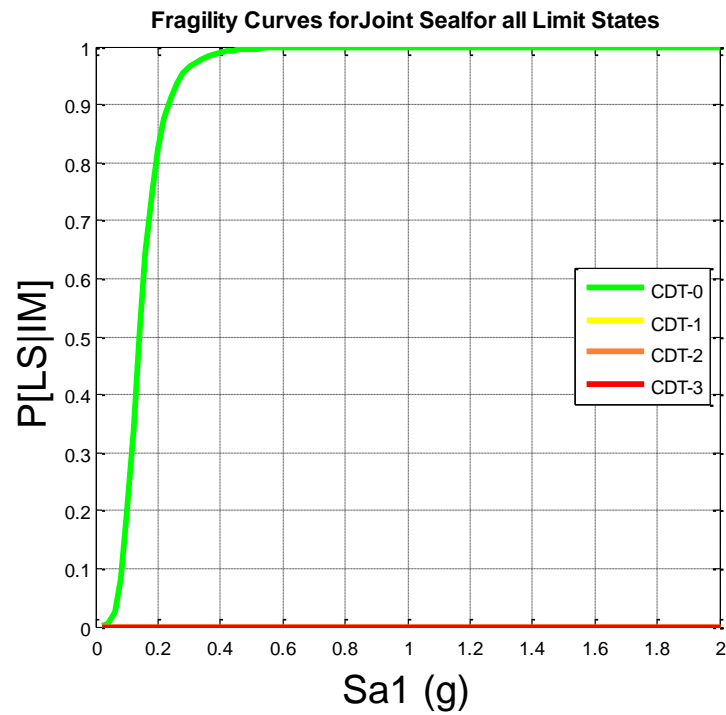

Figure 107: Fragility curves for the joint seals component response at all damage states, with Sa1.
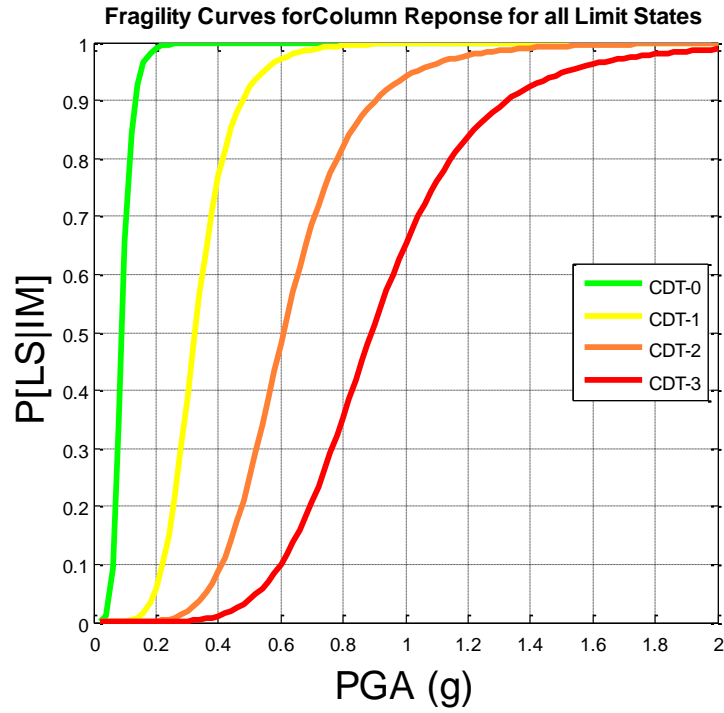
Figure 108: Fragility curves for the column component response at all damage states, with PGA.
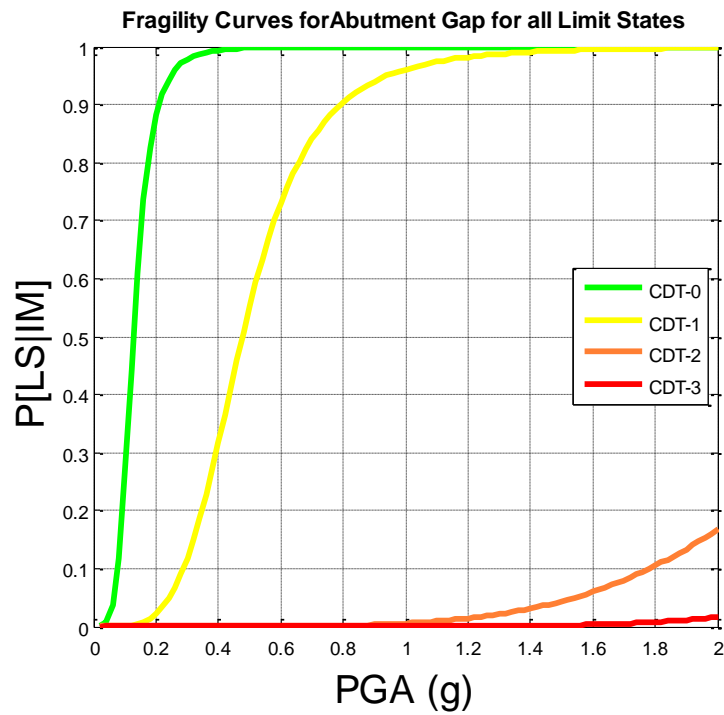

Figure 109: Fragility curves for the abutment gap component response at all damage states, with PGA.
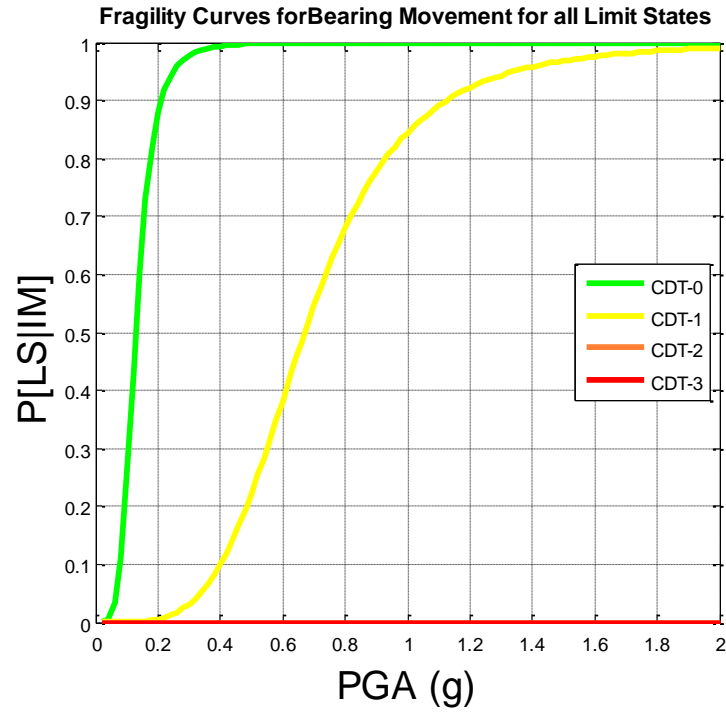
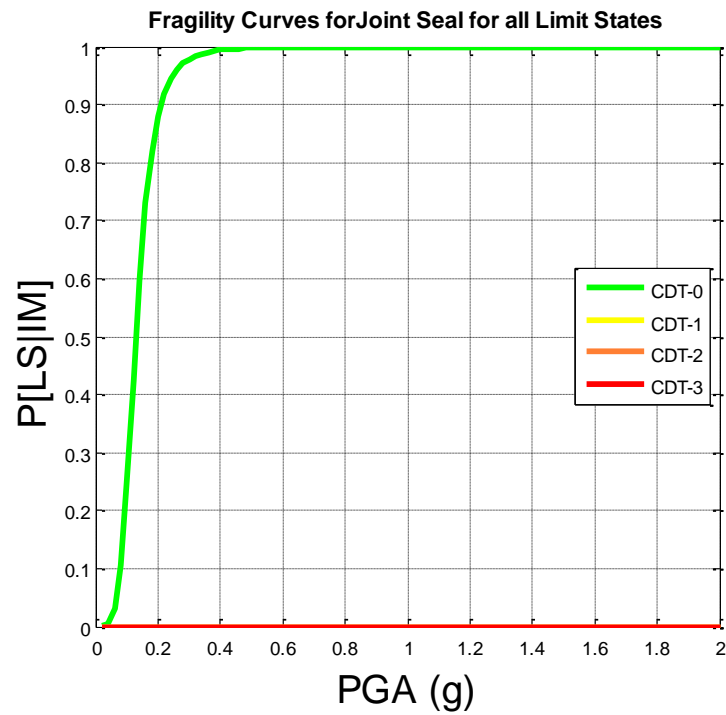Figure 110: Fragility curves for the bearing component response at all damage states, with PGA.

Figure 111: Fragility curves for the joint seals component response at all damage states, with PGA.

APPENDIX E

DESIGN SUPPORT TOOL FRAGILITY CURVES FROM DESIGN EXAMPLE

In Chapter 8, an example was given using the design support tool for an existing bridge. In that chapter, column component fragility curves were shown corresponding to the design details of the example bridge, with and without upper and lower bounds that showed the change in performance due to variations in the longitudinal steel ratio. In this appendix, additional fragility curves are shown corresponding to the same example bridge for the other components. Also shown are fragility curves that include the upper and lower bounds fragility curves corresponding to the changes in longitudinal steel ratio. As is shown, the upper and lower bounds of the longitudinal steel ratio had a significant effect on the fragility estimation of the bridge system, but not on the other bridge component fragility curves.

Figure 112: Bridge specific fragility curves for bridge system at all damage levels.

Figure 113: Bridge specific fragility curves for bridge system at all damage levels including the upper and lower bounds.

Figure 114: Bridge specific fragility curves for abutment gap component at all damage levels.

Figure 115: Bridge specific fragility curves for abutment gap component at all damage levels, including the upper and lower bounds.
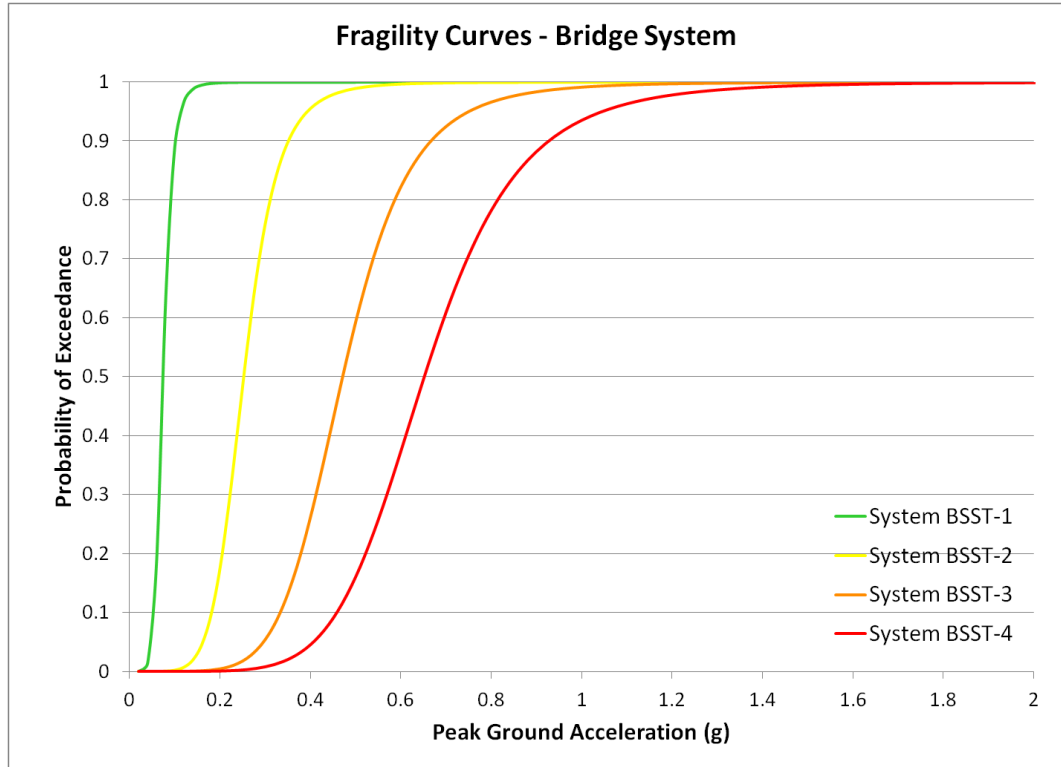
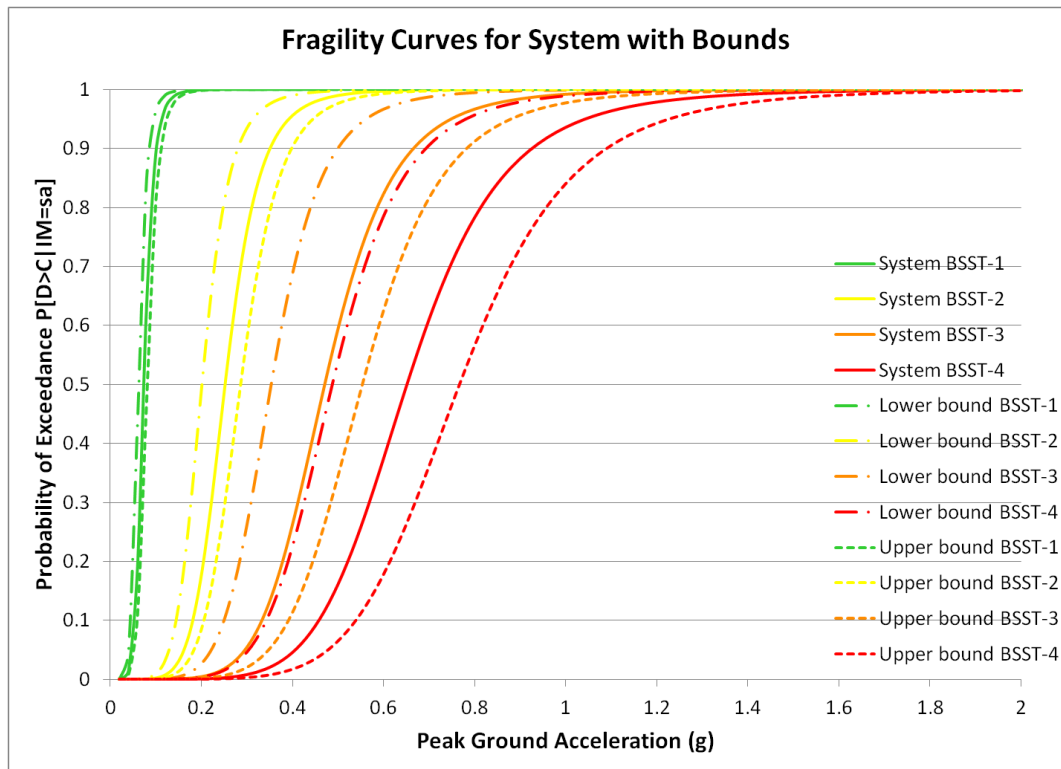Figure 116: Bridge specific fragility curves for bearing component at all damage levels.

Figure 117: Bridge specific fragility curves for bearing component at all damage levels with upper and lower bounds.
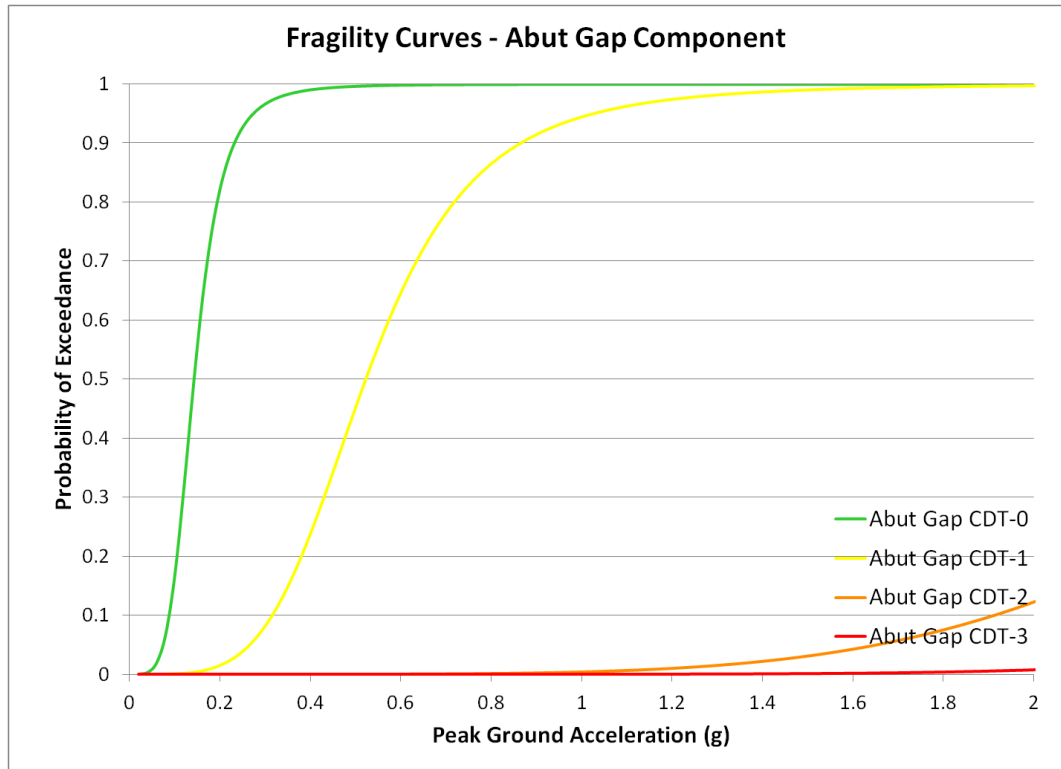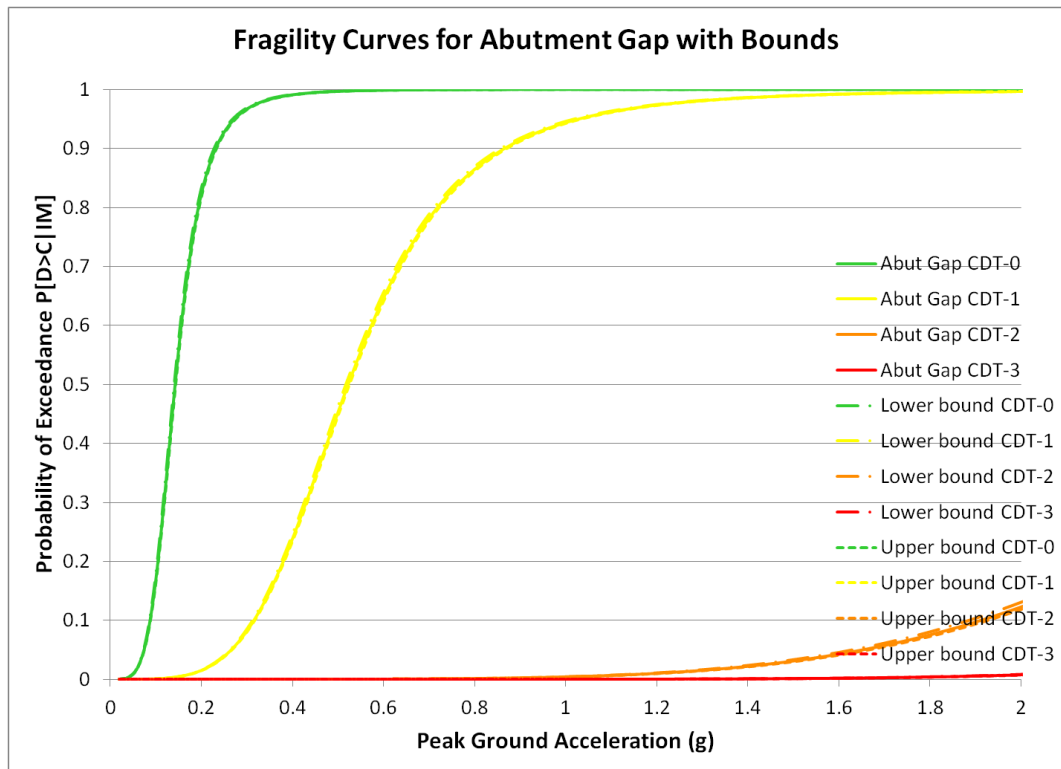
Figure 118: Bridge specific fragility curves for joint seals component at all damage levels.

Figure 119: Bridge specific fragility curves for joint seals component at all damage levels with upper and lower bounds.

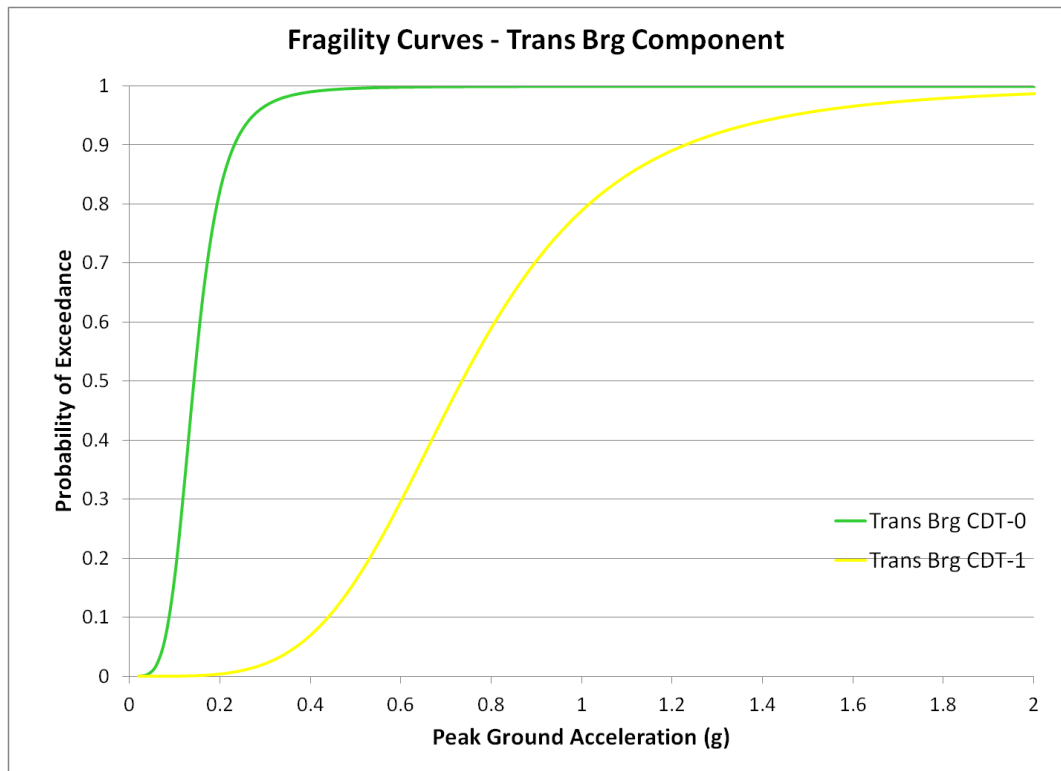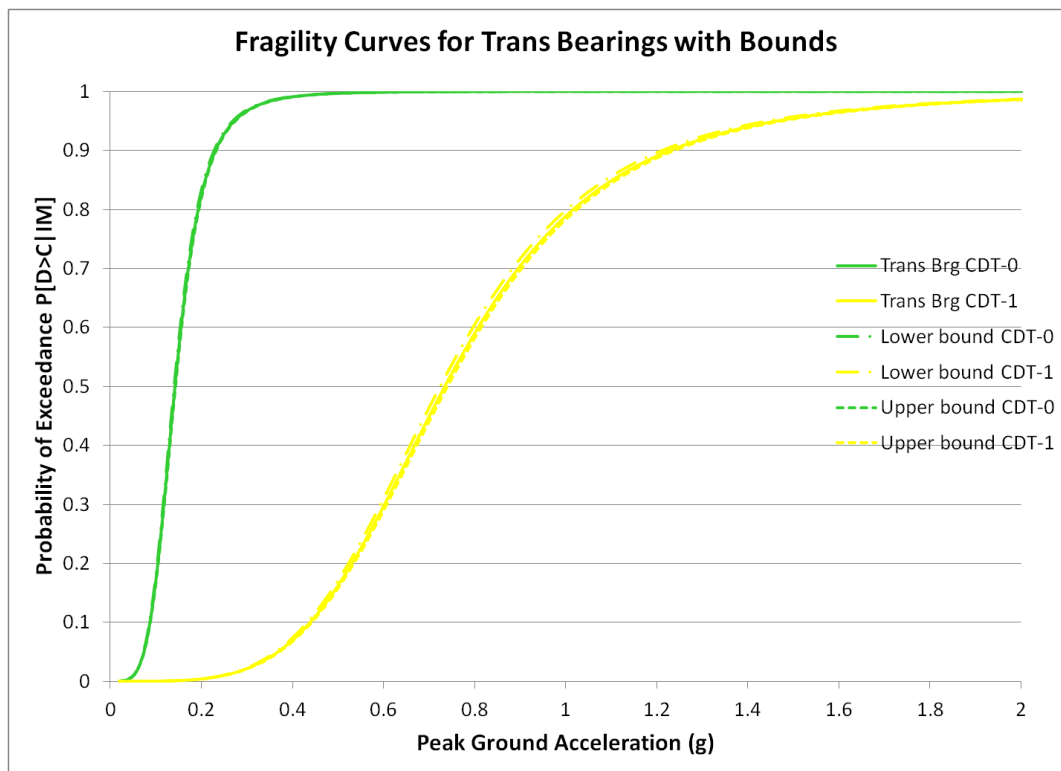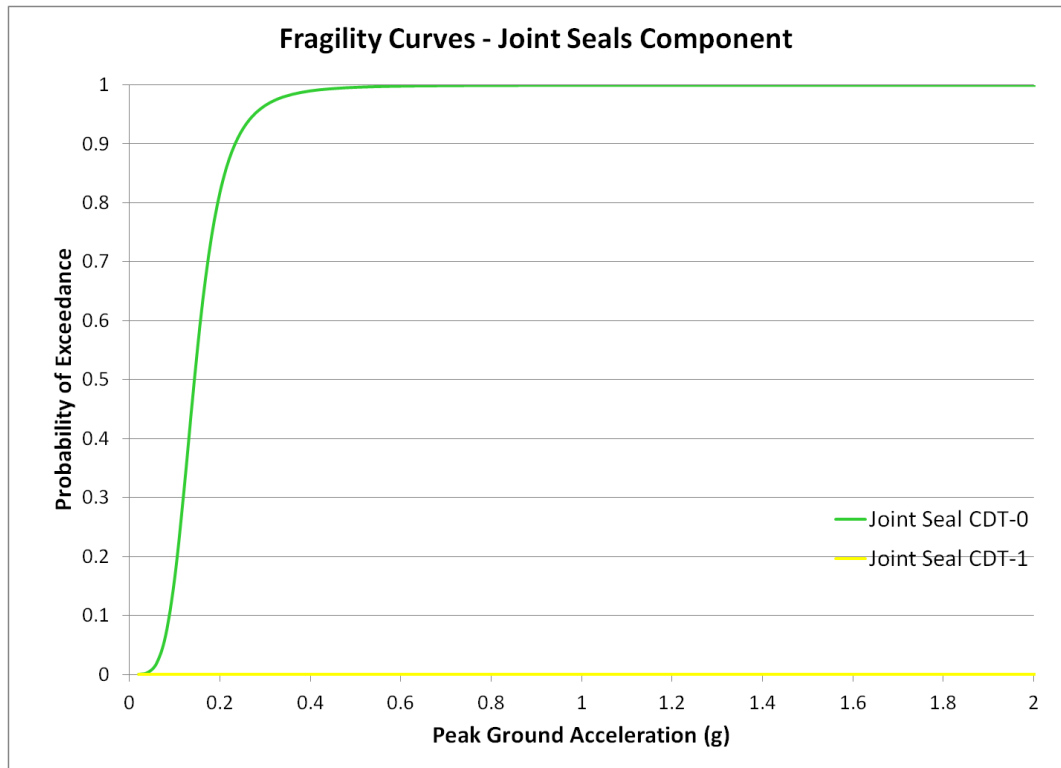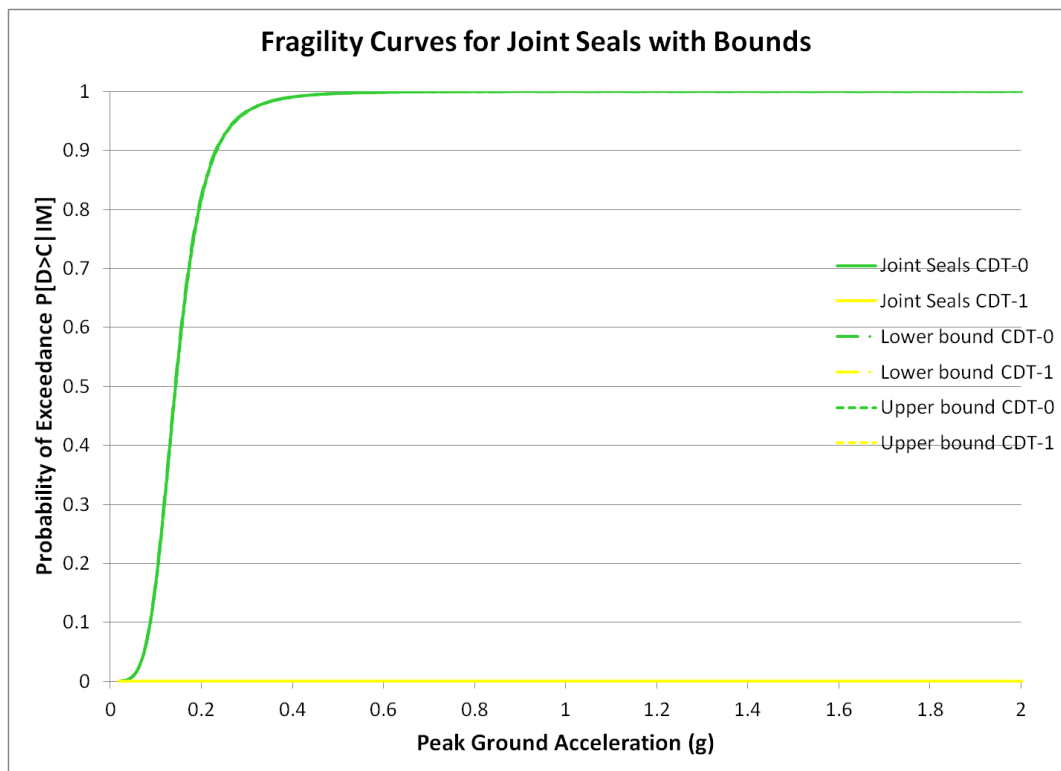# REFERENCES

AASHO. (1961). *Standard Specifications for Highway Bridges, 8th Edition.* American Association of State Highway Officials.

AASHTO. (2010). *AASHTO LRFD Bridge Design Specifications, 5th Edition.* American Association of State Highway and Transportation Officials.

AASHTO. (1977). *Standard Specifications for Highway Bridges, 12th Edition.* American Association of State Highway and Transportation Officials.

ACI. (2008). *building Code Requirements for Structural Concrete (ACI 318-08) and Commentary.* Farmington Hills, MI: American Concrete Institute.

Applied Technology Council. (2012). *Seismic Performance Assessment of Buildings: Volume 1 - Methodology.* Federal Emergency Management Agency.

Aslani, H., & Miranda, E. (2005). *Probabilistic Earthquake Loss Estimation and Loss Disaggregation in Buildings.* Stanford University, Department of Civil and Environmental Engineering. The John A. Blume Earthquake Engineering Center.

ATC. (1985). *Earthquake Damage Evaluation Data for California.* Applied Technology Council.

Baker, J. W., & Cornell, C. A. (2005). A Vector-valued Ground Motion Intensity Measure Consisting of Spectral Acceleration and Epsilon. *Earthquake Engineering and Structural Dynamics , 34*.

Baker, J., Lin, T., Shahi, S., & Jayaram, N. (2011). *New Ground Motion Selection Procedures and Selected Motions for the PEER Transportation Research Program.* Pacific Earthquake Engineering Research Center Report.

Bandyopadhyay, K., & Hofmayer, C. (1985). Component Fragilities: Data Collection, Analysis and Interpretation. *Conference 13: Water Reactor Safety Research Information Meeting.* Sponsored by the US Nuclear Regulatory Commission.

Bandyopadhyay, K., & Hofmayer, C. (1986). Synthesizing Seismic Fragility of Components by Use of Existing Data. *Conference 14: Water Reactor Safety Information Meeting.* Sponsored by the US Nuclear Regulatory Commission.

Basoz, N., & Kiremidjian, A. S. (1998). *Evaluation of Bridge Damage Data from the Loma Prieta and Northridge, California Earthquakes.* Techinal Report MCEER 98-0004, John A. Blume Earthquake Engineering Center, Stanford, California.

Basoz, N., & Mander, J. (1999). *Enhancement of the Highway Transportation Module in HAZUS.* Draft #7, Prepared for the National Institute of Building Sciences .

Caltrans. (2008). *Restrainer Material Propeties and Design.* California Department of Transportation.

Caltrans. (2010). *Seismic Design Criteria.* California Department of Transporation.

Caltrans. (2006). *Seismic Design Criteria, Version 1.4.* California Department of Transportation.

Caltrans. (2010, July). Seismic Design Methodology. *Memo To Designers 20-1* .

Calvi, G., Pinho, R., Magenes, G., Bommer, J., Restrepo-Velez, L., & and Crowley, H. (2006). Development Of Seismic Vulnerability Assessment Methodologies Over The Past 30 Years. *ISET Journal of Earthuake Technology* , Paper No. 472, Vol 43, No 3.

CEN. (2002). *Eurocode - Basis of Structural Design.* Brussels: European Committee for Standardization.

CEN. (2004). *Eurocode 8: Design of Structures for Earthquake Resistance. Part 1: General rules, seismic actions and rules for buildings.* European Committee for Standardization.

Chiou, B., Darragh, R., Gregor, N., & Silva, W. (2008). NGA Project Strong-Motion Database. *Earthquake Spectra , 23* (1), 23-44.

Choi, E. (2002). *Seismic Analysis and Retrofit of Mid-America Bridges.* PhD Thesis, Georgia Institute of Technology, Civil and Environmental Engineering.

Choi, E., Desroches, R., & Nielson, B. (2004). Seismic Fragility of Typical Bridges in Moderate Seismic Zones. *Engineering Structures , 26*, 187-199.

Choi, E., Nielson, B., & DesRoches, R. (2004). Seismic Fragility of Typical Bridges in Moderate Seismic Zones. *Engineering Structures , 26* (2), 187-199.

Choi, E., Nielson, B., & DesRoches, R. (2004). Seismic Fragility of Typical Bridges in Moderate Seismic Zones. *Engineering Structures 26 (2), 187-199* .

Cimellaro, G., Reinhorn, A., Bruneau, M., & and Rutenburg, A. (2006). *Multi-Dimension Fragility of Structures: Formulation and Evaluation.* University at Buffalo, The State University of New York, Buffalo, N.Y.

Cimellaro, G., Reinhorn, A., D'Ambrisi, A., & De Stefano, M. (2009). Fragility Analysis and Seismic Record Selection. *Journal of Structural Engineering , 137* (3), 379-390.

Cornell, A. C., Jalayer, F., Hamburger, R. O., & Foutch, D. A. (2002). Probabilistic basis for 2000 SAC Federal Emergency Management Agency steel moment frame guidelines. *Journal of Structural Engineering, 128, 526-532* .

Cornell, C., Jalayer, F., Hamburger, R., & Foutch, D. (2002). Probabilistic Basis for 2000 SAC Federal Emergency Management Agency Steel Moment Frame Guidelines. *Journal of Structural Engineering , 128*.

Duan, L., & Li, F. (2003). Seismic Design Philosophies and Performance-Based Design Criteria. In W.-F. Chen, & L. Duan (Eds.), *Bridge Engineering: Seismic Design*. Boca Raton: CRC Press.

Duenas-Osorio, L., Craig, J., & Goodno, B. (2007). Seismic Response of Critical Interdependent Networks. *Earthquake Engineering and Structural Dynamics , 36*, 285-306.

Elnashai, A. (2001). Advanced Inelastic Static (Pushover) Analysis for Earthquake Applications. *Strucutral Engineering and Mechanics , 12* (1), 51-69.

Elnashai, A. S., & Mwafy, A. M. (2008). Seismic Response and Design. In I. o. Engineers, G. Parke, & N. Hewson (Eds.), *ICE Manual of Bridge Engineering* (2nd edition ed.). Thomas Telford Ltd.

Elnashai, A., Borzi, B., & Vlachos, S. (2004). Deformation-based Vulnerability Functions for RC Bridges. *Structural Engineering and Mechanics, Vol 17, No 2* .

Faravelli, L. (1989). Response-Surface Approach for Reliability Analysis. *Journal of Engineering Mechanics , 115*, 2763-2781.

FEMA. (2006). *FEMA 454: Designing for Earthquakes: A Manual for Architects.* Washington, D.C.: U.S Department of Homeland Security.

FEMA. (1997). *HAZUS 97: Technical Manual.* Washington, D.C.: Federal Emergency Management Agency.

FEMA. (2003). *Multi-hazard Loss Estimation Methodology: Earthquake Model.* Technical Manual, HAZUS MR4.

Franchin, P., Lupoi, A., Pinto, P., & Schotanus, M. (2003). Seismic Fragility of Reinforced Concrete Structures using a Response Surface Approach. *Journal of Earthquake Engineering , 7* (Special Issue 1), 45-77.

Gardoni, P., Der Kiureghian, A., & Mosalam, K. (2002). *Probabilistic Models and Fragility Estimates for Bridge Components and Systems.* Pacific Earthquake Engineering Research Center.

Ghosh, J., Padgett, J. E., & Dueñas-Osorio, L. (2012). Comparative Assessment of Different Surrogate Modeling Strategies with Application to Aging Bridge

Seismic Fragility Analysis. *To Appear in the Proceedings of the 11th ASCE Joint Specialty Conference on Probabilistic Mechanics and Structural Reliability (PMC 2012), June 17-20, 2012.* Notre Dame, Indiana.

Goodman, J. (1985). Structural Fragility and Principle of Maximum Entropy. *3*, 37-46.

Hancock, J., Bommer, J., & Stafford, P. (2008). Numbers of Scaled and Matched Accelerograms Required for Inelastic Dynamic Analyses. *Earthquake Engineering and Structural Dynamics , 37*, 1585-1607.

HAZUS MR4:Technical Manual. (2003). *Multi-Hazard Loss Estimation Methodology Earthquake Model.* FEMA.

HAZUS-MH. (2011). *Multi-Hazard Loss Estimation Methodology: Earthquake Model HAZAUS-MH MR5 Technical Manual.* Federal Emergency Management Agency, Washington, DC.

Highway Bridges. (n.d.). Retrieved Jan 7, 2012, from http://nisee.berkeley.edu/northridge/highway_bridges.html

Historic World Earthquakes. (n.d.). Retrieved September 17, 2012, from USGS: http://earthquake.usgs.gov/earthquakes/world/historical_country.php

Hwang, H., & Jaw, J.-W. (1990). Probabilistic Damage Analysis of Structures. *Journal of Structural Engineering , 116* (7), 1992-2007.

Hwang, H., Jernigan, J. B., & Lin, Y. (2000). Evaluation of Seismic Damage to Memphis Bridges and Highway Systems. *Journal of Bridge Engineering , 5* (4), 322-330.

Hwang, H., Liu, J. B., & Chiu, Y.-H. (2001). *Seismic Fragility Analysis of Highway Bridges.* The University of Memphis, Center for Earthquake Research and Information. Mid-America Earthquake Center.

Iervolino, I., & Cornell, C. A. (2005). Record Selection for Nonlinear Seismic Analysis of Structures. *Earthqauke Spectra , 21* (3).

Iervolino, I., Manfredi, G., & Cosenza, E. (2006). Ground Motion Duration Effects on Nonlinear Seismic Response. *Earthquake Engineering and Structural Dynamics , 35*.

Jeong, S., & Elnashai, A. (2007). Probabilistic Fragility Analysis Parameterized by Fundamental Response Quantities. *Engineering Structures 29, 1238-1251* .

Jeong, S.-H., & Elnashai, A. (2007). Probabilistic Fragility Analysis Parameterized by Fundamental Response Quantities. *Engineering Structures 29 pp 1238-1251* .

Ji, J., Elnashai, A., & Kuchma, D. (2007). *Seismic Fragility Assessment for Reinforced Concrete High-Rise Buildings.* MAE Center Report 07-14.

JMP Software. (n.d.). Retrieved April 18, 2012, from www.jmp.com

JMP the Statistical Discovery Software. (2010). *JMP Pro v9.0.2*. Carry, NC.

JPA. (2002). Part V: Seismic Design. In *Design Specifications of Highway Bridges.* Japan Road Association.

Kafali, C., & Grigoriu, M. (2007). Seismic Fragility Analysis: Aplication to Simple Linear and Nonlinear Systems. *Earthquake Engineering and Structural Dynamics , 36*, 1885-1900.

Kappos, A., Stylianidis, K., & Pitilakis, K. (1998). Development of Seismic Risk Scenarios Based on a Hybrid Method of Vulnerability Assessment. *Natural Hazards 17* .

Karim, K., & Yamazaki, F. (2001). Effect Of Earthquake Ground Motions On Fragility Curves Of Highway Bridge Piers Based On Numerical Simulation. *Earthquake Engineering and Structural Dynamics 2001; 30:1839-1856* .

Katsanos, E. I., Sextos, A. G., & Manolis, G. D. (2010). Selection of Earthquake Ground Motion Records: A State-of-the-art Review. *Soil Dynamics and Earthquake Engineering , 30*, 157-169.

Kawashima, K. (2002). Seismic Design.

Kawashima, K., Nakano, M., Nishikawa, K., Fukui, J., Tamura, K., & Unjoh, S. (1997). The 1996 Seismic Design Specifications of Highway Bridges. *Proceedings of the 29th Joint Meeting of U.S.–Japan Panel on Wind and Seismic Effects.* UNJR, Technical MEmorandum of PWRI, No. 3524.

Kennedy, R., Cornell, C., Campbell, R., Kaplan, S., & Perla, H. (1980). Probabilistic Seismic Safety Study of an Existing Nuclear Power Plant. *Nuclear Engineering and Design , 59*, 315-338.

Kim, J., Choi, I.-K., & Park, J.-H. (2011). Uncertainty analysis of System Fragility for Seismic Safety Evaluation of NPP. *Nuclear Engineering and Design , 241*, 2570-2579.

Kircil, M., & Polat, Z. (2006). Fragility Analysis of Mid-Rise R/C Frame Buildings. *Engineering Structures , 28*, 1335-1345.

Kolias, B. (2008). Eurocode 8 - Part 2. Seismic Design of Bridges. *Eurocodes: Background and Applications Workshop.* Brussels.

Koutsourelakis, P. (2010). Assessing Structural Vulnerability Against Earthquakes Using Multi-Dimensaional Fragility Surfaces: A Bayesian Framework. *Probabilistic Engineering Mechanics 25:49-60* .

Koutsourelakis, P. S. (2010). Assessing structural vulnerability against earthquakes using multi-dimensional fragility surfaces: A Bayesian framework. *Probabilistic Engineering Mechanics , 25*.

Kutner, M., Nachtsheim, C., Neter, J., & Li, W. (2005). *Applied Linear Statistical Models* (5th edition ed.). Boston: McGraw-Hill.

Kwon, O., & Elnashai, A. (2006). The effect of material and ground motion uncertainty on the seismic vulnerability curves of RC structure. *Engineering Structures 28, 289-303.*

Kwon, O., & Elnashai, A. (2006). The effect of material and ground motion uncertainty on the seismic vulnerability curves of RC structure. *Engineering Structures 28, 289-303* .

Lemieux, C. (2009). *Monte Carlo and Quasi-Monte Carlo Sampling.* Waterloo, Ontario, Canada: Springer.

Lin, K., & Wald, D. (2008). *ShakeCast Manual Open-File Report 2008-1158.* United States Geological Survey. Washington, DC: United States Department of Interior.

Lu, J., Mackie, K., & Elgamal, A. (2011). *BridgePBEE: OpenSees 3D Pushover and Earthquake Analysis of Single-Column 2-span Bridges.* User Manual, Beta 1.0.

Luco, N., Ellingwood, B. R., Hamburger, R. O., Hooper, J. D., Kimball, J. K., & Kircher, C. A. (2007). Risk-Targeted versus Current Seismic Design Maps for the Conterminous United States. *SEAOC 2007 Convention Proceedings.*

Lupoi, G., Franchin, P., Lupoi, A., & Pinto, P. (2004). Seismic Fragility Analysis of Structural Systems. *13th World Conference on Earthquake Engineering.* Vancouver, BC, Canada.

Mackie, K. R., & Stojadinovic, B. (2007, July/August). R-Factor Parameterized Bridge Damage Fragility Curves. *Journal of Bridge Engineering* .

Mackie, K., & Stojadinović, B. (2005). *Fragility Basis for California Highway Overpass Bridge Seismic Decision Making.* Technical Report, PEER 2005/12.

Mackie, K., & Stojadinovic, B. (2001). Probabilistic Seismic Demand Model For California Highway Bridges. *Journal of Bridge Engineering, 6(6): 468-481* .

Mackie, K., Wong, J.-M., & Stojadinović, B. (2008). *Integrated Probabilistic Performance-Based Evaluation Of Benchmark Reinforced Concrete Bridges.* Technical Report, PEER 2007/09.

Malhotra, P. K. (2003). Strong-Motion Records for Site-Specific Analysis. *Earthquake Spectra , 19* (3).

Mander, J. (1999). Fragility Curve Development for Assessing the Seismic Vulnerability of Highway Bridges. In M. C. Research, *Research Progress and Accomplishments: 1997-1999* (pp. 89-98).

Mander, J., Priestley, M., & Park, R. (1988). Theoretical Stress-Strain Model for Confined Concrete. *Journal of Structural Engineering , 114* (No. 8).

MATLAB. (2011). *(MATLAB R2011b)* . Natick, Massachusetts: The MathWorks Inc.

Matthews, R. (2005). CONSEC: Concrete Section Analysis Program.

Mazzoni, S., McKenna, F., Scott, M. H., & Fenves, G. L. (2009). *Open System for Earthquake Engineering Simulation User Command-Language Manual.* University of California, Berkeley. Pacific Earthquake Engineering Research Center.

Mazzoni, S., McKenna, F., Scott, M. H., & Fenves, G. L. (2009). *Open System for Earthquake Engineering Simulation User Command-Language Manual.* University of California, Berkeley. Pacific Earthquake Engineering Research Center.

Megally, S. H., Silva, P. F., & Seible, F. (2001). *Seismic Response of Sacrificial Shear Keys in Bridge Abutments.* SSRP-2001/23, University of California, San Diego, Department of Structural Engineering.

Melchers, R. (1999). *Structural Reliability Analysis and Prediction* (Second Edition ed.). Chichester, West Sussex, England: John Wiley and Sons.

Microsoft. (n.d.). Get in the Loop with Excel Macros. Retrieved December 30, 2012, from http://office.microsoft.com/en-us/training/get-in-the-loop-with-excel-macros-RZ001150634.aspx

Microsoft. (2007). Microsoft Excel 2007. Redwood , Washington.

Moehle, a., Fenves, G., Mayes, R., Priestley, N., Seible, F., Uang, C.-M., et al. (1995). Highway Bridges and Traffic Management. *Earthquake Spectra , 11* (S2), 287-372.

Moehle, J., & Deierlein, G. (2004). A Framework Methodology for Performance-Based Earthquake Eningeering. *13th World Conference on Earthquake Engineering.* Vancouver, B.C., Canada.

Montgomery, D. (2009). *Design and Analysis of Experiments.* Hoboken, NJ: John Wiley & Sons.

Muthukumar, S. (2003). *A Contact Element Approach with Hysteresis Damping for the Analysis and Design of Pounding in Bridges.* PhD Thesis, Georgia Institute of Technology, Civil and Environmental Engineering.

Myers, R., Khuri, A., & Carter, J. W. (1989). Response Surface Methodology: 1966-1988. *Technometric, Vol 31, No 2* .

Nielson, B. (2005). *Analytical Fragility Curves for Highway Bridges in Moderate Seismic Zones.* PhD Thesis, Georgia Institute of Technology, School of Civil and Environmental Engineering.

Nielson, B., & Bowers, M. (2007). Seismic Bridge Fragilities for Post-design Verification. *1st US-Italy Seismic Bridge Workshop.*

Nielson, B., & DesRoches, R. (2007). Seismic Fragility Methodology for Highway Bridges Using a Component Level Approach. *Earthquake Engineering and Structural Dynamics, 36 (6), 823-839* .

NZTA. (2003). *Bridge Manual*. Retrieved September 17, 2012, from NZ Transport Agency: http://www.nzta.govt.nz/resources/bridge-manual/index.html

O'Rourke, M. J., & So, P. (2000). Seismic Fragility Curves for On-grade Steel Tanks. *Earthquake Spectra , 16* (4).

Ouchi, F. (2004). *A Literature Review on the Use of Expert Opinion in Probabilistic Risk Analysis.* World Bank Policy Research Working Paper 3201.

Padgett, J. E., & DesRoches, R. (2008). Methodology for the Development of Fragility Curves for Retrofitted Bridges. *Earthquake Engineering and Structural Dynamics 37 (8), 1157-1174* .

Padgett, J., Nielson, B., & DesRoches, R. (2008). Selection of Optimal Intensity Measures in Probabilistic Seismic Demand Modelas of Highway Bridge Portfolios. *Earthquake Engineering and Structural Dynamics , 37*, 711-725.

Park, R. (1997). Developements inSesimic Design Procedures for Bridges in New Zealand. *Bulletin of the New Zealand National Society for Earthquake Engineering , Vol. 30* (No. 2).

Park, R. (1996). New Zealand Perspectives on Seismic Design of Bridges. *11th World Conference on Earthquake Engineering.*

Park, Y., & Ang, A.-S. (1985). Mechanistic Seismic Damage Model for Reinforced Concrete. *Journal of Structural Engineering , 111* (4), 722-739.

Rajashekhar, M., & Ellingwood, B. (1993). A New Look at the Response Surface Approach for Reliability Analysis. *Structural Safety , 12*, 205-220.

Ramanathan, K. (2012). *Next Generation Seismic Fragility Curves for California Bridges Incorporating the Evolution in Seismic Design Philosphy.* PhD Thesis, Georgia Institute of Technology, Civil and Environmental Engineering.

Ramanathan, K., DesRoches, R., & Padgett, J. (2010). Analytical Fragility Curves of Multispan Continuous Steel Girder Bridges in Moderate Seismic Zones. *Transportation Research Record: Journal of the Transportation Research Board* (No. 2202), 173-182.

Roblee, C., Sahs, S., Mahan, M., Yashinsky, M., Setberg, H., Maintenance, C., et al. (2011, February). Caltrans-Aligned Limit States Discussion. (J. Dukes, K. Ramanathan, R. DesRoches, & J. Padgett, Interviewers)

Roblee, C., Yashinsky, M., & Mahan, M. (2011, October). Bridge Specific Fragility Discussion. (J. Dukes, R. DesRoches, J. Padgett, & K. Ramanathan, Interviewers)

Rojahn, C. (1997). *Seismic design criteria for bridges and other highway structures.* National Center for Earthquake Engineering Research. Buffalo, N.Y.: National Center for Earthquake Engineering Research, University at Buffalo, The State University of New York,.

Sahs, S. V. (2008). Visual Inspection and Capacity Assessment of Earthquake Damaged Reinforced Concrete Bridge element. *Report CA08-0284 and SSRP-06/12* .

Sahs, S., Veletzos, M., Panagiutou, M., & Restrepo, J. (2008). Visual Inspection & Capacity Assessment of Earthquake Damaged Reinforced Concrete Bridge Element: Integrated Research & Deployment Final Report. *Report No CA08-0284 and SSRP-06/19* .

Schrage, I. (1981). Anchoring of Bearings by Friction. *Joint Sealing and Bearing Systems for Concrete Structures, World Congress on Joints and Bearings. Vol 1.* Niagara Falls, NY: American Concrete Institute.

Seo, J., Duenas-Osorio, L., Craig, J., & Goodno, B. (2012). Metamodel-based regional vulnerability estimate of irregular steel moment-frame structures subjected to earthquake events. *Engineering Structures , 45*, 585-597.

Setberg, H. (2011, February 18). Caltrans Seismic Design Process. (G. Tech, Interviewer)

Shafieezadeh, A. (2011). *Seismic Vulnerability Assessment of Wharf Structures.* PhD Thesis, Georgia Insitute of Technology, Civil and Environmental Engineering.

Shafieezadeh, A., Ramanathan, K., Padgett, J. E., & DesRoches, R. (2011). Fractional Order Intensity Measures For Probabilistic Seismic Demand Modeling Applied to Highway Bridges. *Earthquake Engineering and Structural Dynamics, DOI: 10.1002/eqe.1135* .

Shamsabadi, A., & Yan, L. (2008). Closed-Form Force-Displacement Backbone Curves for Bridge Abutment Backfill Systems. *Geotechnical Earthquake Engineering and Soil Dynamics IV Congress.* American Society of Civil Engineers.

Shamsabadi, A., Rollins, K., & Kapuskar, M. (2007, June). Nonlinear Soil-Abutment-Bridge Structure Interaction for Seismic Performance-Based Design. *Journal of Geotechnical and Geoenvironmental Engineering* .

Shinozuka, M., Banerjee, S., & Kim, S. (2007). *Fragility Considerations in Highway Bridge Design.* University at Buffalo, The State University of New York, Buffalo, N.Y.

Shinozuka, M., Banerjee, S., & Kim, S. (2007). *Statistical and Mechanistic Fragility Analysis of Concrete Bridges.* Technical Report, MCEER-07-0015.

Shinozuka, M., Feng, M. Q., Lee, J., & Naganuma, T. (2000, December). Statistical Analysis of Fragility Curves. *Journal of Engineering Mechanics* .

Shinozuka, M., Feng, M., Kim, H., Uzamwa, T., & Ueda, T. (2003). *Statistical Analysis of Fragility Curves.* Technical Report, MCEER-03-0002.

Simpson, T., Peplinski, J., Koch, P., & and Allen, J. (2001). Metamodels for Computer-based Engineering Design: Survey and Recommendations. *Engineering with Computers 17:129-150* .

Smith, M., & Caracoglia, L. (2011). A Monte Carlo based method for the dynamic ''fragility analysis'' of tall buildings under turbulent wind loading. *Engineering Structures , 33*, 410-420.

Terzic, V. (2011, December). Force-based Element vs. Displacement-based Element. UC Berkeley,OpenSees, NEES, & NEEScomm.

Towashiraporn, P. (2004). *Building Seismic Fragilities Using Response Surface Metamodels.* Georgia Institute of Technology.

Transit New Zealand. (2003). *Bridge Manual.* Wellington: Transit New Zealand.

Unjoh, S. (2000). Seismic Design Practice in Japan. In W.-F. Chen, & L. Duan (Eds.), *Bridge Engineering Handbook.* Boca Raton, London, New York, Washington, D.C.: CRC Press.

Unjoh, S., Nakatani, S.-i., Tamura, K., Fukui, J., & Hoshikuma, J.-i. (2002). 2002 seismic design specifications for highway bridges. *Proceedings of the 34th Joint Panel Meeting, May 13-15, 2002. SP 987.* Gaithersburg, Maryland: National Institute of Standards and Technology.

USGS. (n.d.). Earthquake Facts and Statistics. Retrieved February 19, 2013, from http://earthquake.usgs.gov/earthquakes/eqarchives/year/eqstats.php

USGS. (n.d.). *Hazard Curve Application*. Retrieved 3 25, 2013, from http://geohazards.usgs.gov/hazardtool/

Wen, Y., Ellingwood, B., Veneziano, D., & Bracci, J. (2003). *Uncertainty Modeling in Earthquake Engineering.* MAE Center Project FD-2 Report.

Yao, T., & Wen, Y. (1996). Response Surface Method for Time-Variant Reliability Analysis. *Journal of Structural Engineering , 122* (2).

Zealand, T. N. (2004). *Bridge Manual.* Wellington: Transit New Zealand.

Zhong, J., Gardoni, P., Rosowsky, D., & Haukaas, T. (2008, June). Probabilistic Seismic Demand Models and Fragility Estimates for Reinforced Concrete Bridge with Two-Column Bents. *Journal of Engineering Mechanics .*